

ABSTRACT

CARR, ANN LOUISE. Profiling of Acarine Attractants and Chemosensation. (Under the direction of Dr. R. Michael Roe.)

Acarine Attractants. The Acari are of significant economic and health importance, and consist of two major groups, the mites that demonstrate a wide variety of life strategies, i.e., herbivory, predation and ectoparasitism, and ticks which have evolved obligatory hematophagy. The major sites of chemoreception in the acarines are the palps and tarsi on the forelegs. A unifying name, the “foretarsal sensory organ” (FSO), is proposed for the first time for the sensory site on the forelegs of all acarines. Over the past three to four decades’ significant progress has been made in the chemistry and analysis of function for acarine attractants in mites and ticks. This has been made possible by the variety of laboratory and field bioassay methods that have been developed for the identification and characterization of attractants including a novel ultrasonic micro-dissection method that was developed. In mites, attractants include aggregation, immature female, female sex and alarm pheromones; in ticks, the attraction-aggregation-attachment, assembly and sex pheromones; in mites and ticks host kairomones and plant allomones; and in mites, fungal allomones. There are still large gaps in our knowledge of chemical communication in the acarines compared to insects. However, the use of lure-and-kill and lure-enhanced biocontrol strategies have been investigated for tick and mite control, respectively, with significant environmental advantages which warrant further study.

Haller’s Organ Olfactory Mechanism. Next generation sequencing and comparative analyses suggest that the chemosensory mechanism in the Haller’s organ of ticks is a G-protein coupled receptor (GPCRs) signal cascade. Only olfactory GPCRs were identified suggesting, despite conflicting morphological data, that the Haller’s organ functions only in

olfaction and not gustation. Each component of the olfactory GPCR signal cascade was identified, except for the odorant binding proteins. This suggests that ticks rely on either a novel, unknown class of binding proteins or other methods of sensilla lymph solubilization to deliver odorant molecules from the environment to chemoreceptors. qPCR experiments documenting the expression profile of the olfactory transcripts GPCR, $G_{\alpha o}$, and β -arrestin in unfed and blood-fed adult *D. variabilis* determined that there is hormonal regulation of the olfactory system in ticks. Behavioral assays confirmed the role of the Haller's organ in chemical avoidance, in addition to its known role in chemical attraction. Remarkably, it was determined that the Haller's organ is not required for host attachment or blood-feeding.

Sex Pheromones of the Black-legged Tick. Copulation in *I. scapularis* involves physical contact between the male and female (on or off the host), male mounting of the female, insertion/maintenance of the male chelicerae in the female genital pore (initiates spermatophore production), and the transfer of the spermatophore by the male into the female genital pore. Bioassays determined that male mounting behavior/chelicerae insertion required direct contact with the female likely requiring non-volatile chemical cues with no evidence of a female volatile sex pheromone to attract males. Unfed virgin adult females and replete mated adult females elicited the highest rates of male chelicerae insertion with part fed virgin adult females exhibiting a much lower response. Whole body surface hexane extracts of unfed virgin adult females and males, separately analyzed by GC-MS, identified a number of novel tick surface associated compounds: fatty alcohols (1-hexadecanol and 1-heptanol), a fatty amide (erucylamid), aromatic hydrocarbons, a short chain alkene (1-heptene), and a carboxylic acid ester (5 β -androstane). These compounds are discussed in terms of their potential role in female-male communication. The two most abundant fatty acid esters found

were butyl palmitate and butyl stearate present in ratios that were sex specific. Only 6 n-saturated hydrocarbons were identified in *I. scapularis* ranging from 10-18 carbons.

© Copyright 2015 Ann Louise Carr

All Rights Reserved

Profiling of Acarine Attractants and Chemosensation

by
Ann Louise Carr

A dissertation submitted to the Graduate Faculty of
North Carolina State University
in partial fulfillment of the
requirements for the Degree of
Doctor of Philosophy

Entomology

Raleigh, North Carolina

2015

APPROVED BY:

Dr. R. Michael Roe
Committee Chair

Dr. Coby Schal

Dr. Wes Watson

Dr. Daniel E. Sonenshine

DEDICATION

This dissertation is dedicated to my grandmother, Martha Carr. Her generosity and support have allowed me to pursue my education to the fullest, and for that I will always be grateful.

BIOGRAPHY

Ann Carr was born and raised in Washington, DC making her a 6th generation Washingtonian. She graduated from the Holton-Arms School for Girls and made her way down south to attend Texas A & M University. She has always had an interest in science and research, interning both her freshman and sophomore years at the Walter Reed Army Institute of Research analyzing the genetic variances between SHIV positive and negative rhesus monkeys. She was fortunate enough to obtain a lab technician position her junior and senior years with Dr. Albert Mulenga in the Texas A & M University medical and veterinary entomology research lab. It was during her time spent helping Dr. Mulenga with his research on tick salivary proteins that she first became fascinated with ticks, and developed a desire to pursue a career researching them. Ann graduated from Texas A & M University in 2009 with a BS double major in biomedical science and entomology. She arrived at North Carolina State University and obtained a master's in entomology in 2011 under the direction of Dr. Charles Apperson, Dr. R. Michael Roe and Dr. Coby Schal studying host kairomones and chemical lures for ticks. She continued on for her PhD in Dr. Roe's lab sequencing the first transcriptome to the Haller's organ and researching tick chemical communication and mating behaviors. In addition to her research, Ann is actively involved in EGSA student outreach and the Triangle Beagle Rescue. She also enjoys skiing and kiteboarding in her free time.

ACKNOWLEDGMENTS

I would first and foremost like to thank my advisor Dr. R. Michael Roe for all his support and guidance, in addition to providing me an opportunity to stay on after my master's and pursue a PhD. Dr. Roe's knowledge and insight has been an invaluable resource, and it has been a privilege to work in his lab.

I would also like to thank all the members of my graduate committee Dr. Daniel E. Sonenshine, Dr. Charles Apperson, Dr. Coby Schal, and Dr. Wes Watson, as well as my graduate representatives Dr. Asimina Mila and Dr. Wesley Everman. I very much appreciate their expertise, advice, and participation on my committee.

I would like to thank all the members of the Roe lab for creating such a positive and welcoming work environment. I truly consider all my work colleagues to be friends and have enjoyed all of our collaborations immensely.

Lastly I would like to thank my family for their unwavering love and support throughout my doctoral studies.

TABLE OF CONTENTS

List of Tables	vi
List of Figures	vii
Acarine Attractants: Chemoreception, Bioassay, Chemistry, and Control	1
Abstract	2
Introduction	3
Chemosensory Structure and Function	5
Bioassay Methods for Acarine Attractants	10
Chemistry of Aggregation and Assembly Pheromones	18
Chemistry of Reproductive (Sex) Pheromones	23
Chemistry of Alarm Pheromones	26
Chemistry of Host Kairomones	27
Chemistry of Plant Allomones	32
Chemistry of Fungal Allomones	35
Acarine Trapping: Attraction and Kill	36
Summary and Conclusions	39
Acknowledgments	41
References	41
Tables	55
Figures	66
Putative GPCR Chemosensory Pathway Identified in the Haller’s Organ of Male American Dog Ticks, <i>Dermacentor variabilis</i>	73
Abstract	74
Introduction	76
Results and discussion	77
Conclusions	93
Materials and Methods	94
Acknowledgements	95
References	95
Tables	99
Figures	101
Supplemental Information: Materials and Methods	111
Supplemental Information: Results	121
Supplemental Information: References	126
Supplemental Information: Tables	128
Supplemental Information: Figures	136
Evidence of Female Sex Pheromones and the Characterization and the Characterization of the Cuticular Lipids of Unfed Adult Male versus Female Blacklegged Ticks, <i>Ixodes scapularis</i>	157
Introduction	158
Materials and Methods	161
Results	168
Discussion	173
Acknowledgments	180

Compliance with Ethical Standards	181
References	181
Tables	185
Figures	195
Supplemental Information: Figures	196
Appendices	214
Appendix A. Ionotropic Glutamate Receptors with Putative Olfactory Functions Identified in the Haller’s Organ of the American Dog Tick, <i>Dermacentor variabilis</i> (Acari: Ixodidae)	215
Appendix B. A Novel Method for Micro-Dissection of the Cuticle Covering of the Haller’s Organ Posterior Capsule	226

LIST OF TABLES

Table 1.1. Mite pheromones and chemical components that elicit attractive or aggregative behavioral responses	55
Table 1.2. Tick pheromones and chemical components that elicit attractive or aggregative behavioral responses	57
Table 1.3. Chemical components of host kairomones that elicit attractive behavioral responses in mite species	59
Table 1.4. Chemical components of host kairomones that elicit attractive behavioral responses in tick species	60
Table 1.5. Plants and herbivore induced plant volatiles that elicit attractive behavioral responses in mite species	60
Table 1.6. Plants volatiles that elicit attractive behavioral responses in tick species	64
Table 1.7. Chemical components of fungal allomones that elicit attractive behavioral responses in mite species	65
Table 2.1. Putative transcripts involved in chemoreceptor signal transduction identified exclusively in the Haller's organ transcriptome of unfed, virgin adult male <i>Dermacentor variabilis</i> and their respective tick, nematode and insect matches with the lowest expected value (e-value)	99
Table 2.2. Putative transcripts involved in chemoreceptor signal modulation/termination and xenobiotic metabolism identified exclusively in the Haller's organ transcriptome of unfed, virgin adult male <i>Dermacentor variabilis</i> and their respective tick, nematode and insect matches with the lowest expected value (e-value).....	100
Table 2.S1. Comprehensive list of the acronyms presented in phylogenetic trees and the identifying species and GenBank accession numbers	128
Table 2.S2. The 50 most abundant transcripts from the unfed, virgin adult male <i>Dermacentor variabilis</i> illumina 1 st leg transcriptome.....	130
Table 2.S3. The 50 most abundant transcripts from the unfed, virgin adult male <i>Dermacentor variabilis</i> illumina 4 th leg transcriptome.....	133
Table 3.1. Compounds with a match probability $\geq 80\%$ identified in all replicates of whole body hexane extracts of <i>I. scapularis</i> unfed, virgin adult females versus unfed, virgin adult males (Cas no. = Chemical abstract service number). Mass spectral data are listed in Supplemental Information: Figures	185

Table A.1. Putative ionotropic glutamate receptors identified exclusively in the Haller’s organ of unfed virgin adult male *Dermacentor variabilis* with their respective tick and non-tick arthropod BLASTx matches with the lowest expected value (e-value) 219

Table A.2. Biological and molecular level 2 gene ontology annotation of the two putative ionotropic glutamate receptors (contig 5494 and 9210) identified exclusively in the Haller’s organ of unfed virgin adult male *Dermacentor variabilis* 220

Table A.3. Comprehensive list of the acronyms presented in phylogenetic trees and the identifying species and GenBank accession numbers 221

LIST OF FIGURES

<p>Figure 1.1. The palpal organ (boxed) located on the tip of the palp pedipalp of the <i>Neocarus texanus</i> mite (AE = anterior eye, CH = chelicerae, OP = ovipositor, LI = leg I, P= posterior eye, PdP = pedipalp), used with permission from Wiley & Sons Inc. © 1999 Alberti and Coons</p>	66
<p>Figure 1.2. (A, B) Sensillar organization in the tarsal complex, located on the foretarsus of the first pair of legs of the <i>Varroa jacobsoni</i> mite (1-9 = edge bristles, PTA= ambulacrum, S1-S9 = pit sensilla), used with permission from Wiley & Sons Inc. © 1999 Alberti and Coons</p>	67
<p>Figure 1.3. The Haller’s organ, located on the first tarsus of the first pair of legs of the American dog tick, <i>Dermacentor variabilis</i> (Ap = anterior pit, Ap₁ = large setiform sensillum, Pc = posterior capsule) used with permission from Cambridge © 2004 Sonenshine</p>	68
<p>Figure 1.4. Mouthparts of the tick <i>Hyalomma savignyi</i> with possible chemo-mechanosensory functions (CH = chelicerae, LI = leg I, PA = palps)</p>	69
<p>Figure 1.5. The number of each type of probable olfactory and gustatory messages identified in both the 454 and illumina Haller’s organ transcriptomes that are found in the <i>Ixodes scapularis</i> genome and have annotations and pfam domains (Carr and Roe, personal communication)</p>	70
<p>Figure 1.6. Image of olfactometer with two ports for use in laboratory bioassays of attractants used with permission from Wiley & Sons Inc. © 2012 Carr et al.....</p>	71
<p>Figure 1.7. Image of olfactometer with four ports for use in laboratory bioassays of acarine attractants.....</p>	72
<p>Figure 2.1. The Haller’s organ (boxed) located on the first foretarsus of the first pair of legs of the American dog tick, <i>Dermacentor variabilis</i> (400x magnification).....</p>	101
<p>Figure 2.2. Phylogenetic relationship of transcripts putatively encoding lipocalins (Lip) identified in the Haller’s organ spf (contig 84287) and 1st/4th leg transcriptomes (contigs 42763, 23753) of unfed, virgin adult male <i>Dermacentor variabilis</i> with lipocalins from <i>Caenorhabditis elegans</i>, <i>Ixodes ricinus</i>, and <i>Rattus norvegicus</i>. The phylogenetic tree shows the branch relation of chemosensory lipocalins (red branch) with non-chemosensory lipocalins. Tick lipocalins are highlighted with a blue branch color. Acronyms are as follows: first letter of the genus and species (<i>Caenorhabditis elegans</i>, Ce; <i>Ixodes ricinus</i>, Ir; <i>Rattus norvegicus</i>, Rn) followed by the protein name (Clip or Lip). Putative lipocalin transcripts are boxed. The tree was constructed using Maximum likelihood phylogenetic analysis and bootstrapping set to 500 iterations. Branch values listed are bootstrap percentages (percent confidence), scale set to 10%. A comprehensive list of acronyms</p>	

and associated Genbank accession numbers are listed in Table 2.S1 102

Figure 2.3. Phylogenetic relationship of transcripts putatively encoding G-protein coupled receptors (GPCRs) identified in the Haller's organ spf (contigs 72702, 83622) of unfed, virgin adult male *Dermacentor variabilis* with GPCRs of known clade annotation from *Amblyomma cajennense*, *Amblyomma triste*, *Ixodes ricinus*, *Ixodes scapularis*, *Rhipicephalus microplus*, and *Rhipicephalus pulchellus*. The phylogenetic tree shows four clades, each represented by the following branch colors: blue = clade A; purple = clade C; green = clade D; red = clade B. Acronyms are as follows: first letter of the genus and species (*Amblyomma cajennense*, Ac; *Amblyomma triste*, At; *Ixodes ricinus*, Ir; *Ixodes scapularis*, Is; *Rhipicephalus microplus*, Rm; *Rhipicephalus pulchellus*, Rp) followed by the protein name (GPCR). Putative GCPR transcripts are boxed. The tree was constructed using Maximum likelihood phylogenetic analysis and bootstrapping set to 500 iterations. Branch values listed are bootstrap percentages (percent confidence), scale set to 50%. A comprehensive list of acronyms and associated Genbank accession numbers are listed in Table 2.S1 103

Figure 2.4. Phylogenetic relationship of transcripts putatively encoding G-protein α subunits ($G\alpha$) identified in the Haller's organ (contig 13937) and 1st/4th leg transcriptomes (contigs 2423, 13329, 14072, 46297) of unfed, virgin adult male *Dermacentor variabilis* with $G\alpha$ subunits of known clade annotation from *Caenorhabditis elegans* and insects. The phylogenetic tree shows four clades, each represented by the following branch colors: red = $G\alpha i/o$ clade; green = $G\alpha q$ clade; purple = $G\alpha q12/13$ clade; blue = $G\alpha s$ clade. Acronyms are as follows: first letter of the genus and species (*Anopheles aquasalis*, Aa; *Anopheles gambiae*, Ag; *Drosophila melanogaster*, Dm; *Caenorhabditis elegans*, Ce) followed by the protein name ($G\alpha$) and the letter/number of the associated clade. Putative $G\alpha$ subunit transcripts are boxed. The tree was constructed using Maximum likelihood phylogenetic analysis and bootstrapping set to 500 iterations. Branch values listed are bootstrap percentages (percent confidence), scale set to 20%. A comprehensive list of acronyms and associated Genbank accession numbers are listed in Table 2.S1 104

Figure 2.5. Phylogenetic relationship of transcripts putatively encoding G-protein β subunits ($G\beta$) identified in the Haller's organ (contig 24477) and 1st/4th leg transcriptomes (contig 57459) of unfed, virgin adult male *Dermacentor variabilis* with $G\beta$ subunits of known clade annotation from *Caenorhabditis elegans* and insects. The phylogenetic tree shows four clades, each represented by a branch color as follows: red = $\beta 1$ clade; green = $\beta 2$ clade; blue = $\beta 5$ clade; purple = novel divergent clade. Acronyms are as follows: first letter of the genus and species (*Aedes aegypti*, Aa; *Apis mellifera*, Am; *Drosophila melanogaster*, Dm; *Caenorhabditis elegans*, Ce) followed by the protein name ($G\beta$) and the number of the clade number. Putative $G\beta$ subunit transcripts are boxed. The tree was constructed using Maximum likelihood phylogenetic analysis and bootstrapping set to 500 iterations. Branch values listed are bootstrap percentages (percent confidence), scale set to 20%. A comprehensive list of acronyms and associated Genbank accession numbers are listed in Table 2.S1 105

Figure 2.6. Phylogenetic relationship of transcripts putatively encoding G-protein γ subunits ($G\gamma$) identified in the 4th leg transcriptome (contig 3088) and the 454 1st leg transcriptome (454 transcript) of unfed, virgin adult male *Dermacentor variabilis* with $G\gamma$ subunits of known clade annotation from *Caenorhabditis elegans* and *Drosophila melanogaster*. The phylogenetic tree shows two clades, each represented by a branch color as follows: red = γ 1, chemosensory clade; blue = γ 2 clade. Acronyms are as follows: first letter of the genus and species (*Drosophila melanogaster*, Dm; *Caenorhabditis elegans*, Ce) followed by the protein name ($G\gamma$) and the number of the clade number. Putative $G\gamma$ subunit transcripts are boxed. The tree was constructed using Maximum likelihood phylogenetic analysis and bootstrapping set to 500 iterations. Branch values listed are bootstrap percentages (percent confidence), scale set to 20%. A comprehensive list of acronyms and associated

Genbank accession numbers are listed in Table 2.S1 106

Figure 2.7. Phylogenetic relationship of transcripts putatively encoding cytochrome P450s (CYPs or P450s) identified in the Haller's organ transcriptome of unfed, virgin adult male *Dermacentor variabilis* with P450s of known clan annotation from *Ixodes scapularis* (Is). The phylogenetic tree shows four P450 clades, each represented by a branch color as follows: green = CYP2 clade; red = CYP3 clade; blue = CYP4 clade; purple = mitochondrial CYP or CYPmit clade. Acronyms consist of the first letter of the genus and species (Is) followed by the protein name (CYP) and the number or abbreviation (mit = mitochondrial) of the associated clade. Putative P450s transcripts are boxed. The tree was constructed using Maximum likelihood phylogenetic analysis and bootstrapping set to 500 iterations. Branch values listed are bootstrap percentages (percent confidence), scale set to 20%. A comprehensive list of acronyms and associated GenBank accession numbers

are listed in Table 2.S1 107

Figure 2.8. Phylogenetic relationship of transcripts putatively encoding glutathione S-transferases (GSTs) identified in the Haller's organ transcriptome of unfed, virgin adult male *Dermacentor variabilis* with GSTs of known clade annotation from *Ixodes scapularis* (Is). The phylogenetic tree shows 5 GST clades, each represented by a different branch color as follows: red = epsilon GST clade; blue = delta GST clade; green = mu GST clade; purple = omega GST clade; yellow = zeta GST clade. Acronyms consist of the first letter of the genus and species (Is), followed by protein name (GST) and the first letter of the associated clade (delta, d; epsilon, e; omega, o; mu, m; zeta, z). Putative GST transcripts are boxed. The tree was constructed using Maximum likelihood phylogenetic analysis and bootstrapping set to 500 iterations. Branch values listed are bootstrap percentages (percent confidence), scale set to 20%. A comprehensive list of acronyms and associated

GenBank accession numbers are listed in Table 2.S1 108

Figure 2.9. Relative mRNA expression (Δ Ct) of the chemosensory proteins β -arrestin, G-protein α_o subunit ($G\alpha_o$) and G-protein coupled receptor (GPCR) in unfed versus fully blood fed adult female and male *Dermacentor variabilis* after normalization to expression levels of glyceraldehyde 3-phosphate dehydrogenase (GAPDH; * = $P < 0.05$; error bars = ± 1 SEM; ANOVA and a Sidak's multiple comparison test). Replicates of 5, using 2ng cDNA,

10 μ L reactions 109

Figure 2.10. Observed behavior in response to the removal of either the 1st or 4th pairs of legs in unfed, virgin adult *Dermacentor variabilis*. A, Time to rabbit (*Oryctolagus cuniculus*) and attachment by tick. Statistical analyses were performed using an ANOVA and a Sidak's multiple comparison test (* = P<0.05; error bars = ±1 SEM). Replicates of 4, with a mixed population of 15 female and 15 male ticks. B, Petridish assay two choice repellency assay. Statistical analyses were performed using an ANOVA and a Sidak's multiple comparison test (* = P<0.05; error bars = ±1 SEM). Replicates of 3 and 6 were conducted for the control and treatment, respectively, with a mixed population of 4 female and 4 male ticks 110

Figure 2.S1. Distribution of transcripts annotated at the gene ontology level 2 and their putative involvement in biological functions for the unfed virgin adult male *Dermacentor variabilis* illumina 1st leg transcriptome 136

Figure 2.S2. Distribution of transcripts annotated at the gene ontology level 2 and their putative involvement in biological functions for the unfed virgin adult male *Dermacentor variabilis* illumina 4th leg transcriptome 137

Figure 2.S3. Distribution of transcripts annotated at the gene ontology level 2 and their putative involvement in biological functions for the unfed virgin adult male *Dermacentor variabilis* 454 1st leg transcriptome..... 138

Figure 2.S4. Multiple sequence alignment (Clustal Ω) of the deduced amino acid sequence for the putative salivary-like lipocalin (contig 84287) identified exclusively in the Haller's organ spf transcriptome of unfed virgin adult male *D. variabilis* versus the top BLAST tick hit (lowest expected value; Table 1). Asterisks (*) denote conserved residues, colons (:) indicate conservation between groups of strongly similar properties scoring >0.5 in the Gonnet PAM 250 matrix, and periods (.) indicate conservation between groups of weakly similar properties scoring ≤0.5 on the Gonnet PAM 250 matrix. The acronym consists of the first letter of genus and species (*Amblyomma triste*, At) followed by the GenBank accession number for the protein BLAST hit (JAA54113.1) 139

Figure 2.S5. Multiple sequence alignment (Clustal Ω) of the deduced amino acid sequence for the putative G-protein coupled receptor (contig 72702) identified exclusively in the Haller's organ spf transcriptome of unfed virgin adult male *D. variabilis* versus the top BLAST tick hit (lowest expected value; Table 1). Asterisks (*) denote conserved residues, colons (:) indicate conservation between groups of strongly similar properties scoring >0.5 in the Gonnet PAM 250 matrix, and periods (.) indicate conservation between groups of weakly similar properties scoring ≤0.5 on the Gonnet PAM 250 matrix. The acronym consists of the first letter of genus and species (*Ixodes scapularis*, Is) followed by the GenBank accession number for the protein BLAST hit (EEC06829.1) 140

Figure 2.S6. Multiple sequence alignment (Clustal Ω) of the deduced amino acid sequence for the putative G-protein coupled receptor (contig 83622) identified exclusively in the Haller's organ spf transcriptome of unfed virgin adult male *D. variabilis* versus the top

BLAST tick hit (lowest expected value; Table 1). Asterisks (*) denote conserved residues, colons (:) indicate conservation between groups of strongly similar properties scoring >0.5 in the Gonnet PAM 250 matrix, and periods (.) indicate conservation between groups of weakly similar properties scoring ≤0.5 on the Gonnet PAM 250 matrix. The acronym consists of the first letter of genus and species (*Ixodes scapularis*, Is) followed by the GenBank accession number for the protein BLAST hit (EEC07880.1) 141

Figure 2.S7. Multiple sequence alignment (Clustal Ω) of the deduced amino acid sequence for the putative G-protein α_o subunit (contig 13937) identified exclusively in the Haller's organ spf spf transcriptome of unfed virgin adult male *D. variabilis* versus the top BLAST tick hit (lowest expected value; Table 1). Asterisks (*) denote conserved residues, colons (:) indicate conservation between groups of strongly similar properties scoring >0.5 in the Gonnet PAM 250 matrix, and periods (.) indicate conservation between groups of weakly similar properties scoring ≤0.5 on the Gonnet PAM 250 matrix. The black bar shows the Gα subunit domain. The acronym consists of the first letter of genus and species (*Rhipicephalus pulchellus*, Rp) followed by the GenBank accession number for the protein BLAST hit (JAA58325.1)..... 142

Figure 2.S8. Multiple sequence alignment (Clustal Ω) of the deduced amino acid sequence for the putative G-protein β subunit (contig 24477) identified exclusively in the Haller's organ spf transcriptome of unfed virgin adult male *D. variabilis* versus the top BLAST tick hit (lowest expected value; Table 1). Asterisks (*) denote conserved residues, colons (:) indicate conservation between groups of strongly similar properties scoring >0.5 in the Gonnet PAM 250 matrix, and periods (.) indicate conservation between groups of weakly similar properties scoring ≤0.5 on the Gonnet PAM 250 matrix. The black bar shows the WD Gβ repeat domain. The acronym consists of the first letter of genus and species (*Ixodes ricinus*, Ir) followed by the GenBank accession number for the protein BLAST hit (JAB79904.1)..... 143

Figure 2.S9. Multiple sequence alignment (Clustal Ω) of the deduced amino acid sequence for the putative adenylate/guanylate cyclase (contig 77721) identified exclusively in the Haller's organ spf transcriptome of unfed virgin adult male *D. variabilis* versus the top BLAST tick hit (lowest expected value; Table 1). Asterisks (*) denote conserved residues, colons (:) indicate conservation between groups of strongly similar properties scoring >0.5 in the Gonnet PAM 250 matrix, and periods (.) indicate conservation between groups of weakly similar properties scoring ≤0.5 on the Gonnet PAM 250 matrix. The acronym consists of the first letter of genus and species (*Ixodes scapularis*, Is) followed by the GenBank accession number for the protein BLAST hit (EEC01411.1) 144

Figure 2.S10. Multiple sequence alignment (Clustal Ω) of the deduced amino acid sequence for the putative adenylate/guanylate cyclase (contig 37845) identified exclusively in the Haller's organ spf transcriptome of unfed virgin adult male *D. variabilis* versus the top BLAST tick hit (lowest expected value; Table 1). Asterisks (*) denote conserved residues, colons (:) indicate conservation between groups of strongly similar properties scoring >0.5 in the Gonnet PAM 250 matrix, and periods (.) indicate conservation between groups of weakly

similar properties scoring ≤ 0.5 on the Gonnet PAM 250 matrix. The solid black bar shows the heme NO binding associated domain, and the dashed black bar shows the guanylate cyclase catalytic domain. The acronym consists of the first letter of genus and species (*Ixodes scapularis*, Is) followed by the GenBank accession number for the protein BLAST hit (EEC13610.1) 145

Figure 2.S11. Multiple sequence alignment (Clustal Ω) of the deduced amino acid sequence for the putative cyclic nucleotide-gated ion channel (contig 82720) identified exclusively in the Haller's organ spf transcriptome of unfed virgin adult male *D. variabilis* versus the top BLAST tick hit (lowest expected value; Table 1). Asterisks (*) denote conserved residues, colons (:) indicate conservation between groups of strongly similar properties scoring >0.5 in the Gonnet PAM 250 matrix, and periods (.) indicate conservation between groups of weakly similar properties scoring ≤ 0.5 on the Gonnet PAM 250 matrix. The black bar shows the cyclic nucleotide binding domain. The acronym consists of the first letter of genus and species (*Ixodes scapularis*, Is) followed by the GenBank accession number for the protein BLAST hit (EEC03664.1) 146

Figure 2.S12. Multiple sequence alignment (Clustal Ω) of the deduced amino acid sequence for the putative cyclic nucleotide-gated ion channel (CNG) α - subunit (contig 82720) identified exclusively in the Haller's organ spf transcriptome of unfed virgin adult male *D. variabilis* versus the *Caenorhabditis elegans* and *Drosophila melanogaster* CNG α - subunits (.Asterisks (*) denote conserved residues, colons (:) indicate conservation between groups of strongly similar properties scoring >0.5 in the Gonnet PAM 250 matrix, and periods (.) indicate conservation between groups of weakly similar properties scoring ≤ 0.5 on the Gonnet PAM 250 matrix. The black bar shows the cyclic nucleotide binding domain. The acronym consists of the first letter of genus and species (*Caenorhabditis elegans*, Ce; *Drosophila melanogaster*, Dm) followed by the protein name (CNG) 147

Figure 2.S13. Multiple sequence alignment (Clustal Ω) of the deduced amino acid sequence for the putative β -arrestin (contig 01853) identified exclusively in the Haller's organ spf transcriptome of unfed virgin adult male *D. variabilis* versus the top BLAST tick hit (lowest expected value; Table 2). Asterisks (*) denote conserved residues, colons (:) indicate conservation between groups of strongly similar properties scoring >0.5 in the Gonnet PAM 250 matrix, and periods (.) indicate conservation between groups of weakly similar properties scoring ≤ 0.5 on the Gonnet PAM 250 matrix. The solid black bar shows the arrestin amino terminal domain, and the dashed black bar shows the arrestin carboxyl terminal domain. The acronym consists of the first letter of genus and species (*Ixodes scapularis*, Is) followed by the GenBank accession number for the protein BLAST hit (EEC07926.1) 148

Figure 2.S14. Multiple sequence alignment (Clustal Ω) of the deduced amino acid sequence for the putative β -arrestin (BArr; contig 82720) identified exclusively in the Haller's organ spf transcriptome of unfed virgin adult male *D. variabilis* versus the *Caenorhabditis elegans* and *Drosophila melanogaster* β -arrestins (accession no. CCD67242.1 and AAF32365.1, respectively). Asterisks (*) denote conserved residues, colons (:) indicate conservation between groups of strongly similar properties scoring >0.5 in the Gonnet PAM 250 matrix,

and periods (.) indicate conservation between groups of weakly similar properties scoring ≤ 0.5 on the Gonnet PAM 250 matrix. The solid black bar shows the arrestin amino terminal domain, and the dashed black bar shows the arrestin carboxyl terminal domain. The acronym consists of the first letter of genus and species (*Caenorhabditis elegans*, Ce; *Drosophila melanogaster*, Dm) followed by the protein name (BArr) 149

Figure 2.S15. Multiple sequence alignment (Clustal Ω) of the deduced amino acid sequence for the putative cytochrome p450 (contig 69591) identified exclusively in the Haller's organ spf transcriptome of unfed virgin adult male *D. variabilis* versus the top BLAST tick hit (lowest expected value; Table 2). Asterisks (*) denote conserved residues, colons (:) indicate conservation between groups of strongly similar properties scoring >0.5 in the Gonnet PAM 250 matrix, and periods (.) indicate conservation between groups of weakly similar properties scoring ≤ 0.5 on the Gonnet PAM 250 matrix. The black bar shows the cytochrome p450 domain. The acronym consists of the first letter of genus and species (*Ixodes scapularis*, Is) followed by the GenBank accession number for the protein BLAST hit (EEC03681.1) 150

Figure 2.S16. Multiple sequence alignment (Clustal Ω) of the deduced amino acid sequence for the putative cytochrome p450 (contig 01691) identified exclusively in the Haller's organ spf transcriptome of unfed virgin adult male *D. variabilis* versus the top BLAST tick hit (lowest expected value; Table 2). Asterisks (*) denote conserved residues, colons (:) indicate conservation between groups of strongly similar properties scoring >0.5 in the Gonnet PAM 250 matrix, and periods (.) indicate conservation between groups of weakly similar properties scoring ≤ 0.5 on the Gonnet PAM 250 matrix. The black bar shows the cytochrome p450 domain. The acronym consists of the first letter of genus and species (*Rhipicephalus pulchellus*, Rp) followed by the GenBank accession number for the protein BLAST hit (JAA56317.1) 151

Figure 2.S17. Multiple sequence alignment (Clustal Ω) of the deduced amino acid sequence for the putative cytochrome p450 (contig 06898) identified exclusively in the Haller's organ spf transcriptome of unfed virgin adult male *D. variabilis* versus the top BLAST tick hit (lowest expected value; Table 2). Asterisks (*) denote conserved residues, colons (:) indicate conservation between groups of strongly similar properties scoring >0.5 in the Gonnet PAM 250 matrix, and periods (.) indicate conservation between groups of weakly similar properties scoring ≤ 0.5 on the Gonnet PAM 250 matrix. The black bar shows the cytochrome p450 domain. The acronym consists of the first letter of genus and species (*Ixodes scapularis*, Is) followed by the GenBank accession number for the protein BLAST hit (EEC19065.1) 152

Figure 2.S18. Multiple sequence alignment (Clustal Ω) of the deduced amino acid sequence for the putative cytochrome p450 (contig 14383) identified exclusively in the Haller's organ spf transcriptome of unfed virgin adult male *D. variabilis* versus the top BLAST tick hit (lowest expected value; Table 2). Asterisks (*) denote conserved residues, colons (:) indicate conservation between groups of strongly similar properties scoring >0.5 in the Gonnet PAM 250 matrix, and periods (.) indicate conservation between groups of weakly similar properties

scoring ≤ 0.5 on the Gonnet PAM 250 matrix. The black bar shows the cytochrome p450 domain. The acronym consists of the first letter of genus and species (*Amblyomma triste*, At) followed by the GenBank accession number for the protein BLAST hit (JAC34536.1)..... 153

Figure 2.S19. Multiple sequence alignment (Clustal Ω) of the deduced amino acid sequence for the putative glutathione S-transferase (contig 12057) identified exclusively in the Haller’s organ spf transcriptome of unfed virgin adult male *D. variabilis* versus the top BLAST tick hit (lowest expected value; Table 2). Asterisks (*) denote conserved residues, colons (:) indicate conservation between groups of strongly similar properties scoring >0.5 in the Gonnet PAM 250 matrix, and periods (.) indicate conservation between groups of weakly similar properties scoring ≤ 0.5 on the Gonnet PAM 250 matrix. The solid black bar shows the glutathione S-transferase amino terminal domain, and the dashed black bar shows the glutathione S-transferase carboxyl terminal domain. The acronym consists of the first letter of genus and species (*Amblyomma triste*, At) followed by the GenBank accession number for the protein BLAST hit (JAC32911.1)..... 154

Figure 2.S20. Multiple sequence alignment (Clustal Ω) of the deduced amino acid sequence for the putative glutathione S-transferase (contig 04931) identified exclusively in the Haller’s organ spf transcriptome of unfed virgin adult male *D. variabilis* versus the top BLAST tick hit (lowest expected value; Table 2). Asterisks (*) denote conserved residues, colons (:) indicate conservation between groups of strongly similar properties scoring >0.5 in the Gonnet PAM 250 matrix, and periods (.) indicate conservation between groups of weakly similar properties scoring ≤ 0.5 on the Gonnet PAM 250 matrix. The solid black bar shows the glutathione S-transferase amino terminal domain, and the dashed black bar shows the glutathione S-transferase carboxyl terminal domain. The acronym consists of the first letter of genus and species (*Amblyomma triste*, At) followed by the GenBank accession number for the protein BLAST hit (JAC32978.1)..... 155

Figure 2.S21. Multiple sequence alignment (Clustal Ω) of the deduced amino acid sequence for the putative superoxide dismutase (contig 83534) identified exclusively in the Haller’s organ spf transcriptome of unfed virgin adult male *D. variabilis* versus the top BLAST tick hit (lowest expected value; Table 2). Asterisks (*) denote conserved residues, colons (:) indicate conservation between groups of strongly similar properties scoring >0.5 in the Gonnet PAM 250 matrix, and periods (.) indicate conservation between groups of weakly similar properties scoring ≤ 0.5 on the Gonnet PAM 250 matrix. The black bar shows the copper/zinc superoxide dismutase domain. The acronym consists of the first letter of genus and species (*Rhipicephalus pulchellus*, Rp) followed by the GenBank accession number for the protein BLAST hit (JAA58838.1)..... 156

Figure 3.1 The 4-port olfactometer used to examine possible volatile secretions produced by *I. scapularis* unfed virgin adult females that would be attractive to unfed virgin adult males. A vacuum hose attached to the bottom of the central arena of the olfactometer creates a unidirectional airflow from each glass bulb toward the center of the apparatus 187

Figure 3.2 (a) Petri dish assays used to examine *I. scapularis* mounting behavior between free roaming unfed virgin adult males and unfed virgin adult females. This experiment was also used to examine the affects of detergent washing and blood feeding on female attraction, and impacts on chelicerae insertion/maintenance behavior in unfed virgin adult males. This Petri dish assay was used to examine chelicerae insertion/maintenance behavior of unfed virgin adult males with 1) detergent washed unfed virgin adult females, 2) unfed virgin adult females, 3) part-fed virgin adult females and 4) replete mated adult females. (b) Petri dish assays used to examine *I. scapularis* mounting behavior between free roaming unfed virgin adult males and unfed virgin adult females secluded inside a mesh to prevent direct contact between the sexes..... 188

Figure 3.3 Mean percentage (± 1 SEM) of *I. scapularis* unfed virgin adult males attracted to odors produced by unfed virgin adult females in olfactometer assays (Fig.3. 1). Attraction is defined as males found between the females and point of choice (Fig. 3.1) 24h after release in the center of the apparatus. Unresponsive males did not leave the central area of the apparatus. Treatments were compared using a paired Student's *t*-test (* = $P < 0.05$)..... 189

Figure 3.4 Mean percentage mounting (± 1 SEM) of *I. scapularis* unfed virgin adult males with free roaming unfed virgin adult females, and with unfed virgin adult females enclosed in mesh bags in Petri dish bioassays (Fig. 3.2a and 3.2b). Attraction is defined as males mounting females and orienting towards the female genital pore. Arrows denote zero values. Treatments were compared using a 2-way ANOVA and a Sidak's multiple comparisons test at each time point (* = $P < 0.05$) 190

Figure 3.5 Mean percentage chelicerae insertion/maintenance (± 1 SEM) of *I. scapularis* unfed virgin adult males with unfed virgin adult females following female whole body washing with distilled water or with 1% Triton-X 100 detergent in Petri dish bioassays (Fig. 3.2a). Treatments were compared using a 2-way ANOVA and a Sidak's multiple comparison test at each time point (* = $P < 0.05$)..... 191

Figure 3.6 Mean percentage chelicerae insertion/maintenance of *I. scapularis* unfed virgin adult males with unfed virgin adult females, part-fed virgin adult females, and replete mated adult females in Petri dish assays (Fig. 3.2a). Arrows denote zero values. Treatments were compared using a 2-way ANOVA and a Tukey's multiple comparison test for each time point. Treatments with the same letter at each time point are not statistically significant ($P < 0.05$)..... 192

Figure 3.7 Example of a GC-MS chromatogram of a whole body surface hexane extraction of 10 unfed virgin adult female *I. scapularis* ticks. The compounds identified with $\geq 80\%$ match probability are numbered and further described in Table 3.1 and Fig. 3.9. Missing numbers represent compounds not identified in females. Abundances were determined using flame ionization detection. Time = min..... 193

Figure 3.8 Example of a GC-MS chromatogram of a whole body surface hexane extraction of 10 unfed virgin adult male *I. scapularis* ticks. The compounds identified with $\geq 80\%$ match

probability are numbered and further described in Table 3.1 and Fig. 3.9. Missing numbers represent compounds not identified in males. Abundances were determined using flame ionization detection. Time = min 194

Figure 3.9 Mean percent abundance (± 1 SEM) of compounds identified (Table 3.1) in whole body hexane extractions of *I. scapularis* unfed virgin adult females versus unfed virgin males. Mean abundance for a compound was calculated by averaging the peak areas identified in all 5 female and 6 male replicate GC-MS runs. Percentages were calculated out of the total abundance obtained for all 18 compounds identified. Arrows denote zero values. Treatments were compared using a paired student's *t*-test (* = $P < 0.05$). Numbers in parenthesis correlate to assigned numbers in Table 1 and peak numbers in Fig. 3.7 and Fig. 3.8 195

Figure 3.S1 Example of the GC-MS mass spectral data obtained for 1-heptene identified in whole body hexane extractions of *I. scapularis* unfed virgin adult females (Table 3.1 and Fig. 3.9). *M/Z* = mass to charge ratio for each ion. Abundance = the intensity or abundance of each ion. 196

Figure 3.S2 Example of the GC-MS mass spectral data obtained for 1,2,3-trimethylbenzene identified in whole body hexane extractions of *I. scapularis* unfed virgin adult females and males (Table 3.1 and Fig. 3.9). *M/Z* = mass to charge ratio for each ion. Abundance = the intensity or abundance of each ion..... 197

Figure 3.S3 Example of the GC-MS mass spectral data obtained for 1-heptanol identified in whole body hexane extractions of *I. scapularis* unfed virgin adult females (Table 3.1 and Fig. 3.9). *M/Z* = mass to charge ratio for each ion. Abundance = the intensity or abundance of each ion. 198

Figure 3.S4 Example of the GC-MS mass spectral data obtained for dodecane identified in whole body hexane extractions of *I. scapularis* unfed virgin adult females and males (Table 3.1 and Fig. 3.9). *M/Z* = mass to charge ratio for each ion. Abundance = the intensity or abundance of each ion..... 199

Figure 3.S5 Example of the GC-MS mass spectral data obtained for thymol identified in whole body hexane extractions of *I. scapularis* unfed virgin adult males (Table 3.1 and Fig. 3.9). *M/Z* = mass to charge ratio for each ion. Abundance = the intensity or abundance of each ion.. *M/Z* = mass to charge ratio for each ion. Abundance = the intensity or abundance of each ion. 200

Figure 3.S6 Example of the GC-MS mass spectral data obtained for butyl benzoate identified in whole body hexane extractions of *I. scapularis* unfed virgin adult females and males (Table 3.1 and Fig. 3.9). *M/Z* = mass to charge ratio for each ion. Abundance = the intensity or abundance of each ion. 201

Figure 3.S7 Example of the GC-MS mass spectral data obtained for tetradecane identified in whole body hexane extractions of <i>I. scapularis</i> unfed virgin adult females (Table 3.1 and Fig. 3.9). M/Z = mass to charge ratio for each ion. Abundance = the intensity or abundance of each ion.....	202
Figure 3.S8 Example of the GC-MS mass spectral data obtained for pentadecane identified in whole body hexane extractions of <i>I. scapularis</i> unfed virgin adult females and males (Table 3.1 and Fig. 3.9). M/Z = mass to charge ratio for each ion. Abundance = the intensity or abundance of each ion	203
Figure 3.S9 Example of the GC-MS mass spectral data obtained for hexadecane identified in whole body hexane extractions of <i>I. scapularis</i> unfed virgin adult males (Table 3.1 and Fig. 3.9). M/Z = mass to charge ratio for each ion. Abundance = the intensity or abundance of each ion.	204
Figure 3.S10 Example of the GC-MS mass spectral data obtained for heptadecane identified in whole body hexane extractions of <i>I. scapularis</i> unfed virgin adult females and males (Table 3.1 and Fig. 3.9). M/Z = mass to charge ratio for each ion. Abundance = the intensity or abundance of each ion.	205
Figure 3.S11 Example of the GC-MS mass spectral data obtained for ethyl-4-ethoxybenzoate identified in whole body hexane extractions of <i>I. scapularis</i> unfed virgin adult females and males (Table 3.1 and Fig. 3.9). M/Z = mass to charge ratio for each ion. Abundance = the intensity or abundance of each ion.....	206
Figure 3.S12 Example of the GC-MS mass spectral data obtained for 5 β -androstane identified in whole body hexane extractions of <i>I. scapularis</i> unfed virgin adult females and males (Table 3.1 and Fig. 3.9). M/Z = mass to charge ratio for each ion. Abundance = the intensity or abundance of each ion.....	207
Figure 3.S13 Example of the GC-MS mass spectral data obtained for octadecane identified in whole body hexane extractions of <i>I. scapularis</i> unfed virgin adult females and males (Table 3.1 and Fig. 3.9). M/Z = mass to charge ratio for each ion. Abundance = the intensity or abundance of each ion.	208
Figure 3.S14 Example of the GC-MS mass spectral data obtained for phytol identified in whole body hexane extractions of <i>I. scapularis</i> unfed virgin adult females and males (Table 3.1 and Fig. 3.9). M/Z = mass to charge ratio for each ion. Abundance = the intensity or abundance of each ion.....	209
Figure 3.S15 Example of the GC-MS mass spectral data obtained for butyl palmitate identified in whole body hexane extractions of <i>I. scapularis scapularis</i> unfed virgin adult females and males (Table 1 and Fig. 9). M/Z = mass to charge ratio for each ion. Abundance = the intensity or abundance of each ion.	210

Figure 3.S16 Example of the GC-MS mass spectral data obtained for 1-hexadecanol identified in whole body hexane extractions of *I. scapularis scapularis* unfed virgin adult females and males (Table 3.1 and Fig. 3.9). M/Z = mass to charge ratio for each ion. Abundance = the intensity or abundance of each ion. 211

Figure 3.S17 Example of the GC-MS mass spectral data obtained for butyl stearate identified in whole body hexane extractions of *I. scapularis scapularis* unfed virgin adult females and males (Table 3.1 and Fig. 3.9). M/Z = mass to charge ratio for each ion. Abundance = the intensity or abundance of each ion..... 212

Figure 3.S18 Example of the GC-MS mass spectral data obtained for erucylamide identified in whole body hexane extractions of *I. scapularis scapularis* unfed virgin adult females and males (Table 3.1 and Fig. 3.9). M/Z = mass to charge ratio for each ion. Abundance = the intensity or abundance of each ion..... 213

Figure A.1. Multiple sequence alignment (Clustal Ω) of the deduced amino acid sequence for the putative ionotropic glutamate receptor (contig 5494) identified exclusively in the Haller's organ transcriptome of unfed virgin adult male *D. variabilis* versus the top BLAST tick hit (lowest e-value). Asterisks (*) denote conserved residues, colons (:) indicate conservation between groups of strongly similar properties scoring >0.5 in the Gonnet PAM 250 matrix, and periods (.) indicate conservation between groups of weakly similar properties scoring ≤ 0.5 on the Gonnet PAM 250 matrix. The acronym consists of the first letter of genus and species (*Rhipicephalus pulchellus*, Rp) followed by the GenBank accession number for the protein BLAST hit (JAA54415.1)..... 222

Figure A.2. Multiple sequence alignment (Clustal Ω) of the deduced amino acid sequence for the putative ionotropic glutamate receptor (contig 9210) identified exclusively in the Haller's organ transcriptome of unfed virgin adult male *D. variabilis* versus the top BLAST tick hit (lowest e-value). Asterisks (*) denote conserved residues, colons (:) indicate conservation between groups of strongly similar properties scoring >0.5 in the Gonnet PAM 250 matrix, and periods (.) indicate conservation between groups of weakly similar properties scoring ≤ 0.5 on the Gonnet PAM 250 matrix. The acronym consists of the first letter of genus and species (*Rhipicephalus pulchellus*, Rp) followed by the GenBank accession number for the protein BLAST hit (JAA64048.1)..... 223

Figure A.3. Phylogenetic relationship of transcripts putatively encoding ionotropic glutamate receptors (iGluRs) identified in the Haller's organ (contig 5494 and 9210) transcriptome of unfed virgin adult male *D. variabilis* with iGluRs of known clade annotation from *Ixodes scapularis*, *I. ricinus*, *Metaseiulus occidentalis*, and *Rhipicephalus pulchellus*. The phylogenetic tree shows three clades, each represented by a different branch color as follows: blue = kainate clade; red = α -amino-3-hydroxy-5-methyl-4-isoxazolepropionic acid (AMPA) clade; green = N-methyl-D-aspartate (NMDA) clade. Acronyms consist of the first letter of the genus and species (*Ixodes scapularis*, Is; *I. ricinus*, Ir; *Metaseiulus occidentalis*, Mo; *Rhipicephalus pulchellus*, Rp) followed by the associated clade. Putative iGluRs transcripts are boxed. The tree was constructed using Maximum likelihood phylogenetic analysis and

bootstrapping set to 500 iterations. Branch values listed are bootstrap percentages (percent confidence), scale set to 20%. The *R. pulchellus* genome orthologs (Table A.1) were included in phylogenetic analyses to ensure the short sequence lengths of the contigs were not resulting in false tree delineation (Acronym Rp followed by GenBank accession no.). A comprehensive list of acronyms and associated Genbank accession numbers are listed in Table A.3..... 224

Figure A.4. Phylogenetic relationship of transcripts putatively encoding ionotropic glutamate receptors (iGluRs) identified in the Haller’s organ (contig 5494 and 9210) transcriptome of unfed virgin adult male *D. variabilis* with iGluRs of known clade annotation from *Caenorhabditis elegans*, *Caligus rogercresseyi*, *Daphnia pulex*, *Drosophila melanogaster*, *Ixodes scapularis*, *I. ricinus*, *Metaseiulus occidentalis*, and *Rhipicephalus pulchellus*. The phylogenetic tree shows four clades, each represented by a different branch color as follows: purple = kainate clade; green = α -amino-3-hydroxy-5-methyl-4-isoxazolepropionic acid (AMPA); red = novel ionotropic receptor (IR) clade that contains the IR co-receptor 25a; blue = N-methyl-D-aspartate (NMDA) clade. Arrows show clustering of kainate-2 like iGluRs. Acronyms consist of the first letter of the genus and species (*Caenorhabditis elegans*, Ce; *Caligus rogercresseyi*, Cr; *Daphnia pulex*, Dp; *Drosophila melanogaster*, Dm; *Ixodes scapularis*, Is; *I. ricinus*, Ir; *Metaseiulus occidentalis*, Mo; *Rhipicephalus pulchellus*, Rp). The tree was constructed using Maximum likelihood phylogenetic analysis and bootstrapping set to 500 iterations. Branch values listed are bootstrap percentages (percent confidence), scale set to 20%. The *R. pulchellus* genome orthologs (Table A.1) were included in phylogenetic analyses to ensure the short sequence lengths of the contigs were not resulting in false tree delineation (Acronym Rp followed by GenBank accession no.). A comprehensive list of acronyms and associated Genbank accession numbers are listed in Table A.3..... 225

Figure B.1. The Haller’s organ located on the foretarsus of the first pair of legs of the American dog tick, *Dermacentor variabilis* and its two structural components the anterior pit (boxed) and the posterior capsule (circled) 231

Figure B.2. Schematic of the piezoelectric dental ultrasonic scaler modified for use as the cutting device to remove the cuticle covering of the Haller’s organ posterior capsule (UDS-J; Guilin Woodpecker Medical Instrument Co., Guangxi, China)..... 232

Figure B.3. Schematic representation of the electropolishing set-up used to sharpen the stainless steel scaler tip. The electrolyte solution was 2M NaOH and the voltage through the circuit was maintained between 3 and 7 volts 233

Figure B.4. Schematic representation of the micro-dissection system used to remove the cuticle covering of the posterior capsule of the Haller’s organ. The vibration frequency of the dental piezoelectric ultrasonic scaler was set to 13.2-16.6kHz and the voltage 4.18-5.40V 2

Acarine Attractants: Chemistry, Chemoreception, Bioassay and Control

This chapter was formatted for submission to the *Journal of Pesticide Biochemistry and Physiology* with the coauthor Dr. R. Michael Roe¹.

¹Department of Entomology, North Carolina State University, Raleigh, NC 27695-7613

Abstract

The Acari are of significant economic importance in crop production and human and animal health. Acaricides are essential for the control of these pests, but at the same time, the number of available pesticides is limited, especially for applications in animal production. The Acari consist of two major groups, the mites that demonstrate a wide variety of life strategies, i.e., herbivory, predation and ectoparasitism, and ticks which have evolved obligatory hematophagy. The major sites of chemoreception in the acarines are the chelicerae, palps and tarsi on the forelegs. A unifying name, the “foretarsal sensory organ” (FSO), is proposed for the first time in this review for the sensory site on the forelegs of all acarines. The FSO has multiple sensory functions including olfaction, gustation, and heat detection. Preliminary transcriptomic data in ticks suggest chemoreception in the FSO is achieved by a different mechanism from insects. There are a variety of laboratory and field bioassay methods that have been developed for the identification and characterization of attractants but minimal techniques for electrophysiology studies. Over the past three to four decades’ significant progress has been made in the chemistry and analysis of function for acarine attractants in mites and ticks. In mites, attractants include aggregation, immature female, female sex and alarm pheromones; in ticks, the attraction-aggregation-attachment, assembly and sex pheromones; in mites and ticks host kairomones and plant allomones; and in mites, fungal allomones. There are still large gaps in our knowledge of chemical communication in the acarines compared to insects, especially relative to acarine pheromones, and more so for mites than ticks. However, the use of lure-and-kill and lure-enhanced biocontrol strategies have been investigated for tick and mite control, respectively, with significant environmental advantages which warrant further study.

Introduction

Mites and ticks are two different but evolutionary related groups of arthropods found in the subphylum Chelicerata, in the class Arachnida and in the subclass Acari. The feeding habits are quite different between mites and ticks. Mites exhibit diverse feeding behaviors as herbivores, predators, and blood and keratin feeding parasites. In contrast, ticks are obligatory blood feeders on humans and animals. Mites and ticks are also of significant economic and health importance. For example, herbivorous mites can cause plant damage resulting in decreased crop production [1]. In contrast, predatory mites can be used as biocontrol agents in crop production to control herbivorous mites while parasitic mites and ticks cause painful skin irritations producing stress and reducing meat, milk, wool, and leather production. They also vector pathogens of importance to plants, insects, humans, and animals [2]. Ticks for example vector the microbial agents of more animal diseases than any other arthropod [3]. The acarines are of special significance because of their significant economic, nuisance, and health impacts; their ancient origin, which goes back to the Devonian period; the unique biology and diversity of mites versus ticks; and the importance of their control as pests [2,3]. Also the Acari in general are an understudied taxon within the Arthropoda especially compared to insects.

The acarines have a unique chemosensory system. Mites and ticks have four pairs of walking legs. The first pair of these legs is used in chemoreception in many ways like the insect antennae (acarines lack antennae). The foretarsal sensory organ, most commonly called the Haller's organ in ticks, is located on the foretarsi of the first pair of legs in mites and ticks. At the gross anatomical level, and based on origin, this organ has little similarity to the insect antennae and is unique to the acarines. Foretarsal organs are involved in the

detection of food, pheromones, aggregation chemicals, host kairomones, plant allomones, fungal allomones, and arthropod repellents [4-9]. Despite the importance of attractants in development, reproduction, and the ecology of mites and ticks, little is understood about the types of chemicals recognized, mechanism for chemoreception, and the relative importance of the Haller's organ and its similarity of function versus other chemosensory organs like the chelicerae and palps of acarines.

Unfortunately, the mostly medical versus agricultural significance of ticks versus mites, respectively; the lack of synergistic research efforts between these two taxonomic groups; gaps in data collection; conflicting results; and overlapping-repetitive studies have limited research progress in chemical communication in the acarines as a whole and the use of this information in control. This has been further exacerbated by the challenges associated with acarine morphology and biology (segmental reductions and difficulty of rearing), and the much smaller size of mites versus that of ticks. A review of chemical communication for the acarines as a whole should be valuable to future research, and the use of this knowledge to develop control solutions. Comprehensive reviews already exist on tick pheromones and chemical communication [7,9] and on tick repellents [10,11]. There also are reviews on mite pheromones [12], on control of insects and mites in certain crops and produce [13-15], and control of individual mite species [16-19]. This is the first review of their chemosensory systems, bioassay methods, chemistry, chemical ecology, and control.

Chemosensory Structure and Function

Any use of chemical attractants for control will depend on chemical detection. An understanding of chemosensory structures and mechanisms of chemosensation is a critical aspect for pesticide development.

Mite Sensory Structures

Chemosensory stimuli are detected in mites by receptors located on the palps and the foretarsi of the first pair of legs. Chemoreceptors on the palps are localized to the palpal organ (Fig. 1.1). The mite palpal organ is located on the tip of each palp, consisting of 10-30 sensilla innervated by 6-7 bipolar sensory neurons. The sensory sensilla represent five morphological types of basiconic sensilla: single walled multipore sensilla with the pore configuration in longitudinal grooves (olfactory receptors), double walled pore sensilla (contact chemo-mechanoreceptors), two types of double walled pore sensilla with distinct internal radial spoke structures (chemo-thermoreceptors), and fine apical processes and cones without pores (cold and humidity receptors) [6]. Similar morphological types of sensilla are found in tick chemosensory structures also located on the palps and the foretarsi of the first pair of legs [4,6]. The structure and organization of the palpal organ in mites remains somewhat uniform across mite families, with the exception of endoparasitic mites in the family *Rhinonyssidae*. Most endoparasitic mites do not actively host seek but are transferred from one host to another through close, direct contact. The loss of host seeking behavior is reflected in the structure and organization of the palpal organ with a reduction in both sensilla number and diversity of morphological sensilla types. This reduction in

chemosensory structures is a common adaptation observed in species that transition from ectoparasites to endoparasites [20].

The mite tarsal complex (Fig. 1.2) is a localization of chemoreceptors on the foretarsi of the first pair of legs, and is homologous to the Haller's organ found in ticks. The tarsal complex consists of 9-28 sensilla innervated by 6-15 bipolar sensory neurons [6]. These sensilla represent similar morphological types to those found in the palpal organ [21]. Topography of the tarsal complex, the number of sensilla, and morphological types are dependent on the phylogenetic history of the mite and degree of specialization [22]. Endoparasitic mites also exhibit reductions of the tarsal complex similar to those observed in the palpal organ [20].

Information describing the mite palpal organ and tarsal complex is limited and primarily consists of morphological descriptions of sensilla structure and organization. This is primarily due to the difficulties associated with the minute size of mites. The apparent similarities in location and gross structure between mite and tick chemosensory systems suggest that ticks could be an ideal model for functional and mechanistic studies of chemoreception which just are not possible with mites because of their small size. Drawing comparisons between mites and ticks could help relate structure to function; so far, there has been minimal comparative work, especially at the molecular level and in understanding detailed functions.

Tick Sensory Structures

Chemosensation in ticks is mainly ascribed to the Haller's organ (Fig. 1.3). The Haller's organ is a localization of chemoreceptors on the foretarsi of the first pair of legs [23]. Similar

to mites, ticks also have chemoreceptors present on their palps (Fig. 1.4), which are not well characterized. Research on chemosensation in ticks has primarily focused on determining the structure and function of the Haller's organ. The Haller's organ consists of two main parts, the posterior capsule and the anterior pit. The anterior pit contains 6-7 sensilla innervated by 2-9 bipolar sensory neurons. The posterior capsule contains 4-13 sensilla, each innervated by 4-5 bipolar sensory neurons. In addition to the sensilla, there are other pleomorph structures present in both the anterior pit and posterior capsule [4]. In ixodid ticks, 13 different structural types of sensilla have been identified with 11 of these 13 also found in argasid ticks [24]. These sensilla represent four morphological types of basiconic sensilla, similar to those described in mites: single walled multipore sensilla with evenly distributed plugged pores (olfactory receptors), double walled pore sensilla with longitudinal grooves (contact chemo-mechanoreceptors), double walled pore sensilla with internal cutical spoke wheel arrangements (chemo-thermoreceptors), and apical processes without pores (hypothesized to function as cold and humidity receptors) [25,26].

The structure and organization of the Haller's organ is diverse across ixodid and argasid genera, though there is uniformity among species of the same genus. The Haller's organ also consistently contains a combination of chemoreceptors, chemo-mechanoreceptors, and presumed chemo-thermoreceptors. The unique placement of these structures on the tarsi of the first pair of legs may advantageously allow for the coordination of chemo-, mechano-, and thermoreception. Of the chemoreceptors present in the Haller's organ, very few are specialized, which suggests that the detection of varying compositions and concentrations of compounds induce tick host seeking and mating behavior [26,27]. The ratio of signals from more generalized sensilla may provide the tick with a systematic method of host

identification and pheromone recognition [28]. Coordinating signals from chemo-, mechano-, and thermoreceptors may increase the accuracy of host detection and location as well as courtship and mating. Since mites have similar numbers and morphological types of sensilla present in the tarsal complex and palpal organ, it can be hypothesized that mites also rely on a similar coordination of sensory signals for locating food sources, mating, and other activities.

Since the Haller's organ is only found in ticks, with homologous organs present in mites (most commonly called the tarsal complex), the distinct combination of different sensory receptors and the mechanisms of sensory detection of the acarines may not be present in other organisms, and may be especially different from that of well-studied insects. Comparative morphological data of sensillar organization in acarines and lower arthropods suggests that all types of chemosensory sensilla have evolved from a common multifunctional presensillum [29]. With clear similarities in the morphological types of sensilla between ticks and mites, it is likely that both groups have evolved chemosensory sensilla from the same presensillum. The general reference to the Haller's organ on the front legs of ticks versus that of the tarsal complex for mites unfortunately is misleading, suggesting differences in origin and function, when most likely this is not the case. We are recommending a unifying name for the acarines, which also denotes function for both mites and ticks, i.e., the foretarsal sensory organ (FSO).

Mechanism of Chemosensation

Acarines use chemosensory sensilla present on their palps and tarsi to identify olfactory and gustatory chemicals in the environment. Olfactory sensilla detect volatilized chemicals while gustatory sensilla detect chemicals through direct contact [20,27]. The presence of both

receptor types in acarine chemosensory structures makes the differentiation between spatial and direct contact chemical responses very difficult. It is also hypothesized that the molecular mechanism involved in the binding of chemical molecules and neuron depolarization in olfactory and gustatory receptor cells share a similar signal cascade mechanism, though the exact proteins involved are still unknown [Carr, Sonenshine and Roe, unpublished].

Current research investigating these olfactory and gustatory mechanisms is primarily focused on ticks. The published mite genome is the only data currently available that could potentially provide information about chemosensation mechanisms in mites, but presently no chemosensory proteins have been identified [30]. For ticks, multiple transcriptome data sets have been generated, specifically for the Haller's organ in our laboratory. The analysis of this transcriptome data is still in process but already has resulted in the identification of probable olfactory and gustatory messages (Fig. 1.5). Transcriptomes of the Haller's organ from males of the American dog tick, *Dermacentor variabilis*, have identified specific G protein-coupled receptors (GPCRs) found in the front legs, but absent from the hind legs, which likely are acting as olfactory and gustatory receptors. We have also identified from this same work multiple messages involved in the GPCR signal cascade mechanism and enzymes involved in the degradation of chemical molecules in the sensillar lymph described for other organisms [31,32], including cytochrome P450, glutathione S-transferase, protein kinase C, and serine threonine kinase [Carr, Sonenshine and Roe, unpublished]. It is thought that the degradation enzymes may help prevent overstimulation of chemoreceptors, which could potentially lead to receptor cell death. Degradation enzymes break down odor molecules into alternative structures that no longer bind to chemoreceptors and/or can be easily removed from the sensillar lymph [32]. Despite finding multiple messages involved in sensory signal initiation,

regulation, and cytoprotection, none of the specialized odorant binding proteins found in insects have been identified in ticks [Carr, Sonenshine and Roe, unpublished]. One possible explanation is that ticks are using lipocalins to transport chemicals from the sensillar lymph to GPCRs instead of specialized odorant binding proteins. Lipocalins may give ticks the ability to respond to a variety of chemicals in a single sensillum at one time. Additional research is needed to confirm the GPCR signal cascade mechanism as the chemosensory mechanism in the Haller's organ of ticks. Since palps also contain known chemoreceptors, similar research will be needed to understand their function at the molecular level. At the same time, comparative work is needed with the mite genome to determine if the mechanism of chemoreception is a common feature for the acarines. Understanding chemosensory systems at the molecular level can be useful in the reverse engineering or screening of novel chemical attractants.

Bioassay Methods for Acarine Attractants

Laboratory Bioassays

Laboratory bioassays are the first experiments needed for attractant identification and to assess their importance in acarine biology or to determine their utility for pest control.

Bioassays also are an easy, fast, and inexpensive approach for screening chemical libraries for attractants and evaluating different formulations. Bioassays for testing acarine attractants are basically repellency bioassays (recently reviewed for ticks by Bissinger and Roe [10,11] but in reverse. When provided with the opportunity to choose between a test compound and a control substrate, movement towards the test compound is indicative of an attractive

behavioral response [33]. On the other hand, repellency assays describe repellent behavioral responses as movements away from test compounds.

There are two primary types of laboratory bioassays used for testing attractants, the Petri dish design and olfactometer methods. The Petri dish assay uses treated filter paper to expose mites and ticks to test chemicals versus an appropriate control in an enclosed petri dish [34]. Two pieces of filter paper, one treated with a test chemical and the second a control, are placed along the bottom of a Petri dish. When test subjects are introduced into the Petri dish, pausing or arrestment of subjects on the treated surface would be indicative of an attractive behavioral response. Subjects arresting on the control surface would indicate that there was no attraction to the test chemical [35]. Comparing the number of mites or ticks on the treated surface versus the control can easily determine if a test chemical is an attractant and can be used as a measure of the effectiveness of the attractant. Additionally, conducting assays at different times after the application of the attractant can provide information on treatment persistence. The Petri dish design requires minimal supplies and space for execution, and is an effective method for identifying chemical attractants. The main disadvantages of this design are due to the fact that test subjects come in direct contact with chemically treated surfaces. Because ticks and mites crawl across treated filter paper, this design is incapable of differentiating between attraction to olfactory stimuli from contact or gustatory stimuli. Additionally, this design cannot differentiate between chemicals that are toxicants and those that are simply not attractive. If test chemicals are toxic, mites and ticks may perish after contact and remain on the treated surface for the duration of the experiment. Since attractive behavioral responses are determined by observing the location of test

subjects, a test compound may falsely present as an attractant. Due to these limitations, the Petri dish design is best suited for rapid screening of test chemicals.

Chemicals identified as attractants using the Petri dish design should be further evaluated using olfactometers. The main advantage of an olfactometer is that mites and ticks do not come in direct contact with chemically treated surfaces and gustatory responses are excluded by this method. Olfactometers use airflow to expose subjects to test chemicals carried typically as a vapor in the air, making them capable of identifying only compounds detected by olfaction [36].

There are multiple designs of olfactometer instruments available for screening acarine attractants, though the most widely used is the Y-tube or two-way olfactometer. As illustrated in Fig. 1.6, the Y-tube is a glass tube that bifurcates into two distinct arms. Removable glass bulbs that fit onto the ends of each arm provide a location for the placement of a test chemical, on one arm, and the appropriate control on the other. Independent air input into each glass bulb carries the test and control odors into each arm, respectively, and then into the common adjoining tube where the air streams become mixed. A vacuum attached to the end of the common adjoining tube ensures unidirectional airflow. When test subjects are introduced into the common adjoining tube distal to the bifurcation, based on attraction to the test compound, they move to its source, entering into the arm associated with the test compound. Test subjects that remain in the common tube, or crawl into the arm associated with the control would indicate that there was no attraction to odors of the test chemical [37]. Documenting the location of mites and ticks in the Y-tube at the end of a timed interval determines if a test chemical is an olfactory attractant.

One modification of the Y-tube design is the addition of two extra arms, with associated glass bulbs, creating a 4-way olfactometer (Fig. 1.7). The 4-way olfactometer functions similarly to the Y-tube except that the four arms are all attached to a common central chamber rather than an adjoining tube. The common chamber is also the location for the attachment of the vacuum. An added advantage of the 4-way olfactometer is that mites and ticks can be exposed to more than one test odor during a single experiment. Comparing multiple chemicals in one trial can determine if there is a preference for one chemical over another. The 4-way olfactometer can help identify the most attractive chemical to ticks or mites from a group of acarine attractants.

The cost for running olfactometer experiments is higher than that for Petri dish assays, and requires either the purchase or construction of the olfactometer instrument. Additionally, olfactometer methods are more time consuming than the Petri dish design. The number of assays is limited by the number of olfactometer instruments available, and the instruments need to be cleaned between experiments while the Petri dish method using plastic plates is unlimited and disposable.

Other factors to consider in laboratory bioassays include selection of species, life stage, and the formulation and delivery method for test chemicals. Unfortunately, these variables make it difficult to draw conclusions from one study to the next, and more highly controlled research is needed for the identification and characterization of common attractants among the acarines.

Electrophysiological Assays

Electrophysiological assays can provide information on specific chemosensory cell functions, and also potentially be used to detect and screen compounds of chemosensory activity.

Electrodes inserted into chemoreceptors record action potentials produced when chemical molecules trigger receptor cell depolarization. Electrodes can be placed in areas to record multicellular function or attached to an individual sensillum for more specific recordings.

This can be done utilizing either tungsten electrodes inserted into the sensillum or with glass electrodes placed over the tip of a spliced sensillum. Electrophysiology recordings can identify specific regions and potentially specific cells involved in the detection of attractants of varying types, as well as exposure to other stimulants, e.g., heat, humidity, and mechanical.

Unfortunately, electrophysiological assays have only been conducted in ticks and, even so problems with sensilla visualization have restricted most electrophysiological work to the anterior pit of the Haller's organ [38]. The strength and thickness of the cuticle covering the posterior capsule makes it difficult to cut away and gain visualization of the sensilla inside. Additionally, the nerve bundles originating from the anterior pit and posterior capsule are in close proximity to each other, so visualization of electrode placement is important to differentiate recordings from these two structures. Visualization of electrode placement is also needed to differentiate recordings obtained from chemosensory cells versus muscle cells. Steullet and Guerin [39,40] performed recordings in the capsule of the Haller's organ. Steullet and Guerin [40] created a hand-drawn diagram of the posterior capsule, dividing the capsule surface into numbered regions and arbitrarily inserting electrodes into each region until recordings could be obtained. The electrodes were placed without good

visualization of the sensilla and at unknown depths. Using these methods, it is unclear if the recordings obtained are from the posterior capsule or if they inadvertently were recording from the anterior pit or even from muscle. These difficulties associated with targeted electrode placement have limited the amount and value that comes from electrophysiology studies in ticks. To date, only a few published experiments have been conducted on ticks, and no work currently is available on mites. Future research is needed to develop better micro-dissecting tools, microscopy, and procedures for accurate visualization of the chemosensory sensilla and for better electrode placement. Additionally, more research is needed documenting the location of neurons within the tarsi, metatarsi, and tibia of the front pair of legs to aid in the discrimination between recordings from the anterior pit, posterior capsule, and muscle, and overall to obtain a better understanding of the function of the FSO in general.

Field Bioassays

Field bioassays are critical for the evaluation of any final proof of concept for acarine attraction, especially associated with their practical use in control (discussed in more detail later). Since field bioassays are time consuming, labor intensive, and the results can be highly variable, they are typically conducted after laboratory bioassays. The ideal would be to have a laboratory assay system that would be a certain mimic of uses in the field. Bissinger et al. [41] for example, found an excellent correlation between tick Petri dish repellency assays and human subject tests in the field for two commercial products, DEET and BioUD. They concluded, at least for these two products that the laboratory assay was an acceptable predictor of their practical use in the field. However, it is difficult to argue, especially for

new chemistries, that field studies simulating practical uses are not critical for a final proof of concept.

There are multiple experimental methods for conducting field bioassays, which range from basic designs to more complex ones. A basic approach would be to simply count the number of mites or ticks attracted to a chemical point source over a period of time. Chemical sources are often incorporated into trapping devices to determine the efficiency of capture. This basic design can easily determine if a chemical can function as an attractant in field applications. By examining capture rates over time, information is obtained about the duration of attractant activity [41,42]. While on the surface, such an assay may seem simple to conduct, the placement of treatments and controls can be problematic because acarine populations are not always evenly distributed in the landscape. Another iteration of this bioassay, and to deal with non-homogenous acarine distribution, employs ticks or mites physically marked and then released at different distances from a chemical source. The experiment can be replicated varying the distances between the release location and chemical source to determine the maximum effective range for capture; information on attraction in the form of a capture percentage for each distance tested can also be obtained [43]. This assay design has been used successfully with ticks, though not with mites because of the past difficulty in marking individuals for release. There are now examples in the insect literature where animal casein and albumin proteins have been used to mark insect parasitoids in laboratory experiments [44,45]. Additionally in field experiments, adult insects exposed to vegetation covered in either casein or albumin were capable of picking up the protein markers within 5 min and retaining them for approximately 2 days [45]. These and other marking systems could potentially be used in the future for mites and ticks.

The primary advantage of field bioassays is to test attractants in practical field settings. Unfortunately, field conditions are also the main source of problems associated with field tests. Working in field settings limits the time frame for conducting experiments because of the seasonal distribution of wild acarine populations. Additionally, since wet weather decreases mite and tick activity, experiments cannot be conducted during rainstorms or on days immediately following rainfall. These time constraints can make it difficult to obtain sufficient, consistent experimental replicates. Changes in temperature from one day to the next, or even during a typical day, also affect vaporization of chemical compounds and acarine motor activity. Working in the field also exposes the researcher to wild populations of mites, ticks, and other animals, some of which produce a level of risk to the researcher, for example, exposing them to venoms or vector borne pathogens. Additionally, human subjects research requires special regulatory approvals that may be difficult and timely to obtain. Since there are no standardized methods for field bioassays, it is important that the experimental design is described in detail; otherwise replication of results between studies is difficult. More research is needed to develop standard methods, including both positive and negative controls, for the evaluation of attractants and repellents in field assays. This is especially relevant to cases where the goal is to develop a commercial use for compounds. More studies are also needed to develop correlations between lab bioassays and field tests for a variety of compounds to determine if reliable lab methods can be developed to effectively predict and minimize the need for field assays.

Chemistry of Aggregation and Assembly Pheromones

Because of the common evolutionary history of the acarines, there likely is some level of uniformity in this group relative to the evolution of pheromones in general and their use in development and reproduction. The same is probable for environmental chemistries and the chemical ecology of the acarines. One of the challenges in the review of the work in this area is the naming of pheromones and other environmental compounds of importance to the acarines; to some degree the nomenclature has been affected by the many different life strategies of mites, the specialized obligatory hematophagy and reproductive strategies of ticks, which is quite different from mites, and likely some degree of isolation of work between the mite versus tick scientific communities. Because there has been no coordination in nomenclature across the acarines, in some cases the terminology appears to be contradictory or confusing. Since the nomenclature for specific acarine systems has already been established in the scientific literature, we have chosen to adhere to this nomenclature to minimize confusion, but it is clear that an effort is needed, as we go forward with new research, to identify similar acarine features versus those that are novel and specific to particular life strategies (or species), and to develop more unifying approaches by which we reference compounds which affect acarine behavior and development. Understanding the known chemistry of acarine attraction is the first step in developing strategies for their use as a pesticide and novel chemical or functional mimics.

Mite Aggregation Pheromone

The aggregation pheromone causes clustering of conspecific male and female mites of all developmental stages to protected and viable habitats while not on a host. Currently only one

aggregation pheromone, lardolure (Table 1.1), has been identified in the acariform mites *Caloglyphus polyphyllae* and *Lardoglyphus konoii* [46]. However, there are many mite sex pheromones that have a dual aggregation function; this makes the identification of solely aggregation pheromones problematic. Despite the limited availability of information describing mite aggregation pheromones, a reasonable role for this pheromone is the clustering of conspecifics into a well-protected habitat to reduce the mortality associated with unfavorable environments. It is difficult to draw additional conclusions or make comparisons to ticks.

Tick Attraction-Aggregation-Attachment Pheromone

Attraction-aggregation-attachment pheromone (AAAP) (Table 1.2) is a tick pheromone secreted by feeding adult males to attract non-feeding conspecific immature and mature males and females, forming feeding clusters on bovine or large ungulate hosts [47]. AAAP is only produced by a subset of species in the genus *Amblyomma* that have a preference for large animal hosts. AAAP alerts unfed questing ticks of nearby feeding ticks and works in combination with host kairomones to orient unfed ticks towards the host [9]. Currently AAAP is known to be produced by *A. cajennense*, *A. gemma*, *A. hebraeum*, *A. lepidum*, *A. marmoreum* and *A. variegatum* [48]. The chemical composition of AAAP varies by tick species, but the primary active chemical component typically consists of 1-2 phenolic fatty acids. AAAP of *A. variegatum*, the tropical bont tick, is the most studied. It is composed of methyl salicylate, *O*-nitrophenol, and nonanoic acid (Table 1.2) in a 2:1:8 ratio [49]. *A. hebraeum* ticks also exhibit attractive behavioral responses to the AAAP components methyl salicylate and *O*-nitrophenol [50,51]. AAAP in combination with carbon dioxide, produced

by the host, creates a strong bioactive mixture capable of attracting host-seeking ticks from a distance of 5 to 10 m in field experiments [50,52]. Attraction of *A. variegatum* increased from 35 to 90% when 6.6 mg of synthetic AAAP was tested in the presence of carbon dioxide gas delivered from 50 and 500 g of dry ice [47].

AAAP induces the formation of species specific aggregations on host animals. This pheromone benefits both emitting and responding ticks. Responding unfed ticks use AAAP to locate hosts and commence blood feeding. Also, blood feeding in a large aggregation may protect ticks from physical damage inflicted by the host by reducing the individual risk of injury by increasing the group size. The emitting adult males have the added benefit of possibly attracting adult females to the feeding aggregation for subsequent mating.

Despite differences between AAAP and the mite aggregation pheromone, i.e., the sex that emits the pheromone and the location of the aggregation on a host, both pheromones act to cluster conspecifics to increase their viability. The mite aggregation pheromone induces clustering to help protect mites from unfavorable environmental conditions while not on a host. AAAP induces clustering on hosts to increase access to blood meals and protect ticks from starvation. It is currently unknown if other genera of ticks, outside of *Amblyomma*, exhibit similar clustering behavior on hosts in response to aggregation pheromones. This phenomenon may also be present in parasitic mites that blood feed, but that is currently undetermined. AAAP has been successfully incorporated into *Amblyomma* tick control strategies. However, since the pheromone is species specific it is ineffective against other tick species. Investigating on-host aggregations in other genera of ticks and in mites could be useful in the identification of other attractive pheromone chemistries for use in acarine control.

Tick Assembly Pheromone

The assembly pheromone (Table 1.2) causes clustering of conspecific individuals in protected, viable habitats off the host [53]. The tick assembly pheromone differs from the mite aggregation pheromone and AAP in the behavior elicited to form the off-host aggregation. Typical aggregation pheromones are volatile compounds that cause responding ticks to actively search for emitters and cluster at the source, forming an aggregation. The assembly pheromone is non-volatile, and is detected by ticks through direct contact. When ticks encounter the pheromone, locomotor activity is arrested. Assemblies are formed as a result of multiple ticks encountering the pheromone and all pausing together. Assembly pheromones are typically species specific and active against unfed larvae, nymphs, and adult male and female ticks. Though, there are exceptions, especially among argasid ticks [48]. Fed immature ticks are unresponsive to the assembly pheromone, but regain responsiveness after molting [54]. Assembly pheromones are produced by multiple ixodid and argasid species including *A. cohaerens* [33], *Aponomma concolor* [55], *Argas persicus*, *A. reflexus*, *A. polonicus* [56], *Hyalomma dromedarii* [57], *I. holocylus* [55], *I. ricinus* [58], *I. scapularis* [59], *I. uriae* [54], *Ornithodoros moubata* [60], *Rhipicephalus appendiculatus* [33], and *R. evertsi* [61]. Assembly pheromones are found in excreta, cast skins, and on the cuticle of larvae, nymphs, and adult male and female ticks [9,62]. In Petri dish bioassays, larval fecal deposits on filter paper caused 67% of tested *I. uriae* larvae to pause and aggregate on the treated filter paper. Similar results were observed with nymph feces causing 66% of tested *I. uriae* nymphs to pause and aggregate, 64% of tested *I. uriae* adult males paused in response to adult male feces, and 71% of tested *I. uriae* adult females in response to adult female feces

[54]. *I. ricinus* ticks also exhibit similar behavior in response to fecal matter with 48% of tested adult males and females ceasing activity and clustering [58,63].

GC-MS analysis of fecal material, caste skins, and whole body tick extracts identified the primary components of assembly pheromone to be hematin, guanine, xanthine, uric acid, and several other purines [54,62] (Table 1.2). Synthetic mixtures of these components applied to filter paper caused both adult and immature males and females to pause on the treated surface and aggregate. For *I. scapularis*, a 25:1:1 mixture of guanine, xanthine and adenine, respectively, applied to filter paper caused 28-48% of tested adult and nymph males and females to pause and aggregate on the treated filter paper [62]. Similar responses were observed when *I. uriae* was tested against varying mixtures of guanine and uric acid [54].

The tick assembly pheromone regulates clustering of unfed individuals into well-protected habitats to reduce mortality caused by predation and exposure to unfavorable environments while not on a host, as well as to sites frequented by hosts [Sonenshine, personal communication]. The risk of desiccation is highest for ticks when they are not on a host. Clustering of immature and mature ticks helps decrease water loss by establishing a group transpiration rate. When the group transpiration rate is distributed among aggregation members, it typically results in lower individual transpiration rates than when ticks are not part of an aggregation [3,48]. This same theory of “power in numbers” also applies to the formation of aggregations to reduce individual risk of predation and physical injury. Additionally, when a host encounters a tick aggregation, clustering conspecific male and female ticks will attach to the host and begin to blood feed as a cohort. Since large tick densities enhance feeding and molting success, it may be advantageous for ticks to form large aggregations off the host to improve success on the host [64]. The aggregation of adult

males and females also may increase the reproductive success of ticks by increasing successful feeding of both sexes on the same host, creating the opportunity for blood fed adults to subsequently mate. Additionally, *Ixodes* species that produce assembly pheromones can engage in mating without a blood meal and before host attachment. Further research is needed to better characterize the behavioral responses associated with the assembly pheromone in ticks that can mate prior to blood feeding and those that mate after blood feeding. It would also be interesting to determine if mites produce similar assembly pheromones.

Chemistry of Reproductive (Sex) Pheromones

Mite Immature Female Pheromone

Male mites must commonly compete to reproduce with conspecific females. Adult female mites have a short period of time for fertilization after eclosion, so the first males to mate are typically the most successful. Males increase fecundity by guarding quiescent deutonymph females and then mating with the emerging reproductives. Male mites are able to differentiate deutonymph females from protonymphs with a high degree of accuracy due to the mite immature female pheromone produced only by deutonymphs [65]. Table 1.1 lists the currently known components of the immature female pheromone, i.e., farnesol, nerolidol, geraniol and citronellol. *Tetranychus urticae* males were significantly attracted to crude extracts of the immature female pheromone and to its individual chemical components citronellol [66], farnesol [67], and nerolidol [68]. Similar behavior of males associating with deutonymph females has been observed in *Hericia* sp. [69], *Macrocheles muscaedomesticae* [70], *Proctophyllodes stylifer*, *P.picae* [71], and *T. kanzawai* [72], though there has been no

identification of the pheromones involved. Male mite guarding of deutonymph females enhances male reproductive success by increasing the likelihood of guarding males mating first with emerging mature females. It would be interesting to evaluate immature female pheromones and the chemical components as potential attractant lures in novel control methods (discussed in more detail later).

Mite Female Sex Pheromone

Fecundity of both male and female mites relies heavily on proper nutrition. Reproduction only occurs after feeding to ensure that adequate nutrients and energy are available for successful mating and egg development. Female mites release female sex pheromone after feeding to attract males for reproduction [73,74]. Currently female sex pheromone and its chemical components have been identified in 9 species of Argasid mites (Table 1.1): 2-hydroxy-6-methylbenzaldehyde in *Acarus immobilis* [73], *Aleuroglyphus ovatus* [74], *Cosmoglyphus hughesi* [75], and *Dermatophagoides farinae* [76]; undecane in *C. rodriguezii* Sams [77]; (2R, 3R)-epoxyneral in *Caloglyphus* sp. [78]; rosefuran in *Caloglyphus* sp. [79]; β -acaridial in *Caloglyphus* sp. [35]; α -acaridial in *Rhizoglyphus robini* [80]; S-isorobinal in *R. setosus* [81]; and S-isopiperitenone in *Tyrophagus similis* [82]. S-isorobinal has also been identified in seven other species of Astimata mites, though its role as a pheromone is unknown. Table 1.1 lists all the currently identified attractive chemical components of female sex pheromone.

The female sex pheromone is also not exclusively produced by females, and is often found in conspecific males in lower concentrations [81,83]. It is currently unknown why male mites would produce small amounts of female sex pheromone, though it may allow

males to identify other conspecifics competing to reproduce with females. The presence of small amounts of female sex pheromone in males may also explain why mounting behavior is often observed between male mites [83]. Mounting behavior between males may be an act of ascendancy with larger, stronger males asserting dominance over smaller, weaker conspecifics. This delineation of dominant and submissive male mites may also explain why dominant males typically mate with the larger, more reproductively successful females and submissive males with smaller, less reproductively successful females [84]. This mating hierarchy is a form of reproductive natural selection important for the survival of the species.

Tick 2,6-Dichlorophenol Sex Pheromone

Ixodid adults become sexually mature shortly after initiating blood feeding. In adult female ticks, consumption of blood triggers production of the sex pheromone, 2,6-dichlorophenol (2,6-DCP) [85] (Table 1.2). Nearby feeding conspecific males detecting 2,6-DCP will stop feeding, detach, and begin searching for emitting females to begin courtship and mating [53]. Additional pheromones are involved in tick mating, though they are not currently known to be volatile attractants. The sex pheromone 2,6-DCP is currently known to be produced by seven genera and 12 species of ticks, listed in Table 1.3 [9,26]. There is currently no evidence of 2,6-DCP in the genus *Ixodes*. Females primarily utilize 2,6-DCP as a sex pheromone, though *A. hebraeum* and *A. variegatum* males will secrete 2,6-DCP to stimulate attraction and attachment of immature and mature males and females on the host [86]. The sex pheromone 2,6-DCP is extremely potent for adult male ticks. Plastic spherical baits impregnated with 50 ng of 2,6-DCP induced 100% of *Anocentor (Dermacentor) nitens* adult males to engage in mate-seeking and mounting behavior on the impregnated plastic baits

[87]. Similar behavior was observed in *A. cajennense* when exposed to 500 ng of 2,6-DCP [88] and in *A. americanum* when exposed to 100 ng [89]. *A. cajennense* [90], *D. andersoni*, *D. variabilis* [85], and *R. sanguineus* [90] also exhibit attractive behavior when exposed to 2,6-DCP in olfactometer bioassays. Electrophysiological studies determined that sensilla in the anterior pit of the Haller's organ of *A. cajennense* [91], *A. variegatum*, *D. variabilis*, and *R. appendiculatus* [92] immature and mature males are responsible for detecting 2,6-DCP.

The sex pheromone 2,6-DCP plays a vital role in reproduction being responsible for alerting males to the presence of proximal, reproductive females. This only applies to adult ticks that must blood feed to become sexually mature and mate. The exception is ticks in the *Ixodes* genus. *Ixodes* sp. can mate prior to blood feeding, though the sex pheromones involved in courtship and reproduction are currently unknown. *Ixodes* sp. may utilize 2,6-DCP as a sex pheromone or some other uncharacterized compound. It is also possible that males secrete small amounts of 2,6-DCP to function as an aggregation pheromone increasing the feeding success of both immature and mature males and females. Similarly, although there is evidence of sex pheromones regulating courtship and mating in argasid ticks, nothing is known about their identity.

Chemistry of Alarm Pheromones

Neral and neryl formate (Table 1.1) have been identified in 16 species of astigmatid mites as alarm pheromones produced in response to bodily injury [5,93]; there also is recent evidence of an additional attractant function for these compounds. In olfactometer studies, *Schwiebia elongata* exhibited an attractive behavioral response walking towards and clustering near filter paper treated with 1 and 3 ng of neral [94] (Table 1.1). When *S. elongata* were

presented with filter paper treated with 30 ng of neral, mites moved away from the neral source. *D. farinae* and *D. pteronyssinus* adults also exhibited attractive responses to low doses of neryl formate in olfactometer bioassays [95] (Table 1.1).

Attraction and clustering of mites in response to low concentrations of alarm pheromone may represent a novel group survival strategy with clustering mites forming a “safety net”. Once mites detect higher concentrations of alarm pheromone they may transition from performing group survival strategies to individual survival strategies, i.e., scattering and hiding. Group survival strategies could be implemented in response to sources of indirect injury, such as unfavorable environmental conditions. Individual survival strategies would be executed in response to direct physical injury. More research is needed to examine the role of alarm pheromone in mite self-preservation. It is also unknown if alarm pheromone and the associated behaviors are expressed in ticks. It would be interesting to determine if ticks have similar group and individual survival strategies as mites, and what compounds might regulate these behaviors. Group clustering in both mites and ticks could also be used as lures for their control.

Chemistry of Host Kairomones

Mite Attractive Host Chemistry

Host seeking in parasitic mites is heavily dependent on the detection of host kairomones. Behavioral assays have demonstrated the attractive quality of a few chemicals against mites that parasitize insect and mammal hosts. Unfortunately, the information available is limited to a few select parasitic mite species. Chemical components of host kairomones that are attractive to parasitic mites are listed in Table 1.3. *Macrocheles muscaedomesticae* is a

predatory mite of *Musca domestica* housefly eggs and first instar larvae. *M.*

muscaedomesticae commonly engages in phoresy with adult *M. domestica* to gain access to offspring. *N*-phenyl-*N*-glucoside and *N*-phenyl-*N*-mannoside identified in whole body extracts of both male and female adult houseflies, 5-7 d after emergence, were documented as being significantly attractive to *M. muscaedomesticae* adults [96] (Table 1.3). These attractive compounds are also present in younger houseflies, though at lower concentrations which did not elicit strong attraction in *M. muscaedomesticae* [97]. Since it has been documented that the release of *M. muscaedomesticae* results in extremely high levels of house fly parasitism [98], one control strategy for houseflies could use applications of *N*-phenyl-*N*-glucoside and *N*-phenyl-*N*-mannoside with or without the release of *M. muscaedomesticae*.

Mites are also the most successful parasites of honeybees [99]. Honeybee hives have an abundance of food and a constant regulation of temperature and humidity despite external conditions, which could be favorable for mite development. *Varroa destructor*, a parasitic honeybee mite, lays eggs in capped honeybee brood cells that have been stocked with nutrients. This makes the detection of honeybee colonies and brood cells essential for the reproduction and survival of *V. destructor* [100]. *V. destructor* are attracted to fatty acid esters including methyl palmitate and methyl linolenate found in the cuticle extracts of *Apis mellifera* workers and drone larvae, with no differentiation between these two honeybee castes [101,102] (Table 1.3). Lab exposure of *V. destructor* in a y-tube bioassay to methyl palmitate resulted in 50% of the tested mites arriving at the chemical source in 30 sec, and 70% after 400 sec [101]. Additionally, the parasitic mites *D. farinae*, *D. pteronyssinus*, *L.*

konoii and *T. putrescentiae* are attracted to saturated and unsaturated fatty acids C₁₆–C₁₈ and methyl esters of C₁₆–C₁₈ [73].

Dermanyssus gallinae, the red poultry mite, is a parasitic mite that blood feeds on poultry. *D. gallinae* relies on the detection of heat, vibrations, and carbon dioxide levels higher than ambient air to detect and locate poultry (Table 1.3). Though, *D. gallinae* will cease locomotor activity and pause in response to large concentrations of carbon dioxide alone [103]. The latter appears to be a defense mechanism to prevent being eaten by the host; the host detects the mite, the mite is exposed to a high level of carbon dioxide from the breath of the host, and the mite decreases its chance of further detection by the cessation of movement. After a period of 30-40 sec, without further exposure to high concentrations of carbon dioxide, the mite will resume searching for the poultry host. Despite this defense mechanism, *D. gallinae* mites still exhibit attraction to lower concentrations of carbon dioxide [103]. *D. gallinae* also exhibits attractive responses to sebaceous gland secretions present on old feathers. When old feathers were tested in a y-tube bioassay against new feathers, 60-70% of tested mites exhibited attraction to the old feathers [104]. It is apparent that research investigating mite attractive host chemicals is sparse resulting in the identification of few chemical attractants. Mite attractive host chemicals have potential as putative lures in novel control methods, though this currently hindered by the limited information available and requires additional research.

Tick Attractive Host Chemistry

The main determinant of tick host-seeking behavior can be attributed to the presence of host kairomones [105]. Ticks utilize host kairomones to detect host type and proximity.

Behavioral assays have demonstrated the attractive quality of dermal pelage [106], host breath [105,107], gland secretions, and urine [105,108]. Acetone, ammonia, carbon dioxide, and 1-octen-3-ol (Table 1.4) are all attractive components of human and animal breath [36,109]. Carbon dioxide has long been recognized as an attractant for multiple species of ixodid ticks [107]. Ixodid ticks have both long-range and short-range sensilla in the Haller's organ that respond to small and large amounts of carbon dioxide, respectively. Sensilla cell responses to carbon dioxide have been recorded in *A. americanum*, *A. maculatum*, *D. variabilis* [110], and *A. variegatum* ticks [39]. Lab and field bioassays have also demonstrated the attractive quality of carbon dioxide to *A. americanum* [36], *A. hebraeum* [111], *A. triguttatum* [112], *A. variegatum* [109], *D. andersoni* [113], *D. variabilis* [36], *I. dammini* [113], *I. ricinus* [114], *I. scapularis* [115], *R. microplus* [28], and *R. sanguineus* [116]. Attractive behavioral responses to acetone and ammonia dissolved in water have been recorded for *A. americanum* [36] and to acetone alone in *A. hebraeum* [109]. Sensory cell responses to NH₃ [39,117] and acetone [109] have also been recorded in *A. variegatum*.

1-Octen-3-ol (Table 1.4) is an important attractive component specifically associated with bovine breath and bovine odors [28]. 1-Octen-3-ol is attractive to *A. hebraeum* unfed adults [118] and *R. microplus* unfed nymphs [28,119] in field settings. Both *A. hebraeum* and *R. microplus* exclusively parasitize bovine hosts. 1-Octen-3-ol also elicited attractive behavioral responses from *A. americanum* in studies with an olfactometer [36] and electrophysiological responses in *A. cajennense* using tip-recording techniques [89].

Nitrogenous wastes, i.e., ammonia and ammonium hydroxide, are major components of mammal dermal pelage and urine. *D. variabilis* exhibits aggregative behavior in response to canine urine [120]. *A. americanum* and *D. variabilis* both exhibit aggregative behavior in

response to domestic canine ear pelage and deer tarsal gland extracts [105,106]. Deer tarsal pelage and its odor are created by bacterial fermentation of urine that is retained in the gland after urination. Lipids secreted by sebaceous glands provide a habitable environment for microbial organisms [121,122]. Canine ear pelage consists of dog-ear wax, lipids from sebaceous glands, and a natural fauna of bacteria that live in the external ear canal [123]. *D. variabilis* does not parasitize white-tailed deer, but this tick has been reported to congregate around deer carcasses, increasing the likelihood of encountering canine scavengers, its primary host type. Its attraction to deer tarsal gland extracts reflects a means of feeding behavior, with tick aggregations in high host traffic areas identified by cervid odors [124]. *D. variabilis*, *I. scapularis*, and *I. persulcatus* also exhibit arrestant behavior in response to canine fur odors [120,125]. *A. variegatum* exhibits attractive behavior in response to rabbit and bovine dermal odors [40], *I. ricinus* to bovine and porcine dermal odors [28], and *R. microplus* to only bovine dermal odors [28]. Electrophysiological and bioassay studies paired with GC-MS analysis identified the attractive components of the rabbit and bovine dermal odors to be aliphatic and aromatic aldehydes, carboxylic acids, alcohols, phenols, as well as lactones [28,39,40,126]. Unfortunately, the majority of these compounds are currently unknown. Osterkamp et al. [28] identified 11 chemical compounds, mainly carboxylic acids, from bovine dermal odors that elicited questing activity in *R. microplus* larvae when presented at high doses; 2-ethylhexanoic acid, 2-nitrophenol, 1-octen-3-ol, benzoic acid, butyric acid, heptanoic acid, hexanal, hexanoic acid, isobutyric acid, pentanoic acid, and pyruvate (Table 1.4). Aliphatic aldehydes were detected by three different sensilla in the Haller's organ of *A. variegatum* adult ticks [40] and additional chemosensory cell responses to lactones recorded in the Haller's organ of *I. ricinus* adult ticks [126].

Although there has been research and development in the use of tick pheromones to attract ticks for the purpose of control, considerably less research is available on the use of host-associated attractants. One obvious disadvantage for the use of some of these host-associated attractants like carbon dioxide is the practical storage and long term delivery of dry ice or compressed gas at an economical cost; these are mostly engineering challenges. The use of dry ice to attract ticks, as one example, is a well-established research tool for tick collection and monitoring [111-115]. The use of other host-associated attractants in acarine control needs further consideration. Host-associated attractants could potentially have a wider range of activity for different acarines than a pheromone that is often species specific. Furthermore, research is needed to characterize both the bacteria associated with host-associated attractants and the volatiles that are produced from bacterial fermentation of mammal sebaceous gland secretions and urine. Since mites are attracted to similar sebaceous gland secretions, it is possible that they are also attracted to odors from bacterial fermentation in addition to host kairomones.

Chemistry of Plant Allomones

Mite Attractive Plant Chemistry

Herbivore-induced plant volatiles (HIPVs) elicited by arthropod feeding, attract predatory mites that may help alleviate plant injury through predation. For example, the predatory mite *Neoseiulus cucumeris* is attracted to volatiles from arthropod infested cucumber plants, and is unresponsive to undamaged plants, plants with artificial damage, and volatiles from pest arthropods [127]. Similar results have been reported with *N. cucumeris* and tulip bulbs [128], *N. womersleyi* and tea plants [129], and *Phytoseiulus macropilis* and bean plants [130]. Table

1.5 lists four HIPVs that were detected from infestation damaged cucumber plants, i.e., linalool, methyl salicylate, α -ocimene and 4,8-dimethyl-1,3,7-nonatriene. One or more of these compounds may be responsible for attracting *N. cucumeris* to arthropod infested plants [127]. These four compounds are also involved in the attraction of the predatory mite *P. persimilis* to infested lima bean plants [131,132]. Additionally, Gols et al. [133] identified a fifth compound from the lima bean HIPVs, jasmonic acid (Table 1.5), to which *P. persimilis* exhibits attractive responses. Linalool and methyl salicylate have been shown to be successful attractants to *N. californicus* in field studies [134,135]. Slow release of methyl salicylate resulted in increased carnivorous predation of herbivorous pests over a 2-year period [42]. Predatory mites also show preference towards HIPVs that are produced by plants to which they have been previously exposed. *N. womersleyi*, previously associated with infested tea leaves, exhibited increased attraction to tea leaf volatiles, i.e., (*E*)-4,8-dimethyl-1,3,7-nonatriene, (*E,E*)- α -farnesene, and (*E*)- β -ocimene (Table 1.5) while remaining unresponsive to other HIPVs. Likewise, *N. womersleyi* previously associated with infested kidney bean plants exhibited 82% attraction to kidney bean plant volatiles, i.e., (*E*)-4,8-dimethyl-1,3,7-nonatriene, (*E,E*)-4,8,12-trimethyl-1,3,7,11-tridecatetraene, β -caryophyllene, and methyl salicylate (Table 1.5), while remaining unresponsive to other HIPVs [129].

Biotic stresses on plants have caused the evolution of tritrophic interactions between plants, herbivores, and herbivore enemies. HIPVs released by plants promote the effectiveness of natural enemies of herbivorous arthropods as a mechanism of indirect plant defense [136]. Interestingly, predatory mite species have been conditioned to associate certain HIPVs with the presence of herbivorous prey, becoming attracted to these volatile chemicals. Since HIPVs are produced in larger quantities than prey kairomones, they may be

easier to detect and possibly become the primary chemical cue regulating hunting in predatory mites. The shift from utilizing prey kairomones to HIPVs would also result in changes in the olfactory sensory system, sensilla detecting prey kairomones losing function and sensilla detecting HIPVs becoming more active and robust. The phenomena of mite preference for HIPVs produced by plants to which they have been previously exposed can be explained by “imprinting”. Mites early in development associate specific plant HIPVs with prey and become dependent on that association for hunting throughout their life span. Though, it is still unclear how this preference for certain HIPVs over others is acquired and retained.

Tritrophic interactions between plants and predatory mites are interesting phenomena, although there is little information available on how these systems develop and function. Research has focused mostly on HIPVs, predatory mites, and their use in biological control. Tritrophic systems are unstable and continually changing as herbivorous pests evolve to evade detection by predators. The mechanisms by which these interactions are established could have significant value in development of biological based novel control strategies.

Tick Attractive Plant Chemistry

A few plants have been found to be attractive to *Rhipicephalus* ticks. Freshly picked leaves from the *Acalypha fruticosa* plant were attractive to *R. appendiculatus* larvae [137], and oil extracts of dry leaves of *Calpurnia aurea* attractive to both *R. appendiculatus* and *R. pulchellus* adults (Table 1.6). A dose of 100 mg/ml of *C. aurea* extract attracted 52.2% of released *R. pulchellus* ticks and 44.4% of released *R. appendiculatus* ticks from a distance of 1 m in field settings [37]. The active ingredients in these plant extracts are currently

unknown. It has been hypothesized that plant odors may mimic pheromones or represent safe habitat selection for ticks searching for protected locations to aggregate. Since *Rhipicephalus* ticks actively hunt or ambush hosts, they are more susceptible to environmental conditions than questing ticks, which remain on or near plants. *Rhipicephalus* ticks may need to identify specific plants in their environment as designated safe habitats to retreat back to during adverse weather conditions. Removing these plants could possibly force ticks to leave the area in search of new safe habitats or increase tick mortality since they no longer have protection from unsuitable environmental conditions. This phenomenon has obvious control implementations and warrants considerably more research emphasis. It at least suggests that ground landscaping could be used to create unviable habitats for ticks and reduce tick feeding on animals and humans. Tick questing behavior and plant preference would be of similar interest. Lastly, since mites exhibit similar aggregative behavior to that of ticks, the same study approaches might apply to mite control.

Chemistry of Fungal allomones

Stored food mites are not ectoparasitic but exhibit attractive behavior in response to fungal allomones. Both *cis*- and *trans*-octa-1,5-dien-3-ol isolated from the fungi, *Trichothecium roseum*, have been determined to be attractive to *T. putrescentiae* mites [138] (Table 1.7). It has been suggested that in the absence of a traditional food source, stored food mites may utilize xerophilic fungi as a source of nutrients [139]. Because xerophilic fungi prefer dry environments, they are likely to thrive while traditional food sources for stored food mites may be limited or absent. This adaptation to obtain nutrients from nontraditional food sources, such as fungi, may have evolved in stored food mites to promote survival during

long starvation periods. The ability of mites to obtain nutrients from nontraditional food sources during starvation periods should be of great interest. The availability of these nontraditional food sources under varying environmental conditions might be significant to the population dynamics of mites. Understanding these alternate food sources may be helpful in modifying current food preparation and storage methods for improved stored food mite control. This could also apply to other systems where mites are important, and therefore microbial-mite interactions will likely grow in importance in the future.

Acarine Trapping: Attraction and Kill

Tick Lure and Kill Strategies

Lure and kill strategies combine attractants with an acaricide into a slow-release formulation or device. The attractive compound(s) lure the tick to some object that contains a contact acaricide [140]. Combining attractants and acaricides with slow release technology allows impregnated delivery devices, as one example, to remain attractive to ticks, and lethal for a period of up to 14 wk [141]. The delivery device provides a safer means of acaricide application both for the pest control operator and the environment since the amount of the pesticide applied is reduced with restricted bioavailability to the general landscape.

Arrestment pheromone, 2,6-DCP sex pheromone, and AAAP (discussed earlier) are examples of proven lures. Allan et al. [142] patented a device that incorporated *I. scapularis* arrestment pheromone (a mixture of guanine, xanthine and adenine) and permethrin acaricide into an oil formulation (Last Call™, IPM technologies, Portland OR) that was applied to ground cover and vegetation with a pump sprayer. The pheromone-acaricide mixture resulted in 95% *I. scapularis* mortality in treated areas over that of the untreated controls [142]. Two

delivery devices have been evaluated incorporating 2,6-DCP and acaricides. The first involves a water emulsion of gelatin-microencapsulated 2,6-DCP combined with propoxur. The emulsion was applied to dogs infested with the American dog tick, *D. variabilis*, where the slow-release microcapsules continuously attracted ticks for multiple days. Tick mortality was observed, with a higher percentage of male ticks killed by the treatment than females. Mating disruption was also observed resulting in a 90% decrease in oviposition in females compared to untreated controls [143]. The second delivery device utilizing 2,6-DCP involved impregnating tick decoys with the pheromone-acaricide mixture. Tick decoys were plastic spherules made from polyvinyl chloride plastic. The decoys (5 mm x 5 mm) were impregnated with 2,6-DCP, cholesteryl oleate and propoxur and adhesively attached to rabbits infested with *D. variabilis*. Mortality of all the male ticks was observed, and there was no oviposition in females compared to untreated controls [144]. Similar results were observed when the impregnated tick decoys were placed onto tick-infested cattle [92] and camels [145]. AAAP was also effectively utilized as a chemical lure to control ticks. Plastic tags impregnated with AAAP and pyrethroids were placed on the tails of cattle infested with the ticks, *A. hebraeum* and *A. variegatum*. Tick control over a 3-month trial averaged 94.9% over that of the untreated controls [51,141].

Current tick control methods are heavily dependent on the use of acaricides. This approach can effectively control tick populations but typically requires multiple, large-scale applications [146,147]. Unfortunately, our dependency on traditional spraying promotes the application of large amounts of pesticides into the environment and fosters the development of pesticide resistance; these negative side effects could be limited by the use of lure and kill strategies focused not on the general pest populations but just on the resource needing

protection. The current research on lure and kill technologies is limited and does not provide enough supporting evidence for their broad implementation as alternatives to chemical sprays.

Mite Biological Control and Attractants

A different type of lure and kill strategy has been used for mite control in crop production using a biocontrol agent, i.e., predatory mites, as the kill mechanism. Attractive HIPVs, primarily methyl salicylate, have been shown to enhance natural enemies in laboratory experiments with a variety of plants [134,148,149]. Field-testing of methyl salicylate has been limited to grape vineyards [150], hops [42], cotton [151], and strawberry fields [150,152]. Methyl salicylate formulated for slow release dispensers (Predalure®, AgBio, Westminster, CO) have demonstrated the most effective predator attraction for the longest time period. Predalure dispensers repeatedly distributed in hops fields reduced infestations by the herbivorous mite *T. koch* 41-90% over a two year period over that of untreated controls [42]. Predalure dispensers placed in strawberry fields also consistently attracted predators from up to 10 m away from the dispenser site [152]. It is apparent that chemically enhanced biocontrol is effective in reducing herbivory of a variety of crop plants. Though, research investigating HIPVs and the tritrophic interactions with predatory mites is still very limited and require additional study. There is also the potential for the development and implementation of lure and kill strategies (as previously described in ticks) to control parasitic mites of humans and animals using chemical attractants and miticides, though that also requires further study.

Summary and Conclusions

The Acari are of significant economic importance in crop production and human and animal health, and chemical control an essential component for pest management. The acarines represent an ancient divergence in the Arthropoda and likely have unique strategies for the use of chemistry in their growth, development, and ecological interactions. However, the study of acarine attractants is limited as compared to that of insects. The acarines consists of two major groups, the mites that demonstrate a wide variety of life strategies, i.e., herbivory, predation, and endo- and ectoparasitism, and ticks which have evolved obligatory hemtophagy. Much of the research on attractants in mites versus ticks has occurred in relative isolation to each other. In addition, advances in the physiology and molecular biology of mite chemical communication have been limited by the small size of mites versus that of ticks. Although we now have genomes and transcriptomes to mites and ticks, which should rapidly advance our understanding of chemical communication, the larger size of ticks will still be important in correlating structure to function and be the driver for translational work with mites.

The important chemosensory organs in the acarines are the palps, chelicerae, and an organ on the tarsus on the front pair of legs called the Haller's organ in ticks and the tarsal organ in mites. The relative importance of these different organs in their chemical ecology is poorly understood. Also the molecular mechanisms for attractant detection in these organs are a black box with no published papers. Data are presented in this review that suggests that the mechanism of olfaction in ticks is unlike that of insects. The tarsal organ of mites and the Haller's organ of ticks have a common evolutionary origin and have apparent similar functions; we recommend they be called the "foretarsal sensory organ" (FSO) in both mites

and ticks. The FSO in acarines is not found in other arthropods and has multiple sensory functions, which are not clearly understood. New electrophysiology techniques are needed to map the function of individual sensilla in the FSO, chelicerae and palps. Transcriptomics coupled to genomics is needed along with new techniques like RNAseq, RNAi, and cell imaging to understand molecular mechanisms and the regulation of chemoreception; these studies are essentially lacking in the acarines, yet essential to any advancement for finding targets in these receptors for mite and tick control.

This review clearly demonstrates that over the past three to four decades, significant progress has been made in identifying chemical attractants and their associated behaviors in acarine species. However, there are still large gaps in the data currently available compared to insects and the application of this knowledge for control. The gaps are even greater for acarine pheromones with essentially all of the research on ticks as compared to mites. The importance of chemical communication on ecological positioning, aggregation, communication between conspecifics, courtship, and reproduction needs further attention. There appears to be a steady decline of research focusing on attractants and the role of attractants in development, reproduction, and control; research investigating acarine repellents for ticks has overshadowed the study of acarine attractants. Although repellents have a high commercial and military importance for protection against arthropod vectored diseases, the use of repellents for crop protection from mites has received essentially no consideration. Lure and kill and lure-enhanced biocontrol strategies have significant environmental advantages, which warrant further study. Also the use of pheromones and other compounds to disrupt chemical communication in insects has not been applied yet to acarines, even though proven technologies exist and are ready for commercial use.

Finally, mechanisms need to be established to encourage interactions between scientists working on mites and those with ticks. Certainly with the common evolutionary history of mites and ticks, even if they have evolved quite different life strategies, the acari must share many similar mechanisms in chemical communication. The tick model and employing techniques like organ specific transcriptomics, RNAi, and classical physiological techniques likely will be a driver for understanding mite function in the future and along with bioassay, chemical screening, and structure-activities studies will be the mechanism for the practical use of attractants for the control of tick and mite populations. There is also the need for translational research to examine chemical control approaches exploiting both attractants and repellents from ticks to mites and the reverse.

Acknowledgments

This work was funded by grants from NIH (1R21AI096268) and NSF (IOS-0949194) to RMR and the North Carolina Agricultural Experiment Station. ALC was supported in part by a Graduate Student Teaching Assistantship from the Department of Entomology at North Carolina State University and a Research Assistantship funded by the NIH grant mentioned earlier. We would also like to thank Dr. Daniel E. Sonenshine and Dr. Lewis B. Coons for their images of mite and tick sensory structures and for their review of the manuscript.

References

- [1] J. Degenhardt, J. Gershenzon, I.T. Baldwin, A. Kessler, Attracting friends on foes: engineering terpene emission to make crop plants more attractive to herbivore enemies, *Curr. Opin. Biotech.* 14 (2003) 169–176.
- [2] S. Jared, F. Khan, M. Ramirez-Fort, S.K. Tying, Bites and mite: prevention and protection of vector-borne disease, *Curr. Opin. Pediatr.* 25 (2013) 488–491.

- [3] D.E. Sonenshine, R.M. Roe, *Biology of Ticks*, vol. 1, Oxford University Press, New York, 2014.
- [4] I.S. Balashov, *An Atlas of the Ixodid Tick Ultrastructure*, Nauka Press, Leningrad, 1983.
- [5] Y. Kuwahara, Chemical ecology in astigmatid mites, in: T. Hidaka, Y. Matsumoto, K. Honda, H. Honda, S. Tatsuki (Eds), *Environmental Entomology: Behavior, Physiology and Chemical Ecology*, University of Tokyo Press, Tokyo, 1999, pp. 380–393.
- [6] S.A. Leonovich, *Sensory Systems of Parasitic Ticks and Mites*, Nauka Press, St. Petersburg, 2006.
- [7] A. Mulenga, Molecular biology and physiology of chemical communication, in: D.E. Sonenshine, R.M. Roe (Eds), *Biology of Ticks*, Oxford University Press, New York, 2014, pp. 368–397.
- [8] L. Šimo, D.E. Sonenshine, Y. Park, D. Žitňan, Nervous and sensory system, function, genomics, and proteomics, in: D.E. Sonenshine, R.M. Roe (Eds), *Biology of Ticks*, Oxford University Press, New York, 2014, pp. 309–367.
- [9] D.E. Sonenshine, Tick pheromones and their use in tick control, *Annu. Rev. Entomol.* 51 (2006) 557–580.
- [10] B.W. Bissinger, R.M. Roe, Tick repellents: Past, present, and future, *Pestic. Biochem. Phys.* 96 (2010) 63–79.
- [11] B.W. Bissinger, R.M. Roe, Tick repellent research, methods and development, in: D.E. Sonenshine, R.M. Roe (Eds.), *Biology of Ticks*, Oxford University Press, New York, 2014, pp. 382–402.
- [12] Y. Kuwahara, Chemical ecology of astigmatid mites, *Nippon Nogeik. Kaishi.* 11 (1990) 1754–1757.
- [13] J.E. Peña, A.I. Mohyuddin, M. Wysoki, A review on the pest management situation in mango agrosystems, *Phytoparasitica.* 26 (1998) 129–148.
- [14] J.L. Shipp, G.J. Boland, L.A. Shaw, Integrated pest management of disease and arthropod pests of greenhouse vegetable crops in Ontario: Current state and future possibilities, *Can. J. Plant Sci.* 71 (1991) 887–914.
- [15] I. Yamamoto, Some chemical ecological approaches to the control of stored-product insects and mites, *A.C.S. Sym. Ser.* 276 (1985) 219–224.
- [16] S. Attia, K.L. Grissa, G. Lognay, E. Bitume, T. Hance, A.C. Mailleux, A review of the

major biological approaches to control of the worldwide pest *Tetranychus urticae* (Acari: Tetranychidae) with special reference to natural pesticides, *J. Pest. Sci.* 86 (2013) 361–386.

[17] T.J. Ridsdill-Smith, Biology and control of *Halotydeus destructor* (Tucker) (Acarine: Penthaleidae): A review, *Exp. Appl. Acarol.* 21 (1997) 195–224.

[18] O.A.E. Sparagano, D.R. George, D.W. Harrington, A. Giangaspero, Significance and control of the poultry red mite, *Dermanyssus gallinae*, *Ann. Rev. Entomol.* 59 (2014) 447–466.

[19] A. Strachecka, M. Sawicki, G. Borsuk, K. Olszewski, J. Paleolog, M. Bajda, J. Chobotow, Use of acaricides for fighting *Varroa destructor* mites in bee colonies: efficiency and risk, *Med. Weter.* 69 (2013) 219–224.

[20] S.A. Leonovich, M.K. Stanyukovich, Sensory organs of mesostigmatic mites (Acarina, Mesostigmata) dwelling in body cavities of mammals and birds, *P. Zool. Ins. Russ. Ac. Sc.* 315 (2011) 263–273.

[21] S.A. Leonovich, Tarsal sensory complex in the red chicken mite *Dermanyssus gallinae* (Gamasina), *Parazitologiya.* 40 (2006) 124–131.

[22] S.A. Leonovich, Adaptation of sensory systems of gamasid mites (Parasitiformes, Gamasina) to dwelling in different environment, *Parazitologiya.* 42 (2008) 271–279.

[23] A.D. Lees, The sensory physiology of the sheep tick, *Ixodes ricinus* L., *J. Exp. Biol.* 25 (1948) 145–207.

[24] R. Gothe, P. Beelitz, H. Schol, Morphology and structural organization of Haller's organ during postembryonic development of *Argas (Persicargas) walkerae* (Ixodoidea: Argasidae), *Exp. Appl. Acarol.* 11 (1991) 99–109.

[25] R.F. Foelix, R.C. Axtell, Ultrastructure of Haller's organ in the tick *Amblyomma americanum*, *Z. Zellforsch. Mikrosk. Anat.* 124 (1972) 275–292.

[26] D.E. Sonenshine, *Biology of Ticks*, vol. 1, Oxford University Press, New York, 1991.

[27] S.M. Waladde, M.J. Rice, The sensory basis of tick feeding behavior, in: F.D. Obenchain, R. Galun (Eds), *Physiology of Ticks*, Pergamon Press, Oxford, 1982, pp. 71–118.

[28] J. Osterkamp, U. Wahl, G. Schmalfluss, W. Haas, Host odor recognition in two tick species coded in a blend of vertebrate volatiles, *J. Comp. Physiol.* 185 (1999) 59–67.

- [29] S.A. Leonovich, F. Dushbábek, Pheromone sensory subsystem in ticks: correlation between structure of sensilla and evolution of behavior, in: F. Dushbábek, V. Bukva (Eds), *Modern Acarology*, vol. 1, Academia Press, Prague, 1991, pp. 53–58.
- [30] M. Grbić, T. Van Leeuwen, R.M. Clark, S. Rombauts, P. Rouzé, V. Grbić, E.J. Osbourne, W. Dermauw, P.C.T. Ngoc, F. Ortego, P. Hernández-Crespo, I. Diaz, M. Martinez, M. Navajas, E. Sucena, S. Magalhães, L. Nagy, R.M. Pace, S. Djuranović, G. Smagghe, M. Iga, O. Christiaens, J.A. Veenstra, J. Ewer, R.M. Villalobos, et al., The genome of *Tetranychus urticae* reveals herbivorous pest adaptations, *Nature*. 479 (2011) 487–492.
- [31] S.B. Liggett, Phosphorylation barcoding as a mechanism of directing GPCR signaling, *Sci. Sig.* 4 (2011) 36.
- [32] M.E. Rodgers, M.K. Jani, R.G. Vogt, An olfactory-specific glutathione-S-transferase in the sphinx moth *Manduca sexta*, *J. Exp. Biol.* 202 (1999) 1625–1237.
- [33] D.A. Otieno, A. Hassanali, F.D. Obenchain, A. Steinberg, R. Galun, Identification of guanine as an assembly pheromone of ticks, *Insect Sci. Appl.* 6 (1985) 667–670.
- [34] L.G. Arlian, D.L. Vyszenski-Moher, Response of *Sarcoptes scabiei* var. *canis* (Acari: Sarcoptidae) to lipid of mammalian skin, *J. Med. Entomol.* 32 (1995) 34–41.
- [35] H. Shimizu, N. Mori, H. Kuwahara, Aggregation pheromone activity of the female sex pheromone, β -acaridial, in *Caloglyphus polyphyllae* (Acari: Acarididae), *Biosci. Biotech. Bioch.* 65 (2001) 1724–1728.
- [36] A.L. Carr, R.M. Roe, C. Arellano, D.E. Sonenshine, C. Schal, C.S. Apperson, Responses of *Amblyomma americanum* and *Dermacentor variabilis* to odorants that attract haematophagous insects, *Med. Vet. Entomol.* 27 (2013) 86–95.
- [37] P. Nana, N.K. Maniania, R.O. Maranga, H.L. Kutima, H.I. Boga, F. Nchu, J.N. Eloff, Attraction response of adult *Rhipicephalus appendiculatus* and *Rhipicephalus pulchellus* (Acari: Ixodidae) ticks to extracts from *Calpurnia aurea* (Fabaceae), *Vet. Parasitol.* 174 (2010) 124–130.
- [38] S.M. Waladde, Tip-recording from ixodid tick olfactory sensilla: Responses to tick related odours, *J. Comp. Physiol.* 148 (1982) 411–418.
- [39] P. Steullet, P.M. Guerin, Perception of breath components by the tropical bont tick, *Amblyomma variegatum* Fabricius (Ixodidae), *J. Comp. Physiol.* 170 (1992) 665–676.
- [40] P. Steullet, P.M. Guerin, Identification of vertebrate volatiles stimulating olfactory receptors on the tarsus I of the tick *Amblyomma variegatum* Fabricius (Ixodidae), *J. Comp. Physiol.* 174 (1993) 27–38.

- [41] B.W Bissinger, C.S Apperson, D.W Watson, C. Arellano, D.E Sonenshine, R.M Roe, Novel field assays and the comparative repellency of BioUD®, DEET and permethrin against *Amblyomma americanum*, Med. Vet. Entomol. 25 (2011) 217–226.
- [42] J.L. Woods, D.G. James, J.C. Lee, D.H. Gent, Evaluation of airborne methyl salicylate for improved conservation biological control of two-spotted spider mite and hop aphid in Oregon hop yards, Exp. Appl. Acarol. 55 (2011) 401–416.
- [43] J.F Carroll, Development of a bioassay for evaluating tick (Acari: Ixodidae) attractants in the field, P. Entomol. Soc. Wash. 110 (2006) 82–91.
- [44] A.I. Irvin, J.R. Hagler, M.S. Hoddie, Laboratory investigation of triple marking the parasitoid *Gonatocerus ashmeadi* with a fluorescent dye and two animal proteins, Entomol. Exp. Appl. 143 (2012) 1–12.
- [45] J.R Hagler, V.P. Jones, A protein-based approach to mark arthropods for mark-capture type research, Entomol. Exp. Appl. 2 (2010) 177–192.
- [46] Y. Kuwahara, N. Asami, M. Morr, S. Matsuyama, T. Suzuki, Chemical ecology of astigmatid mites. XXXVIII. Aggregation pheromone and kairomone activity of lardolure and its analogues against *Lardoglyphus konoi* and *Carpoglyphus lactis*, Appl. Entomol. Zool. 29 (1994) 253–257.
- [47] R.O. Maranga, A. Hassanali, G.P. Kaaya, J.M. Mueke, Attraction of *Amblyomma variegatum* (ticks) to the attraction-aggregation-attachment pheromone with or without carbon dioxide, Exp. Appl. Acarol. 29 (2003) 121–130.
- [48] A.S. Bowman, P. Nuttal, Ticks: Biology, Disease and Control, Cambridge University Press, Cambridge, 2008.
- [49] R. Schoni, E. Hess, W. Blum, K. Ramstein, The aggregation-attachment pheromone of the tropical bont tick *Amblyomma variegatum* Fabricius (Acari: Ixodidae); isolation, identification and action of its components, J. Insect Physiol. 30 (1984) 613–668.
- [50] R.A.I. Norval, T. Peter, C.E. Yunker, D.E. Sonenshine, M.J. Burrridge, Responses of the ticks *Amblyomma americanum* and *A. variegatum* to known or potential components of the aggregation-attachment pheromone. I. Long-range attraction, Exp. Appl. Acarol. 13 (1991) 11–18.
- [51] R.A.I. Norval, T. Peter, C.E. Yunker, D.E. Sonenshine, M.J. Burrridge, Response of the ticks *Amblyomma hebraeum* and *A. variegatum* to known or potential components of the aggregation-attachment pheromones. III. Aggregation, Exp. Appl. Acarol. 16 (1992) 237–245.

- [52] N. Barré, G.I. Garris, O. Lorvelec, Field sampling of the tick *Amblyomma variegatum* (Acari: Ixodidae) on pastures in Guadeloupe: attraction of CO₂ and/or tick pheromones and conditions of use, *Exp. Appl. Acarol.* 21 (1997) 95–108.
- [53] D.E. Sonenshine, Pheromones and other semiochemicals of the Acari, *Annu. Rev. Entomol.* 30 (1985) 1–28.
- [54] J.B. Benoit, G. Lopez-Martinez, S.A. Philips, M.A. Elnitsky, J.A. Yoder, R.E. Lee Jr., D.L. Denlinger, The seabird tick, *Ixodes uriae*, uses uric acid in penguin guano as a kairomone and guanine in tick feces as an assembly pheromone on the Antarctic Peninsula. *Polar Biol.* 31 (2008) 1445–1451.
- [55] N.L. Treverrow, B.F. Stone, M. Cowie, Aggregation pheromone in two Australian hard ticks, *Ixodes holocyclus* and *Aponomma concolor*, *Experientia.* 33 (1977) 680–682.
- [56] F. Dusbábek, P. Šimek, A. Jegorov, J. Tříška, Identification of xanthine and hypoxanthine as components of assembly pheromone in excreta of argasid ticks, *Exp. Appl. Acarol.* 11 (1991) 307–316.
- [57] M.G. Leahy, Z. Hajkova, J. Bourchalova, Two female pheromones in the metastriate tick, *Hyalomma dromedarii* (Acarina: Ixodidae), *Acta Entomol. Bohemos.* 78 (1981) 224–230.
- [58] S. Grenacher, T. Kröber, P.M. Guerin, M. Vlimant, Behavioral and chemoreceptor cell response of the tick *Ixodes ricinus* to its own feces and faecal constituents, *Exp. Appl. Acarol.* 25 (2001) 641–660.
- [59] S.A. Allan, D.E. Sonenshine, Evidence of an assembly pheromone in the black-legged deer tick, *Ixodes scapularis*, *J. Chem. Ecol.* 28 (2002) 15–27.
- [60] M.G. Leahy, S. Sternberg, C. Mango, R.J. Galun, Lack of specificity in assembly pheromones of soft ticks (Acari: Argasidae), *Med. Entomol.* 31 (1975) 413–414.
- [61] R. Gothe, A.W.H. Neitz, Investigation into the participation of male pheromones of *Rhipicephalus evertsi evertsi* during infestation, *Onderstepoort J. Vet.* 52 (1985) 67–70.
- [62] D.E. Sonenshine, T. Adams, S.A. Allan, J. McLaughlin, F.X. Webster, Chemical composition of some components of the arrestment pheromone of the black-legged tick, *Ixodes scapularis* (Acari: Ixodidae) and their use in tick control, *J. Med. Entomol.* 40 (2003) 849–859.
- [63] C. McMahon, T. Kröber, P.M. Guerin, In vitro assay for repellents and deterrents for ticks: Differing effects of products when tested with attractant or arrestment stimuli, *Med. Vet. Entomol.* 17 (2003) 370–378.

- [64] J.L. Brunner, L. Cheney, F. Keesing, M. Killilea, K. Logiudice, A. Previtali, R.S. Ostfeld, Molting success of *Ixodes scapularis* varies among individual blood meal hosts and species, *J. Med. Entomol.* 48 (2011) 860–866.
- [65] M. Colloff, *Dust Mites*, CSIRO Publishing, Melbourne, 2009.
- [66] S. Regev, W.W. Cone, Evidence of farnesol as a male sex attractant of the two spotted spider mite, *Tetranychus urticae* Koch (Acarina: Tetranychidae), *Environ. Entomol.* 4 (1975) 307–311.
- [67] S. Regev, W.W. Cone, Analyses of pharate female two spotted spider mites for nerolidol and geraniol: evaluation for sex attraction of males, *Environ. Entomol.* 5 (1976) 133–138.
- [68] S. Regev, W.W. Cone, The monoterpene citronellol, as a male sex attractant of the two spotted spider mite, *Tetranychus urticae* (Acarina: Tetranychidae), *Environ. Entomol.* 9 (1980) 50–52.
- [69] N.J. Fashing, Morphological adaptations associated with mate-guarding behavior in the genus *Hericia* (Acari: Algophagidae), in: R.B. Halliday, D.E. Walter, H.C. Proctor, R.A. Norton, M.J. Colloff, M.J. (Eds), *Acarology: Proceedings of the 10th International Congress*, CSIRO Publishing, Melbourne, 2001, pp. 176–179.
- [70] I. Yasui, The receptor sites of sex pheromone eliciting precopulatory mite guarding behavior of male predatory mite *Macrocheles muscaedomesticae* (Scopoli), *J. Ethol.* 10 (1992) 81–83.
- [71] W. Witalinski, J. Dabert, M.G. Walzl, Morphological adaptation for precopulatory guarding in astigmatic mites (Acari: Acarididae), *Int. J. Acarol.* 18 (1992) 49–54.
- [72] K. Oku, Effects of density experience on mate guarding behavior by adult male Kanzawa spider mite, *J. Ethol.* 27 (2009) 279–283.
- [73] M. Sato, Y. Kuwahara, S. Matsuyama, Chemical ecology of astigmatid mites XXXVII; Fatty acids as food attractant of astigmatid mites, its scope and limitations, *Appl. Entomol. Zool.* 28 (1993) 565–569.
- [74] Y. Kuwahara, M. Sato, T. Koshii, T. Suzuki, Chemical ecology of astigmatid mites. XXXII. 2-Hydroxy-6-methyl-benzaldehyde, the sex pheromone of the brown-legged grain mite, *Aleuroglyphus ovatus* (Troupeau) (Acarina: Acaridae), *Jpn. Soc. Appl. Entomol. Zool.* 27 (1992) 253–260.
- [75] A. Ryono, N. Mori, K. Okabe, Y. Kuwahara, Chemical ecology of astigmatid mites, LVIII. 2-Hydroxy-6-methylbenzaldehyde: Female sex pheromone of *Cosmoglyphus hughesi* Samsinak (Acari: Acaridae), *Appl. Entomol. Zool.* 36 (2001) 77–81.

- [76] K. Tatami, N. Mori, R. Nishida, Y. Kuwahara, 2-hydroxy-6-methylbenzaldehyde: the female sex pheromone of the house dust mite *Dermatophagoides farinae* (Astigmata: Pyroglyphidae), *Jpn. Soc. Med. Entomol. Zool.* 52 (2001) 279–286.
- [77] N. Mori, Y. Kuwahara, K. Kurosa, R. Nishida, T. Fukushima, Chemical ecology of astigmatid mites. XLI. Undecane: The sex pheromone of the acarid mite *Caloglyphus rodriguezii* Samsinak (Acarina: Acaridae), *Appl. Entomol. Zool.* 30 (1995) 415–423.
- [78] N. Mori, Y. Kuwahara, K. Kuroas, Chemical ecology of astigmatid mites. XLV. (2R, 3R)-Epoxyneral: Sex pheromone of the acarid mite *Caloglyphus* sp. (Acarina: Acaridae), *Bioorgan. Med. Chem.* 4 (1996) 289–295.
- [79] N. Mori, Y. Kuwahara, K. Kuroas, Rosefuran: The sex pheromone of the acarid mite *Caloglyphus* sp., *J. Chem. Ecol.* 24 (1998) 1771–1779.
- [80] A. Mizoguchi, N. Mori, R. Nishida, Y. Kuwahara, α -Acaridial a female sex pheromone from an alarm pheromone emitting mite *Rhizoglyphus robini*, *J. Chem. Ecol.* 29 (2003) 1681–1690.
- [81] A. Mizoguchi, K. Murakami, N. Shimizu, N. Mori, R. Nishida, Y. Kuwahara, S-Isorobinal as the female sex pheromone from an alarm pheromone-emitting mite, *Rhizoglyphus setosus*, *Exp. Appl. Acarol.* 36 (2005) 107–117.
- [82] G. Maruno, N. Mori, Y. Kuwahara, Chemical ecology of the Astigmatid mites. LXXXVII. S-(+)-Isopiperitenone: Re-identification of the alarm pheromone as the female sex pheromone in *Tyrophagus similis* (Acari: Acaridae), *J. Chem. Ecol.* 38 (2012) 36–41.
- [83] N. Mori, Y. Kuwahara, Comparative studies of the ability of males to discriminate between sexes in *Caloglyphus* sp., *J. Chem. Ecol.* 26 (2000) 1299–1309.
- [84] Y. Saito, *Plant Mites and Sociality: Diversity and Evolution*, Springer Publishing, Tokyo, 2010.
- [85] D.E. Sonenshine, 2,6-Dichlorophenol, the sex pheromone of the Rocky Mountain wood tick, *Dermacentor andersoni* (Stiles) and the American dog tick, *Dermacentor variabilis* (Say), *J. Chem. Ecol.* 2 (1976) 201–211.
- [86] T. Price, D.E. Sonenshine, R.A.I. Norval, C.E. Yunker, M.J. BurrIDGE, Pheromonal composition of two species of African *Amblyomma* ticks: Similarities, difference and possible species specific components, *Exp. Appl. Acarol.* 18 (1994) 37–50.
- [87] L. Borges, A.E. Eiras, P.H. Ferri, A.C.C. Lobo, The role of 2,6-dichlorophenol as a sex pheromone of the tropical horse tick *Anocentor nitens* (Acari: Ixodidae), *Exp. Appl. Acarol.* 27 (2002) 223–230.

- [88] K.K. Gachoka, L.L. Ferreira, C.C.B. Louly, L.M.F. Borges, Induction of complete courtship ritual in *Amblyomma cajennense* using 2,6-dichlorophenol at female-equivalent quantities, *Rev. Bras. Parasitol. Vet.* 20 (2011) 347–350.
- [89] R.S. Berger, 2,6-dichlorophenol, sex pheromone of the lone star tick. *Science*. 177 (1972) 704–705.
- [90] C.C.B. Louly, D.D. Silveira, S.F. Soares, P.H. Ferri, A.C.C. de Melo, L.M.F. Borges, More about the role of 2,6-dichlorophenol in tick courtship: Identification and olfactometer bioassay in *Amblyomma cajennense* and *Rhipicephalus sanguineus*, *Mem. I. Oswaldo Cruz*. 103 (2008) 60–65.
- [91] S.F. Soares, M.L.F. Borges, Electrophysiological responses of the olfactory receptors of the tick *Amblyomma cajennense* (Acari: Ixodidae) to host-related and tick pheromone-related synthetic compounds, *Acta Trop.* 124 (2012) 192–198.
- [92] D.E. Sonenshine, J.G. Hamilton, W.R. Lusby, Use of cholesteryl esters as mounting sex pheromone in combination with 2,6-dichlorophenol and pesticides to control populations of hard ticks, United States Patent, patent no. 5,149,526, 1992.
- [93] Y. Kuwahara, How astigmatic mites control the emission of two or even three types of pheromones from the same gland, in: M.W. Sabelis, J. Bruin (Eds), *Trends in Acarology: Proceedings on the 12th International Conference*, Springer Publishing, London, 2010, pp. 241-246.
- [94] K. Nishimura, N. Shimizu, N. Mori, Y. Kuwahara, Chemical ecology of astigmatid mites. LXIV. The alarm pheromone neral functions as an attractant in *Schwiebea elongata* (Banks) (Acari: Acaridae), *Appl. Entomol. Zool.* 37 (2002) 13–18.
- [95] A.C. Skelton, M.M. Cameron, J.A. Pickett, M.A. Birkett, Identification of neryl formate as the airborne aggregation pheromone for the American house dust mite and the European house dust mite (Acari: Epidermoptidae), *Med. Vet. Entomol.* 47 (2010) 798–804.
- [96] K.A. Achiano, J.H. Giliomee, Feeding behavior of the potential predators of the house flies *Musca domestica* L. and *Fannia canicularis* (L.) (Diptera: Muscidae), *Afr. Entomol.* 14 (2006) 69–75.
- [97] M.C. Wicht, J.G. Rodriguez, W.T. Smith Jr., M. Jalil, Attractant to *Macrocheles muscaedomesticae* (Acarina) present in the housefly, *Musca domestica*, *J. Insect. Physiol.* 17 (1971) 63–67.
- [98] P.E. Kaufman, M. Burgess, D.A. Rutz, C. Glenister, Population dynamics of manure inhabiting arthropods under an integrated pest management (IPM) program in New York poultry facilities - 3 case studies, *J. Appl. Poultry Res.* 11 (2002) 90–103.

- [99] D.R. Tarpy, J. Summers, Managing *Varroa* Mites in Honeybee Colonies, North Carolina Cooperative Extension Service, N.C. State University: Raleigh, 2014.
- [100] D. Sammataro, U. Gerson, G. Needham, Parasitic mites of honeybees: Life history, implications and impacts, *Annu. Rev. Entomol.* 45 (2000) 519–548.
- [101] Y. Le Conte, G. Arnold, J. Trouiller, C. Masson, B. Chappe, G. Ourisson, Attraction of the parasitic mite *Varroa jacobsoni* to the drone larvae of honeybees by simple aliphatic esters, *Science. PRS* (1989) 638–639.
- [102] N.W. Calderone, S. Lin, Behavioral responses of *Varroa destructor* (Acari: Varroidae) to extracts of larvae, cocoons, and food brood of worker and drone honey bees, *Apis mellifera* (Hymenoptera: Apidae), *Physiol. Entomol.* 26 (2001) 341–350.
- [103] O. Kilpinen, How to obtain a bloodmeal without being eaten by a host: the case of poultry red mite, *Dermanyssus gallinae*, *Physiol. Entomol.* 30 (2005) 232–240.
- [104] C.J.M. Koenraadt, M. Dick, The role of volatiles in aggregation and host-seeking of the haematophagous poultry red mite *Dermanyssus gallinae* (Acari: Dermanyssidae), *Exp. Appl. Acarol.* 50 (2010) 191–199.
- [105] J.F. Carroll, Notes on the responses of host-seeking nymphs and adults of the ticks *Ixodes scapularis* and *Amblyomma americanum* (Acari: Ixodidae) to canine, avian and deer-produced substances, *P. Entomol. Soc. Wash.* 104 (2002) 73–78.
- [106] J.F. Carroll, Responses of three species of adult ticks (Acari: Ixodidae) to chemicals in the coats of principal and minor hosts, *J. Med. Entomol.* 36 (1999) 238–241.
- [107] R. Garcia, Carbon dioxide as an attractant for certain ticks (Acarina: Argasidae and Ixodidae), *Ann. Entomol. Soc. Am.* 55 (1962) 605–606.
- [108] J.F. Carroll, Interdigital gland substances of white-tailed deer and the response of host-seeking ticks (Acari: Ixodidae). *J. Med. Entomol.* 38 (2001) 114–117.
- [109] C. McMahon, P.M. Guerin, Attraction of the tropical bont tick, *Amblyomma variegatum* to human breath and to the breath components acetone, NO, and CO₂, *Naturwissenschaften.* 89 (2002) 311–315.
- [110] K.H. Holscher, H.L. Gearhart, R.W. Barker, Electrophysiological response of three tick species to carbon dioxide in the laboratory and field, *Ann. Entomol. Soc. Am.* 73 (1980) 288–292.
- [111] R.B. Anderson, G.J. Scrimgeour, W.R. Kaufman, Responses of the tick, *Amblyomma hebraeum* (Acari: Ixodidae) to carbon dioxide, *Exp. Appl. Acarol.* 22 (1998) 667–681.

- [112] A.A. Gugliemone, E.D. Morehouse, G. Wolf, Attraction to carbon dioxide of unfed stages of *Amblyomma trigutatum* under field conditions. *Acarologia*. 26 (1985) 123–9.
- [113] R.C. Falco, D. Fish, Horizontal movement of adult *Ixodes dammini* (Acari: Ixodidae) attracted to CO₂ baited traps, *J. Med. Entomol.* 28 (1991) 726–729.
- [114] C.M. Gherman, A.D. Mihalca, M.O. Dumitrache, A. Gyorke, I. Oroian, M. Sandor, V. Cozma, CO₂ flagging, an improved method for collection of questing ticks, *Parasit. Vectors*. 5 (2012) 125.
- [115] A. Mackay, L. Foil, Seasonal distribution of adult *Ixodes scapularis* Say (Acari: Ixodidae) in Louisiana, *J. Vector. Ecol.* 30 (2005) 168–170.
- [116] E.A Dykstra, P.D. Teel, Influence of daily activity of adult *Rhipicephalus sanguineus* (Acari: Ixodidae) on CO₂-trap sampled in acaricide efficacy trials, *Southwest Entomol.* 19 (1994) 119–128.
- [117] P. Steullet, P.M. Guerin, Identification of vertebrate volatiles stimulating olfactory receptors on tarsus I of the tick *Amblyomma variegatum* Fabricius (Ixodidae) II, Receptors outside the Haller's organ capsule, *J. Comp. Physiol.* 174 (1994) 39–47.
- [118] R.A.I. Norval, Field sampling of unfed adults of *Amblyomma hebraeum* Koch, *Exp. Appl. Acarol.* 3 (1987) 213–217.
- [119] R.A.I. Norval, C.E. Yunker, J.D. Gibson, S.L.D. Deem, Field sampling of unfed nymphs of *Amblyomma hebraeum*, *Exp. Appl. Acarol.* 4 (1988) 173–177.
- [120] C.N. Smith, M.M. Cole, H.K. Gouk, Biology and control of the American dog tick, *USDA Tech. Bull.* 905 (1946) 74.
- [121] D.A. Osborn, K.V. Miller, D.M. Hoffman, W.H. Dickerson, J.W. Gasset, C.F. Quist, Morphology of the white-tailed deer tarsal gland, *Acta Theriol.* 45 (2000) 117–122.
- [122] K.J. Alexy, J.W. Gasset, D.A. Osburn, K.V. Miller, S.M. Russell, Bacterial fauna of the tarsal tufts of White-tailed deer (*Odocoileus virginianus*), *Am. Midl. Nat.* 149 (2003) 237–240.
- [123] R.G. Harvey, J. Harari, A.J. Delauche, *Ear Diseases of the Dog and Cat*, Manson Publishing, London, 2001.
- [124] J.F. Carroll, J.J. Grasela, Occurrence of adult American dog ticks, *Dermacentor variabilis* (Say) around small animal traps and vertebrate carcasses, *P. Entomol. Soc. Wash.* 88 (1998) 253–256.

- [125] A.K. Dobrotvorský, A.V. Tkachev, R.I. Naumov, C.F. Carroll, Study of host odour determinants of questing behavior in *Ixodes* ticks, in: M. Kazimírová, M. Labuda, P.A. Nuttall (Eds), Proceedings of the 3rd International Conference on Tick and Tick Borne Diseases, High Tatra Mountains Press, Slovakia, 2000, pp. 229-233.
- [126] S.A. Leonovich, Phenol and lactone receptors in the distal sensilla of the Haller's organ in *Ixodes ricinus* ticks and their possible role in host perception, *Exp. Appl. Acarol.* 32 (2004) 89–102.
- [127] S. Tatemoto, T. Shimoda, Olfactory Responses of the predatory mites (*Neoseiulus cucumeris*) and insects (*Orius strigicollis*) to two different plant species infested with onion thrips (*Thrips tabaci*), *J. Chem. Ecol.* 34 (2008) 605–613.
- [128] N.S. Aratchige, I. Lesna, M.W. Sabelis, Below ground plant parts emit herbivore-induced volatiles: olfactory responses of a predatory mite to tulip bulbs infested by rust mites, *Exp. Appl. Acarol.* 33 (2004) 21–30.
- [129] H. Ishiwari, T. Suzuki, T. Maeda, Essential compounds in herbivore-induced plant volatiles that attract the predatory mite *Neoseiulus womersleyi*, *J. Chem. Ecol.* 33 (2007) 1670–1681.
- [130] M.M. Amin, R.F. Mizell III, R.W. Flowers, Response of the predatory mite *Phytoseiulus macropilis* (Acari: Phytoseiidae) to pesticides and kairomones of three spider mite species (Acari: Tetranychidae) and non-prey food, *Fla. Entomol.* 92 (2009) 554–562.
- [131] M. Dicke, T.A. Van Beek, M.A. Posthumus, N. Ben Don, H. Van Bokhoven, A.E. De Groot, Isolation and identification of volatile kairomone that affects acarine predator-prey interactions: Involvement of host plant in its production, *J. Chem. Ecol.* 16 (1990) 381–396.
- [132] J.G. De Boer, M.A. Posthumus, M. Dicke, Identification of volatiles that are used in discrimination between plants infested with prey or non-prey herbivores by a predatory mite, *J. Chem. Ecol.* 30 (2004) 2215–2230.
- [133] R. Gols, M. Roosjen, H. Dijman, M. Dicke, Induction of direct and indirect plant response by jasmonic acid, low spider mite densities, or a combination of jasmonic acid treatment and spider mite infestation, *J. Chem. Ecol.* 29 (2003) 2651–2666.
- [134] T. Shimoda, A key volatile infochemical that elicits a strong olfactory response of the predatory mite *Neoseiulus californicus*, an important natural enemy of the two-spotted spider mite *Tetranychus urticae*, *Exp. Appl. Acarol.* 50 (2009) 9–22.
- [135] T. Shimoda, R. Ozawa, K. Sano, E. Yano, J. Takabayashi, The involvement of volatile infochemicals from spider mites and from food-plants in prey location of the generalist predatory mite, *Neoseiulus californicus*, *J. Chem. Ecol.* 31 (2005) 2019–2032.

- [136] M.W. Sabelis, A. Janssen, J. Takabayashi, Can plants evolve stable alliances with the enemies of enemies?, *J. Plant Interact.* 6 (2011) 71–75.
- [137] S.M. Hassan, O.O. Dipeolu, M.M. Malonza, Natural attraction of livestock ticks by the leaves of a shrub, *Trop. Anim. Health Pro.* 26 (1994) 87–91.
- [138] M. Vanhaelen, R. Vanhaelen-Fastré, J. Geeraets, T. Wirthlin, *Cis*- and *trans*-octa-1, 5-dien-3-ol; new attractants to the cheese mite *Tyrophagus putrescentiae* (Schrank) (Acaridae) identified in *Trichothecium roseum* (Fungi imperfecti), *Microbios.* 23 (1979) 199–212.
- [139] M. Vanhaelen, R. Vanhaelen-Fastré, J. Geeraets, Occurrence in mushrooms (Homobasidiomycetes) of *cis*- and *trans*-octa-1, 5-dien-3-ol: attractants to the cheese mite *Tyrophagus putrescentiae* (Schrank) (Acaridae), *Experientia.* 36 (1980) 406–407.
- [140] S.A. Allan, N. Barré, D.E. Sonenshine, M.J. Burrridge, Efficiency of tags impregnated with pheromone and acaricide for control of *Amblyomma variegatum*, *Med. Vet. Entomol.* 12 (1998) 141–150.
- [141] R.A.I. Norval, D.E. Sonenshine, M.I. Meltzer, M.J. Burrridge, Attractant decoy for controlling bont ticks, United States Patent Office, patent no. 5,296,277, 1994.
- [142] S.A. Allan, D.E. Sonenshine, M.J. Burrridge, Tick pheromones and uses thereof, United States Patent Office. Patent no. 6,331,297, 2002.
- [143] D.E. Sonenshine, D. Taylor, G. Corrigan, Studies to evaluate the effectiveness of sex pheromone impregnated formulations for control of populations of the American dog tick *Dermacentor variabilis* (Say) (Acari: Ixodidae), *Exp. Appl. Acarol.* 1 (1985) 23–24.
- [144] J.G. Hamilton, D.E. Sonenshine, Methods and apparatus for controlling arthropods populations, United States Patent Office, patent no. 4,884,361, 1989.
- [145] M.S. Abdel-Rahman, M.M. Fahmy, M.G. Aggour, Trials for control of ixodid ticks using pheromone-acaricide tick decoys, *J. Egypt. Soc. Parasitol.* 28 (1998) 551–557.
- [146] J.E. George, Present and future technologies for tick control, *Ann. N.Y. Acad. Sci.* 916 (2000) 583–588.
- [147] H.S. Ginsberg, Tick control: Trapping, biocontrol, host management, and other alternative strategies, in: D.E. Sonenshine, R.M. Roe (Eds), *Biology of ticks*, Oxford University Press, New York, 2014, pp. 409–434.
- [148] B. Drukker, J. Bruin, M.W. Sabelis, Anthocorid predators learn to associate herbivore induced plant volatiles with presence or absence of prey, *Physiol. Entomol.* 25 (2000) 260–265.

[149] J.A. Pickett, T.J.A. Bruce, K. Chamberlain, A. Hassanali, Z.R. Khan, M.C. Matthes, J.A. Napier, L.E. Smart, L.J. Wadhams, C.M. Woodcock, Plant volatiles yielding new ways to exploit plant defense, in: M. Dicke, W. Tekken (Eds), *Chemical Ecology: From Gene to Ecosystem*, Springer Press, The Netherlands, 2006, pp. 161–173.

[150] Z.R. Khan, D.G. James, C.A.O. Midega, J.A. Pickett, Chemical ecology and conservation biological control, *Biol. Control*. 45 (2008) 210–224.

[151] H. Yu, Y. Zang, K. Wu, X.W. Gao, Y.Y. Guo, Field-testing of synthetic herbivore-induced plant volatiles as attractants for beneficial insects, *Environ. Entomol.* 37 (2008) 1410–1415.

[152] J.C. Lee, Methyl salicylate as a natural enemy attractant in strawberry fields, *Environ. Entomol.* 39 (2010) 653–660.

Tables

Table 1.1. Mite pheromones and chemical components that elicit attractive or aggregative behavioral responses

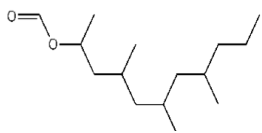
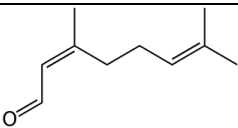
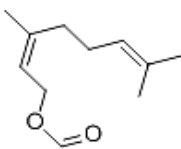
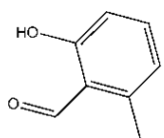
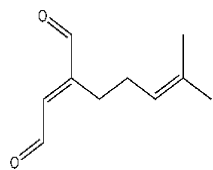
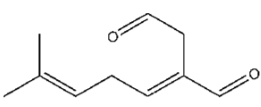
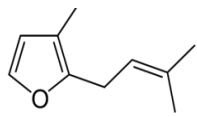
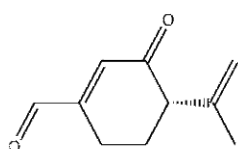
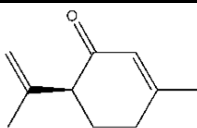
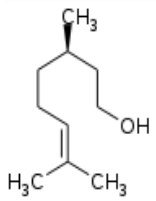
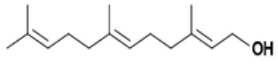
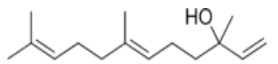
Pheromone	Attractive components	Mite species ^a	Reference	Formula	Structure
Mite aggregation pheromone	Lardolure	<i>C. polyphyllae</i> <i>L. konoii</i>	[46]	C ₁₅ H ₃₀ O ₂	
Mite alarm pheromone	Neral	<i>S. elongata</i>	[93], [94]	C ₁₀ H ₁₆ O	
	Neryl formate	<i>D. farinae</i> <i>D. pteronyssinus</i>	[93], [95]	C ₁₁ H ₁₈ O ₂	
Mite female sex pheromone	(2R,3R)-Epoxyneral	<i>Caloglyphus</i> sp.	[78]	C ₁₀ H ₁₆ O ₂	
	2-Hydroxy-6-methylbenzaldehyde	<i>A. immobilis</i> <i>A. ovatus</i> <i>C. hughesi</i> <i>D. farinae</i>	[73], [74], [75], [76]	C ₈ H ₈ O ₂	
	α-Acaridial	<i>R. robini</i>	[80]	C ₁₀ H ₁₄ O ₂	
	β-Acaridial	<i>Caloglyphus</i> sp.	[35]	C ₁₀ H ₁₄ O ₂	
	Rosefuran	<i>Caloglyphus</i> sp.	[79]	C ₁₀ H ₁₄ O	
	S-Isorobinal	<i>R. setosus</i>	[81]	C ₁₀ H ₁₂ O ₂	

Table 1.1. Continued

Pheromone	Attractive components	Mite species ^a	Reference	Formula	Structure
Mite female sex pheromone	S-Isopiperitenone	<i>T. similis</i>	[82]	C ₁₀ H ₁₄ O	
	Undecane	<i>C. rodriguezi</i>	[78]	C ₁₁ H ₂₄	
Mite Immature female pheromone	Citronellol	<i>T. urticae</i>	[66]	C ₁₀ H ₂₀ O	
	Farnesol	<i>T. urticae</i>	[67]	C ₁₅ H ₂₆ O	
	Nerolidol	<i>T. urticae</i>	[68]	C ₁₅ H ₂₆ O	

^a*Acarus immobilis*, *Aleuroglyphus ovatus*, *Caloglyphus polyphyllae*, *Caloglyphus rodriguezi*, *Cosmoglyphus hughesi*, *Dermatophagoides farinae*, *Dermatophagoides pteronyssinus*, *Lardoglyphus konoi*, *Rhizoglyphus robini*, *Rhizoglyphus setosus*, *Schwiebea elongata*, *Tetranychus urticae*, *Tyrophagus similis*

Table 1.2. Tick pheromones and chemical components that elicit attractive or aggregative behavioral responses

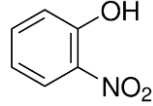
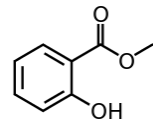
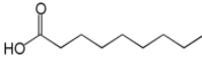
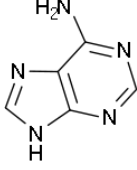
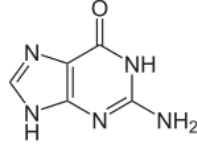
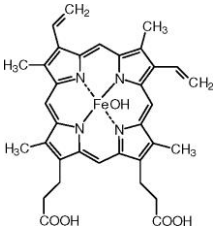
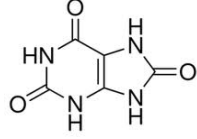
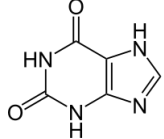
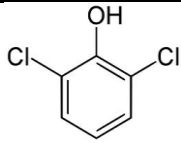
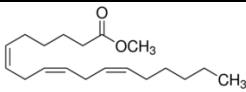
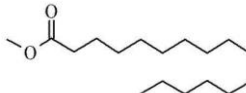
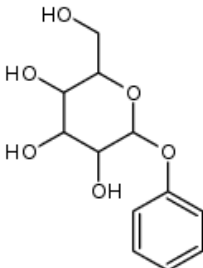
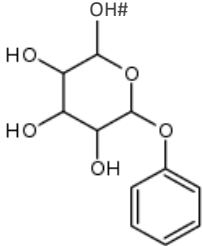
Pheromone	Attractive components	Tick species ^a	Reference	Formula	Structure
Tick attraction-aggregation-attachment pheromone	<i>O</i> -Nitrophenol	<i>A. hebraeum</i> <i>A. variegatum</i>	[49], [50], [51], [52]	C ₆ H ₅ NO ₃	
	Methyl salicylate	<i>A. hebraeum</i> <i>A. variegatum</i>	[49], [50], [51], [52]	C ₈ H ₈ O ₃	
	Nonanoic acid	<i>A. variegatum</i>	[49], [52]	C ₉ H ₁₈ O ₂	
Tick assembly pheromone	Adenine	<i>I. scapularis</i>	[54], [62]	C ₅ H ₅ N ₅	
	Guanine	<i>I. ricinius</i> <i>I. scapularis</i> <i>I. uriae</i>	[54], [58], [62]	C ₅ H ₅ N ₅ O	
	Hematin	<i>I. ricinius</i>	[54], [58]	C ₃₄ H ₃₃ N ₄ O ₅ F _e	
	Uric acid	<i>I. ricinius</i> <i>I. uriae</i>	[54], [58]	C ₅ H ₄ N ₄ O ₃	
	Xanthine	<i>I. ricinius</i> <i>I. scapularis</i>	[54], [58], [62]	C ₅ H ₄ N ₄ O ₂	

Table 1.2. Continued

Pheromone	Attractive components	Tick species ^a	Reference	Formula	Structure
Tick sex pheromone	2,6-Dichlorophenol	<i>A. nitens</i> <i>A. americanum</i> <i>A. cajennense</i> <i>A. hebraeum</i> <i>A. variegatum</i> <i>D. andersoni</i> <i>D. variabilis</i> <i>H. anatolicum</i> <i>H. dromedarii</i> <i>R. appendiculatus</i> <i>R. microplus</i> <i>R. sanguineus</i>	[9], [26], [38], [85], [86], [87], [88], [89], [90], [91],	C ₆ H ₃ Cl ₂ OH	

^a*Amblyomma americanum*, *Amblyomma cajennense*, *Amblyomma hebraeum*, *Amblyomma variegatum*, *Anocentor (Dermacentor) nitens*, *Dermacentor andersoni*, *Dermacentor variabilis*, *Hyalomma anatolicum*, *Hyalomma dromedarii*, *Ixodes ricinus*, *Ixodes scapularis*, *Ixodes uriae*, *Rhipicephalus appendiculatus*, *Rhipicephalus microplus*, *Rhipicephalus sanguineus*

Table 1.3. Chemical components of host kairomones that elicit attractive behavioral responses in mites

Chemical component	Associated host	Mite species ^a	Reference	Formula	Structure
Methyl linolenate	Honeybee	<i>V. destructor</i>	[101], [102]	C ₁₉ H ₃₂ O ₂	
Methyl palmitate	Honeybee	<i>V. destructor</i>	[101], [102]	C ₁₇ H ₃₄ O ₂	
N-Phenyl-N-glucoside	Housefly	<i>M. muscaedomesticae</i>	[96], [97]	C ₁₂ H ₁₆ O ₆	
N-Phenyl-N-mannoside	Housefly	<i>M. muscaedomesticae</i>	[96], [97]	C ₁₂ H ₁₆ O ₆	
Carbon dioxide	Poultry	<i>D. gallinae</i>	[103]	CO ₂	O=C=O

^a*Dermanyssus gallinae*, *Macrocheles muscaedomesticae*, *Varroa destructor*

Table 1.4. Chemical components of host kairomones that elicit attractive behavioral responses in ticks

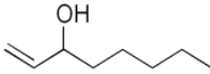
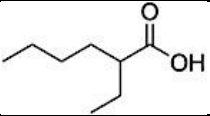
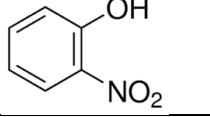
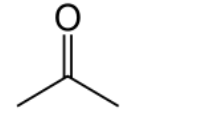
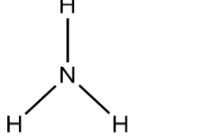
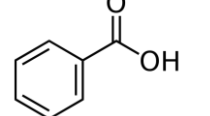
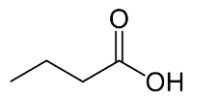
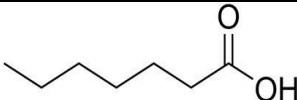
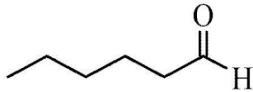
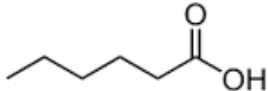
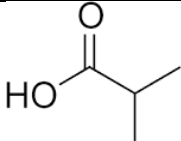
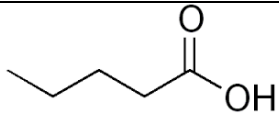
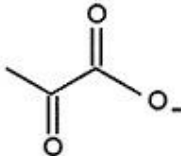
Chemical component	Associated host	Tick species ^a	Reference	Formula	Structure
1-Octen-3-ol	Cattle	<i>A. americanum</i> <i>A. cajennense</i> <i>A. hebraeum</i> <i>R. microplus</i> <i>I. ricinus</i>	[28], [36], [89], [118], [119]	C ₈ H ₁₆ O	
2-Ethylhexanoic acid	Cattle	<i>R. microplus</i>	[28]	C ₈ H ₁₆ O ₂	
2-Nitrophenol	Cattle	<i>R. microplus</i>	[28]	C ₆ H ₅ NO ₃	
Acetone	Cattle, Dogs, Humans, White-tailed deer	<i>A. americanum</i> <i>A. hebraeum</i>	[36], [109]	C ₃ H ₆ O	
Aliphatic aldehydes	Cattle Rabbit	<i>A. variegatum</i>	[40]	N/A	Specific chemical structures are unknown
Ammonia	Cattle, Dogs, Humans, White-tailed deer	<i>A. americanum</i>	[36]	NH ₄	
Aromatic aldehydes	Cattle Rabbit	<i>A. variegatum</i>	[39]	N/A	Specific chemical structures are unknown
Benzoic acid	Cattle	<i>R. microplus</i>	[28]	C ₇ H ₆ O ₂	
Butyric acid	Cattle	<i>R. microplus</i>	[28]	C ₄ H ₈ O ₂	

Table 1.4. Continued

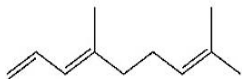
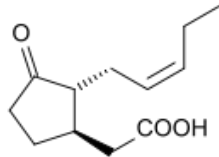
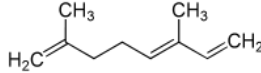
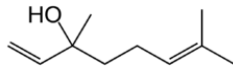
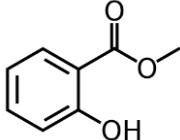
Chemical component	Associated host	Tick species ^a	Reference	Formula	Structure
Carbon dioxide	Cattle, Dogs, Humans, White-tailed deer	<i>A. americanum</i> <i>A. hebraeum</i> <i>A. maculatum</i> <i>A. triguttatum</i> <i>A. variegatum</i> <i>D. andersoni</i> <i>D. variabilis</i> <i>I. dammini</i> <i>I. ricinus</i> <i>I. scapularis</i> <i>R. microplus</i> <i>R. sanguineus</i>	[26], [36], [39], [110], [111], [112], [113], [114], [115], [116]	CO ₂	O=C=O
Heptanoic acid	Cattle	<i>R. microplus</i>	[28]	C ₇ H ₁₄ O ₂	
Hexanal	Cattle	<i>R. microplus</i>	[28]	C ₆ H ₁₂ O	
Hexanoic acid	Cattle	<i>R. microplus</i>	[28]	C ₆ H ₁₂ O ₂	
Isobutyric acid	Cattle	<i>R. microplus</i>	[28]	C ₄ H ₈ O ₂	
Lactones	Cattle Rabbit	<i>I. ricinus</i>	[126]	N/A	Specific chemical structures are unknown
Pentanoic acid	Cattle	<i>R. microplus</i>	[28]	C ₅ H ₁₀ O ₂	
Pyruvate	Cattle	<i>R. microplus</i>	[28]	C ₃ H ₃ O ₃	

^a*Amblyomma americanum*, *Amblyomma hebraeum*, *Amblyomma maculatum*, *Amblyomma triguttatum*, *Amblyomma variegatum*, *Dermacentor andersoni*, *Dermacentor variabilis*, *Ixodes dammini*, *Ixodes persulcatus*, *Ixodes ricinus*, *Ixodes scapularis*, *Rhipicephalus microplus*, *Rhipicephalus sanguineus*

Table 1.5. Plants and herbivore induced plant volatiles that elicit attractive behavioral responses in mites

Plant	Chemical components	Mite species ^a	Reference	Formula	Structure
Camellia tea plant	4,8-Dimethyl-1,3,7-nonatriene	<i>N. womersleyi</i>	[129]	C ₁₁ H ₁₈	
	α-Farnesene	<i>N. womersleyi</i>	[129]	C ₁₅ H ₂₄	
	β-Ocimene	<i>N. womersleyi</i>	[129]	C ₁₀ H ₁₆	
Cucumber plant	4,8-Dimethyl-1,3,7-nonatriene	<i>N. cucumeris</i>	[127]	C ₁₁ H ₁₈	
	α-Ocimene	<i>N. cucumeris</i>	[127]	C ₁₀ H ₁₆	
	Linalool	<i>N. californicus</i> <i>N. cucumeris</i>	[127], [134], [135]	C ₁₀ H ₁₈ O	
	Methyl salicylate	<i>N. californicus</i> <i>N. cucumeris</i>	[127], [134], [135]	C ₈ H ₈ O ₃	
Kidney bean plant	4,8-Dimethyl-1,3,7-nonatriene	<i>N. womersleyi</i>	[129]	C ₁₁ H ₁₈	
	4,8,12-Trimethyl-1,3,7,11-tridecatetraene	<i>N. womersleyi</i>	[129]	C ₁₆ H ₂₆	
	β-Caryophyllene	<i>N. womersleyi</i>	[129]	C ₁₅ H ₂₄	
	Methyl salicylate	<i>N. womersleyi</i>	[129]	C ₈ H ₈ O ₃	

Table 1.5. Continued

Plant	Chemical components	Mite species ^a	Reference	Formula	Structure
Lima bean plant	4,8-Dimethyl-1,3,7-nonatriene	<i>P. persimilis</i>	[131], [132]	C ₁₁ H ₁₈	
	Jasmonic acid	<i>P. persimilis</i>	[133]	C ₁₂ H ₁₈ O ₃	
	α-Ocimene	<i>P. persimilis</i>	[131], [132]	C ₁₀ H ₁₆	
	Linalool	<i>P. persimilis</i>	[131], [132]	C ₁₀ H ₁₈ O	
	Methyl salicylate	<i>P. persimilis</i>	[131], [132]	C ₈ H ₈ O ₃	

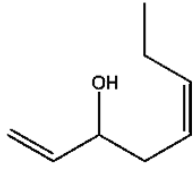
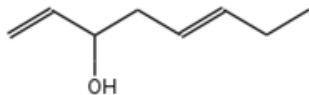
^a*Neoseiulus cucumeris*, *Neoseiulus womersleyi*, *Neoseiulus californicus*, *Phytoseiulus persimilis*

Table 1.6. Plant volatiles that elicit attractive behavioral responses in ticks

Plant	Chemical components	Tick species^a	Reference	Formula	Structure
Acalypha plant	Unknown	<i>R. appendiculatus</i>	[137]	Unknown	Unknown
Calpurnia plant	Unknown	<i>R. appendiculatus</i> <i>R. pulchellus</i>	[37]	Unknown	Unknown

^a*Rhipicephalus appendiculatus*, *Rhipicephalus pulchellus*

Table 1.7. Chemical components of fungal allomones that elicit attractive behavioral responses in mites

Chemical component	Associated host	Mite species ^a	Reference	Formula	Structure
<i>cis</i> -Octa-1,5-dien-3-ol	Fungi	<i>T. putrescentiae</i>	[138], [139]	C ₈ H ₁₄ O	
<i>trans</i> -Octa-1,5-dien-3-ol	Fungi	<i>T. putrescentiae</i>	[138], [139]	C ₈ H ₁₄ O	

^a*Tyrophagus putrescentiae*

Figures

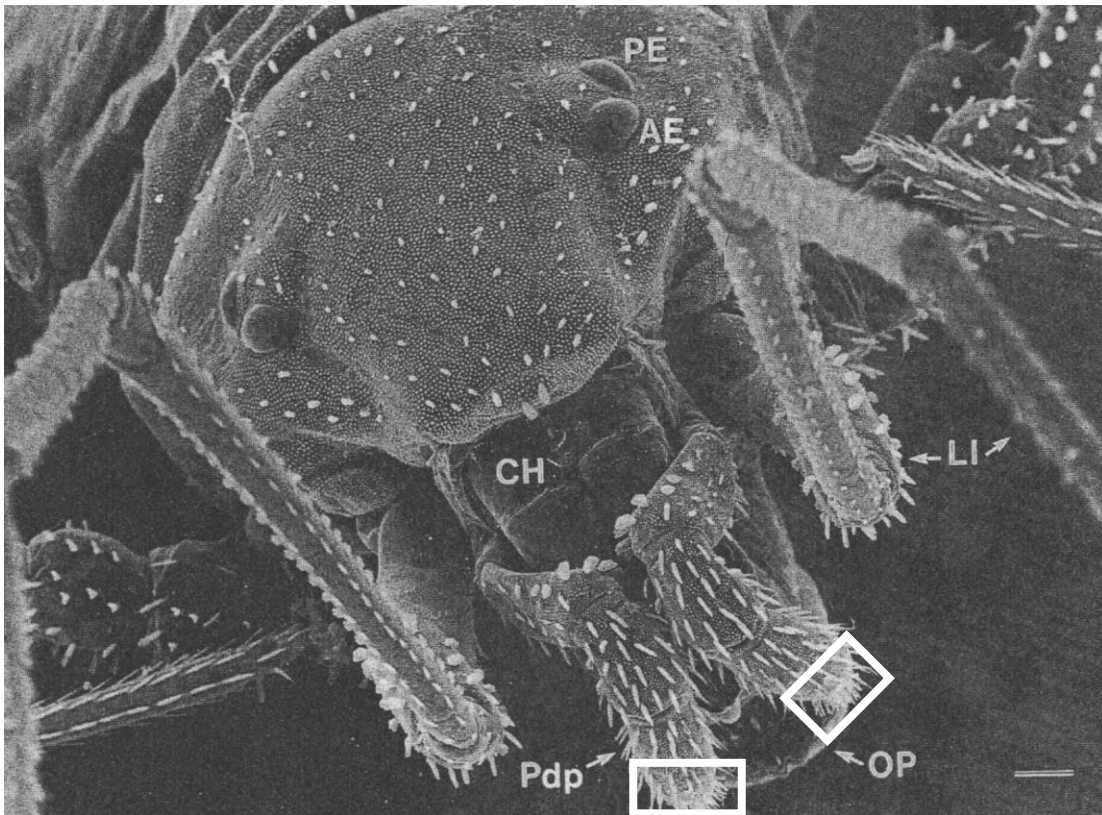


Figure 1.1. The palpal organ (boxed), located on the tip of the palp pedipalp of the *Neocarus texanus* mite (AE = anterior eye, CH = chelicera, OP = ovipositor, LI = leg I, PE = posterior eye, Pdp = pedipalp), used with permission from Wiley-Liss © 1999 Alberti and Coons

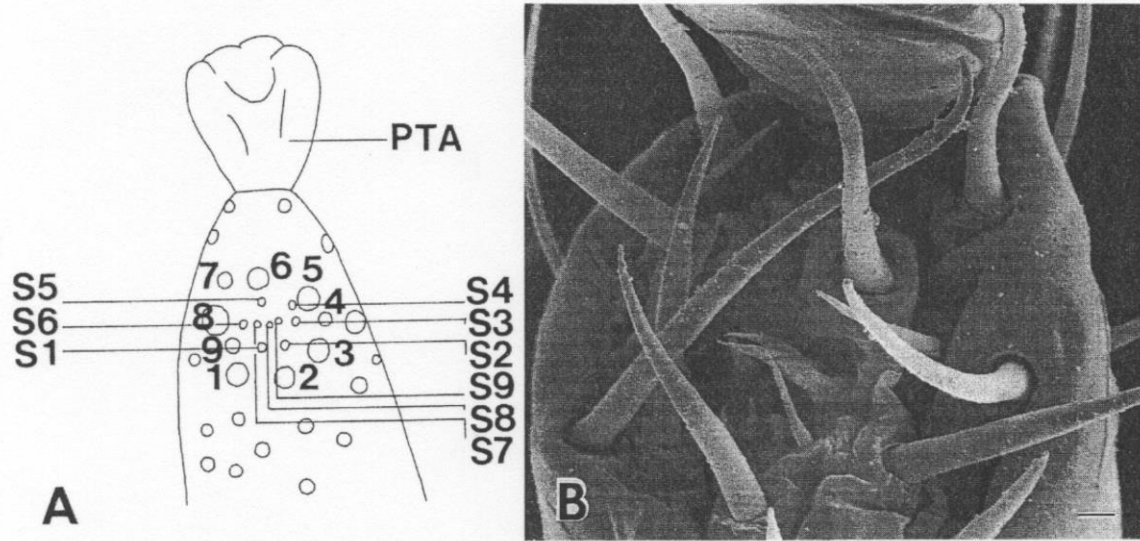


Figure 1.2. (A, B) Sensillar organization in the tarsal complex, located on the foretarsus of the first pair of legs of the *Varroa jacobsoni* mite (1-9 = edge bristles, PTA = ambulacrum, S1-S9 = pit sensilla), used with permission from Wiley-Liss © 1999 Alberti and Coons

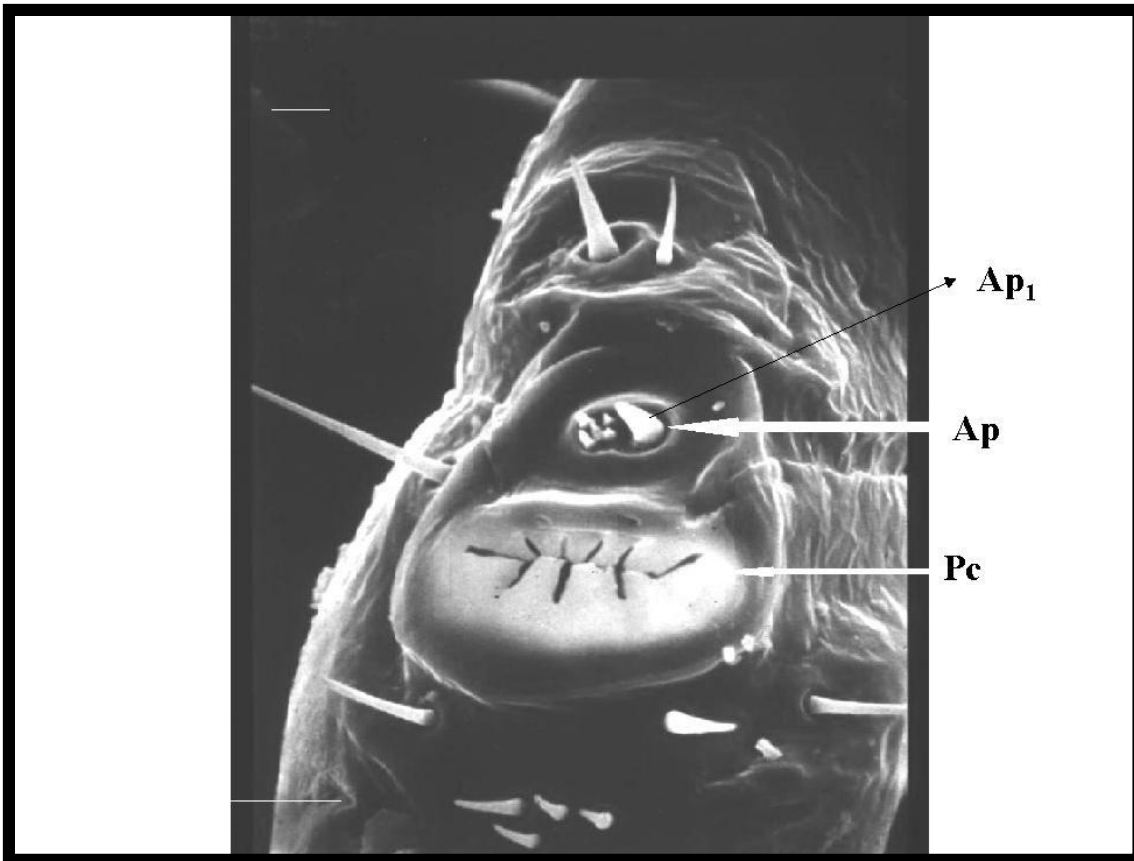


Figure 1.3. The Haller's organ, located on the first tarsus of the first pair of legs of the American dog tick, *Dermacentor variabilis* (Ap = anterior pit, Ap₁ = large setiform sensillum, Pc = posterior capsule), used with permission from Cambridge © 2004 Sonenshine

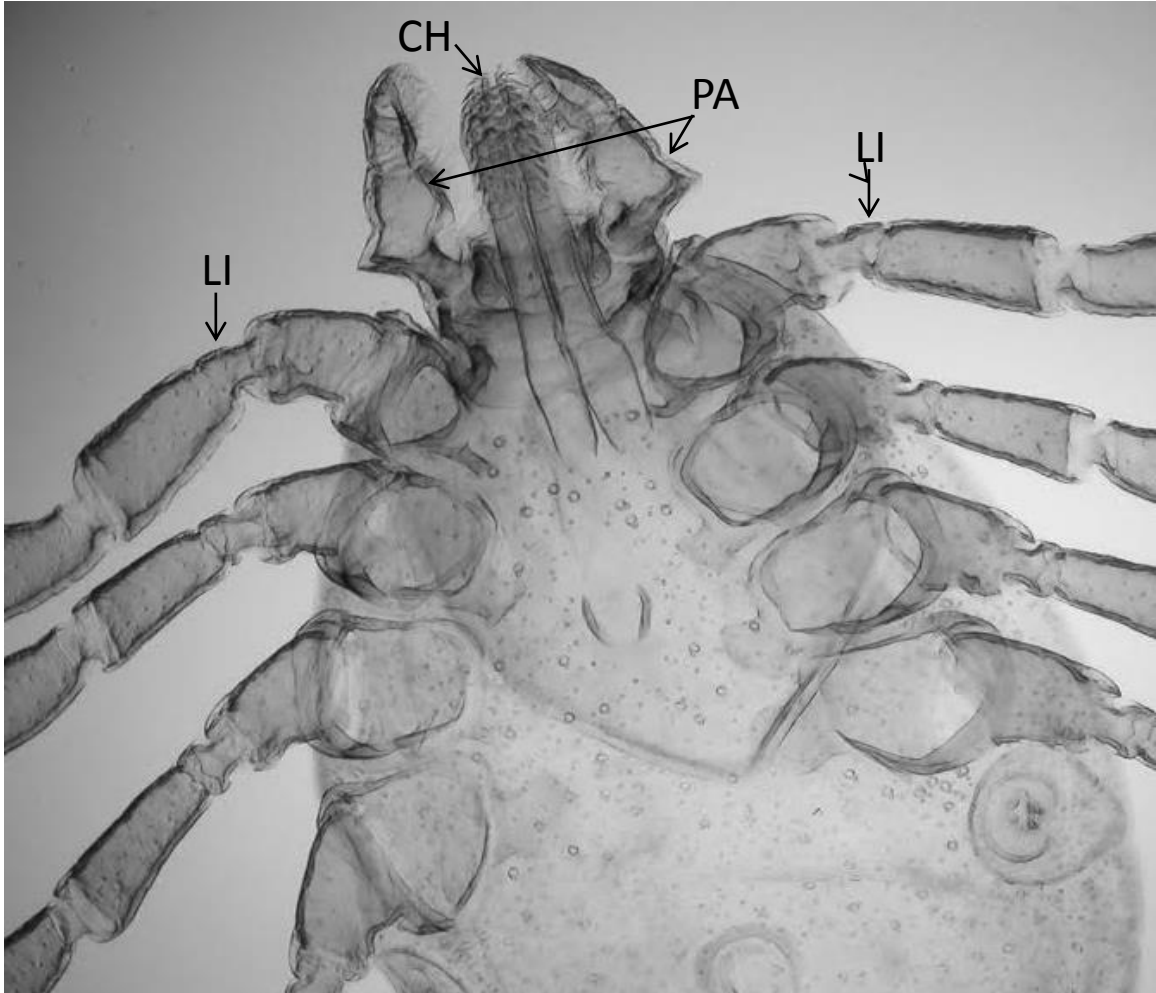


Figure 1.4. Mouthparts of the tick *Hyalomma savignyi* with possibly chemo-mechanosensory functions (CH = chelicerae, LI = leg I, PA = palps)

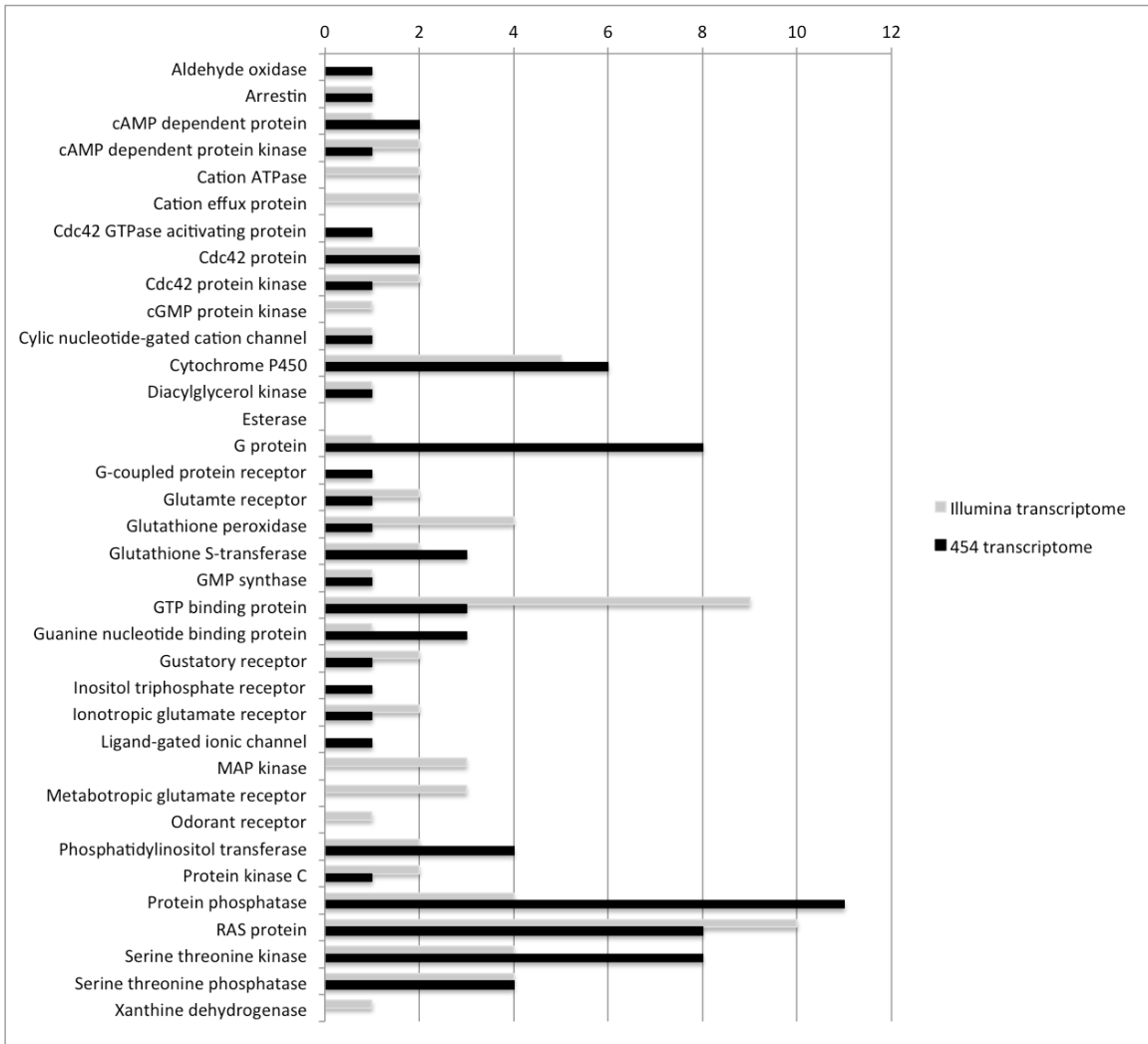


Figure 1.5. The number of each type of probable olfactory and gustatory messages identified in both the 454 and Illumina Haller’s organ transcriptomes that are found in the *Ixodes scapularis* genome and have annotations and pfam domains [Carr and Roe, unpublished]

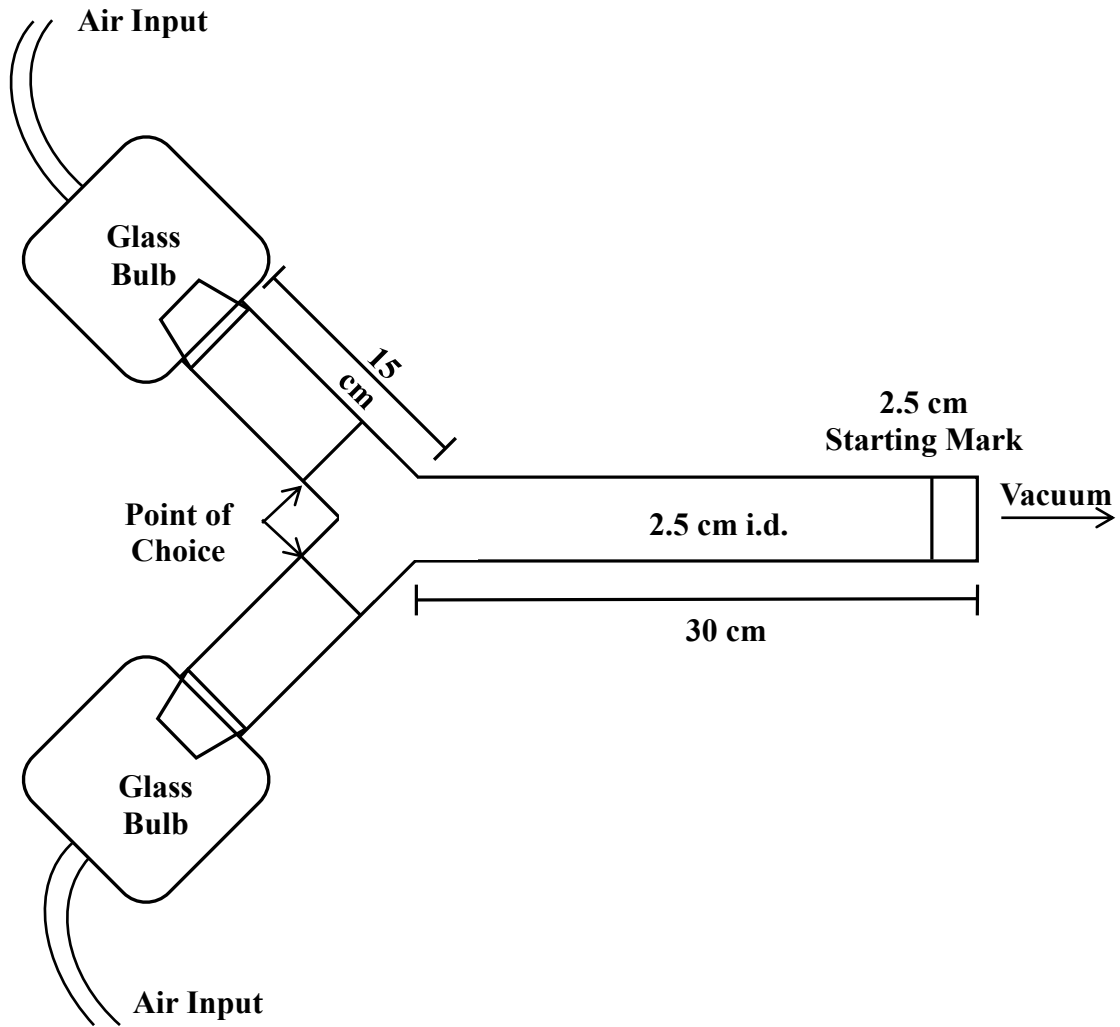


Figure 1.6. Image of olfactometer with two ports for use in laboratory bioassays of acarine attractants, used with permission from Wiley & Sons Inc. © 2012 Carr et al.

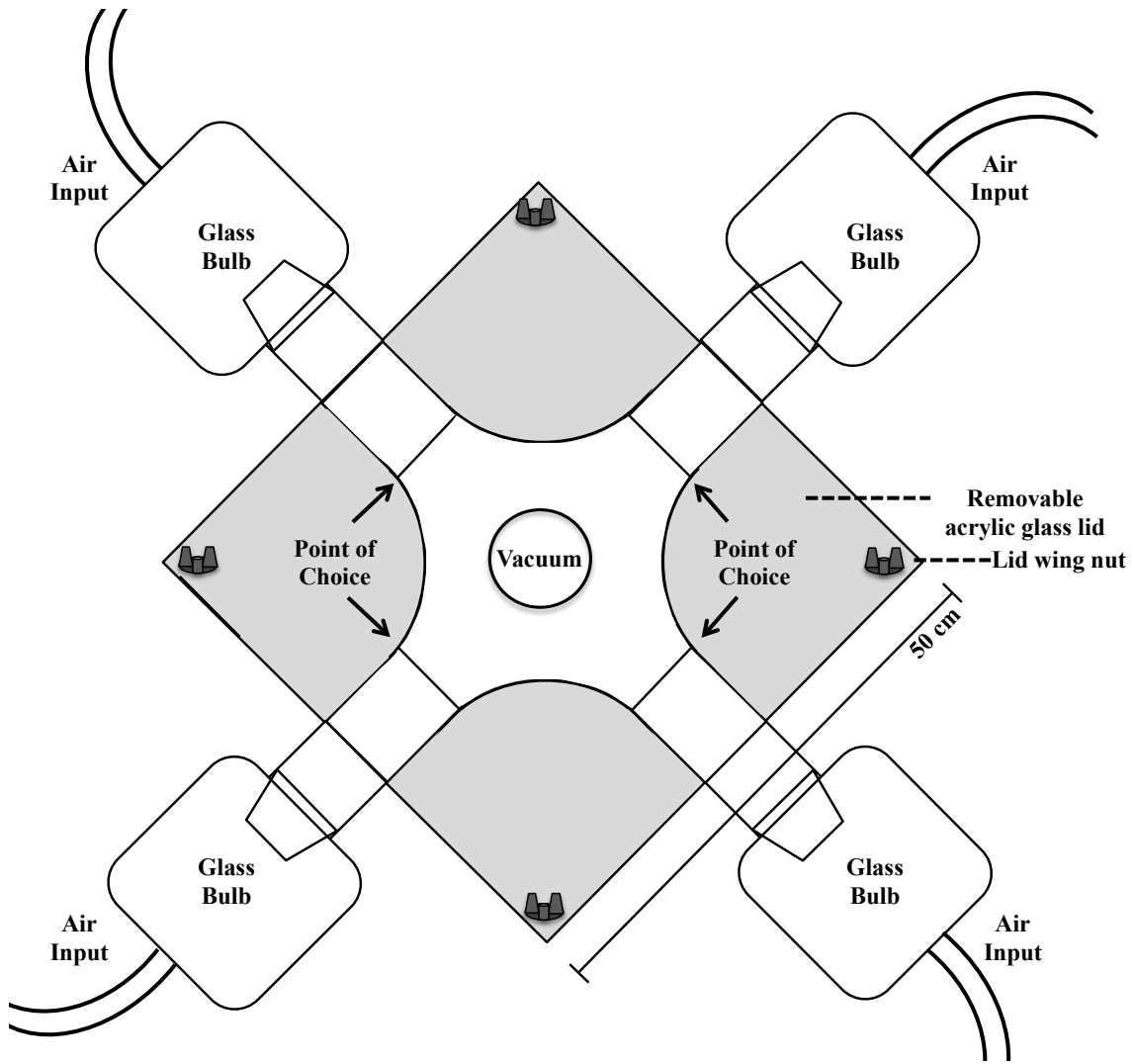


Figure 1.7. Image of olfactometer with four ports for use in laboratory bioassays of acarine attractants

Putative GPCR Signaling Pathway Identified in the Haller's Organ of Male American Dog Ticks, *Dermacentor variabilis*

This chapter was formatted for submission to the *PLoS One Neuroscience* with the coauthors Robert D. Mitchell III¹, Anirudh Dhammi¹, Dr. Brooke Bissinger², Dr. Daniel E. Sonenshine³, and Dr. R. Michael Roe¹.

¹ Department of Entomology, North Carolina State University, Raleigh, North Carolina, 27695 USA

² Tyratech, Raleigh, North Carolina, 27560

³ Department of Biological Sciences, Old Dominion University, Norfolk, Virginia, 23529 USA

Abstract

The Haller's organ is a unique chemosensory organ of ticks that is not found in any other animal. Through next-generation sequencing technology and comparative analyses we have generate the first transcriptome to the Haller's organ. Results of BLAST analyses of the Haller's organ specific transcriptome suggest that the chemosensory mechanism is a G-protein coupled receptor (GPCRs) signal cascade. Additionally, only olfactory GPCRs were identified suggesting, despite conflicting morphological data, that the Haller's organ functions only in olfaction and not gustation. Each component of the olfactory GPCR signal cascade was identified, except for the odorant binding proteins. This suggests that ticks rely on either a novel, unknown class of binding proteins and/or other methods of sensilla lymph solubilization to deliver odorant molecules from the environment to chemoreceptors. qPCR experiments documenting the expression profile of the olfactory transcripts GPCR, G_{α} , and β -arrestin in unfed and blood-fed adult female and male *D. variabilis* determined that there is hormonal regulation of the olfactory system in tick. Behavioral assays confirmed the role of the Haller's organ in chemical avoidance, in addition to its known role is chemical attraction. Remarkably, it was determined that the Haller's organ is not required for host attachment or blood-feeding.

Introduction

Ticks are blood-feeding ectoparasites that cause direct harm to humans and animals. They inflict painful wounds and skin irritations during feeding, as well as vector microbial agents that cause debilitating diseases. Ticks in the genus *Dermacentor* are distributed worldwide and vector pathogens responsible for various types of encephalitis, spotted fever, tick fever,

typhus, and additional diseases (1). In the US, the American dog tick, *D. variabilis* (Acari: Ixodidae), is the most prolific member of the genus and the primary vector of *Rickettsia rickettsii*, the causative agent of Rocky Mountain spotted fever (1, 2). Tick physiology requires blood meals for molting, sexual maturation, reproduction; blood-feeding provides a means of pathogen transmission between ticks and hosts (3, 4).

Successful blood feeding is dependent on the efficient detection of hosts within the proximate environment of the tick. Ticks rely heavily on chemosensation to identify and locate hosts. Chemosensation is mainly ascribed to the Haller's organ, a unique structure found on the foretarsus of the first pair of legs (Fig. 2.1) that is not found in any other animal except ticks. In addition to detecting host kairomones, these chemoreceptors are also involved in the detection of pheromones, aggregation chemicals, repellents and environmental cues needed for life off the host (5). Despite the pivotal role of the Haller's organ as the primary component of the tick peripheral sensory system, and its presence only in ticks, little is known about its genetic structure or molecular function. The Haller's organ is essentially a molecular black box with no information on its mechanism of chemosensation.

Through next-generation sequencing and comparative transcriptomics between the 1st and 4th pair of legs (the latter without the Haller's organ) in *D. variabilis* we have generated the first transcriptome to the Haller's organ. Haller's organ specific transcripts were then compared to proteins associated with chemosensation in insects and nematodes to identify putative odorant binding proteins (OBPs), chemosensory proteins (CSPs), odorant receptors (ORs), gustatory receptors (GRs), odorant receptor kinases (ORKs), odorant degrading enzymes (ODEs; refs 6, 7) and to determine the mechanism of chemoreception in ticks. The

protein functions of putative tick chemosensory transcripts were characterized through sequence alignments, phylogenetic analyses, identification of conserved functional domains and gene expression analysis. The findings in this study are consistent with the role of the Haller's organ in olfactory chemoreception but not gustatory function, despite the conflicting morphological data. Our evidence from next-generation sequencing suggests that the chemosensory signal pathway of ticks is a G-protein coupled receptor (GPCR) signal cascade that lacks the odorant binding proteins described in insects. The gene expressions of putative chemosensory proteins were successfully characterized before and after blood feeding, providing valuable insight into the links between chemosensory signaling, tick endocrinology, and behavior providing new leads for the development of tick acaricides and repellents. In addition to the molecular findings, the results of bioassays stipulate a new understanding of the role of the Haller's organ in host seeking versus blood feeding behavior.

Results and Discussion

Sequencing and Transcriptomic Assembly. Two transcriptome datasets were generated using the normalized 1st and 4th leg cDNA libraries and constructed from individual reads from Illumina RNA Hiseq 2000 (Illumina, San Diego, CA). In total, 106 million reads were obtained for the 1st legs, assembled into 88,289 contigs establishing the illumina 1st leg transcriptome; 180 million reads were obtained from the 4th legs, assembled into 105,827 contigs establishing the illumina 4th leg transcriptome. Using Blast2Go and the GenBank non-redundant database, at least one putative function with an expected value (e-value) of <10 was identified for 71,114 of the illumina 1st leg contigs (80.5% of the total number of contigs) and 83,647 of the illumina 4th leg contigs (79.0% of contigs). Due to the exclusive

location of the Haller's organ on the 1st pair of legs, an *in silico* subtraction was performed between the illumina 1st and 4th leg contigs for only those contigs with putative functions. Removal of illumina 1st leg contigs with identical counterparts, based on putative function and accession number, in the illumina 4th leg transcriptome resulted in the identification of 38,087 contigs exclusive to the 1st legs, and what will be referenced in this paper as the Haller's organ spf (specific) transcriptome. Permission was also obtained to include a combined unfed virgin adult female and male *D. variabilis* 1st leg transcriptome generated using 454 pyrosequencing in BLAST searches for chemosensory transcripts. The fasta file for the 454 1st leg transcriptome contained 33,981 contigs with at least one putative function, with an e-value of <10, was identified for 22,151 of the contigs (65.2% of the total number of contigs). The nomenclature for the four transcriptomes used throughout this manuscript is as follows: the 454 1st leg transcriptome, the Haller's organ spf transcriptome, the illumina 1st leg transcriptome, and the illumina 4th leg transcriptome. Additional analysis results of the 454 1st leg, illumina 1st leg, and illumina 4th leg transcriptome, including gene ontology annotation and the top 50 most abundant transcripts are described in *Supplemental Information: Results* (Figs. 2.S1-2.S3 and Tables 2.S1 and 2.S2).

No Odorant Binding Proteins in Ticks. BLASTx and BLASTn searches of the illumina 1st leg, illumina 4th leg, and Haller's organ spf transcriptome did not identify any transcripts putatively encoding OBPs or pheromone binding proteins (PBPs; e-value ≤ 1.0).

Additionally, BLASTx and BLASTn searches of the 454 1st leg transcriptome did not identify any putative OBPs or PBPs (e-value ≤ 1.0). To further validate these findings, the NCBI BLAST+ toolkit and the 'makeBLASTdb' UNIX coding were used to create a

BLASTable illumina 1st leg BLAST database from the illumina 1st leg transcriptome fasta file. The illumina 1st leg BLAST database was uploaded into the program Geneious (Biomatters, Auckland, New Zealand), and discontinuous BLASTn searches of the illumina 1st leg BLAST database conducted for OBPs and PBPs (e-value ≤ 1.0). OBPs and PBPs have been well characterized in the Dipteran species *Aedes aegypti*, *Anopheles gambiae* and *Drosophila melanogaster*. All of the OBPs and PBPs for these Dipteran species reviewed and verified by Uniprot (*A. aegypti* GOBP, accession no. AAA29347.1; *A. aegypti* OBP45, accession no. EAT37277.1; *A. aegypti* OBP83a, accession no. CAF02084.1; *A. gambiae* OBP66, accession no. EAU77642.1; *A. gambiae* OBP67, accession no. EAL42143.2; *A. gambiae* OBP68, accession no. EAU77839.1; *A. gambiae* OBP69, accession no. EGK96890.1; *A. gambiae* OBP70, accession no. EAA11535.2; *A. gambiae* OBP71, accession no. EAL42442.3; *A. gambiae* OBP72, accession no. EDO64833.1; *D. melanogaster* LUSH, accession no. AAB58940.1; *D. melanogaster* OBP19a, accession no. AAF50910.2; *D. melanogaster* OBP19d, accession no. AAC46475.1; *D. melanogaster* OBP28a, accession no. AAC46478.1; *D. melanogaster* OBP56a, accession no. AAL49345.1; *D. melanogaster* OBP56d, accession no. AAF57520.1; *D. melanogaster* OBP56h, accession no. AAY55796.1; *D. melanogaster* OBP57a, accession no. AAM69286.1; *D. melanogaster* OBP57b, accession no. AAM69285.1; *D. melanogaster* OBP57c, accession no. AAF57467.1; *D. melanogaster* OBP57d, accession no. AAM69287.1; *D. melanogaster* OBP57e, accession no. AAF57460.2; *D. melanogaster* OBP69a, accession no. AAC46474.1; *D. melanogaster* OBP83a, accession no. AAC46476.1; *D. melanogaster* OBP84a, accession no. AAC46477.1; *D. melanogaster* OBP99a, accession no. AAM29630.1; *D. melanogaster* OBP99b, accession no. AAM50904.1; *D. melanogaster* PBP6, accession no. AAA21356.1)

were used in discontinuous BLASTn searches of the illumina 1st leg BLAST database, and no putative OBPs or PBPs were identified (e-value ≤ 1.0). BLASTn and BLASTx searches of all the tick and mite sequence data in GenBank using the same OBPs and PBPs described above also did not identify any putative tick OBPs or PBPs (e-value ≤ 1.0). OBPs and PBPs were not present in the 454 1st leg, Haller's organ spf, illumina 1st leg, or illumina 4th leg transcriptomes of *D. variabilis*, and were not present in any of the tick sequence data in GenBank or in the *Ixodes scapularis* genome (8).

In vertebrates all OBPs are lipocalins with no sequence homology with insect OBPs (9). Vertebrate chemosensory lipocalins are identified exclusively in chemosensory tissues and are structurally different from non-chemosensory lipocalins. Since there were no OBPs or PBPs identified in the 454 1st leg, illumina 1st leg, illumina 4th leg or Haller's organ spf transcriptomes or any of the other databases examined, it is possible that tick lipocalins act as OBPs. One transcript encoding a putative salivary-like lipocalin was identified exclusively in the Haller's organ spf transcriptome (Table 2.1) and two additional lipocalins identified in both the illumina 1st and 4th leg transcriptomes. An alignment of the putative Haller's organ spf salivary-like lipocalin with the top tick BLAST hit, an *Amblyomma triste* salivary-like lipocalin, was weak with few conserved residues that are spaced sporadically and are not continuous (Table 2.1; Fig. 2.S3). Based on the alignment it is questionable if the function of this Haller's organ spf transcript is indeed a salivary-like lipocalin. Phylogenetic analysis of the putative Haller's organ spf salivary-like lipocalin suggested it was not related to vertebrate chemosensory lipocalins (Fig. 2.2). The putative salivary-like lipocalin did not cluster in the same node as the vertebrate chemosensory lipocalins. Phylogenetic analysis also determined that there were no structural or functional differences between the Haller's

organ spf salivary-like lipocalin and the two lipocalins identified in the illumina 1st and 4th leg transcriptomes, with all proteins clustering in the same node (Fig. 2.2). With no lipocalins identified exclusively in the Haller's organ spf transcriptome that are functionally related to vertebrate chemosensory lipocalins, it is unlikely that tick lipocalins function as a chemosensory lipocalin. To further verify these findings, BLASTn and BLASTx searches of all the tick and mite sequence data in GenBank were performed searching for vertebrate chemosensory lipocalins with no putative OBPs or PBPs (e-value ≤ 10) found.

There is no evidence in multiple Haller's organ transcriptomes, in current tick and mite sequences in GenBank, and in the *I. scapularis* genome that ticks use OBPs, PBPs or chemosensory lipocalins for chemosensation. These same proteins also are not involved in chemosensation in nematodes (6) suggesting ticks are more like nematodes than insects in relying on either a novel, unknown class of binding proteins and/or other methods of sensilla lymph solubilization not yet described to deliver odorant molecules from the environment to chemoreceptors.

Haller's Organ Not Involved in Gustation. The morphologies of the chemosensory sensilla of the Haller's organ have always inferred that the Haller's organ functions in both olfaction and gustation, presenting with both multipore and tip-pore sensilla. Interestingly, BLASTx and BLASTn searches of the 454 1st leg, illumina 1st leg, illumina 4th leg, and Haller's organ spf transcriptomes did not find any gustatory receptors (e-value ≤ 1). There are gustatory receptors present in ticks, with 56 gustatory receptors identified in the *I. scapularis* genome. Annotation of the *I. scapularis* gustatory receptors determined that they were G-protein coupled receptors (GPCRs) as well as members of the 7-transmembrane chemosensory

receptor family (8). BLASTn searches of the illumina 1st leg BLAST database for the 56 *I. scapularis* gustatory receptors also did not identify any putative gustatory receptors (e-value ≤ 1). The complete lack of gustatory receptors in the 1st legs suggests that primary role of the Haller's organ is olfaction, and that there is a secondary chemosensory organ in ticks, most likely on the pedipalps, associated with gustation. These findings are consistent with results obtained from bioassays that determined the Haller's organ is not required for host attachment or feeding, and only functions in host finding and repellent detection, discussed later in further detail.

G-Protein Coupled Receptors Function as Chemoreceptors in Ticks. Since gustatory receptors in ticks are GPCRS, is it likely that olfactory receptors are also GPCRs. A total of 20 putative GPCRs were identified in the 454 1st leg, illumina 1st leg and illumina 4th leg transcriptomes, and two putative olfactory GPCRs identified exclusively in the Haller's organ spf transcriptome (Table 2.1). In insects, GPCRs can be divided into 4 clades, clade A (rhodopsin-like), B (secretin-like), C (metabotropic glutamate-like), and D (atypical; ref 10). All GPCR chemoreceptors in insects and *C. elegans* belong to either clade A and D, with expression exclusively in chemosensory organs (6, 11). Annotation and phylogenetic analyses of the two putative olfactory GPCR transcripts identified exclusively in the Haller's organ determined that one transcript was a clade A, rhodopsin-like GPCR and the second a clade D, atypical GPCR (Fig. 2.3). Though there was difficulty in conducting the phylogenetic analyses with the clade association of the putative GPCRs changing from A to D depending on the phylogenetic algorithm. This was due to the short nature of the putative olfactory GPCR transcripts, and the inclusion of the *I. scapularis* genome counterparts did

not help to alleviate the problem. With such few olfactory GPCRs identified in the Haller's organ spf transcriptome, and the identified transcripts short in nature, additional BLAST searches were performed in attempts to identify more olfactory GPCRs or additional olfactory receptors. BLASTn searches of the illumina 1st leg BLAST database were performed looking for analogues to *C. elegans* chemosensory GPCRs (str-2, accession no. AAF23508.1; odr-3, accession no. AAG32095.1; nucleotide translations), the insect OR co-receptor OR83b also known as Orco (*A. gambiae*, accession no. AAR14938.1; *D. melanogaster*, accession no. AAT71306.1; nucleotide translations), and several randomly selected odorant receptors from *D. melanogaster* with no results found (e-value ≤ 1.0). It is probable that the identified putative rhodopsin-like and/or atypical GPCR transcripts, exclusive to the Haller's organ, are olfactory receptors. Though, it is also possible that the majority of tick olfactory GPCRs were not identified due to inconsistencies in the 1st leg transcriptome sequencing and assembly.

G-Proteins Involved in Odorant Reception. Heterotrimeric G-proteins are the intracellular components of GPCRs that function to initiate intracellular signaling cascades in response to extracellular stimuli that bind GPCRs. Heterotrimeric G-proteins consist of 3 subunits G_α , G_β , and G_γ (12). The binding of a ligand to the GPCR results in a conformational change that activates the G_α subunit and prompts the dissociation of all G-protein subunits (see illustration in Table 2.1). G_α subunits functions to activate secondary messengers such as AGCs, whereas G_β and G_γ subunits form a dimer and function as signal modulators of G_α (12). In the Haller's organ spf transcriptome, transcripts putatively encoding a G_α and G_β chemosensory-specific subunits were identified (Table 2.1). In *C. elegans* and insects,

particular clades of the G_α , G_β , and G_γ subunits are exclusively expressed in chemosensory neurons while others are associated with GPCRs distributed throughout the whole organism (6, 13). In addition to the G_α and G_β subunits identified in the Haller's organ *spf* transcriptome, five additional transcripts putatively encoding four G_α subunits and one G_β subunit were found common in the 454 1st leg, illumina 1st leg, and illumina 4th leg transcriptomes, and were included in phylogenetic analyses. The G_α subunits can be classified into four clades: $G_{\alpha i}/G_{\alpha o}$, $G_{\alpha q}$, $G_{\alpha s}$, and $G_{12/13}$ (14). Alignment and phylogenetic analysis of the putative G_α subunit transcripts determined that the Haller's organ exclusive transcript encoded a putative $G_{\alpha o}$ subunit, while the common 1st/4th leg transcripts encoded $G_{\alpha q}$ and $G_{\alpha 12/13}$ subunits (Figs. 2.4 and 2.S6). Gene ontology (GO) annotation and pathway identification of the putative $G_{\alpha 12/13}$, $G_{\alpha o}$ and $G_{\alpha q}$ subunits revealed functional roles in G-protein coupled receptor signal pathway and signal transduction (GO term identification no. GO:0007186, GO:0007165, respectively). $G_{\alpha 12/13}$ subunits are primarily associated with cell proliferation, cell survival, cytoskeleton remodeling, and calcium signaling, and are not of interest as possible chemosensory G-proteins (15, 16). In *C. elegans* and insects, $G_{\alpha o}$ and $G_{\alpha q}$ subunits are involved in chemosensation with evidence of G_α protein compartmentalism within chemosensory neurons; $G_{\alpha q}$ subunits are localized to the dendrites, whereas only one $G_{\alpha o}$ subunit is exclusively located along the chemosensory neuron axon (13, 17). The $G_{\alpha o}$ subunit is required for potentiating signals initiated by $G_{\alpha q}$ subunits (18). It is possible that ticks exhibit the same G_α protein compartmentalism as *C. elegans* and insects, establishing a two-step chemosensory signal transduction system. A two-step chemosensory signal transduction system would establish a quorum number of chemoreceptors that must be activated in order for signal transduction. It would also allow for multiple chemoreceptors,

responding to either the same or variant stimuli, to simultaneously build an action potential, allowing for the integration of multiple chemoreceptor inputs into neuron signaling to the tick brain.

G_{β} subunits are important chemoreceptor signal modulators that can function as a dimer with G_{γ} subunits to regulate G_{α} subunits (13,19). G_{γ} subunits are not required for the proper function of G_{β} . In invertebrates G_{β} subunits can be divided in three clades: $\beta 1$, $\beta 2$, and $\beta 5$ (14). Alignment and phylogenetic analysis of the putative G_{β} transcripts determined that both the Haller's organ exclusive and 1st/4th leg transcripts encoded a divergent clade of G_{β} subunits (Figs. 2.5 and 2.S7). GO annotation and pathway identification of the putative G_{β} transcripts revealed functional roles in GTPase regulation (GO term identification no. GO:0043547). The GTPase activity of G_{β} subunits deactivates G_{α} subunits and instigates the re-association of all G-protein subunits with the GPCR (13,19). G_{β} subunits are not well documented in Acari and their roles in sensory signal modulation remain unclear. In *C. elegans* and *D. melanogaster* two G_{β} subunits, a $\beta 2$ and $\beta 5$ like, are expressed in chemosensory neurons and can function in part with or without G_{γ} subunits as negative regulators of G_{α} subunits (13, 19). BLASTx and BLASTn searches of the illumina 1st leg and Haller's organ specific transcriptomes did not find any G_{γ} subunits (e-value ≤ 1). Though, BLASTx and BLASTn searches of the illumina 4th leg and 454 1st leg transcriptomes did identify two G_{γ} subunits. *C. elegans* and insects have two G_{γ} subunits, a chemosensory type 1 and a non-chemosensory type 2 (19). Phylogenetic analysis of the two putative G_{γ} subunits determined that neither were chemosensory (Fig. 2.6). Since G_{β} subunits can form functional dimers with any protein that contains functional domains similar to the G_{γ} domain, the novel type of G_{β} subunit expressed exclusively in the Haller's organ of ticks may function

independently of G_γ subunits with an unknown protein regulator, explaining their absence in both the Haller's organ and illumina 1st leg transcriptomes.

Secondary Messenger Proteins in Odorant Reception. Adenylate/Guanylate cyclases (AGCs) are important enzymes that catalyze the formation of secondary messenger proteins, i.e., cyclic nucleotides (cNMPs). All chemosensory AGCs in insects and nematodes have been identified as transmembrane AGCs, though their classification into different subtypes has not been studied (6, 12). BLASTx and BLASTn searches of the illumina 1st leg, illumina 4th leg, and Haller's organ spf transcriptome identified two transcripts putatively encoding AGCs, an adenylate cyclase and a guanylate cyclase, exclusive to the Haller's organ spf transcriptome (Table 2.1). Alignments and phylogenetic analysis of the two putative AGCs transcripts determined that both transcripts encoded transmembrane AGCs (Figs. 2.S9 and 2.S10). GO annotation and pathway identification of the putative AGC transcripts using revealed functional roles in cNMP biosynthesis and signal transduction (GO term identification no. GO:0006182, GO:0035556, respectively). Since $G_{\alpha o}$ subunits are associated with guanylate cyclase and $G_{\alpha q}$ subunits with adenylate cyclase, it is reasonable to assume that chemosensory AGCs also exhibit the same neuron compartmentalism as seen with G_α subunits (7). The identification of both adenylate and guanylate cyclase exclusively in the Haller's organ further supports the presence of a two-step chemosensory signal transduction system in ticks.

Odorant Ion Channels. Cyclic nucleotide-gated ion channels (CNGs) control the cellular influx of Na^+ and Ca^{2+} ions that leads to neuron depolarization and signal transduction

(illustration in Table 2.1). They are the ultimate targets of the cNMPs generated by AGCs in the GPCR signaling pathway (20). CNG ion channels are thought to function as hetero-oligomers, consisting of various combinations of α - and β -subunits (21). BLASTx and BLASTn searches of the illumina 1st leg, illumina 4th leg, and Haller's organ spf transcriptome identified one transcript putatively encoding a CNG ion channel exclusive to the Haller's organ spf transcriptome. A similar CNG transcript was also identified in the 454 1st leg transcriptome. Alignments and phylogenetic analysis of the putative CNG ion channel transcript determined that it encoded a α - subunit (Fig. 2.S11). GO annotation and pathway identification revealed function roles in ion transmembrane transport (GO term identification no. GO:0034220). No β -subunits were identified. In *C. elegans* and *D. melanogaster* a single type of CNG ion channel α - subunit is expressed in chemosensory neurons and required for chemosensation. *C. elegans* also express a CNG ion channel β -subunit in their chemosensory neurons, but a β -subunit has yet to be identified in *D. melanogaster* antennae (20, 22). The percent identities between the putative CNG ion channel α - subunit and the α - subunits of *C. elegans* and *D. melanogaster* were calculated to be 61% and 66%, respectively, having homologous cNMP binding functional domains (Fig. 2.S12). The percent identity between the *C. elegans* and *D. melanogaster* CNG ion channel α - subunit was calculated to be 30%. Additionally, the putative tick and *C. elegans* CNG ion channel α - subunits were determined to be transcribed from orthologous genes by OrthoDB. It is probable that ticks utilize one CNG ion channel to depolarize chemosensory neurons, and the identified α - subunit is the sole component of that CNG ion channel.

Putative Proteins Involved in Chemoreceptor Modulation. The Haller's organ spf transcriptome was then examined for transcripts encoding proteins involved in chemoreceptor signal termination and stimuli adaptation. BLASTx and BLASTn searches of the illumina 1st leg, illumina 4th leg, and Haller's organ spf transcriptome yielded one putative arrestin transcript that was exclusive to the Haller's organ spf transcriptome (Table 2.2). The same putative arrestin transcript was also identified in the 454 1st leg transcriptome. Arrestins are important protein modulators of GPCR signaling that bind activated GPCRs and sterically inhibit the GPCR signal cascade (illustration in Table 2. 2). Arrestins can be classified into two clades, visual and non-visual otherwise known as β -arrestins (23, 24). Alignment and phylogenetic analysis determined that the identified arrestin transcript encoded a putative cystolic β -arrestin (Fig. 2.S13). GO annotation and pathway identification of the putative β -arrestin transcript revealed a functional role in environmental information processing and signal transduction (GO term identification no. GO:007165). In *C. elegans* and *D. melanogaster* a single cystolic β -arrestin has been identified in chemosensory neurons that is required for the maintenance of GPCR sensitivity. The *C. elegans* and *D. melanogaster* β -arrestins promote the internalization of GPCRs, resulting in signal termination and adaptation to persistent stimuli (23, 24). The percent identity between the putative β -arrestin transcript and the β -arrestins of *C. elegans* and *D. melanogaster* were calculated to be 61% and 68%, respectively, having homologous amino and carboxyl β -arrestin functional domains (Fig. 2.S14). The percent identity between the *C. elegans* and *D. melanogaster* β -arrestins was calculated to be 58%. Additionally, these three β -arrestins were determined to be transcribed from orthologous genes by OrthoDB. It is probable that ticks

only possess one β -arrestin that functions to desensitize chemoreceptors and maintain GPCR sensitivity, and the identified transcript encodes that β -arrestin.

BLASTx and BLASTn searches of the illumina 1st leg transcriptome identified several proteins involved in chemoreceptor signal termination and chemosensory neuron recovery, though these transcripts were also present in the illumina 4th leg transcriptome. The putative calmodulin transcript (contig 01632) responds to increases in intracellular calcium and closes the CNG ion channel, while also promoting the elimination of excess intracellular calcium to help return the chemosensory neuron back to its resting state (25). Putative cNMP phosphodiesterase transcripts (contigs 01856, 04376, 04511, 20766) respond to increases in intracellular cNMP and promote cNMP degradation and signal termination (26). Similar calmodulin and cNMP phosphodiesterase transcripts were also identified in the 454 1st leg transcriptome.

BLASTx and BLASTn searches of the illumina 1st leg, illumina 4th leg, and 454 transcriptomes did not identify any G-protein kinases (GPKs; e-value ≤ 1). But, GPKs are a specialized family of serine threonine kinases (STKs), and several transcripts encoding putative STKs were present in all three transcriptomes. STKs phosphorylate the serine and threonine residues of activated GPCRs, creating binding sites for arrestin (25). GPCRs are involved in a variety of signal transduction pathways in ticks, which may account for the lack of exclusivity of these enzyme modulators. In *C. elegans* several confirmed chemoreceptor signal modulator enzymes are distributed throughout the animal's nervous system, exhibiting similar functions in various types of neurons (6, 23). In ticks and *C. elegans* there may be a limited diversity of GPCR modulator enzymes available, with the function of each enzyme determined by its location rather than its protein identity.

Odorant Degrading Enzymes Involved in Olfaction. BLASTx and BLASTn searches of the illumina 1st leg, illumina 4th leg, and Haller's organ spf transcriptome identified several odorant degrading enzymes (ODEs) that were exclusive to the Haller's organ spf transcriptome including 4 transcripts for cytochrome P450 (P450s and CYPs), 1 transcript for glutathione S-transferase (GSTs), and 2 transcripts for superoxide dismutase (SODs; Table 2.2.). Several putative epoxide hydrolases, esterases and methyltransferases were also identified in the illumina 1st leg transcriptome, but were also found in the illumina 4th leg transcriptome.

P450s are hemethiolate membrane proteins that catalyze the oxidation of lipophilic molecules into reactive oxygen species (ROSs) that are then degraded by GSTs or SODs (27, 28). GSTs and SODs metabolize ROSs into readily excretable hydrophilic products (28). This two-phase odorant degradation metabolism has been detected specifically in insect antennal chemosensory sensilla (29), and this is the first documentation of set odorant degradation metabolic pathway in the Haller's organ of ticks.

P450s can be classified into four clades: CYP2, CYP3, CYP4 and mitochondrial P450s. Alignment and phylogenetic analysis of the 4 putative P450 transcripts determined that one transcript belongs to the CYP2 clade, two to CYP3, and one to CYP4 (Figs. 2.7 and 2.S15-2.S18). GO annotation and pathway identification of the putative CYP transcripts revealed function roles in oxidation-reduction processes (GO term identification no. GO:0055114). The majority of chemosensory specific P450s identified in insects belong to CYP2, CYP3 and CYP4 (30). CYP2s, CYP3s and CYP4s are also commonly found in the gut and fat bodies of insects, though this does not preclude these enzymes from chemosensory specific functions (25). In insect chemosensory CYP4s are primarily

associated with the metabolism of odorants and pheromones, whereas CYP3s are linked to the metabolism of toxic and/or harmful odorant molecules (29). CYP2s are orphan enzymes of unknown function. There is evidence of certain CYP2s being tissue specific in vertebrates, but this has yet to be examined in invertebrates (31). The exclusive presence of these putative P450 transcripts in the Haller's organ, as well as their functional annotations, makes it highly probable that these encoded P450s function as ODEs.

GSTs are important antioxidant enzymes that degrade ROSs created in response to the CYP inactivation of pheromones and harmful chemical molecules (32). GSTs can be classified into 7 clades: delta, epsilon, mu, omega, sigma, theta and zeta (33, 34). All GST clades except for sigma and theta have been documented in ticks (35). Alignment and phylogenetic analysis of the two putative GST transcripts determined that one transcript encoded a cytosolic epsilon GST and the second a cytosolic mu GST (Figs. 2.8, 2.S19 and 2.S20). GO annotation and pathway identification of the putative GST transcripts revealed functional roles in the metabolism of xenobiotics following CYP oxidation (GO term identification no. GO:008152). In insects, epsilon GSTs are highly expressed in antennal chemosensory sensilla and associated with the degradation of pheromones and harmful odorant molecules (30, 35, 36). Mu GSTs were previously recognized as vertebrate-specific, and associated with odorant degradation in nasal mucosa (37). Several mu GSTs have been identified in multiple Acari species, though their roles in odorant degradation and general xenobiotic metabolism are still being studied (33).

SODs function in a similar manner to GSTs to prevent cellular oxidative damage from ROSs. Eukaryotic SODs can be classified into three clades, cytosolic, extracellular, and mitochondrial (38). Alignment and phylogenetic analysis of the putative SOD transcript

determined that it encoded a Cu/Zn binding cytosolic SOD (Fig. 2.S21). GO annotation of the putative SOD transcript revealed a functional role in the removal of superoxide radicals (GO term identification no. GO:0019430). Currently there are discrepancies in the reported functions of cytosolic SODs in insects and Acari, but it is clear that SODs play a role in protecting chemosensory cells from ROS damage (38).

ODEs in chemosensory sensilla protect chemosensory neurons from xenobiotic damage and odor desensitization. Efficient metabolism of odorant molecules, toxic or benign, may limit the duration of odorant activity and neural stimulation allowing for apt behavioral responses (32). ODEs warrant further investigation as putative targets of novel tick control strategies.

Developmental/Hormonal Regulation of Chemoreception in the Haller's Organ. In male *D. variabilis* blood feeding had no statistically significant effect on transcript levels in the front pair of legs for GPCR (contig 83622), $G_{\alpha o}$ (contig 13937), or β -arrestin (contig 01853; Fig. 2.9). This is not surprising since blood-fed males remain on the host, and are attracted to part-fed females for copulation. In females the situation was different; mating and blood feeding to repletion resulted in a dramatic down-regulation of these same three chemosensory transcripts when compared to unfed females. The GPCR expression decreased 5.0 fold ($t = 5.677$, $dF = 12$, $P = 0.0001$); $G_{\alpha o}$ expression decreased 10.0 fold ($t = 7.598$, $dF = 12$, $P < 0.0001$); and β -arrestin expression decreased 4.2 fold ($t = 4.324$, $dF = 12$, $P = 0.0010$). In *D. variabilis*, blood feeding to repletion is initiated in part-fed virgin females by the transfer of the spermatophore into the female genital tract by the male. This transfer initiates the 'big sip', where the female consumes a large volume of blood and increase in size to

approximately 100 times their unfed body weight. Mating and blood feeding also initiates the synthesis of the hormone 20-hydroxyecdystone; this hormone starts the process of egg development (1).

Blood feeding has been shown to impact chemosensory genes in other arthropods. For example, in adult female *Anopheles gambiae* blood feeding resulted in the down-regulation of most antennal chemosensory gene transcripts with the exception of a subset of odorant receptors (AgORs) that were significantly up-regulated. These changes in chemosensory gene expression resulted in observable changes in odorant sensitivity and responsiveness. Blood-fed *A. gambiae* females were less receptive to host-associated attractants and more receptive to oviposition attractants (40). In *D. variabilis* and other prostriate ticks, replete females lose their host seeking behavior, detach, and drop from the host into the leaf litter where they oviposit their eggs and subsequently die (41). It is not surprising that there is a down-regulation of chemosensory function at this time since all of the female tick's energy is aimed at egg production and oviposition. Since increases in ecdysteroids are associated with this reduction in gene expression in the Haller's organ, this might provide a new practical mechanism for repelling ticks and to reduce host seeking and biting using hormone mimics.

Role of the Haller's Organ in Tick Repellency Versus Host Attachment. It has been well documented that the Haller's organ is involved in host-seeking and mating behaviors; the general assumption has been that the Haller's organ is also important in tick repellency and host biting and attachment, though this is not well documented (1). In Petri dish bioassays removal of the 1st pairs of legs, which includes the Haller's organ, prevented both female and

male unfed virgin adult *D. variabilis* from detecting the presence of a DEET treated surface (Fig. 2.10). Without the 1st pairs of legs, DEET repellent was greatly reduced and ticks were found on both the treated and control surfaces (treated with absolute ethanol; $F = 22.430$, $dF = 34$, $P < 0.0001$). In comparison, ticks were repelled from the DEET treated surface when the 4th pairs of legs were removed ($F = 143.042$, $dF = 34$, $P < 0.0001$). Since there was no evidence of gustatory receptors in the Haller's organ (discussed earlier), the mechanism of this repellency in the Haller's organ must be spatial (not contact) and involve the mechanism of olfaction. More bioassay work is needed to further validate this hypothesis. This discovery is significant in showing that the development of new tick repellents, like DEET, must target the Haller's organ and the odorant receptor system in this organ.

Also surprising, removal of the 1st pair of legs, which includes the Haller's organ, had no significant impact on host biting, attachment or feeding when compared to ticks that had their 4th pair of legs removed at any of the time points examined, 1h ($t = 0.0$, $dF = 10$, $P = 1.00$), 3h ($t = 1.112$, $dF = 10$, $P = 0.293$), 6h ($t = 1.320$, $dF = 10$, $P = 0.216$) or 24h ($t = 0.508$, $dF = 10$, $P = 0.623$; Fig 10). We can only hypothesize at this point that the pedipalps are used in controlling biting and host attachment, and that the Haller's organ is required for host seeking, mating, and possibly strategic positioning on the host animal body. Our preliminary studies have shown the removal of the pedipalps prevents tick attachment in *D. variabilis*. The discovery of an organ, other than the Haller's organ, that is critical in host attachment and feeding is exciting because this suggests a novel mechanism for the development of tick repellent that function to prevent tick attachment. Future repellents could potentially be a mixture of compounds, which repel ticks from the host and also prevent host attachment.

Conclusions

Utilizing RNA-seq technology we have generated the first Haller's organ specific transcriptome in addition to two new *D. variabilis* 1st and 4th leg transcriptomes. Analyses of the multiple transcriptomes have determined that there are no known odorant binding proteins or chemosensory lipocalins in ticks. Additionally, it appears that the Haller's organ is only involved in olfaction and not gustation, and the olfactory signaling mechanism is a GPCR signal cascade. Each component of the olfactory GPCR signal cascade was identified either exclusively in the Haller's organ spf transcriptome or in the 1st leg and/or 4th transcriptomes, and all functions of putative chemosensory transcripts confirmed using alignments, annotation and phylogenetic analyses. Additionally, the expressions of GPCR, G_{αo}, and β-arrestin transcripts identified in the Haller's organ specific transcriptome were documented in unfed and blood-fed adult female and male *D. variabilis*. Blood feeding to repletion in adult females down-regulated the expression of all three chemosensory transcripts. This represents the first documentation of hormonal regulation of the chemosensory system in Acari. Behavioral assays confirmed the role of the Haller's organ in chemical avoidance, in addition to its known role is chemical attraction. Though, it was determined that while the Haller's organ is essential for host-seeking, mating, and possibly strategic orientation on the host body, once ticks are present on the host chemoreceptors present on the pedipalps are responsible for attachment and feeding.

Materials and Methods

Adult *D. variabilis* ticks were obtained from laboratory colonies of Dr. Daniel E. Sonenshine at Old Dominion University (Norfolk, VA). Total RNAs extracted from dissected 1st and 4th

legs of unfed virgin adult male *D. variabilis* were used for Illumina RNA Hiseq sequencing. Total RNAs extracted from dissected 1st legs of unfed and fully blood-fed adult female and male *D. variabilis* were used to generate cDNA templates for qPCR expression analyses. Behavioral bioassays utilized unfed virgin adult female and male *D. variabilis*, with either the 1st or 4th legs removed, in host attachment/feeding assays on live rabbit hosts (*Oryctolagus cuniculus*) and Petri dish assays with exposure to absolute ethanol and/or the repellent DEET. A more detailed description is provided in *Supplemental Information: Materials and Methods*.

Acknowledgements

This work was funded by grants to RMR and DES from NIH (1R21AI096268) and NSF (IOS-0949194). ALC was also supported in part by a Graduate Student teaching Assistantship from the Department of Entomology at North Carolina State University.

References

1. Sonenshine DE, Roe RM (2014) *Biology of Ticks Vol. 2* (Oxford University Press, New York City, NY).
2. Lin L, Decker CF (2012) Rocky Mountain spotted fever. *Dis Mon* 58(6):361-369.
3. Liu XY, Bonnet SI (2014) Hard tick factors implicated in pathogen transmission. *PLoS Neglect Trop D* 8(1):e2566.
4. Brunner JL, et al. (2011) Molting success of *Ixodes scapularis* varies among individual blood meal hosts and species. *J Med Entomol* 48(4):860-866.
5. Leonovich SA (2006) *Sensory Systems of Parasitic Ticks and Mites* (Nauka press, St. Petersburg, Russia).

6. Bargmann CI (2006) Chemosensation in *C. elegans*. *Wormbook*, ed The C. elegans Research Community (Wormbook) doi/10/1895/wormbook.1.123, <http://www.wormbook.org>.
7. Nakagawa T, Vosshall LB (2009) Controversy and consensus: Non-canonical signaling mechanism in the insect olfactory system. *Curr Opin Neurobiol* 19(3):284-292.
8. Gulia-Nuss M, et al. (2015) Genomic insights into the parasitic vector of Lyme disease, *Ixodes scapularis*. *Nature Comm* in press.
9. Nespoulous C, et al. (2004) Odorant binding and conformation changes of a rat odorant-binding protein. *Chem Senses* 29(3):189-198.
10. Hill CA (2002) G Protein-coupled receptors in *Anopheles gambiae*. *Science* 298(5591):176-178.
11. Kaupp UB (2010) Olfactory signaling in vertebrates and insects: differences and commonalities. *Nat Rev Neurosci*. 11(3):188-200.
12. Broeck JV (2001) Insect G protein-coupled receptors and signal transduction. *Archive Insect Biochem* 48(1):1-12.
13. Boto T, Gomez-Diaz C, Alcorta E (2010) Expression analysis of the 3 G-protein subunits G α , G β , and G γ in the olfactory receptor organs of adult *Drosophila melanogaster*. *Chem Senses* 35(3):183-193.
14. Tu H, Qin Y (2014) Cloning and expression analysis of G-protein G α_{aq} subunit and G β 1 subunit from *Bemisia tabaci* Gennadius (Homoptera:Aleyrodidae). *Arch Insect Biochem* 87(2):53-71.
15. Hull JJ, Wan M (2015) Molecular cloning and characterization of G alpha proteins from the western tarnished plant bug, *Lygus Hesperus*. *Insects* 6(1):54-76.
16. Yau DM, et al. (2003) Identification and molecular characterization of the G alpha12-Rho guanine nucleotide exchange factor pathway in *Caenorhabditis elegans*. *PNAS* 100(25):14748-14753.
17. Rützler M, Lu T, Zwiebel LJ (2006) G α encoding gene family of the malaria vector mosquito *Anopheles gambiae*: expression analysis and immunolocalization of AG α_{aq} and AG α_{ao} in female antennae. *J Comp Neurol* 499(4):533-545.
18. Chatterjee A, Roman G, Hardin PE (2009) G α_o contributes to olfactory reception in *Drosophila melanogaster*. *BMC Physiol* 9:22.

19. Khan SM, et al. (2013) The expanding roles of G $\beta\gamma$ subunits in G protein-coupled receptor signaling and drug action. *Pharmacol Rev* 65(2):545-577.
20. Komatsu H, Mori I, Rhee J (1996) Mutations in a cyclic nucleotide-gated channel lead to abnormal thermosensation and chemosensation in *C. elegans*. *Neuron* 17(4):707-718.
21. Finn JT, Grunwald ME, Yau K (1996) Cyclic nucleotide-gated ion channels: an extended family with diverse functions. *Annu Rev Physiol* 58:395-426.
22. Baumann A, et al. (1994) Primary structure and functional expression of a *Drosophila* cyclic nucleotide-gated channel present in eyes and antennae. *EMBO J* 13(21):5040-5050.
23. Fukuto HS, et al. (2004) G protein-coupled receptor kinase function is essential for chemosensation in *C. elegans*. *Neuron* 42(4):581-593.
24. Ge H, et al. (2006) A *Drosophila* nonvisual arrestin is required for the maintenance of olfactory sensitivity. *Chem Senses* 31(1):49-62.
25. Gilbert LI (2012) *Insect Endocrinology* (Academic Press, Waltham, MA).
26. Dmochowska-Ślęzak K, et al. (2015) Variations in antioxidant defense during the development of the solitary bee *Osmia bicornis*. *Apidologie* 246(4):432-44.
27. Linblom TH, Dodd AK (2006) Xenobiotic detoxification in the nematode *Caenorhabditis elegans*. *J Exp Zool* 305(9):720-729.
28. Liu B, et al. (2011) Analysis of transcriptome differences between resistant and susceptible strains of the citrus red mite *Panonychus citri* (Acari: Tetranychidae). *PLoS ONE* 6(1):e28516.
29. Feyereisen R (2012) Insect CYP genes and P450 enzymes. *Insect Molecular Biology and Biochemistry*, ed Gilbert LI (Academic Press, San Diego, CA), pp 236-316.
30. Younus F, et al. (2014) Identification of candidate odorant degrading gene/enzyme systems in the antennal transcriptome of *Drosophila melanogaster*. *Insect Biochem Molec* 53:30-43.
31. Karlgren M, Miura S, Ingelman-Sundberg M (2005) Novel extrahepatic cytochrome P450s. *Toxicol Appl Pharm* 207(2):57-61.
32. Rogers ME, Jani MK, Vogt RG (1999) An olfactory-specific glutathione-S-transferase in the sphinx moth *Manduca sexta*. *J Exp Biol* 202(12):1625-1637.

33. Liao C, et al. (2013) Identification and characterization of seven glutathione S-transferase genes from citrus red mite, *Panonychus citri* (McGregor). *Int J Mol Sci* 14(12):24255-24270.
34. Tan X, et al. (2014) Antenna-specific glutathione S-transferase in male silkworm *Bombyx mori*. *Int J Mol Sci* 15(5):7429-7443.
35. Reddy BP, Prasad GBKS, Raghavendra K (2011) *In silico* analysis of glutathione S-transferase supergene family revealed hitherto unreported insect specific δ - and ϵ -GSTs and mammalian specific μ -GSTs in *Ixodes scapularis* (Acari: Ixodidae). *Comput Biol Chem* 35(2):114-120.
36. Lumjuan N, et al. (2005) Elevated activity of an epsilon class glutathione transferase confers DDT resistance in the dengue vector, *Aedes aegypti*. *Insect Biochem Molec* 35(8):861-871.
37. Krishna NSR, Getchell TV, Getchell ML (1994) Differential expression of alpha-class, mu-class, and pi-class of glutathione S-transferases in chemosensory mucosae of rats during development. *Cell Tissue Res* 275(3):435-450.
38. Feng Y, et al. (2015) Regulation of three isoforms of SOD gene by environmental stresses in citrus red mite, *Panonychus citri*. *Exp Appl Acarol* 67(1):43-69.
39. Ogoma SB, Moore SJ, Maia MF (2012) A systematic review of mosquito coils and passive emanators: defining recommendations for spatial repellency testing methodologies. *Parasite Vector* 5:287.
40. Rinker, et al. (2013) Blood meal-induced changes to antennal transcriptome profiles reveal shifts in odor sensitivities in *Anopheles gambiae*. *PNAS* 110(20):8260-8265.
41. Sonenshine DE, Roe RM (2014) *Biology of Ticks Vol. 1* (Oxford University Press, New York City, NY).

Tables

Table 2.1. Putative transcripts involved in chemoreceptor signal transduction identified exclusively in the Haller's organ transcriptome of unfed, virgin adult male *Dermacentor variabilis* and their respective tick, nematode and insect matches with the lowest expected value (e-value).

Chemoreceptor signal transduction	Protein	Contig (length, bp)	Top tick hit ^a accession no. (%identity & e-value)	Top <i>C. elegans</i> hit ^b accession no. (%identity & e-value)	Top insect hit ^c accession no. (%identity & e-value)	Contig conserved domain(s) ^d
	Salivary-like Lipocalin	84287 (237)	<i>A. triste</i> JAA54113.1 (48% & 9.10E-12)	No match	No match	None found
	OR , Odorant receptor: G-protein coupled receptor	72702 (245)	<i>I. scapularis</i> EEC06829.1 (92% & 8.40E-28)	<i>C. elegans</i> CCF23345.1 (25% & 2.00E-3)	<i>F. arisanus</i> JAG78630.1 (35% & 8.50E-4)	None found
		83622 (322)	<i>I. scapularis</i> EEC07880.1 (62% & 1.90E-32)	<i>C. elegans</i> CCD63420.1 (29% & 1.00E-4)	<i>D. melanogaster</i> AAF49949.2 (33% & 1.20E-11)	None found
	RP , Receptor protein: G _α protein	13937 (7348)	<i>R. pulchellus</i> JAA58325.1 (99% & 0.00E+00)	<i>C. elegans</i> CAA96595.1 (89% & 0.00E+00)	<i>H. saltator</i> EFN90078.1 (75% & 8.00E-166)	G_alpha
	RP : G _β protein	24477 (354)	<i>I. ricinus</i> JAB79904.1 (75% & 4.70E-28)	<i>C. elegans</i> CAA93514.1 (73% & 4.00E-25)	<i>D. ponderosae</i> AEE61583.1 (94% & 3.40E-36)	WD40
	SP , Secondary protein: Adenylate/guanylate cyclase	77721 (242)	<i>I. scapularis</i> EEC01411.1 (70% & 1.90E-30)	No match	<i>D. plexippus</i> KDR07447.1 (58% & 4.60E-7)	None found
		37845 (534)	<i>I. scapularis</i> EEC13610.1 (92% & 1.60E-105)	<i>C. elegans</i> CCD67191.1 (36% & 2.00E-19)	<i>Z. nevadensis</i> KDR07447.1 (61% & 6.20E-67)	Guanlate_cyc, HNOBA
	IC , Ion channel: Cyclic nucleotide-gated ion channel	82720 (266)	<i>I. scapularis</i> EEC03664.1 (99% & 3.00E-51)	<i>C. elegans</i> CAB63418.2 (61% & 8.00E-26)	<i>A. echinator</i> EGI67156.1 (93% & 3.00E-49)	cNMP_bindin g

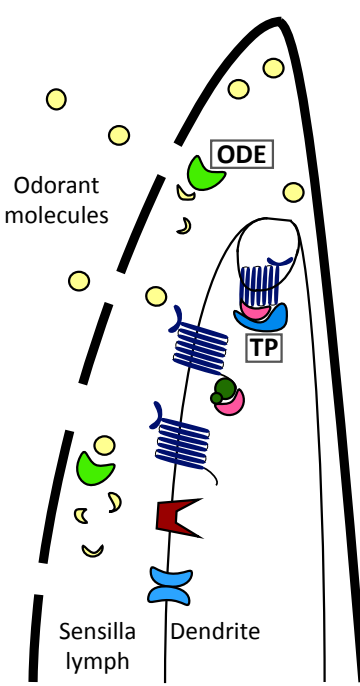
^a*Amblyomma triste*, the hard tick; *Ixodes scapularis*, the blacklegged tick; *Ixodes ricinus*, the castor bean tick; *Rhipicephalus pulchellus*, the zebra tick.

^b*Caenorhabditis elegans*, the roundworm.

^c*Acromyrmex echinator*, the Panama leaf cutting ant; *Danaus plexippus*, the Monarch butterfly; *Dendroctonus ponderosae*, the mountain pine bark beetle; *Drosophila melanogaster*, the fruit fly; *Fopius arisanus*, the solitary endoparasitoid; *Harpegnathos saltator*, the Indian jumping ant; *Pediculus humanus*, the body louse; *Zootermopsis nevadensis*, the dampwood termite.

^dcNMP_binding, cyclic nucleotide binding domain; G_alpha, G-protein alpha subunit; Guanylate_cyc, adenylate and guanylate cyclase catalytic domain; HNOBA, heme NO binding associated domain; WD40, WD domain G-beta repeat.

Table 2.2. Putative transcripts involved in chemoreceptor signal modulation/termination and xenobiotic metabolism identified exclusively in the Haller's organ transcriptome of unfed, virgin adult male *Dermacentor variabilis* and their respective tick, nematode and insect matches with the lowest expected value (e-value).

Chemoreceptor modulation & odorant degradation enzymes	Protein	Contig (length, bp)	Top tick hit ^a accession no. (%identity & e-value)	Top <i>C. elegans</i> hit ^b accession no. (%identity & e-value)	Top insect hit ^c accession no. (%identity & e-value)	Contig conserved domain(s) ^d
	TP , Terminator protein: β -Arrestin	01853 (3390)	<i>A. cajennense</i> EEC07926.1 (93% & 0.00E+00)	<i>C. elegans</i> CCD67242.1 (63% & 5.80E-160)	<i>L. hesperus</i> JAG24601.1 (83% & 0.00E+00)	Arrestin_C, Arrestin_N
	ODE , Odorant degradation enzyme: Cytochrome P450	69591 (575)	<i>I. scapularis</i> EEC03681.1 (57% & 1.30E-69)	<i>C. elegans</i> CCD68717.1 (43% & 2.00E-39)	<i>D. mojavensis</i> EDW16611.1 (42% & 1.30E-48)	p450
		01691 (1001)	<i>R. pulchellus</i> JAA56317.1 (90% & 4.80E-79)	<i>C. elegans</i> CAB60436.1 (30% & 7.00E-7)	<i>C. biroi</i> EZA58513.1 (32% & 2.70E-9)	p450
		06898 (1170)	<i>I. scapularis</i> EEC19065.1 (64% & 6.10E-123)	<i>C. elegans</i> CAB07222.1 (33% & 3.00E-30)	<i>L. bostrychophila</i> ABN80241.2 (40% & 3.0E-54)	p450
		14383 (1167)	<i>A. triste</i> JAC34536.1 (69% & 2.30E-157)	<i>C. elegans</i> CAA91268.1 (31% & 2.00E-27)	<i>B. tabaci</i> AEK21811.1 (33% & 2.70E-41)	p450
	ODE , Glutathione S-transferase	12057 (902)	<i>A. triste</i> JAC32911.1 (74% & 5.00E-110)	<i>C. elegans</i> CCD73730.1 (31% & 6.00E-7)	<i>A. glabripennis</i> JAB67323.1 (34% & 7.80E-38)	GST_C_3, GST_N
		04931 (2250)	<i>A. triste</i> JAC32978.1 (88% & 3.30E-140)	<i>C. elegans</i> CCD62297.1 (30% & 7.00E-18)	<i>A. rosae</i> XP_012268124 (31% & 1.00E-13)	GST_C, GST_N
	ODE , Superoxide dismutase	83534 (332)	<i>R. pulchellus</i> JAA58838.1 (70%, 2.20E-38)	<i>C. elegans</i> CAR97839.1 (55%, 3.00E-26)	<i>P. cochleariae</i> AEY77316.1 (65% & 4.90E-36)	Sod_Cu

^a*Amblyomma cajennense*, the Cayenne tick; *Amblyomma triste*, the hard tick; *Ixodes scapularis*, the blacklegged tick; *Rhipicephalus pulchellus*, the zebra tick.

^b*Caenorhabditis elegans*, the roundworm.

^c*Anoplophora glabripennis*, the Asian long-horned beetle; *Athalia rosae*, the turnip sawfly; *Bemisia tabaci*, the silverleaf whitefly; *Cerapachys biroi*, the clonal raider ant; *Drosophila mojavensis*, the fruit fly; *Liposcelis bostrychophila*, the booklouse; *Lygus hesperus*, the Western tarnished plant bug; *Phaedon cochleariae*, the mustard beetle.

^dArrestin_C, arrestin C-terminal domain; Arrestin_N, arrestin N-terminal domain; GST_C, glutathione S-transferase C-terminal domain; GST_C_3, glutathione S-transferase C-terminal domain; GST_N, glutathione S-transferase N-terminal domain; P450, cytochrome p450 domain; Sod_Cu, copper/zinc superoxide dismutase.

Figures

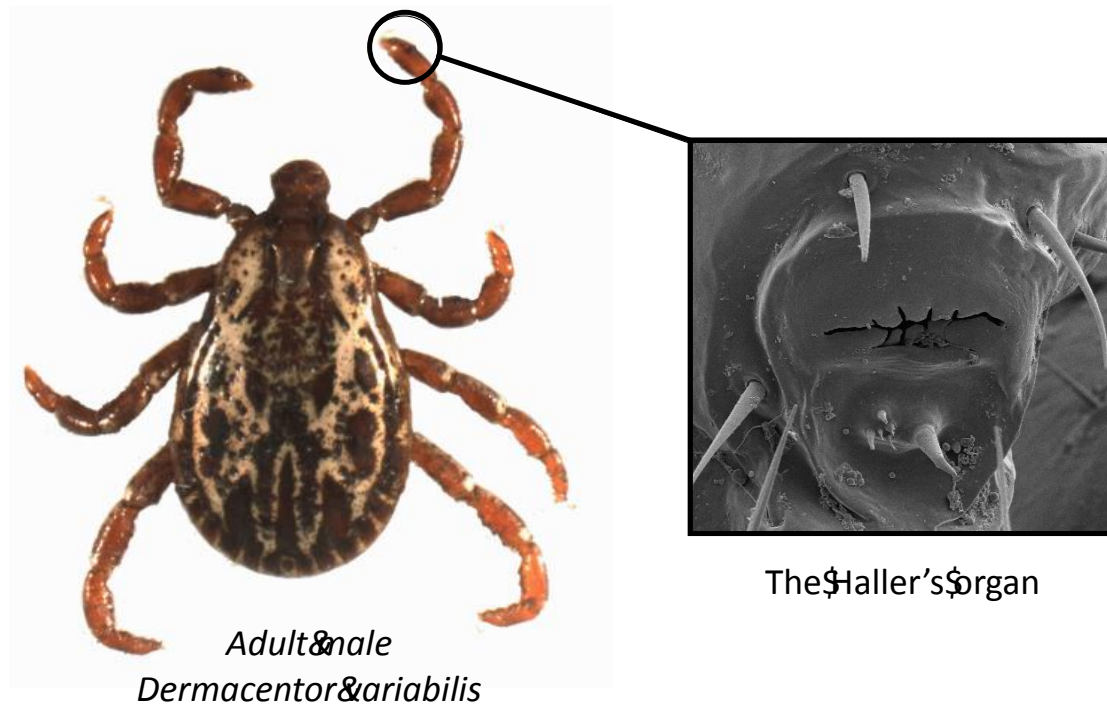


Figure 2.1. The Haller's organ (boxed) located on the first foretarsus of the first pair of legs of the American dog tick, *Dermacentor variabilis* (400x magnification).

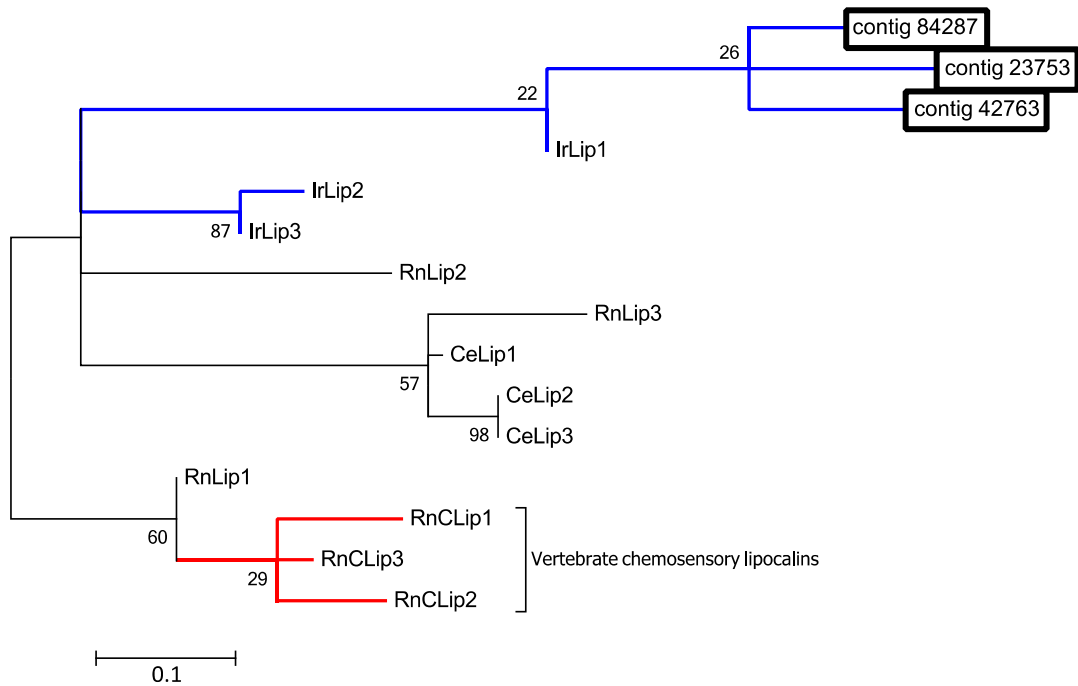


Figure 2.2. Phylogenetic relationship of transcripts putatively encoding lipocalins (Lip) identified in the Haller's organ spf (contig 84287) and 1st/4th leg transcriptomes (contigs 42763, 23753) of unfed, virgin adult male *Dermacentor variabilis* with lipocalins from *Caenorhabditis elegans*, *Ixodes ricinus*, and *Rattus norvegicus*. The phylogenetic tree shows the branch relation of chemosensory lipocalins (red branch) with non-chemosensory lipocalins. Tick lipocalins are highlighted with a blue branch color. Acronyms are as follows: first letter of the genus and species (*Caenorhabditis elegans*, Ce; *Ixodes ricinus*, Ir; *Rattus norvegicus*, Rn) followed by the protein name (Clip or Lip). Putative lipocalin transcripts are boxed. The tree was constructed using Maximum likelihood phylogenetic analysis and bootstrapping set to 500 iterations. Branch values listed are bootstrap percentages (percent confidence), scale set to 10%. A comprehensive list of acronyms and associated Genbank accession numbers are listed in Table 2.S1.

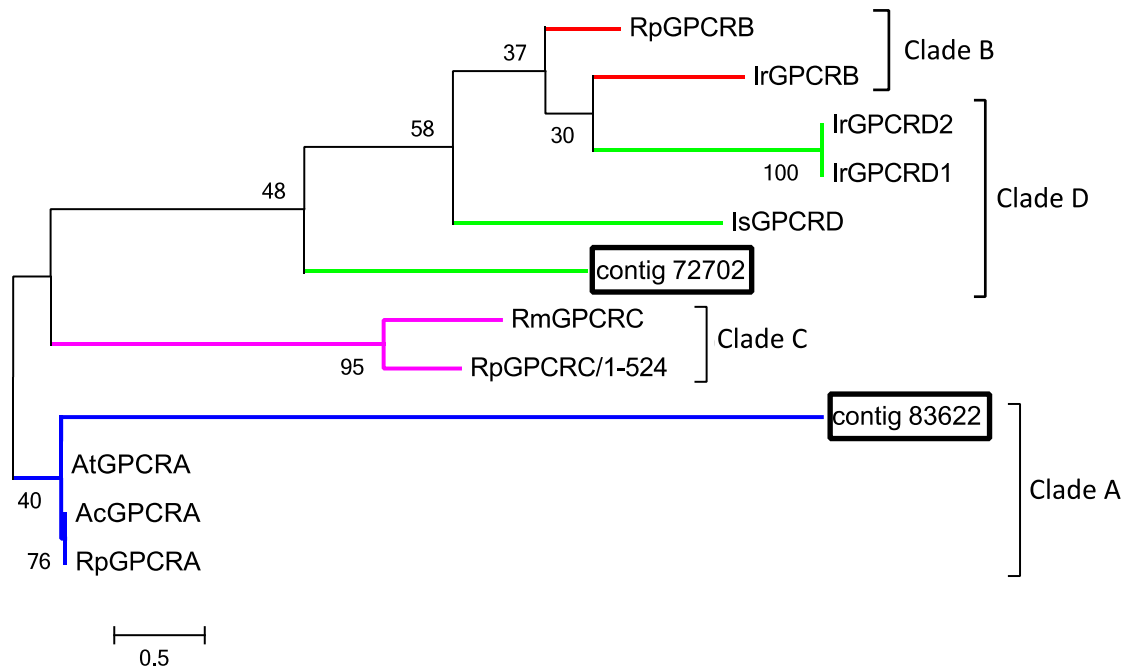


Figure 2.3. Phylogenetic relationship of transcripts putatively encoding G-protein coupled receptors (GPCRs) identified in the Haller's organ spf (contigs 72702, 83622) of unfed, virgin adult male *Dermacentor variabilis* with GPCRs of known clade annotation from *Amblyomma cajennense*, *Amblyomma triste*, *Ixodes ricinus*, *Ixodes scapularis*, *Rhipicephalus microplus*, and *Rhipicephalus pulchellus*. The phylogenetic tree shows four clades, each represented by the following branch colors: blue = clade A; purple = clade C; green = clade D; red = clade B. Acronyms are as follows: first letter of the genus and species (*Amblyomma cajennense*, Ac; *Amblyomma triste*, At; *Ixodes ricinus*, Ir; *Ixodes scapularis*, Is; *Rhipicephalus microplus*, Rm; *Rhipicephalus pulchellus*, Rp) followed by the protein name (GPCR). Putative GPCR transcripts are boxed. The tree was constructed using Maximum likelihood phylogenetic analysis and bootstrapping set to 500 iterations. Branch values listed are bootstrap percentages (percent confidence), scale set to 50%. A comprehensive list of acronyms and associated Genbank accession numbers are listed in Table 2.S1.

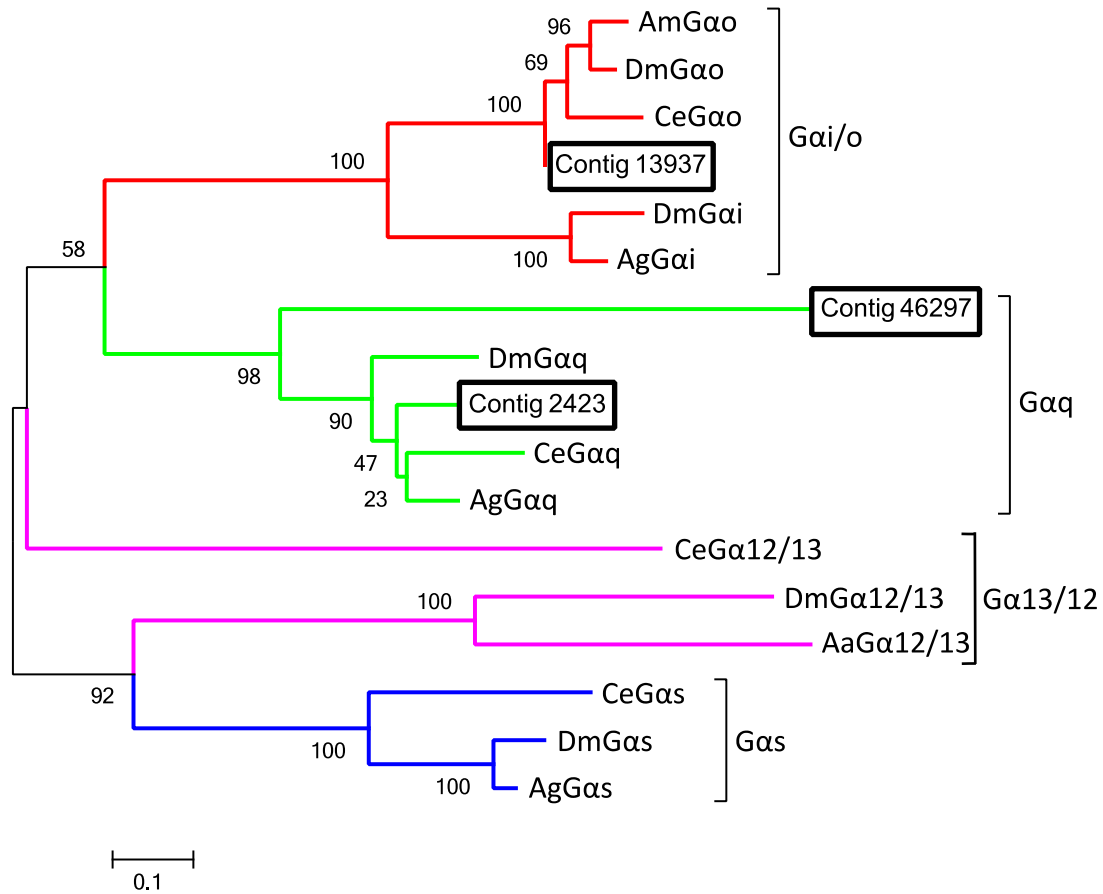


Figure 2.4. Phylogenetic relationship of transcripts putatively encoding G-protein α subunits ($G\alpha$) identified in the Haller's organ (contig 13937) and 1st/4th leg transcriptomes (contigs 2423, 13329, 14072, 46297) of unfed, virgin adult male *Dermacentor variabilis* with $G\alpha$ subunits of known clade annotation from *Caenorhabditis elegans* and insects. The phylogenetic tree shows four clades, each represented by the following branch colors: red = Gai/o clade; green = Gaq clade; purple = Gaq12/13 clade; blue = Gas clade. Acronyms are as follows: first letter of the genus and species (*Anopheles aquasalis*, Aa; *Anopheles gambiae*, Ag; *Drosophila melanogaster*, Dm; *Caenorhabditis elegans*, Ce) followed by the protein name ($G\alpha$) and the letter/number of the associated clade. Putative $G\alpha$ subunit transcripts are boxed. The tree was constructed using Maximum likelihood phylogenetic analysis and bootstrapping set to 500 iterations. Branch values listed are bootstrap percentages (percent confidence), scale set to 20%. A comprehensive list of acronyms and associated Genbank accession numbers are listed in Table 2.S1.

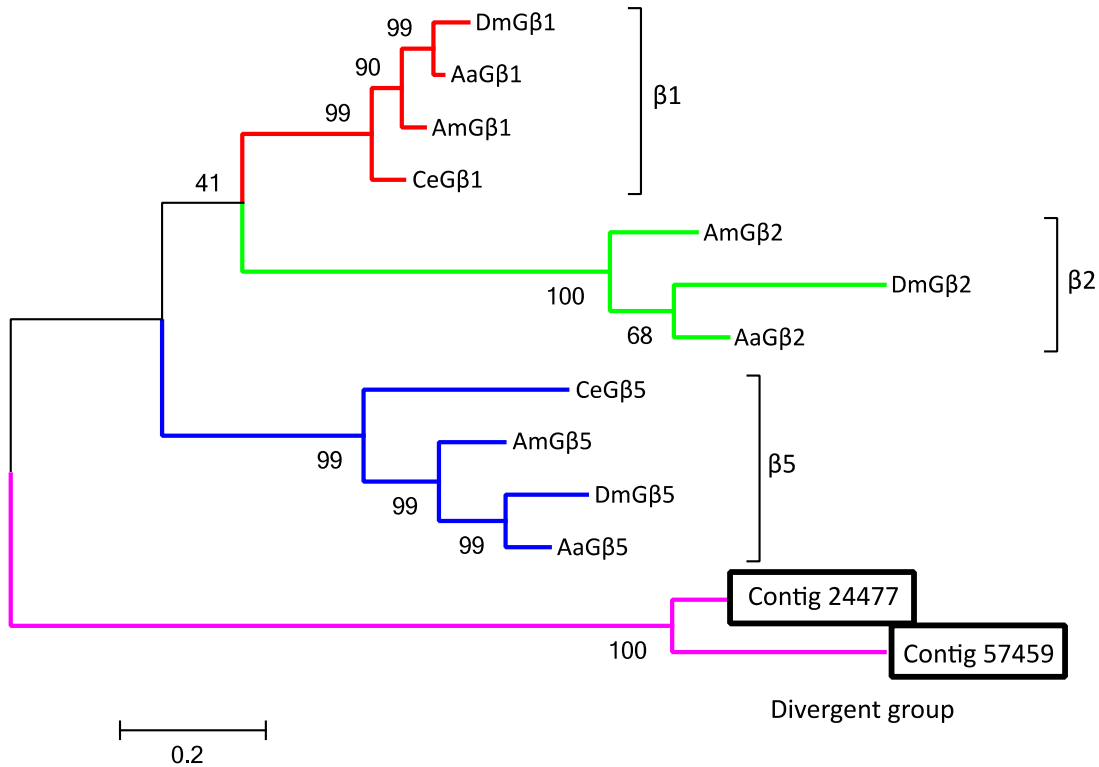


Figure 2.5. Phylogenetic relationship of transcripts putatively encoding G-protein β subunits ($G\beta$) identified in the Haller's organ (contig 24477) and 1st/4th leg transcriptomes (contig 57459) of unfed, virgin adult male *Dermacentor variabilis* with $G\beta$ subunits of known clade annotation from *Caenorhabditis elegans* and insects. The phylogenetic tree shows four clades, each represented by a branch color as follows: red = $\beta 1$ clade; green = $\beta 2$ clade; blue = $\beta 5$ clade; purple = novel divergent clade. Acronyms are as follows: first letter of the genus and species (*Aedes aegypti*, Aa; *Apis mellifera*, Am; *Drosophila melanogaster*, Dm; *Caenorhabditis elegans*, Ce) followed by the protein name ($G\beta$) and the number of the clade number. Putative $G\beta$ subunit transcripts are boxed. The tree was constructed using Maximum likelihood phylogenetic analysis and bootstrapping set to 500 iterations. Branch values listed are bootstrap percentages (percent confidence), scale set to 20%. A comprehensive list of acronyms and associated Genbank accession numbers are listed in Table 2.S1.

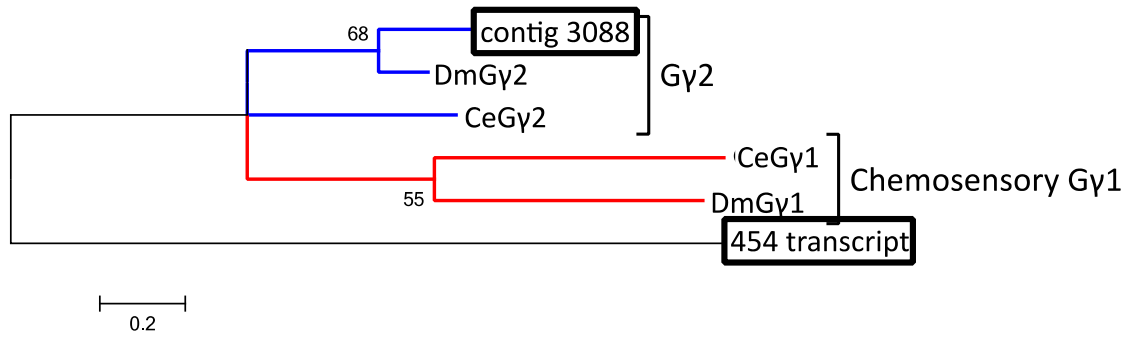


Figure 2.6. Phylogenetic relationship of transcripts putatively encoding G-protein γ subunits ($G\gamma$) identified in the 4th leg transcriptome (contig 3088) and the 454 1st leg transcriptome (454 transcript) of unfed, virgin adult male *Dermacentor variabilis* with $G\gamma$ subunits of known clade annotation from *Caenorhabditis elegans* and *Drosophila melanogaster*. The phylogenetic tree shows two clades, each represented by a branch color as follows: red = γ 1, chemosensory clade; blue = γ 2 clade. Acronyms are as follows: first letter of the genus and species (*Drosophila melanogaster*, Dm; *Caenorhabditis elegans*, Ce) followed by the protein name ($G\gamma$) and the number of the clade number. Putative $G\gamma$ subunit transcripts are boxed. The tree was constructed using Maximum likelihood phylogenetic analysis and bootstrapping set to 500 iterations. Branch values listed are bootstrap percentages (percent confidence), scale set to 20%. A comprehensive list of acronyms and associated Genbank accession numbers are listed in Table 2.S1.

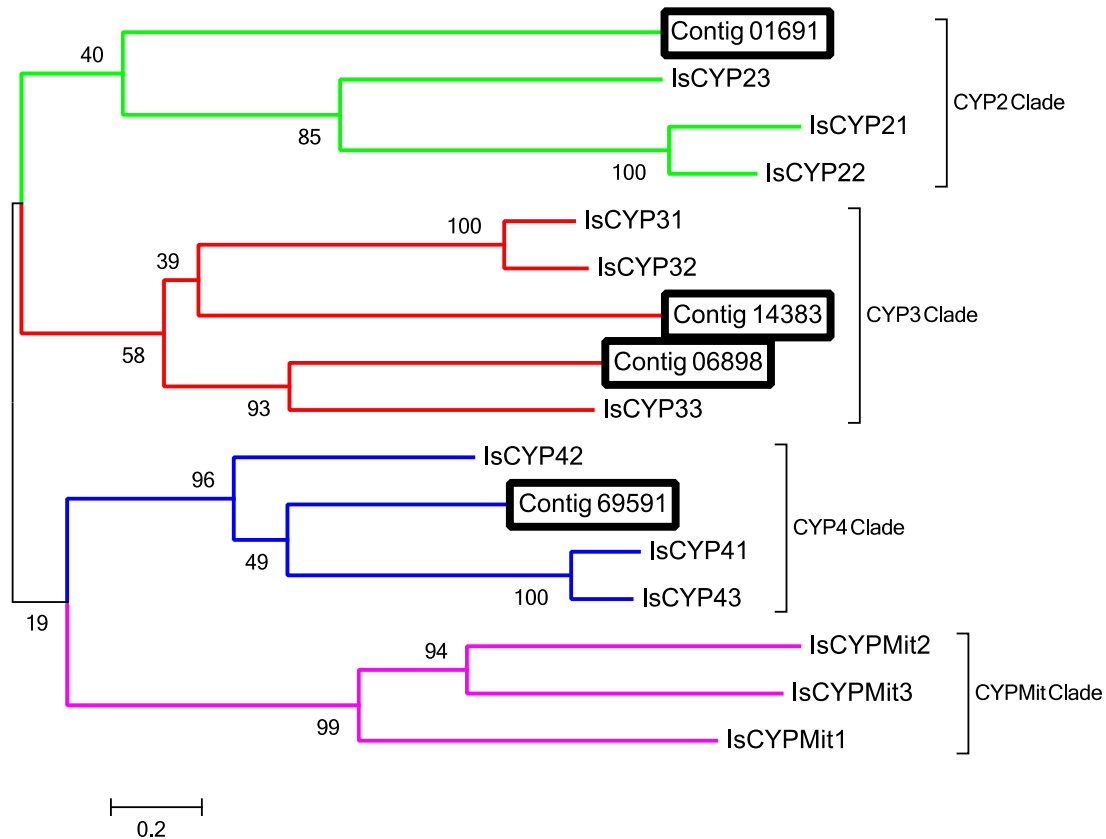


Figure 2.7. Phylogenetic relationship of transcripts putatively encoding cytochrome P450s (CYPs or P450s) identified in the Haller's organ transcriptome of unfed, virgin adult male *Dermacentor variabilis* with P450s of known clan annotation from *Ixodes scapularis* (Is). The phylogenetic tree shows four P450 clades, each represented by a branch color as follows: green = CYP2 clade; red = CYP3 clade; blue = CYP4 clade; purple = mitochondrial CYP or CYPmit clade. Acronyms consist of the first letter of the genus and species (Is) followed by the protein name (CYP) and the number or abbreviation (mit = mitochondrial) of the associated clade. Putative P450s transcripts are boxed. The tree was constructed using Maximum likelihood phylogenetic analysis and bootstrapping set to 500 iterations. Branch values listed are bootstrap percentages (percent confidence), scale set to 20%. A comprehensive list of acronyms and associated GenBank accession numbers are listed in Table 2.S1.

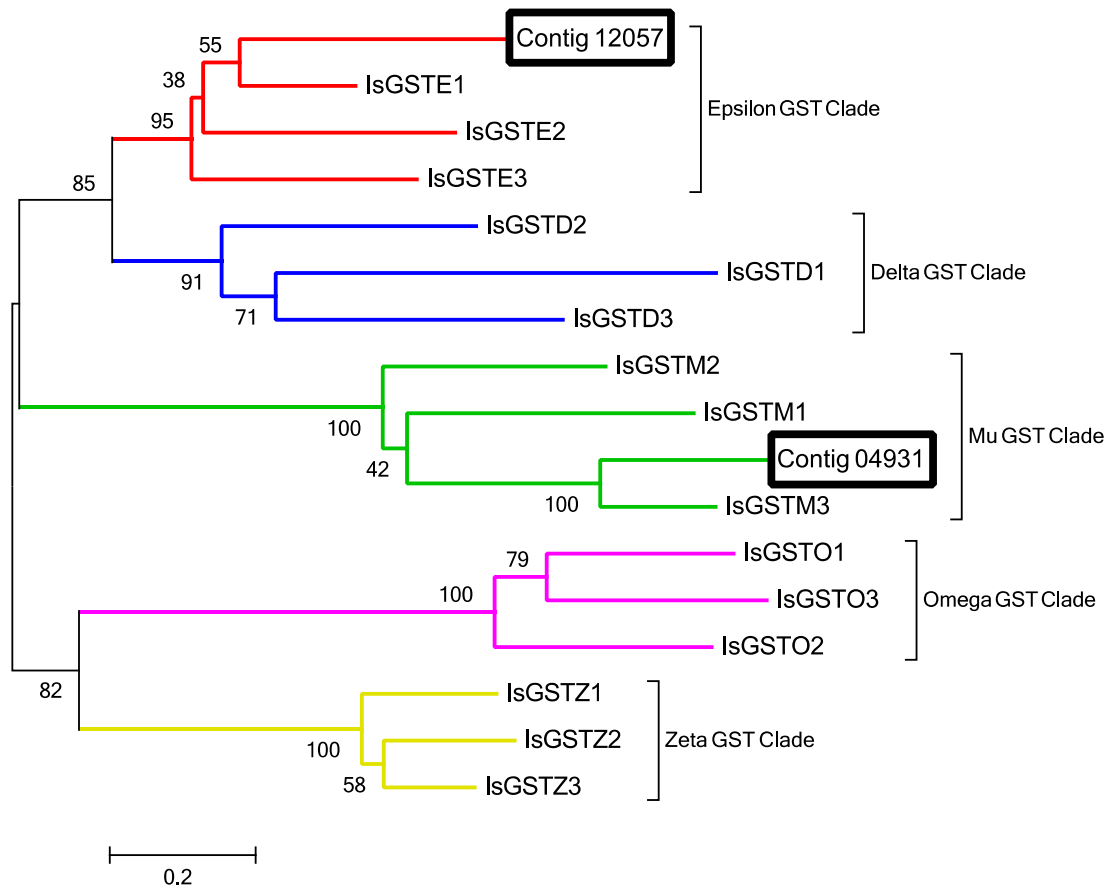


Figure 2.8. Phylogenetic relationship of transcripts putatively encoding glutathione S-transferases (GSTs) identified in the Haller’s organ transcriptome of unfed, virgin adult male *Dermacentor variabilis* with GSTs of known clade annotation from *Ixodes scapularis* (Is). The phylogenetic tree shows 5 GST clades, each represented by a different branch color as follows: red = epsilon GST clade; blue = delta GST clade; green = mu GST clade; purple = omega GST clade; yellow = zeta GST clade. Acronyms consist of the first letter of the genus and species (Is), followed by protein name (GST) and the first letter of the associated clade (delta, d; epsilon, e; omega, o; mu, m; zeta, z). Putative GST transcripts are boxed. The tree was constructed using Maximum likelihood phylogenetic analysis and bootstrapping set to 500 iterations. Branch values listed are bootstrap percentages (percent confidence), scale set to 20%. A comprehensive list of acronyms and associated GenBank accession numbers are listed in Table 2.S1.

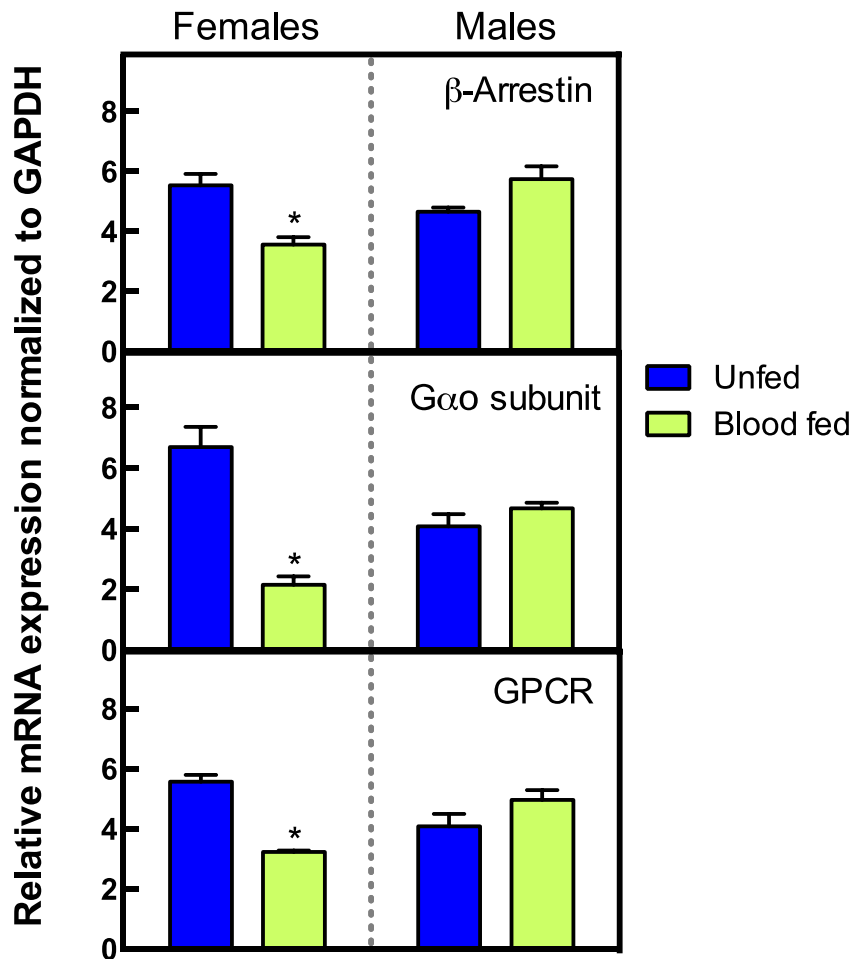


Figure 2.9. Relative mRNA expression (ΔC_t) of the chemosensory proteins β -arrestin, G-protein α_o subunit ($G\alpha_o$) and G-protein coupled receptor (GPCR) in unfed versus fully blood fed adult female and male *Dermacentor variabilis* after normalization to expression levels of glyceraldehyde 3-phosphate dehydrogenase (GAPDH; * = $P < 0.05$; error bars = ± 1 SEM; ANOVA and a Sidak's multiple comparison test). Replicates of 5, using 2ng cDNA, 10 μ L reactions.

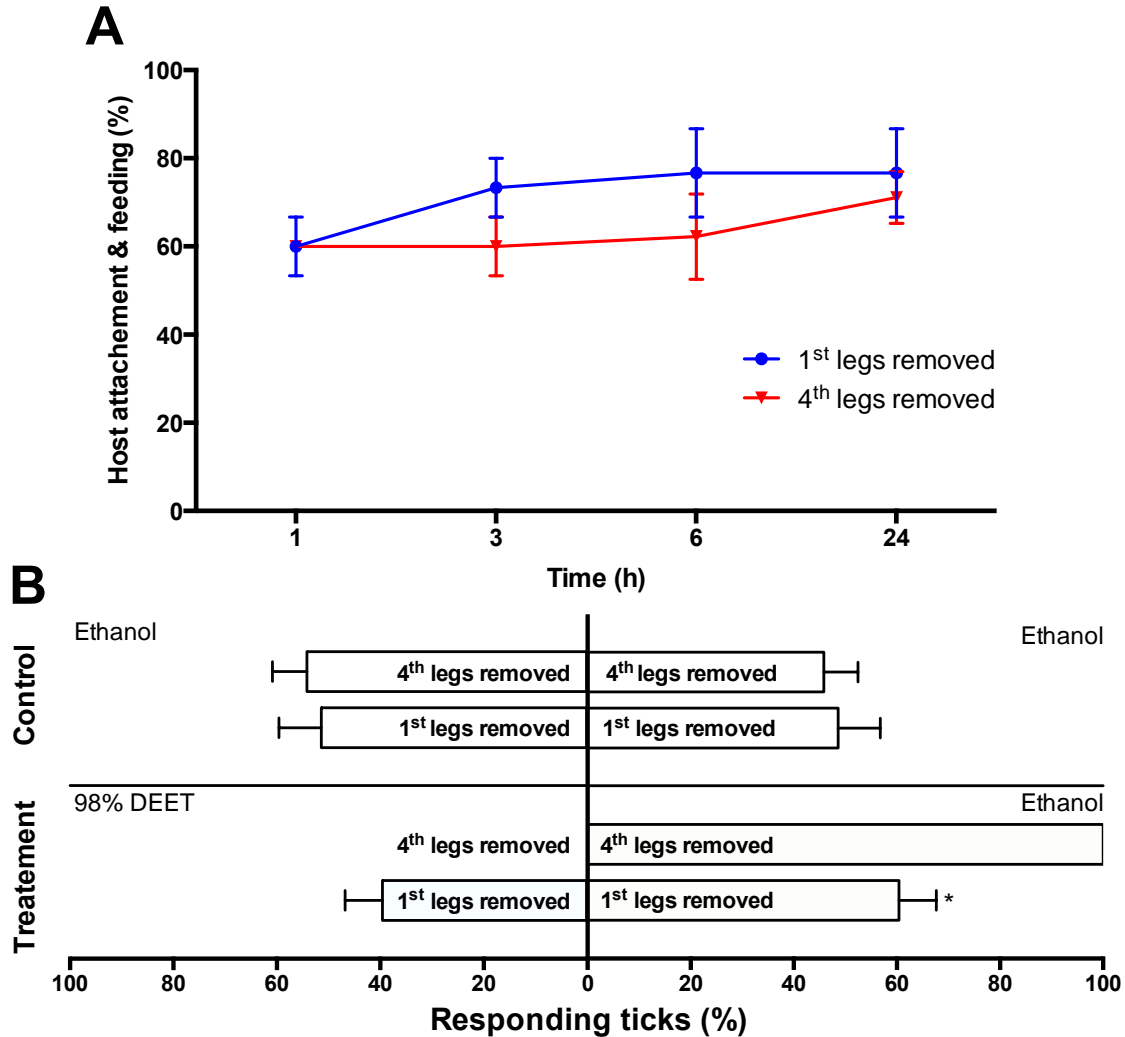


Figure 2.10. Observed behavior in response to the removal of either the 1st or 4th pairs of legs in unfed, virgin adult *Dermacentor variabilis*. A, Time to rabbit (*Oryctolagus cuniculus*) and attachment by tick. Statistical analyses were performed using an ANOVA and a Sidak's multiple comparison test (* = $P < 0.05$; error bars = ± 1 SEM). Replicates of 4, with a mixed population of 15 female and 15 male ticks. B, Petridish assay two choice repellency assay. Statistical analyses were performed using an ANOVA and a Sidak's multiple comparison test (* = $P < 0.05$; error bars = ± 1 SEM). Replicates of 3 and 6 were conducted for the control and treatment, respectively, with a mixed population of 4 female and 4 male ticks.

Supplemental Information: Materials and Methods

Ticks. Adult *Dermacentor variabilis* were obtained from a highly inbred laboratory colony of Dr. Daniel E. Sonenshine at Old Dominion University (Norfolk, VA). The colony was started with field collected *D. variabilis* obtained from a single site near Richmond, VA, and reared for at least 30 generations by feeding larval and nymph stages on Norway rats, *Rattus norvegicus*, and adult stages on New Zealand white rabbits, *Oryctolagus cuniculus*. When not feeding, *D. variabilis* larvae, nymphs, adult females, and adult males were maintained in different containers at $23 \pm 1^{\circ}\text{C}$, 97% humidity, and with a photoperiod of 16-hour light: 8-hour dark (dusk and dawn periods of 1 h each at the beginning and ending of the scotophase).

Ethics Statement. All applicable international, national, and/or institutional guidelines for the care and use of animals were followed to minimize pain and discomfort. All use of animals in this study was done under the protocol #10-032 approved by the Old Dominion University Institutional Animal Care and Use Committee (Animal Welfare Assurance Number: A3172-01). This protocol is on file at the Office of Research, Old Dominion University, Norfolk, VA.

RNA Extraction. Total RNAs extracted from the 1st and 4th legs of *D. variabilis* ticks were used in Illumina Hiseq sequencing and qPCR studies. Ten batches of 100 1st legs and 100 4th legs were dissected from unfed virgin adult males for use only in Illumina Hiseq sequencing. An additional five batches of 60 1st legs and 60 4th legs were dissected, separately, from unfed virgin adult males, unfed virgin adult females, fully blood-fed virgin adult males, and fully (replete) blood-fed mated adult females for use in qPCR studies. Unfed virgin adult *D.*

variabilis females and males used for dissections were 3-4 months post molt, with females and male stored separately after molting. Fully blood-fed virgin adult males were fed on rabbit hosts (*O. cuniculus*) for 4-5 days and forcible detached. Fully (replete) blood-fed mated adult females were 1-2 days post-drop off from the rabbit host (*O. cuniculus*). Dissections of each sex (female and male) and feeding stage (unfed and blood-fed) were performed on separate days to prevent cross-contamination. Additionally, all ticks were handled using gloves, and all dissection equipment washed thoroughly with glassware detergent and autoclaved between dissections. One tick specimen allotted two 1st legs and two 4th legs, removed at the femur. To maintain tissue viability, 1st and 4th leg dissections were conducted congruently. Leg dissections required two persons, one to dissect the 1st legs and one to dissect the 4th legs, with each person assigned a distinct set of sterile dissection tools. The 4th legs were dissected first to prevent cross-contamination of the hemolymph secreted from dissection sites. Dissections were performed during the day between 1100 h and 1300 h under ambient (fluorescent) lighting at RT ($24 \pm 1^\circ\text{C}$) and a relative humidity of 40%. Dissected 1st and 4th legs were collected into two distinct mortars each containing 3mL liquid nitrogen (LN2; Airgas, Radnor, PA), and two separate pestles used to grind the legs into fine particles. Once the LN2 evaporated, 350 μL of beta-mercaptoethanol in RTL lysis buffer (10 $\mu\text{L}/1\text{mL}$; Qiagen, Valencia, CA, USA) was added to each mortar and the appropriate pestle used to homogenize the leg particles and lysis buffer. The mixtures were thawed, and an additional 350 μL of beta-mercaptoethanol in RTL lysis buffer (10 $\mu\text{L}/1\text{mL}$; Qiagen, Valencia, CA, USA) was added to each mortar and homogenized using the appropriate pestle. All 700 μL of the lysis buffer containing either the 1st or 4th leg particles was transferred into a labeled 1.5mL centrifuge tube and frozen overnight at -70°C . Total

RNA was extracted from the 1st and 4th leg particles, in lysis buffer, according to the manufacturer's protocol using the RNeasy mini kit (Qiagen, Valencia, CA). This process was repeated for each dissection batch, and the extracted RNAs kept separate to allow for biological replicates pertinent to qPCR studies. Total RNA concentrations and purities were measured using RNA pico chips in combination with the Agilent 2100 Bioanalyzer (Agilent Tech., Santa Clara, CA).

Illumina Hiseq Paired-end Sequencing. Deep sequencing utilizing Illumina RNA-Seq technology (Illumina, San Diego, CA) was conducted at the University of North Carolina High Throughput Sequencing Facility. Hiseq paired-end sequencing was conducted using mRNAs extracted from the 1st and 4th legs of unfed virgin adult male *D. variabilis*. Poly(A) mRNAs were isolated, separately, from 2 μ g of total RNA collected from the 1st legs, and 2 μ g of total RNA collected from the 4th legs for library preparation and barcoding. The mRNAs were fragmented and cDNA synthesized, amplified, digested, and purified utilizing Illumina TruSeq chemistry protocols (Illumina, San Diego, CA). The purified cDNA fragments generated were ligated with adaptor constructs creating the 1st and 4th leg cDNA libraries. In preparation for sequencing, the 1st and 4th leg cDNA libraries were barcoded with a 6bp barcode (GCCAAT or CTTGTA) to distinguish the sequencing data generated from each library. The barcoded 1st and 4th leg cDNA libraries were hybridized onto one Illumina Hiseq flow cell for cBOT (Illumina, San Diego, CA) cluster generation and sequencing (paired-end, 2 x 100bp; total 200 cycles). Two raw data sets of sequencing outputs, one per library, were generated using the Illumina software assembler (Illumina, San Diego, CA).

Illumina Bioinformatics. The 1st and 4th leg Illumina Hiseq data sets generated were cleaned using BLASTN, quality trimmed (Q15) using the FASTX-Toolkit (http://hannonlab.cshl.edu/fastx_toolkit), and assembled de novo using the CLC pipeline assembler and scaffolder (Qiagen, Valencia, CA) with k-mer set to “N”, minimum overlap set to 100 bases, seed length set to 5kbp, and npairs set to 5. Putative functions and gene ontology (GO) annotations of contigs were predicted using the program Blast2Go (BioBam, Valencia, Spain) and the GenBank non-redundant protein (nr) database with an expected value (e-value) cut-off of <10. An *in silico* subtraction was then performed between the illumina 1st and 4th leg contigs, for only those contigs with putative functions. Removal of the illumina 1st leg contigs with identical counterparts, based on putative function and accession number, in the illumina 4th leg transcriptome resulted in the identification of contigs exclusive to the 1st legs, creating the Haller’s organ spf transcriptome. The assumption is that since the Haller’s organ is exclusive to the 1st legs, contigs exclusive to the illumina 1st leg transcriptome are associated with the Haller’s organ and chemosensation. BLASTx and BLASTn searches of the illumina 1st leg, illumina 4th leg and Haller’s organ spf transcriptome were conducted to identify putative chemosensory transcripts using insect and nematode chemosensory systems as models. BLASTx and BLASTp searches of all the tick sequence data contained in GenBank were also performed to identify putative chemosensory transcripts in other Ixodid species. Lastly, using the NCBI BLAST+ toolkit and the ‘makeBLASTdb’ UNIX coding, the illumina 1st leg transcriptome fasta file was used to create a BLASTable database. This illumina 1st leg BLAST database was uploaded into the program Geneious (Biomatters, Auckland, New Zealand), and BLASTn searches for insect and nematode chemosensory messages (coding sequences) conducted to identify putative

contig matches in the illumina 1st leg BLAST database. The functions and GO annotations of identified putative chemosensory transcripts were verified against the Uniprot knowledgebase using BLAST (BLAST; EBI, Cambridge, UK) and Argot² (FEM-IASMA, Trento, Italy; Ref. 1-3). Protein families and domains were identified using the Pfam program and database (4). Alignments and trees were constructed using Clustal Omega (EBI, Cambridge, UK) and MAFFT (5) with default E-INS settings, and visualized using Jalview v. 2.8.2 (6) and the Molecular Evolutionary Genetics Analysis program v.5.2.2 (MEGA; Biodesign Institute, Tempe, AZ). Orthologous genes to putative *D. variabilis* chemosensory transcripts were predicted using OrthoDB (7).

454 1st Leg Transcriptome. In addition to analyzing the illumina 1st leg, illumina 4th leg, and Haller's organ spf transcriptomes to elucidate the chemosensory mechanism of ticks, permission was obtained to conduct BLASTx searches for putative chemosensory transcripts of a female and male *D. variabilis* 1st leg transcriptome generated using 454 pyrosequencing. The 454 1st leg transcriptome was made using 1st legs dissected at the femur from unfed virgin adult female and male *D. variabilis* 3-4 months post-molt. Tissue processing, RNA extraction and 454 pyrosequencing were performed as described by Donohue et al. (8). Dissected 1st legs were homogenized in TRI reagent (Sigma-Aldrich, St. Louis, MO) and the total RNAs precipitated into a pellet that was rehydrated in 100mM aurintricarboxylic acid to prevent dehydration. mRNA isolation from the precipitated total RNAs was performed using the Oligotex mRNA isolation kit (Qiagen, Valencia, CA) according to the manufacturer's protocol. A cDNA library was synthesized from the isolated mRNAs using the SMART cDNA library construction kit and protocol (Clontech, Mountain View, CA). Purification of

the cDNA library was performed using a PCR purification kit (Qiagen, Valencia, CA) according to the manufacturer's protocol. The purified cDNA library was prepared for pyrosequencing on the GS-FLX sequencer using GS-FLX Titanium library preparation and adaptors kits (Roche, Indianapolis, IN). The raw dataset of sequencing output generated by the GS-FLX sequencer was assembled using the GS Assembler (Roche, Indianapolis, IN) with default settings. The fasta file containing all the contigs for the 454 1st leg transcriptome was obtained and the putative functions and gene ontology (GO) annotations of contigs were predicted using the program Blast2Go (BioBam, Valencia, Spain) and the GenBank non-redundant protein (nr) database with an expected value (e-value) cut-off of <10. The functions and GO annotations of identified putative chemosensory transcripts were verified against the Uniprot knowledgebase using BLAST (BLAST; EBI, Cambridge, UK) and Argot² (FEM-IASMA, Trento, Italy; Ref. 1-3).

Quantitative Analysis of Putative Chemosensory Transcript Levels. Quantitative PCR (qPCR) experiments were conducted to determine the levels of putative chemosensory transcripts in unfed versus blood-fed adult female and male *D. variabilis*. qPCR experiments used total RNAs extracted from dissected 1st legs of unfed virgin adult females, unfed virgin adult males, fully blood-fed virgin adult males, and fully (replete) blood-fed mated females (Ref. *SI Total RNA extraction*). Total RNA was reverse transcribed into cDNA using the SuperScript® III First-Strand Synthesis System (Life Technologies, Carlsbad, CA) according to the manufacturer's protocol. qPCR was performed using the C1000 Touch™ Thermal Cycler (Bio-Rad, Hercules, CA) in combination with SsoFast™ EvaGreen® Supermix technology and protocol (Bio-Rad, Hercules, CA). Primer3Plus (9) was used to design

primer pairs for the following messages: β -arrestin (contig 01853), $G_{\alpha o}$ subunit (contig 13937), and GPCR (contig 83622). Primer pairs were also designed for glyceraldehyde 3-phosphate dehydrogenase (GAPDH), used as a reference housekeeping message. The primer pairs are as follows; β -arrestin: forward (Fw) 5'-CTTCCAGTTCTGCCTTTTTGTC-3'; reverse (Rv) 5'-TGCAAGACCATATCGCTGAG-3'; $G_{\alpha o}$ subunit: Fw 5'-AATACACAGGTGCCCAGGAG-3'; Rv 5'-CAAACCTGGATGTTGGTCGTG-3'; GPCR: Fw 5'-TTCGGAAGACGTTCAAGGAT-3'; Rv 5'-CTCTCCGGTTACATCGAGGA-3'; GAPDH: Fw 5'-TGTCGGCAGCTTAGGTTATTCTT-3'; Rv 5'-GCCGATCTTCACGCTCATGT. Primers were validated in PCR studies and the subsequent products sequenced (Eton Bioscience Inc., Research Triangle Park, NC) to confirm target identity prior to use in qPCR studies. qPCR experiments were conducted with 5 biological replicates for each sex and feeding stage, and each biological replicate repeated twice for a total of 10 replicates for each sex (female and male) and feeding stage (unfed and fully blood-fed). Expression data generated by qPCR experiments was normalized against GAPDH and analyzed using ANOVA and a Sidak's multiple comparison test using Prism™ (GraphPad, La Jolla, CA).

Repellency Bioassays. Petri dish assays were conducted to determine the relationship between the Haller's organ and chemical avoidance behavior in *D. variabilis*. Unfed virgin adult male and female *D. variabilis* were tested in Petri dish assays against DEET following the removal of either the 1st or 4th legs. Petri dish assays were performed using black, glass Petri dishes (148 mm diam x 20 mm) and lids (150 mm diam x 20 mm). Filter paper was employed during these experiments as the means of chemical delivery in Petri dish assays,

testing 98% DEET (Sawyer, Safety Harbour, FL) and absolute ethanol (control). Tests were conducted during the day between 1100 h and 1500 h at RT and a relative humidity of 40%. The use of black Petri dishes eliminated light contamination from ambient (fluorescent) lighting and created a dark testing environment. Adult ticks used in Petri dish assays were 3-4 months post-molt with females and males stored separately after molting. All ticks were handled using gloves and sterile, soft-tipped forceps cleaned with absolute ethanol. Additionally, all dissection equipment was washed thoroughly with glassware detergent and autoclaved between dissections to prevent contamination. The 1st or 4th legs of unfed virgin adult female and male *D. variabilis* were dissected at the femur under the same experimental conditions previously described. Ticks were permitted a recovery period of 24 h after leg dissections to confirm mobility and viability before use in assays. During the recovery period ticks were housed in an insectary maintained at $23 \pm 1^\circ \text{C}$, 97% humidity and with a photoperiod of 16-hour light: 8-hour dark (dusk and dawn periods of 1 h each at the beginning and ending of the scotophase). In preparation for Petri dish assays, a piece of circular filter paper (6 cm^2) was divided into two halves (3 cm^2), and each half treated with $100\mu\text{L}$ of either DEET or absolute ethanol (control). To allow for thorough chemical dispersal on the filter paper and solvent evaporation, all filter papers were chemically treated at least 30 min prior to use in assays. Control experiments employed two half pieces of filter paper (3 cm^2) both treated with absolute ethanol. Treatment experiments employed two half pieces of filter paper (3 cm^2) with one treated with DEET and the second with absolute ethanol. Sterile forceps were used to place the chemically treated filter papers into the bottom of the Petri dish. Filter papers treated with absolute ethanol were always handled first to prevent cross-contamination. After placement of the chemically treated filter papers into the

Petri dish, sterile soft tipped forceps were used to introduce the test subjects to the experimental arena (Petri dish). Test subjects, 8 unfed virgin adult females and males (50:50) with either the 1st or 4th legs removed, were allowed 30 min to acclimate to experimental conditions prior to being placed into the Petri dish. Each Petri dish assay was conducted for 30 min, with the location of the test subjects in reference to the chemically treated surfaces documented at 5, 10, 15, 20, 25 and 30 min. Due to the use of black, glass Petri dishes in experiments, the lids were removed briefly to catalog the location of ticks at each time point. Control experiments were conducted to document the normal behavior of test subjects in Petri dish assays, and to verify that there was no experimental bias associated with the Petri dish assay design or experimental conditions. Treatment experiments were conducted to observe the behavior of test subjects when exposed to DEET in Petri dish assays. In treatment experiments subjects arresting on the absolute ethanol treated (control) surface were recorded as exhibiting chemical avoidance behavior, while subjects arresting on the DEET treated surface were recorded as not exhibiting chemical avoidance behavior. *D. variabilis* unfed virgin adults with the 1st legs removed were tested in Petri dish assay treatment experiments a total of 6 replicates, and in Petri dish assay control experiments a total of 3 replicates. These experiments were repeated, with the same number of replicates, using *D. variabilis* unfed virgin adults with the 4th legs removed. Response data was analyzed by SAS (SAS, Cary, NC) GLM and the Mixed-Procedure as well as ANOVA and a Sidak's multiple comparison test using Prism™ (GraphPad, La Jolla, CA).

Host Attachment/Feeding Bioassays. Host attachment/feeding assays were conducted to determine the relationship between the Haller's organ and host biting, attachment and

feeding behaviors in *D. variabilis*. Unfed virgin adult female and male *D. variabilis* were tested in attachment/feeding assays on live rabbit hosts (*O. cuniculus*) following the removal of either the 1st or 4th legs. Attachment/feeding assays were initiated at 900 h and run for a 24 h time period at $20 \pm 1^\circ \text{C}$ and a relative humidity of 40%. The rabbit hosts are maintained in a facility with a photoperiod of 14-hour light: 10-hour dark with dusk and dawn periods of 1 h each at the beginning and ending of each scotophase. Adult ticks used in attachment/feeding assays were 3-4 months post-molt with females and males stored separately after molting. All ticks were handled using gloves and sterile, soft-tipped forceps cleaned with absolute ethanol. Additionally, all dissection equipment was washed thoroughly with glassware detergent and autoclaved between dissections to prevent contamination. The 1st or 4th legs of unfed virgin adult female and male *D. variabilis* were dissected at the femur under the same experimental conditions described above. Ticks were permitted a recovery period of 24 h after leg dissections to confirm mobility and viability before use in assays. During the recovery period, ticks were housed in an insectary maintained at $23 \pm 1^\circ \text{C}$, 97% humidity and with a photoperiod of 16-hour light: 8-hour dark (dusk and dawn periods of 1 h each at the beginning and ending of the scotophase). Prior to conducting the attachment/feeding assays, ticks were allowed to acclimate to the testing environment for a period of 30 min. Test subjects, 30 unfed virgin adult females and males (50:50) with either the 1st or 4th legs removed, were placed into a plastic, dome-shaped feeding chamber (148 mm diam x 76 mm) that was adhered to the shaved flank of an animal using veterinary topical adhesive. To protect the feeding chamber from animal manipulation, the animal was placed into a protective collar and a medical pet shirt (MPS, the Netherlands). The number of test subjects attaching and/or feeding on the animal host was documented at 1, 3, 6 and 24 h.

In addition to the experimental time points, animals were also monitored twice daily by veterinary personal and had continuous access to food and water. During the attachment/feeding assays there were no indications that analgesics or anesthetics were needed to relieve animals of discomfort or stress. Assays were replicated 4 times, twice testing subjects with their 1st legs removed and twice testing subjects with their 4th legs removed. Two different animal hosts were used, and each allowed a recovery period of 3-4 weeks in between assays. Response data was collected and analyzed using ANOVA and a Sidak's multiple comparison test using Prism™ (GraphPad, La Jolla, CA).

Supplemental Information: Results

Raw Reads, Base Pairs, and Assembly. The illumina 1st leg transcriptome consisted of a total of 105,959,590 filtered and trimmed reads assembled into 88,289 contigs representing an assembly of ≥ 2 reads with an average length of 748bp. Using Blast2Go and the GenBank non-redundant (nr) database, at least one putative function with an expected value (e-value) cut-off of 10 was identified for 71,114 of the contigs (80.5% of the total number of contigs).

The illumina 4th leg transcriptome consisted of a total of 180,355,958 filtered and trimmed reads assembled into 105,827 contigs representing an assembly of ≥ 2 reads with an average length of 730bp. Using Blast2Go and the GenBank nr database, at least one putative function with an e-value cut-off of 10 was identified for 83,647 of the contigs (79.0% of the total number of contigs).

The fasta file generated for the 454 1st leg transcriptome contained 33,981 contigs representing an assembly of ≥ 2 reads. Using Blast2Go and the GenBank nr database, at

least one putative function with an e-value cut-off of 10 was identified for 22,151 of the contigs (65.2% of the total number of contigs).

Gene Ontology. Gene ontology (GO) mapping using Blast2Go assigned at least one GO term annotation to the illumina 1st leg transcriptome contigs resulting in 79,601 GO terms assigned to 36,196 contigs, to the illumina 4th leg transcriptome contigs resulting in 85,719 GO terms assigned to 43,319 contigs, and to the 454 1st leg transcriptome contigs resulting in 9,104 GO terms assigned to 8,819 contigs. The 18 putative Level 2 biological functions for the identified GO terms of the illumina 1st leg, illumina 4th leg and 454 1st leg transcriptome are described in Fig. 2.S1-2.S3.

Top 50 Most Abundant Transcripts of the Illumina 1st Leg Transcriptome

Myofibril Proteins. The 50 most abundant transcripts from the unfed virgin adult male *D. variabilis* illumina 1st leg transcriptome are listed in Table 2.S2. All contigs had a sequence similarity to genes in the Uniprot knowledgebase, though 14 contigs were homologous to genes of unknown function including the most abundant contig (77381) with 1,709,234 reads. The second most abundant contig (00308), with 439,971 reads, was homologous to the myofibril scaffold component titin. Titin is a giant elastic protein found in striated muscle sarcomeres that connects the A-band and Z-line. Titin allows for muscle cell elasticity, and is essential for ensuring the mechanical stability of muscle fibers (10). Two additional contigs (00696 and 01517) homologous to titin were sequenced 137,289 and 58,463 times, respectively. Since oblique leg muscles insert in tick legs, it is expected that the illumina 1st leg transcriptome contain components of striated (skeletal) muscle (11). Table 2.S2 lists

several additional components of striated muscle including actin, myosin and troponin. Actin (thin) and myosin (thick) filaments form the striated pattern of sarcomeres, and are responsible for the sliding mechanism that produces the force necessary for muscle contractions (11). One contig (00073) homologous to filamentous actin was sequenced 278,198 times. Myosin filaments are composed of a helix of two heavy chain filaments and one light chain filament. Six contigs (15573, 27862, 00452, 00036, 00233, and 00060) homologous to the myosin heavy chain filament were sequenced 94,585, 82,021, 80428, 72,607, 54,395 and 52,729 times respectively. Table 2.S2 lists only one contig (00430) homologous to the myosin light chain filament sequenced 72,504 times.

Troponin is a protein complex that is vital in regulating muscle contractions. Troponin is present on actin filaments, and acts on the coiled coil protein tropomyosin. When inactive, the troponin-tropomyosin complex blocks the myosin binding sites used during the filament sliding mechanism of muscle contractions. Calcium ions activate troponin and cause a conformational change of the troponin-tropomyosin complex that expose the myosin binding sites for muscle contraction (11). The troponin protein complex consists of three subunits: the tropomyosin-binding subunit (troponin T), the inhibitory subunit (troponin I), and the calcium-binding subunit (troponin C; ref 12). Only contigs homologous to the troponin T and I subunits were identified among the top 50 most abundant transcripts of the illumina 1st leg transcriptome. Contig 00022 homologous to troponin T was sequenced 410,660 times, and contig 00033 homologous to troponin I sequenced 112,728 times. Additionally, one contig (00017) homologous to the coiled coil protein tropomyosin was sequenced 72,240 times (Table 2.S2).

In addition to identifying the structural components of skeletal muscle among the top 50 most abundant transcripts of the illumina 1st leg transcriptome, one contig (03069) homologous to ryanodine receptors was sequenced 167,176 times (Table 2.S2). Ryanodine receptors form calcium channels that control the release of intracellular calcium in excitatory tissue such as muscle and neurons (13). In muscles, ryanodine receptors provide the intracellular calcium required for contractions. One contig (00140) homologous to a calcium pump responsible for restoring intracellular calcium back to resting levels was also sequenced 79,270 times (Table 2.S2). The presence of muscle components in the illumina 1st leg transcriptome is not unexpected because of the presence of striated muscle fibers in the legs of *D. variabilis*. It is highly probable that the dissected 1st legs used in Illumina RNA Hiseq sequencing contained striated muscle fibers.

Cuticle Proteins. The integument of ticks consists of an epidermis and its secreted cuticle (14). Since tick legs are surrounded externally by cuticle, it is not surprising to identify cuticular proteins among the top 50 most abundant transcripts of the illumina 1st leg transcriptome. One contig (00690) homologous to a cuticular protein was sequenced 55,986 times and is listed in Table 2.S2.

Other Messages. House keeping genes are required for the maintenance of basic cellular functions and are expressed in all cells of an organism. Several transcripts homologous to house keeping gene messages are listed in Table 2.S2 including: cytochrome oxidase, cytoskeletal actin (beta), endocytosis proteins, heat shock proteins (crystallins), orithinine decarboxylase, small ATP and GTP binding proteins, transcription elongation factor 1-alpha,

and translation initiation factors 4a2, 4g2 and amb caj-77. There are also several transcripts listed in Table 2.S2 involved in ATP production and the cellular metabolism of amino acids, fatty acids, and carbohydrates (14, 15).

Top 50 Most Abundant Transcripts of the Illumina 4th Leg Transcriptome

Myofibril Proteins. The 50 most abundant transcripts from the unfed virgin adult male *D. variabilis* illumina 4th leg transcriptome are listed in Table 2.S3. All contigs had a sequence similarity to genes in the Uniprot knowledgebase, though 19 contigs were homologous to genes of unknown function including the top three most abundant contigs (20107, 03297, and 29927) with 3,060,443, 2,068,585, and 1,571,479 reads respectively. The next most abundant contig (06805), with 435,907 reads, was homologous to the myofibril scaffold component titin. Similar to the illumina 1st leg transcriptome, several components of striated muscle fibers were among the top 50 most abundant transcripts of the illumina 4th leg transcriptome, including actin, myosin, titin, troponin, and tropomyosin (Table 2.S3). A second contig (00680) homologous to titin was sequenced 126,367 times. One contig (00146) homologous to the actin filament was sequenced 146,196 times, whereas several contigs (00086, 00468, and 00079) homologous to myosin heavy chain filaments were sequenced 344,474, 117,492, and 83,955 times respectively. No myosin light chain filaments were identified among the top 50 most abundant transcripts of the illumina 4th leg transcriptome. Of the three troponin subunits only contigs homologous to troponin I and troponin T were identified among the top 50 most abundant transcripts of the illumina 4th leg transcriptome. One contig (00194) homologous to troponin I was sequenced 150,153 times, and two contigs (00042 and 51752)

homologous to troponin T, also known as ‘wings up A’ protein, were sequenced 316,355 and 89,524 times respectively.

In addition to identifying the structural components of skeletal muscle among the top 50 most abundant transcripts of the illumina 4th leg transcriptome, two contigs (02472 and 00082) associated with intracellular calcium transport were sequenced 200,303 and 133,507 times respectively. In muscle cells the influx and efflux of calcium is essential for proper muscle contraction.

Since tick striated leg muscles insert directly into tick legs, the presence of muscle components in the illumina 4th leg transcriptome is not unexpected. As with the illumina 1st leg transcriptome, it is highly likely that the dissected 4th legs used in RNA-seq contained striated muscle.

Cuticle Proteins. Since tick legs are surrounded externally by cuticle, it is not surprising to identify cuticle proteins among the top 50 most abundant transcripts of the illumina 4th leg transcriptome. One contig (02211) homologous to a cuticular protein was sequenced 92,976 times and is listed in Table 2.S3.

Other Messages. Similar to the illumina 1st leg transcriptome, several transcripts homologous to housekeeping gene messages were identified among the top 50 most abundant transcripts of the illumina 4th leg transcriptome and are listed in Table 2.S3, including: cell adhesion proteins, cytoskeletal actin (beta), endocytosis proteins, ferritin, small DNA and GTP binding proteins, transcription elongation factor 1-alpha, and translation initiation factors 4a2 and 4g2. There are also several transcripts listed in Table 2.S3 involved in ATP

production and the cellular metabolism of amino acids, antioxidants, fatty acids, and carbohydrates (14, 15). Additionally, one contig (07344) associated with the metabolism of the outer protein membrane of invading microbes was sequenced 89,354 times (13).

Supplemental Information: References

1. Fontana P, et al. (2009) Rapid annotation of anonymous sequences from genome projects using semantic similarities and a weighting scheme in gene ontology. *PLoS One* 4(2):e4619.
2. Falda M, et al. (2012) Argot²: a large scale function prediction tool relying on semantic similarity of weighted Gene Ontology terms. *BMC bioinformatics*, 13:S4-S14.
3. Radivojac P, et al. (2013) A large-scale evaluation of computational protein function prediction. *Nat Methods* 10(3):221-227.
4. Finn RD, et al. (2014) The Pfam protein families database. *Nucleic Acids Res* 42(D1):D222–D230.
5. Katoh K, Standley DM (2013) MAFFT Multiple sequence alignment software version 7: improvements in performance and usability. *Mol Biol Evol* 30(4):772–780.
6. Waterhouse AM, et al. (2009) Jalview version 2: a multiple sequence alignment editor and analysis workbench. *Bioinformatics* 25(9):1189–1191.
7. Waterhouse RM, et al. (2015) OrthoDB v8: update of the hierarchical catalog of orthologs and the underlying free software. *Nucleic Acids Res* 41(database issue):D358-365.
8. Donohue KV, et al. (2010) Neuropeptide signaling sequences identified by pyrosequencing of the American dog tick synganglion transcriptome during blood feeding and reproduction. *Insect Biochem Mol Biol* 40(1):79-90.
9. Untergasser A, et al. (2007) Primer3Plus, an enhanced web interface to Primer3. *Nucleic Acids Res* 35(Web Server Issue):W71–W74.
10. Nave R, Weber K (1990) A myofibrillar protein of insect muscle related to vertebrate titin connects Z band and A band: purification and molecular characterization of invertebrate mini-titin. *J Cell Sci* 95(4):535–544.

11. Shoura SM (1989) Fine structure of muscles in the tick *Hyalomma* (*Hyalomma*) *dromedarii* (Ixodoidea: Ixodidae). *Exp Appl Acarol* 7(4):327–335.
12. Gao J, et al. (2008) Cloning and characterization of a cDNA clone encoding troponin T from tick *Haemaphysalis qinghaiensis* (Acari: Ixodidae). *Comp Biochem Phys B* 151:323–329.
13. Thomas NL, Williams AJ (2012) Pharmacology of ryanodine receptors and Ca²⁺ - induced Ca²⁺ release. *WIREs Membr Transp Signal* 1:383-397.
14. Sonenshine DE, Roe RM (2014) *Biology of Ticks Vol. 1* (Oxford University Press, New York City, NY).
15. Bissinger BW, et al. (2011) Synganglion transcriptome and developmental global gene expression in adult females of the American dog tick *Dermacentor variabilis* (Acari: Ixodidae). *PLoS One* 6(9):e24711.

Supplemental Information: Tables

Table 2.S1. Comprehensive list of the acronyms presented in phylogenetic trees and the identifying species and GenBank accession numbers.

Acronym	Species	Accession no.
AaGA12/13	<i>Anopheles aquasalis</i>	JAA99692.1
AcGPCRA	<i>Amblyomma cajennense</i>	JAC21379.1
AgGAI	<i>Anopheles gambiae</i>	ABA56308.1
AgGAO	<i>Anopheles gambiae</i>	AAW50310.1
AgGAQ	<i>Anopheles gambiae</i>	ABA56307.1
AgGAS	<i>Anopheles gambiae</i>	ABA56309.1
AgGPB1	<i>Aedes aegypti</i>	EAT33735.1
AgGPB2	<i>Aedes aegypti</i>	EAT40134.1
AgGPB5	<i>Aedes aegypti</i>	EAT38001.1
AtGPCRA	<i>Amblyomma triste</i>	JAC28848.1
BmGPB1	<i>Apis mellifera</i>	XM_006562979.1
BmGPB2	<i>Apis mellifera</i>	XM_624332.4
BmGPB5	<i>Apis mellifera</i>	XM_006568128.1
CeGA12/13	<i>Caenorhabditis elegans</i>	CCD61930.1
CeGAO	<i>Caenorhabditis elegans</i>	CAA96595.1
CeGAQ	<i>Caenorhabditis elegans</i>	CCD67955.1
CeGAS	<i>Caenorhabditis elegans</i>	CCD73235.2
CeGPB1	<i>Caenorhabditis elegans</i>	CAA35532.1
CeGPB5	<i>Caenorhabditis elegans</i>	CAA95824.1
CeLip1	<i>Caenorhabditis elegans</i>	CAB03391.2
CeLip2	<i>Caenorhabditis elegans</i>	CCD70630.1
CeLip3	<i>Caenorhabditis elegans</i>	CCD70629.1
DmGA12/13	<i>Drosophila melanogaster</i>	AAA28569.1
DmGAI	<i>Drosophila melanogaster</i>	AAA28565.1
DmGAO	<i>Drosophila melanogaster</i>	AAA28586.1
DmGAQ	<i>Drosophila melanogaster</i>	AAA28460.1
DmGAS	<i>Drosophila melanogaster</i>	AAA28579.1
DmGPB1	<i>Drosophila melanogaster</i>	AAB59247.1
DmGPB2	<i>Drosophila melanogaster</i>	AAA73103.1
DmGPB5	<i>Drosophila melanogaster</i>	AAF46336.1
IrGPCRB	<i>Ixodes ricinus</i>	JAB73169.1
IrGPCRD1	<i>Ixodes scapularis</i>	JAB74122.1
IrGPCRD2	<i>Ixodes scapularis</i>	JAB69073.1
IsCYP21	<i>Ixodes scapularis</i>	EEC15754.1
IsCYP22	<i>Ixodes scapularis</i>	EEC15758.1
IsCYP23	<i>Ixodes scapularis</i>	EEC02779.1

Table 2.S1. Continued

Acronym	Species	Accession no.
IsCYP31	<i>Ixodes scapularis</i>	EEC08584.1
IsCYP32	<i>Ixodes scapularis</i>	EEC17346.1
IsCYP33	<i>Ixodes scapularis</i>	EEC05868.1
IsCYP41	<i>Ixodes scapularis</i>	EEC15441.1
IsCYP42	<i>Ixodes scapularis</i>	EEC16313.1
IsCYP43	<i>Ixodes scapularis</i>	ECC15440.1
IsCYPMit1	<i>Ixodes scapularis</i>	EEC14261.1
IsCYPMit2	<i>Ixodes scapularis</i>	EEC01694.1
IsCYPMit3	<i>Ixodes scapularis</i>	EEC13863.1
IsGPCRD	<i>Ixodes ricinus</i>	EEC20264.1
IsGSTD1	<i>Ixodes scapularis</i>	EEC06462.1
IsGSTD2	<i>Ixodes scapularis</i>	EEC09120.1
IsGSTD3	<i>Ixodes scapularis</i>	EEC15339.1
IsGSTE1	<i>Ixodes scapularis</i>	EEC09121.1
IsGSTE2	<i>Ixodes scapularis</i>	EEC09122.1
IsGSTE3	<i>Ixodes scapularis</i>	EEC10833.1
IsGSTM1	<i>Ixodes scapularis</i>	EEC05606.1
IsGSTM2	<i>Ixodes scapularis</i>	EEC05607.1
IsGSTM3	<i>Ixodes scapularis</i>	EEC12982.1
IsGSTO1	<i>Ixodes scapularis</i>	EEC06527.1
IsGSTO2	<i>Ixodes scapularis</i>	EEC08493.1
IsGSTO3	<i>Ixodes scapularis</i>	EEC08494.1
IsGSTZ1	<i>Ixodes scapularis</i>	EEC03386.1
IsGSTZ2	<i>Ixodes scapularis</i>	EEC17074.1
IsGSTZ3	<i>Ixodes scapularis</i>	EEC20054.1
RmGPCRC	<i>Rhipicephalus microplus</i>	ACV07675.1
RnLip1	<i>Rattus norvegicus</i>	ABG24239.1
RnLip2	<i>Rattus norvegicus</i>	AAH99072.1
RnLip3	<i>Rattus norvegicus</i>	AAA41138.1
RnOBP1	<i>Rattus norvegicus</i>	AAA41736.2
RnOBP1	<i>Rattus norvegicus</i>	ABG24236.1
RnOBP1	<i>Rattus norvegicus</i>	AAH86942.1
RpGPCRA	<i>Rhipicephalus pulchellus</i>	JAA57151.1
RpGPCRB	<i>Rhipicephalus pulchellus</i>	JAA63917.1
RpGPCRC	<i>Rhipicephalus pulchellus</i>	JAA54919.1

Table 2.S2. The 50 most abundant transcripts from the unfed, virgin adult male *Dermacentor variabilis* illumina 1st leg transcriptome.

Contig	Unique reads	Accession no.	Best match (lowest e-value) to UniprotKB database	Organism	e-value	Conserved domain(s) ^a	Putative function
77381	1709234	EAW18142	Hypothetical protein	<i>Neosartorya fischeri</i>	6E+00	None	Unknown
00308	439971	JAC35015	Putative titin	<i>Amblyomma triste</i>	00E+00	DUF1136, I-set	Myofibril scaffold
00022	410660	JAC21803	Putative troponin T skeletal muscle	<i>Amblyomma cajennense</i>	1E-179	Troponin	Skeletal muscle contraction
00073	278198	JAC34009	Putative alpha-actin	<i>Amblyomma triste</i>	00E+00	None	Skeletal muscle contraction
00084	181667	AGH19694	Cytochrome oxidase subunit 1	<i>Dermacentor nitens</i>	00E+00	None	Aerobic metabolism
03069	167176	BAK26392	Ryanodine receptor	<i>Tetranychus urticae</i>	00E+00	Ins145_P3_rec, MIR	Intracellular cation transport
00151	137793	JAC30240	Uncharacterized protein	<i>Amblyomma triste</i>	00E+00	PDZ	Unknown
00696	137289	JAC22297	Putative titin	<i>Amblyomma cajennense</i>	00E+00	I-set, fn3	Myofibril scaffold
13661	118729	AAD23988	Beta-actin	<i>Tupaia belangeri</i>	2E-79	None	Cytoskeleton
00033	112728	ABB89211	Troponin I	<i>Rhipicephalus haemaphysaloides</i>	8E-49	None	Skeletal muscle contraction
00545	109190	XP_003739692	Uncharacterized protein	<i>Metaseiulus occidentalis</i>	6E-17	None	Unknown
18048	94602	CCW16442	Xanthine dehydrogenase	<i>Sphingobium japonisum</i>	1.2E+00	None	Amino acid metabolism
15573	94585	JAC34970	Putative myosin class II heavy chain	<i>Amblyomma triste</i>	7E-27	Myosin head	Skeletal muscle contraction
04953	85346	JAA60593	Putative 24 kDa family member	<i>Rhipicephalus pulchellus</i>	4E-38	None	Unknown
27862	82021	JAB83083	Putative myosin class I heavy chain	<i>Ixodes ricinus</i>	3E-33	Myosin head	Skeletal muscle contraction
00452	80428	ECC00524	Myosin heavy chain, skeletal muscle or cardiac muscle	<i>Ixodes scapularis</i>	3E-26	Myosin_N	Skeletal muscle contraction
00140	79270	JAA57343	Calcium transporting ATPase	<i>Rhipicephalus pulchellus</i>	00E+00	Cation ATPase_N	Organelle cation transporter
00619	78855	JAC31893	Putative actin binding cytoskeleton protein filamin	<i>Amblyomma triste</i>	00E+00	CH, filamin	Cytoskeleton

Table 2.S2. Continued

Contig	Unique reads	Accession no.	Best match (lowest e-value) to UniprotKB database	Organism	e-value	Conserved domain(s) ^a	Putative function
08708	77869	ELU14970	Uncharacterized protein	<i>Capitella teleta</i>	1E+00	None	Unknown
02127	75107	JAC34859	Putative mitogen inducible protein product	<i>Amblyomma triste</i>	00E+00	FERM_M	Unknown
00589	74222	JAA62349	Uncharacterized protein	<i>Rhipicephalus pulchellus</i>	1E-112	None	Unknown
00036	72607	JAC22444	Putative myosin class II heavy chain	<i>Amblyomma cajennense</i>	00E+00	None	Skeletal muscle contraction
00430	72504	JAC31335	Putative myosin regulatory light chain	<i>Amblyomma triste</i>	1E-133	EF-hand_6	Skeletal muscle contraction
00017	72240	AAD17324	Tropomyosin	<i>Rhipicephalus microplus</i>	00E+00	None	Skeletal muscle contraction
00471	66789	JAC94084	Putative endocytosis/signaling protein	<i>Ixodes ricinus</i>	00E+00	None	Endocytosis
73407	64871	XP_657842	Uncharacterized protein	<i>Emericella nidulans</i>	2E-10	None	Unknown
00449	62738	AEO34581	Uncharacterized protein	<i>Amblyomma maculatum</i>	00E+00	None	Unknown
00975	62079	JAB81899	Nucleolar GTP-binding protein 1	<i>Ixodes ricinus</i>	00E+00	NOGCT	Biogenesis of 60s
00477	61091	JAC34490	Putative alanine-glyoxylate aminotransferase agt2	<i>Amblyomma triste</i>	00E+00	Aminotran_3	Amino acid metabolism
28761	60162	EEC00415	Putative ornithine decarboxylase	<i>Ixodes scapularis</i>	9E-126	Orn_Arg_deC_N, Orn_DAP_Arg_deC	Polyamine synthesis
07560	60258	JAC93558	Uncharacterized protein	<i>Ixodes ricinus</i>	1E-6	None	Unknown
00055	60152	JAC22069	Elongation factor 1-alpha	<i>Amblyomma cajennense</i>	00E+00	GTP_EFTU, GTP_EFTU_D2, GTP_EFTU_D3	Elongation and nuclear export
10926	60100	JAC29751	Putative alpha crystallins	<i>Amblyomma triste</i>	5E-65	HSP20	Stress response
01517	58463	EEC19998	Putative titin	<i>Ixodes scapularis</i>	00E+00	I-set, fn3	Myofibril scaffold
00690	55986	EEC04237	Putative cuticular protein	<i>Ixodes scapularis</i>	3E-69	CBM_14	Chitin metabolism
00310	55692	JAA60289	Putative eukaryotic translation initiation factor 4a2	<i>Rhipicephalus pulchellus</i>	00E+00	DEAD	Translation initiation

Table 2.S2. Continued

Contig	Unique reads	Accession no.	Best match (lowest e-value) to UniprotKB database	Organism	e-value	Conserved domain(s) ^a	Putative function
00960	55150	EEC14479	Putative stearyl-CoA desaturase	<i>Ixodes scapularis</i>	00E+00	FA_desaturase	Iron binding/ fatty acid metabolism
17549	54635	AAF81900	Beta-actin	<i>Aspergillus terreus</i>	2E-121	None	Cytoskeleton
00960	55150	EEC14479	Putative stearyl-CoA desaturase	<i>Ixodes scapularis</i>	00E+00	FA_desaturase	Iron binding/ fatty acid metabolism
00080	53133	JAC30913	Putative secreted protein	<i>Amblyomma triste</i>	4E-17	None	Unknown
00060	52729	JAC34970	Putative myosin class II heavy chain	<i>Amblyomma triste</i>	00E+00	Myosin_head	Skeletal muscle contraction
00355	52661	JAA61741	Putative eukaryotic translation initiation factor 4g2	<i>Rhipicephalus pulchellus</i>	00E+00	MIF4G	Translation initiation
43456	51562	EKN64830	Uncharacterized protein	<i>Bacillus azotoformans</i>	2E-1	None	Unknown
03024	50391	JAC22994	Putative secreted protein	<i>Amblyomma cajennense</i>	3E-9	None	Unknown
00517	50298	JAA60286	Putative amb caj-77 translation factor	<i>Rhipicephalus pulchellus</i>	00E+00	None	Translation
37644	50066	JAA56007	Putative der- and -36 heat shock-related protein	<i>Rhipicephalus pulchellus</i>	9E-75	None	Stress response
00954	49578	JAC26141	Putative enolase	<i>Amblyomma parvum</i>	00E+00	Enolase_C, enolase_N	Glycolysis
02045	49068	JAA60432	Putative tick thioester protein	<i>Rhipicephalus pulchellus</i>	00E+00	A2M_comp, thil-ester_cl	Fatty acid metabolism
02199	48695	JAA59973	Putative ATP	<i>Rhipicephalus pulchellus</i>	00E+00	ABC_tran, ABC_tran_2	ATPase activity

^aA2M_comp, A-macroglobulin complement component; ABC_tran, ATP-binding cassette transporter; ABC_tran_2, ATP-binding cassette transporter 2; Aminotran_3, aminotransferase class III; Cation ATPase_N, cation transporter/ATPase, amino-terminus; CBM_14, chitin binding peritrophin-A domain; CH, calponin homology domain; COX2, cytochrome C oxidase subunit II periplasmic domain; DEAD, DEAD/DEAH box helicase; DUF1136, domain of unknown function 1136; EF-hand_6, EF-hand domain; Enolase_C, enolase carboxyl-terminus TIM barrel domain; Enolase_N, enolase amino-terminus; FA_desaturase, fatty acid desaturase; FERM_M, 4.1 protein, ezrin, radixin, moesin central domain; fn3, fibronectin type III; GTP_EFTU, elongation factor Tu GTP binding; GTP_EFTU_D2, elongation factor Tu domain 2; GTP_EFTU_D3, elongation factor Tu carboxyl-terminus; HSP20, heat shock protein 20/alpha crystallin family; I-set, immunoglobulin intermediate-set; Ins145_P3_rec, inositol 1,4,5-triphosphate/ryanodine receptor; MIF4G, middle domain of eukaryotic initiation factor 4G; MIR, protein mannosyltransferase; Myosin_head, myosin head motor domain; Myosin_N, myosin amino-terminus; NOGCT, nucleolar GTP-binding protein carboxyl-terminus; Orn_Arg_deC_N, pyridoxal-dependent decarboxylase, pyridoxal binding domain amino-terminus; Orn_DAP_Arg_deC, pyridoxal-dependent decarboxylase carboxyl-terminus sheet domain; PDZ, post synaptic density protein; Thiol-ester_cl, alpha-macro-globulin thiol-ester bond forming region.

Table 2.S3. The 50 most abundant transcripts from the unfed, virgin adult male *Dermacentor variabilis* illumina 4th leg transcriptome.

Contig	Unique reads	Accession no.	Best match (lowest e-value) to UniprotKB database	Organism	e-value	Conserved domain(s) ^a	Putative function
20107	3060443	EEH50655	Uncharacterized protein	<i>Paracoccidioides brasiliensis</i>	6E-5	None	Unknown
03297	2068585	EDW75348	GK19734	<i>Drosophila willistoni</i>	5.9E+00	None	Unknown
29927	1571479	ABQ96857	Uncharacterized protein	<i>Haemaphysalis qinghaiensis</i>	5E-5	None	Unknown
06805	425907	EEC05627	Putative titin	<i>Ixodes scapularis</i>	00E+00	I-set	Myofibril scaffold
00086	344474	JAC22444	Putative myosin class II heavy chain	<i>Amblyomma cajennense</i>	00E+00	None	Skeletal muscle contraction
00042	316355	JAC21807	Putative troponin t skeletal muscle	<i>Amblyomma cajennense</i>	00E+00	None	Skeletal muscle contraction
13801	259741	EAU34989	TATA-box binding protein	<i>Aspergillus terreus</i>	6E-72	TBP	DNA binding/ transcription
02472	200303	Not available	Uncharacterized protein	<i>Tetranychus urticae</i>	00E+00	Ins145_P3_rec, MIR	Intracellular cation transport
03579	194590	EEC12543	Uncharacterized protein	<i>Ixodes scapularis</i>	1E-28	None	Unknown
89009	165386	JAA56423	Uncharacterized protein	<i>Rhipicephalus pulchellus</i>	6E-58	None	Unknown
0194	150153	ABB89211	Putative troponin I	<i>Rhipicephalus haemaphysaloides</i>	2E-24	None	Skeletal muscle contraction
00250	149220	EPQ15604	Actin, cytoplasmic 1	<i>Myotis brandtii</i>	2E-120	None	Cytoskeleton component
00146	146196	JAC34009	Putative actin	<i>Amblyomma triste</i>	00E+00	None	Skeletal muscle contraction
00082	133507	JAA57343	Calcium-transporting ATPase	<i>Rhipicephalus pulchellus</i>	00E+00	Cation ATPase_N	Organelle cation transporter
27571	132321	Unknown	Unknown	Unknown		None	Unknown
10067	131184	JAC31684	Arginyl tRNA protein transferase 1	<i>Amblyomma triste</i>	8E-162	None	Amino acid metabolism
00824	130575	JAC34993	Putative neural cell adhesion molecule L1	<i>Amblyomma triste</i>	00E+00	I-set, fn3	Cytoskeleton component
00023	126693	AGH19694	Cytochrome C oxidase	<i>Dermacentor nitens</i>	00E+00	None	Aerobic metabolism
00680	126367	JAB71798	Putative titin	<i>Ixodes ricinus</i>	3E-14	I-set	Myofibril scaffold
00424	124358	AGH19696	Cytochrome C oxidase	<i>Dermacentor nitens</i>	6E-109	COX2	Aerobic metabolism

Table 2.S3. Continued

Contig	Unique reads	Accession no.	Best match (lowest e-value) to UniprotKB database	Organism	e-value	Conserved domain(s) ^a	Putative function
51752	122349	EEC14950	Uncharacterized protein	<i>Ixodes scapularis</i>	5E-14	None	Unknown
00375	118647	JAC94084	Putative endocytosis/ signaling protein	<i>Ixodes ricinus</i>	00E+00	None	Endocytosis
00468	117492	JAC34970	Putative myosin class II heavy chain	<i>Amblyomma triste</i>	2E-175	Myosin_head	Skeletal muscle contraction
01684	112255	JAC29985	Uncharacterized protein	<i>Amblyomma triste</i>	1E-81	None	Unknown
02213	109709	JAC26409	Uncharacterized protein	<i>Amblyomma parvum</i>	00E+00	A2M_comp, thiol_ester_d	Unknown
17461	109466	EFG04290	Threonine dehydrogenase	<i>Streptomyces clavuligerus</i>	7.2E+00	None	Amino acid metabolism
01153	108934	Not available	Uncharacterized protein	<i>Xenopus tropicalis</i>	1.8E-1	None	Unknown
03566	108685	AAK73728	Uncharacterized protein	<i>Oryza sp.</i>	4.2+00	None	Unknown
00808	107982	EEC14479	Putative stearyl-CoA desaturase	<i>Ixodes scapularis</i>	00E+00	FA_desaturase	Iron binding/ fatty acid metabolism
15365	107585	JAB79130	Putative mitochondrial enolase	<i>Ixodes ricinus</i>	00E+00	MR_MLE, MR_MLE _C MR_MLE_N	Glycolysis
00182	105261	JAA59820	Uncharacterized protein	<i>Rhipicephalus pulchellus</i>	00E+00	Orn_Arg_deC_N, Orn_DAP_Arg_deC	Unknown
00543	105012	JAA64874	Uncharacterized protein	<i>Rhipicephalus pulchellus</i>	00E+00	NOGCT	Unknown
00574	103671	JAC34490	Putative alanine-glyoxylate aminotransferase agt2	<i>Amblyomma triste</i>	00E+00	Aminotran_3	Amino acid metabolism
00516	103502	JAC34859	Putative mitogen inducible protein product	<i>Amblyomma triste</i>	00E+00	FERM_M	Unknown
00006	100338	JAC22069	Elongation factor 1-alpha	<i>Amblyomma cajennense</i>	00E+00	GTP_EFTU, GTP_EFTU_D2, GTP_EFTU_D3	Elongation and nuclear export
15671	94282	BAC31766	Uncharacterized protein	<i>Mus musculus</i>	1E-50	None	Unknown
00912	93884	AEO34581	Uncharacterized protein	<i>Amblyomma maculatum</i>	00E+00	None	Unknown
04838	93041	KGG51869	Uncharacterized protein	<i>Microsporidia sp.</i>	2E-24	None	Unknown
02211	92976	ECC04237	Putative cuticular protein	<i>Ixodes scapularis</i>	3E-69	CBM_14	Chitin metabolism
02753	92396	JAA62349	Uncharacterized protein	<i>Rhipicephalus pulchellus</i>	8E-124	None	Unknown

Table 2.S3. Continued

Contig	Unique reads	Accession no.	Best match (lowest e-value) to UniprotKB database	Organism	e-value	Conserved domain(s) ^a	Putative function
00216	89994	JAA60289	Putative eukaryotic transcription initiation factor 4a2	<i>Rhipicephalus pulchellus</i>	00E+00	DEAD	Translation initiation
51752	89524	JAC25392	Putative wings up A	<i>Amblyomma parvum</i>	7E-32	None	Skeletal muscle contraction
07344	89354	JAA54211	Putative similar to chymotrypsin-elastase inhibitor ixodidin	<i>Rhipicephalus pulchellus</i>	6E-44	TIL	Immune response
00239	89239	AAD17324	Tropomyosin	<i>Rhipicephalus microplus</i>	00E+00	None	Skeletal muscle contraction
01350	88374	JAA61741	Putative eukaryotic translation initiation factor 4 gamma 2	<i>Rhipicephalus pulchellus</i>	00E+00	None	Translation initiation
74084	86871	Unknown	Unknown	Unknown	3E-63	None	Unknown
52616	85798	EEO3672	Putative gamma-glutamyltransferase	<i>Ixodes scapularis</i>	4E-23	None	Antioxidant metabolism
00355	85082	AAL75582	Ferritin	<i>Dermacentor variabilis</i>	1E-115	Ferritin	Iron homeostasis
00079	83955	JAC34970	Putative myosin class II heavy chain	<i>Amblyomma triste</i>	2E-175	Myosin_head	Skeletal muscle contraction
00043	83765	JAA55363	Acetyl Co-enzyme A oxidase	<i>Rhipicephalus pulchellus</i>	00E+00	Acyl_CoA_dh_1, Acyl_CoA_M, Acyl_CoA_ox_N	Metabolism

^aA2M_comp, A-macroglobulin complement component; Aminotran_3, aminotransferase class III; Acyl_CoA_dh_1, Acyl-CoA dehydrogenase carboxyl terminal domain; Acyl_CoA_M, Acyl-CoA dehydrogenase middle domain; Acyl_CoA_ox_N, Acyl-enzyme A oxidase amine terminal domain; Cation ATPase_N, cation transporter/ATPase, amino-terminus; CBM_14, chitin binding peritrophin-A domain; COX2, cytochrome C oxidase subunit II periplasmic domain; DEAD, DEAD/DEAH box helicase; FA_desaturase, fatty acid desaturase; FERM_M, 4.1 protein, ezrin, radixin, moesin central domain; fn3, fibronectin type III; I-set, immunoglobulin intermediate-set; GTP_EFTU, elongation factor Tu GTP binding; GTP_EFTU_D2, elongation factor Tu domain 2; GTP_EFTU_D3, elongation factor Tu carboxyl-terminus; I-set, immunoglobulin intermediate-set; Ins145_P3_rec, inositol 1,4,5-triphosphate/ryanodine receptor; MIR, protein mannosyltransferase; MR_MLE, mandelate racemase/muconate lactonizing enzyme carboxyl terminus; MR_MLE_C, enolase carboxyl terminus; MR_MLE_N, mandelate racemase/muconate lactonizing enzyme amino terminus; Myosin_head, myosin head motor domain; NOGCT, nucleolar GTP-binding protein carboxyl-terminus; Orn_Arg_deC_N, pyridoxal-dependent decarboxylase, pyridoxal binding domain; Orn_DAP_Arg_deC, pyridoxal-dependent decarboxylase carboxyl terminal sheet domain; TBP, TATA-binding protein; Thiol_ester_d, alpha-macro-globulin thiol-ester bond-forming region; TIL, trypsin inhibitor cysteine rich domain.

Supplemental Information: Figures

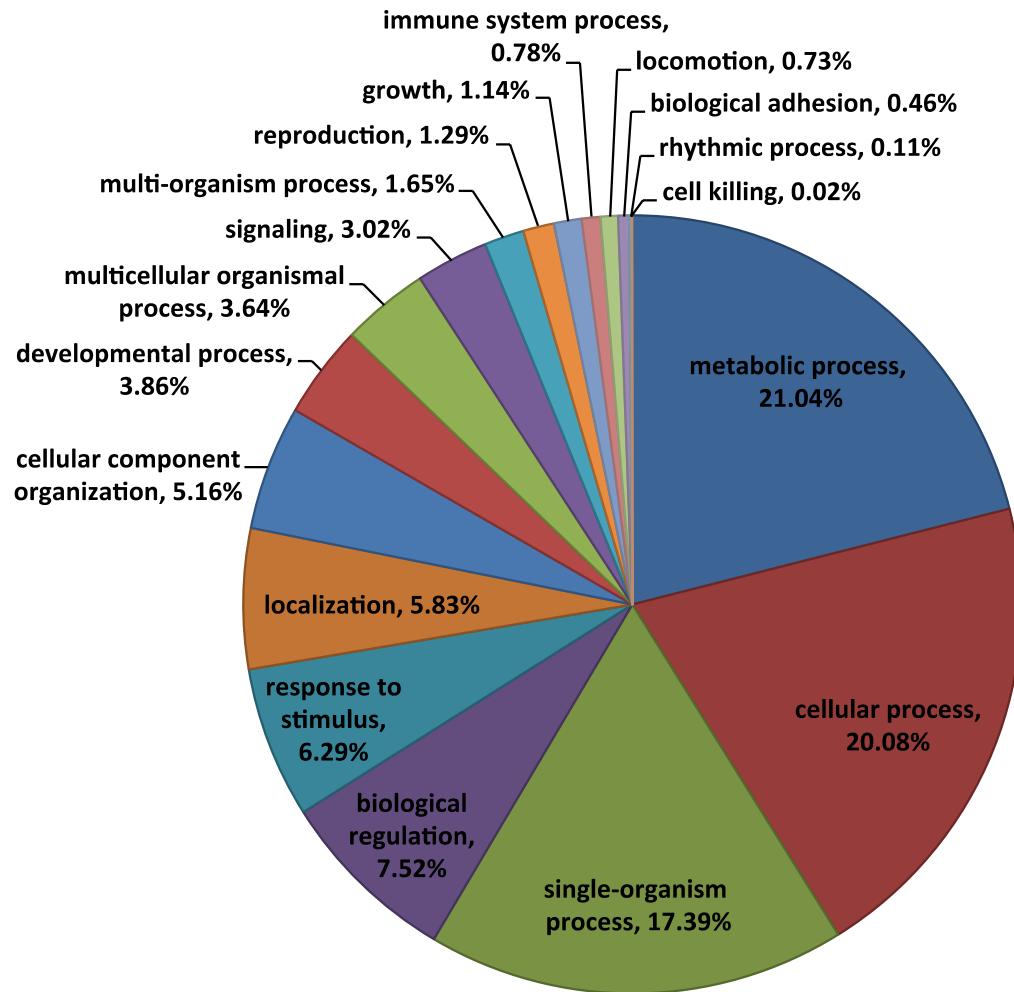


Figure 2.S1. Distribution of transcripts annotated at the gene ontology level 2 and their putative involvement in biological functions for the unfed virgin adult male *Dermacentor variabilis* illumina 1st leg transcriptome.

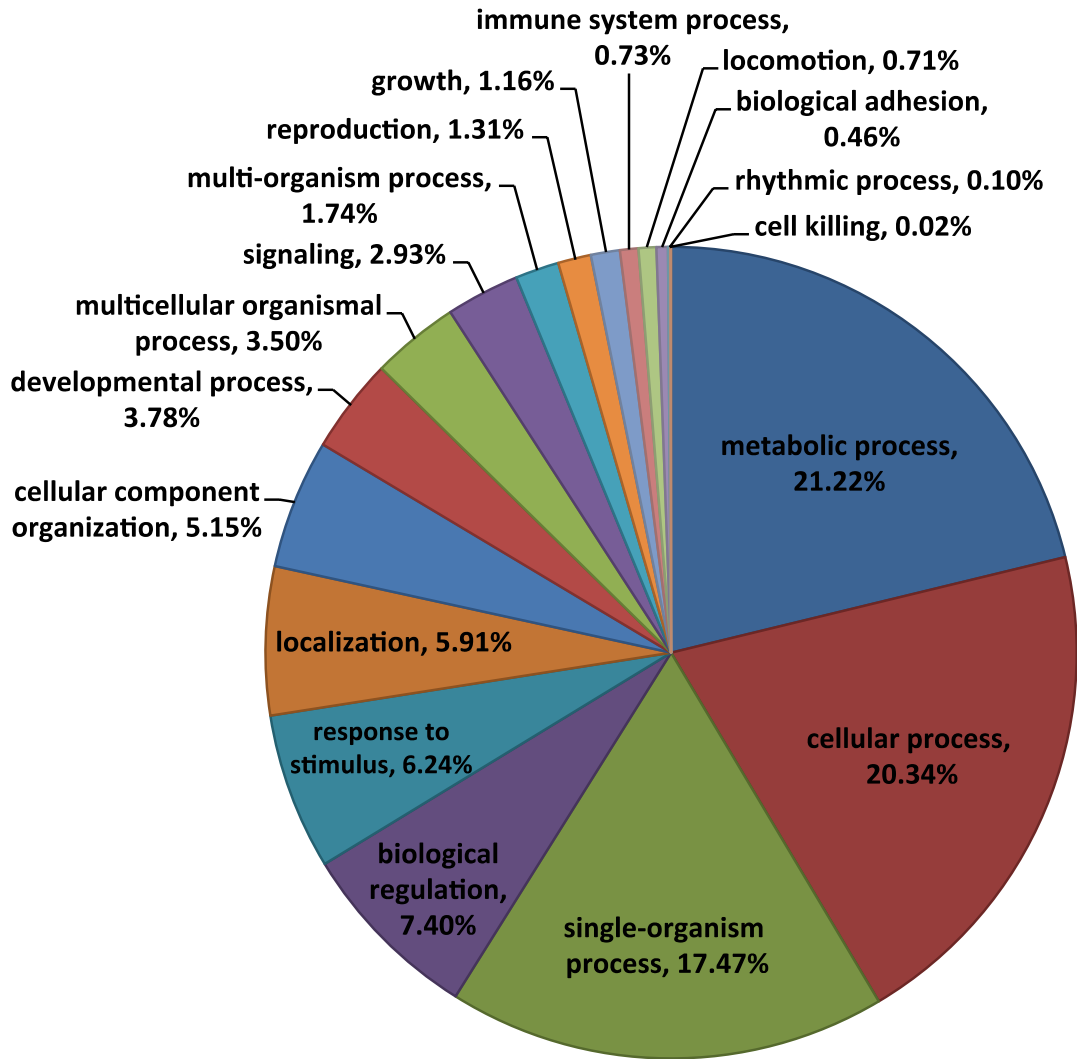


Figure 2.S2. Distribution of transcripts annotated at the gene ontology level 2 and their putative involvement in biological functions for the unfed virgin adult male *Dermacentor variabilis* illumina 4th leg transcriptome.

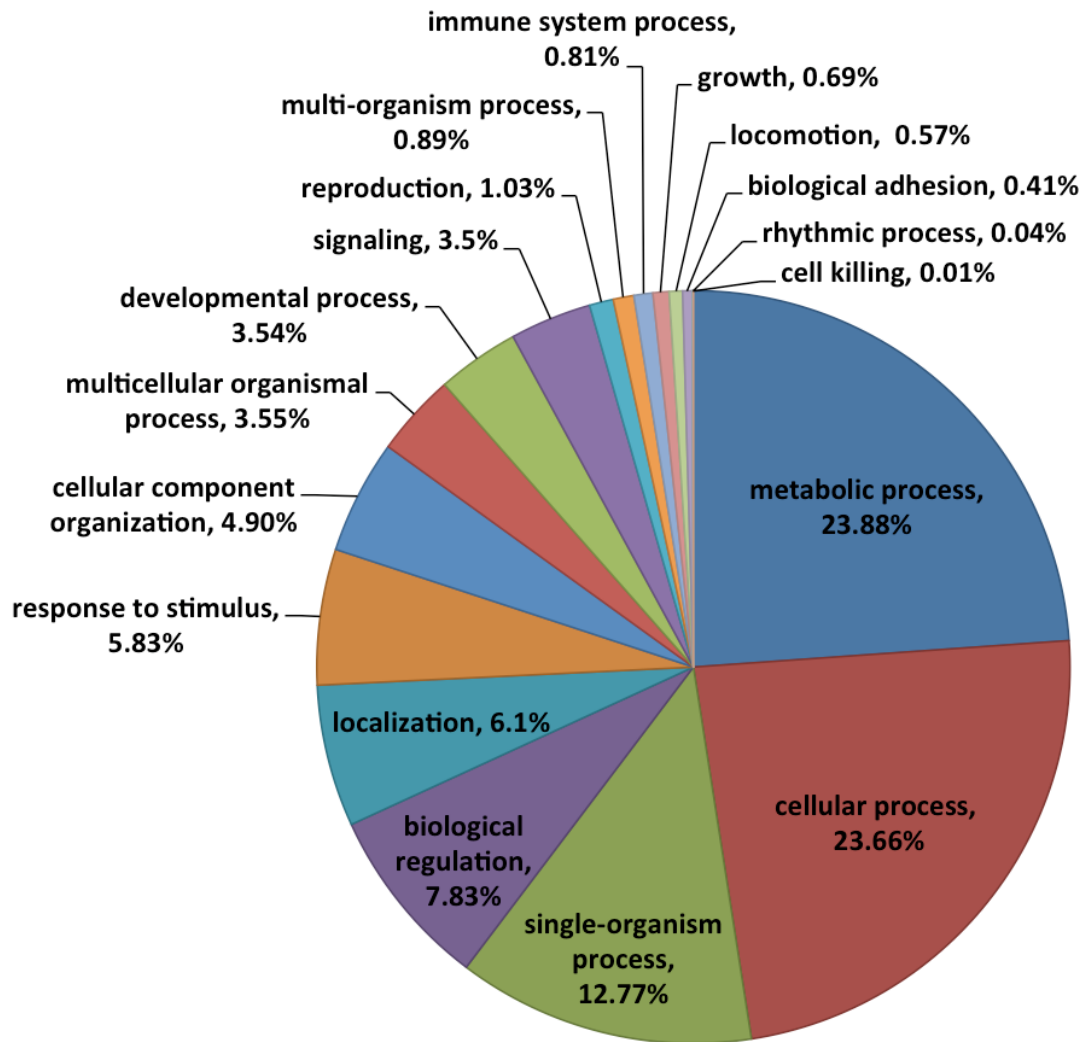


Figure 2.S3. Distribution of transcripts annotated at the gene ontology level 2 and their putative involvement in biological functions for the unfed virgin adult male *Dermacentor variabilis* 454 1st leg transcriptome.

```

contig_84287 -----
AtJAA54113.1 MLLILLGLALPQCMLGAGVSTPGGNGNNIRQPGYGFYLPYEENPQHFHEQLLIDLTDINE

contig_84287 -----AIHIKCVYKVRGIR-----TWL*-----RLHFLSYIFNTVPLQFC
AtJAA54113.1 PIFIKMRNYGTNTPYRCHYAHKVGQLYDGSFWYNLNIRAPTRAGYQYITFPNIAIPLR--
                :* * : : *          ::::: :*:
                :*      : . *:* * :          .*: :::

contig_84287 LYTL*HSSGTSVSIYASVRRSWHPFLSPM-----SCTKIIQP-----
AtJAA54113.1 -----TGQ----HPYPNALWYRFTPAPALRKILTINRRLGCAVLVEQLRGGRRGCQ
                :*      : . *:* * :          .*: :::

contig_84287 -----PFLSRX-----
AtJAA54113.1 LVQTSSTVDNQVPPQCQRAYNENCKGNSITLYEPSCKASQAYFPQHGTKL
                * . *

```

Figure 2.S4. Multiple sequence alignment (Clustal Ω) of the deduced amino acid sequence for the putative salivary-like lipocalin (contig 84287) identified exclusively in the Haller's organ spf transcriptome of unfed virgin adult male *D. variabilis* versus the top BLAST tick hit (lowest expected value; Table 1). Asterisks (*) denote conserved residues, colons (:) indicate conservation between groups of strongly similar properties scoring >0.5 in the Gonnet PAM 250 matrix, and periods (.) indicate conservation between groups of weakly similar properties scoring ≤ 0.5 on the Gonnet PAM 250 matrix. The acronym consists of the first letter of genus and species (*Amblyomma triste*, At) followed by the GenBank accession number for the protein BLAST hit (JAA54113.1).

```

contig_72702      WKHSSRSAKMGQQTSSSLPRAKVKTLKMTAVVFGAFLVTNVPYMVQEAILAFGNPGILDA
IsEEC06829.1     -----MVKTLKMTVVVFGAFLVTNVPYMVQEMILAFGNPGILDH
                   *****.*****
contig_72702      NLVALFGVISASNSAINPYIFL-----
IsEEC06829.1     NVVALFGVISASNSAINPYIYFFFQRSKRQCGKFCALLKDAKTWFSCRRLRLCNSQSA
                   *:*:*****:
contig_72702      -----
IsEEC06829.1     SSPVTMTSLHLNGDYAMTSWNTGTQVEIRSPNKVDV

```

Figure 2.S5. Multiple sequence alignment (Clustal Ω) of the deduced amino acid sequence for the putative G-protein coupled receptor (contig 72702) identified exclusively in the Haller's organ spf transcriptome of unfed virgin adult male *D. variabilis* versus the top BLAST tick hit (lowest expected value; Table 1). Asterisks (*) denote conserved residues, colons (:) indicate conservation between groups of strongly similar properties scoring >0.5 in the Gonnet PAM 250 matrix, and periods (.) indicate conservation between groups of weakly similar properties scoring ≤ 0.5 on the Gonnet PAM 250 matrix. The acronym consists of the first letter of genus and species (*Ixodes scapularis*, Is) followed by the GenBank accession number for the protein BLAST hit (EEC06829.1).

```

contig_83622      DMNDDFWANQDSVTMMVVLIVATFFAAWTPYAVLCLWAVFGKASAVPHLVAVVPPLFCKT
IsEEC07880.1     -----MVALIVVTFFFAWTPYAVLCLWAVFADTKSVPHLLAMVPPLFAKT
                  **.***.*** *****.....:****:*:*****.**

contig_83622      ASAINPFIYFFSNPRIRTDIYALLTCRCKTLGRRS---CSIQEDYC*PPP-
IsEEC07880.1     ASTINPFIYFLSNPCIRADVLQLLGCRARSSPHMAISSDAVEEERCCQQA
                  **:*****:* ** **:*  ** **.: : : : : : *

```

Figure 2.S6. Multiple sequence alignment (Clustal Ω) of the deduced amino acid sequence for the putative G-protein coupled receptor (contig 83622) identified exclusively in the Haller’s organ spf transcriptome of unfed virgin adult male *D. variabilis* versus the top BLAST tick hit (lowest expected value; Table 1). Asterisks (*) denote conserved residues, colons (:) indicate conservation between groups of strongly similar properties scoring >0.5 in the Gonnet PAM 250 matrix, and periods (.) indicate conservation between groups of weakly similar properties scoring ≤ 0.5 on the Gonnet PAM 250 matrix. The acronym consists of the first letter of genus and species (*Ixodes scapularis*, Is) followed by the GenBank accession number for the protein BLAST hit (EEC07880.1).

```

contig_13937      MGCAMSAEERAALARSKQIEKNLKEDGIQAAKDIKLLLLGAGESGKSTIVKQMKI IHDSG
RpJAA58325.1    ---MSAEERAALARSKQIEKNLKEDGIQAAKDIKLLLLGAGESGKSTIVKQMKI IHDSG
                  *****

contig_13937      FTQEDFKQYKPVVYSNTIQSMVAILRAMPNLGISFGNNEREADAKMVFDDVVARMEDTEPF
RpJAA58325.1    FTQEDFKQYKPVVYSNTIQSMVAILRAMPNLGISFGNNEREADAKMVFDDVVARMEDTEPF
                  *****

contig_13937      SEELLSAMKRLWTD SGVQECFGRSNEYQLNDSAKYFLDDLDRLGKKDYMPTEQDILRTRV
RpJAA58325.1    SEELLSAMKRLWTD SGVQECFGRSNEYQLNDSAKYFLDDLDRLGKKKEYMPTEQDILRTRV
                  *****;*****

contig_13937      KTTGIVEVHFSFKNLNFKLFDVGGQRSEKRWIHC FEDVTAIIFCVAMSEYDQVLHEDET
RpJAA58325.1    KTTGIVEVHFSFKNLNFKLFDVGGQRSEKRWIHC FEDVTAIIFCVAMSEYDQVLHEDET
                  *****

contig_13937      TNRMQESLKLFD SICNNKWFDTDSIILFLNKKDLFE EKIKKSPLTICFPEYTGAQEYGEA
RpJAA58325.1    TNRMQESLKLFD SICNNKWFDTDSIILFLNKKDLFE EKIKKSPLTICFPEYTGAQEYGEA
                  *****

contig_13937      AAYIQAQFEAKNKSTTKEIYCHMTCATD TTNIQVFDAVTDVI IANNLRGCGLY
RpJAA58325.1    AAYIQAQFEAKNKSTTKEIYCHMTCATD TTNIQVFDAVTDVI IANNLRGCGLY
                  *****

```

Figure 2.S7. Multiple sequence alignment (Clustal Ω) of the deduced amino acid sequence for the putative G-protein α_0 subunit (contig 13937) identified exclusively in the Haller's organ spf spf transcriptome of unfed virgin adult male *D. variabilis* versus the top BLAST tick hit (lowest expected value; Table 1). Asterisks (*) denote conserved residues, colons (:) indicate conservation between groups of strongly similar properties scoring >0.5 in the Gonnet PAM 250 matrix, and periods (.) indicate conservation between groups of weakly similar properties scoring ≤ 0.5 on the Gonnet PAM 250 matrix. The black bar shows the $G\alpha$ subunit domain. The acronym consists of the first letter of genus and species (*Rhipicephalus pulchellus*, Rp) followed by the GenBank accession number for the protein BLAST hit (JAA58325.1).

```

Contig_24477      -----ISSDGAYAL
IrJAB79904.1     QIATNPKFPDPTVLSSSRDKTLILWRLTRDDASYGVATRRLRGHGHFVTDVVLSSDGGQYAL
                                     :**** **

Contig_24477     SASWDKSLRLWELETGNTTRTFVGHNTDVLVSFSADNRQIVSGSRDRTIKLWNTLGDC-
IrJAB79904.1     SCSWDKTLRLWDLAVGSSTRRFEGHEKDVLSVAFSADNRQIVSGSRDKTIKLWNTLAECK
*.****:****:*  .*.:** * * * :*****:*****:*****.*:

```

Figure 2.S8. Multiple sequence alignment (Clustal Ω) of the deduced amino acid sequence for the putative G-protein β subunit (contig 24477) identified exclusively in the Haller's organ spf transcriptome of unfed virgin adult male *D. variabilis* versus the top BLAST tick hit (lowest expected value; Table 1). Asterisks (*) denote conserved residues, colons (:) indicate conservation between groups of strongly similar properties scoring >0.5 in the Gonnet PAM 250 matrix, and periods (.) indicate conservation between groups of weakly similar properties scoring ≤ 0.5 on the Gonnet PAM 250 matrix. The black bar shows the WD G β repeat domain. The acronym consists of the first letter of genus and species (*Ixodes ricinus*, Ir) followed by the GenBank accession number for the protein BLAST hit (JAB79904.1).

```

contig_77721      -----AFFAGGWGNDPEITHCALL
IsEEC01411.1     TNSFKDDKLELAYQGYSHRQRQTALVIVNLDVFLKVAMLVAFFVAGELDEPR-LTCALL
                                     ***..*  ::*  ****

contig_77721     RYLPWVLVNVLLSLLTCWRFFANNYLHWGAALIWIWALNAQGNNGFVTSGELRFEPGGDV
IsEEC01411.1     RNLPWIAVNLLCCLLYWKFFASNYLHWGALLIWIWALNAEGNGTFGVTWGYLQFEPGGDV
*  ***:  **:*.*** *:***.***** *****:***.*** * *:*****

contig_77721     SX-----
IsEEC01411.1     AGDGSWHVMFTVFVTYAMLPLPLKWCIVCGVLASLGHLLVCCLYRAHLDRPEFERMILTN
:

```

Figure 2.S9. Multiple sequence alignment (Clustal Ω) of the deduced amino acid sequence for the putative adenylate/guanylate cyclase (contig 77721) identified exclusively in the Haller’s organ spf transcriptome of unfed virgin adult male *D. variabilis* versus the top BLAST tick hit (lowest expected value; Table 1). Asterisks (*) denote conserved residues, colons (:) indicate conservation between groups of strongly similar properties scoring >0.5 in the Gonnet PAM 250 matrix, and periods (.) indicate conservation between groups of weakly similar properties scoring ≤ 0.5 on the Gonnet PAM 250 matrix. The acronym consists of the first letter of genus and species (*Ixodes scapularis*, Is) followed by the GenBank accession number for the protein BLAST hit (EEC01411.1).

```

contig_37845 -----RIE
IsEEC13610.1 ASAADLAVSVSTFCRAFPFHFMCDRQLRLTQLGRGLARIFGGRGSAVPSLFFVLEPELLE
                                         :*

contig_37845 MRFDHVVANINLPFLQVRDDAIKHERYKGMEIKGQMVHCPESRALLFLGSPVVDGGLSA
IsEEC13610.1 MRFDHVVAATNLPFLQVRDDAIKHQRYKGMEVKGQMVHCPESRALLFLGSPVVDGGLSA
*****  *****:*****:*****.:*****

contig_37845 MLRRGLYISDVPVHDATRDILLVEEQSRAQDGLKRRMDKIRASIQEANLAVEEERQKNVD
IsEEC13610.1 MLRRGLYISDVPVHDATRDILLVEEQARAQDGLKRRMDKIRSSIQEANLAVEEERQKNVD
*****:*****:*****

contig_37845 LLHLIFPPRVARKLWLGESMEAQQHDQATLLFSDIVGFTAICSTATPMMVINMLX-----
IsEEC13610.1 LLHLIFPPSVARKLWLGESVEAQQHDQVTLFSDIVGFTAICSTATPMMIETVGDAYCVA
*****  *****:*****.*****: .:

```

Figure 2.S10. Multiple sequence alignment (Clustal Ω) of the deduced amino acid sequence for the putative adenylate/guanylate cyclase (contig 37845) identified exclusively in the Haller's organ spf transcriptome of unfed virgin adult male *D. variabilis* versus the top BLAST tick hit (lowest expected value; Table 1). Asterisks (*) denote conserved residues, colons (:) indicate conservation between groups of strongly similar properties scoring >0.5 in the Gonnet PAM 250 matrix, and periods (.) indicate conservation between groups of weakly similar properties scoring \leq 0.5 on the Gonnet PAM 250 matrix. The solid black bar shows the heme NO binding associated domain, and the dashed black bar shows the guanylate cyclase catalytic domain. The acronym consists of the first letter of genus and species (*Ixodes scapularis*, Is) followed by the GenBank accession number for the protein BLAST hit (EEC13610.1).

```

contig_82720      -----QKCSDEERSVGCLPDKLKAET
IsEEC03664.1     MKTHQISKLDAVKTYMRMRHVPDHLQNKVIRWFDYLWLTQKSSDEERSVGCLPDKLKAET
                  ** .*****

contig_82720      AIHVHLDTLKRVEIFQNTTEAGFLCELVLRLRPVLFSPGDYICRKGEVGKEMYIVNRGRLO
IsEEC03664.1     AIHVHLDTLKRVEIFQNTTEAGFLCELVLRLRPVLFSPGDYICRKGEVGKEMYIVNRGRLO
                  *****

contig_82720      VVTDNGK-----
IsEEC03664.1     VVTDNGKTVLATLRAGSYFGEISILNMGTAGNRRTASVRSVGYSDLFCLYKQDMWDVLKD
                  *****

```

Figure 2.S11. Multiple sequence alignment (Clustal Ω) of the deduced amino acid sequence for the putative cyclic nucleotide-gated ion channel (contig 82720) identified exclusively in the Haller’s organ spf transcriptome of unfed virgin adult male *D. variabilis* versus the top BLAST tick hit (lowest expected value; Table 1). Asterisks (*) denote conserved residues, colons (:) indicate conservation between groups of strongly similar properties scoring >0.5 in the Gonnet PAM 250 matrix, and periods (.) indicate conservation between groups of weakly similar properties scoring ≤ 0.5 on the Gonnet PAM 250 matrix. The black bar shows the cyclic nucleotide binding domain. The acronym consists of the first letter of genus and species (*Ixodes scapularis*, Is) followed by the GenBank accession number for the protein BLAST hit (EEC03664.1).

```

CeCGNG      MSAARTEFQNKMDGIKQYMELRKVSKQLEIRVIKWFDFYLTNKSLSLSDQQVLKVLDPDKLQ
Contig_82720 -----QKCSDEERSVGCCLPDKLK
DmCNG      MNVARVEFQNRMDGVKQYMAFRRVGHELEARVIRWFAYTWSQSGALDEERVLAALPDKLK
                . . .::: : *****:

CeCGNG      AEIAMQVHFETLRKVRIFQDCEAGLLAELVLKLQVLFSPGDFICKKGDIGREMYIVKRG
Contig_82720 AEIAIHVHLDLTKRVEIFQNTAEAGFLCELVLRLRPVLFSPGDYICRKGEVKGEMYIVNRG
DmCNG      AEIAIQVHMDTLKQVRIFHDTEPGLLEALVLKLKLQVLFSPGDYICRKGDVKGEMYIVKRG
                *****:***:***:*.***: * *:* ***:* :*****:***:***:*.***:***

CeCGNG      RLQVVDDDGGKVFVTLQEGSVFGELSILNIAGSKNGNRRTANVRVSVGYTDLFVLSKTDLW
Contig_82720 RLQVVTDNGK-----
DmCNG      KLSVVGDDGITVLTATLGAGSVFGEVSVLEIAGNRTGNRRTANVRSGLGYSDLFCLAKRDLW
                :*.** *:*

```

Figure 2.S12. Multiple sequence alignment (Clustal Ω) of the deduced amino acid sequence for the putative cyclic nucleotide-gated ion channel (CNG) α - subunit (contig 82720) identified exclusively in the Haller's organ spf transcriptome of unfed virgin adult male *D. variabilis* versus the *Caenorhabditis elegans* and *Drosophila melanogaster* CNG α - subunits (.Asterisks (*) denote conserved residues, colons (:) indicate conservation between groups of strongly similar properties scoring >0.5 in the Gonnet PAM 250 matrix, and periods (.) indicate conservation between groups of weakly similar properties scoring ≤ 0.5 on the Gonnet PAM 250 matrix. The black bar shows the cyclic nucleotide binding domain. The acronym consists of the first letter of genus and species (*Caenorhabditis elegans*, Ce; *Drosophila melanogaster*, Dm) followed by the protein name (CNG).

```

contig_01853      TIGTEAAAAEESAKRQGGTRVFKKSSPNGKITMYLGKRDFVDHITSVDPIDGVVLIDPDY
IsEEC07926.1     -----IVIPFRVFKKSSPNSKITMYLGKRDFVDHITSVDPIDGVVLIDPDY
                  *****.*****

contig_01853      VKERKVFVGHVLAAFRYGREDLDVLGLTFRKDLYLASEQIYPPLAE--TAGRPLTRLQERL
IsEEC07926.1     VKDRKVFVGHVLAAFRYGREDLDVLGLTFRKDLYLASEQIYPRLTGGENSNRPLTRLQVSS
                  **.****** *: .: *****

contig_01853      LRKLGPNAYPFYFEL-PPHCPASVTLQPAPGDTGKPCGVDYELKGYVADS---PEDKPHK
IsEEC07926.1     ESSFFFFLSFFYYLFVRNLGWGGTTFPATRLPDGFCNP-QRVNGHCSTAEVTQPRFCSY
                  .: *:: * . . * ** * .::: : :

contig_01853      RNSVRLAIRKIMYAPSRQGEQPSVEVSKEFVMSPNKLHLEASLDKELYHHGEDIAVNVHI
IsEEC07926.1     RNSVRLAIRKIMYAPSRQGEQPSVEVSKEFVMSPNKLHLEASLDKELYHHGEDIAVNVHI
                  *****

contig_01853      ANNSNRTVKKVKVSVRQFADICLFSTAQYKCTVAEIDSEEGCPVSPGFVTLKVVYLRPLL
IsEEC07926.1     ANNSNRTVKKVKVSVRQFADICLFSTAQYKCTVAEIDSEEGCPVSPGFVTLKVVHYLRPLL
                  *****:*****

contig_01853      ANNKDKRGLALDGQLKHEDTNLASSTIITDPAQKENLGIIVQYKVKVKLCLGPLGGDLVA
IsEEC07926.1     ANNKDKRGLALDGQLKHEDTNLASSTM-----
                  *****;

contig_01853      ELPFILMHPKPEESSPIRVVSEPKAPGPVPLDTNLIELDTDAAASLDDDDIIFEDFARLR
IsEEC07926.1     -----

```

Figure 2.S13. Multiple sequence alignment (Clustal Ω) of the deduced amino acid sequence for the putative β -arrestin (contig 01853) identified exclusively in the Haller's organ spf transcriptome of unfed virgin adult male *D. variabilis* versus the top BLAST tick hit (lowest expected value; Table 2). Asterisks (*) denote conserved residues, colons (:) indicate conservation between groups of strongly similar properties scoring >0.5 in the Gonnet PAM 250 matrix, and periods (.) indicate conservation between groups of weakly similar properties scoring ≤ 0.5 on the Gonnet PAM 250 matrix. The solid black bar shows the arrestin amino terminal domain, and the dashed black bar shows the arrestin carboxyl terminal domain. The acronym consists of the first letter of genus and species (*Ixodes scapularis*, Is) followed by the GenBank accession number for the protein BLAST hit (EEC07926.1).

```

CeBarr      -----MVDEDKKSGTRVFKKTS PNGKITTYLGKRDFIDRGDYVDLIDGMVLIDEEY
Contig_01853 TIGTEAAAAEESAKRQGGTRVFKKSSPNGKITMYLGKRDFVDHITSVDPIDGVVLIDPDY
DmBarr      SAGD--ETGGDASSRRQATR VFKKSSNGKITVYLGKRDFVDHVTHVDPIDGVVFDPEY
           .: .*****:* ***** *****:*: ** **:*:*:* :*

CeBarr      IKDNRKVT A H L L A A F R Y G R E D L D V L G L T F R K D L I S E T F Q V Y P Q T D K S I S R P L S R L Q E R L K
Contig_01853 VKE-RKVFGHVLA A F R Y G R E D L D V L G L T F R K D L Y L A S E Q I Y P P L A E T A G R P L T R L Q E R L L
DmBarr      VKD-RKVFGQVLA A F R Y G R E D L D V L G L T F R K D L Y L A H E Q I Y P P M Q --LDRP M T R L Q E R L I
           *: ** .:*****:***** ** ** **:*:*****

CeBarr      RKLGANAFPFWF E V A P K S A S S V T L Q P A P G D T G K P C G V D Y E L K T F V A V T D G S S G E K P K K S A
Contig_01853 RKLGPNA Y P F Y F E L P P H C P A S V T L Q P A P G D T G K P C G V D Y E L K G Y V A D S P E -----DKPH
DmBarr      KKLGPNA H P F Y F E V P P Y C P A S V L Q P A P G D V G K S C G V D Y E L K A F V G E N V E -----DKPH
           :*** **.*:*:*: * . :*:*****.* ***** :*. . . *

CeBarr      LSNTVRLA I R K L T Y A P F E S R P Q M V D V S K Y F M M S S G L L H M E V S L D K E M Y Y H G E S I S V N V H
Contig_01853 KRNSVRLA I R K I M Y A P S R Q E Q P S V E V S K E F V M S P N K L H L E A S L D K E L Y H H G E D I A V N V H
DmBarr      KRNSVRLT I R K V M Y A P S K V G E Q P S I E V S K E F M M K P N K I H L E A T L D K E L Y H H G E K I S V N V H
           *:***:***: *** . ** :*:** *:. :*:*:***:*:*:*.*:***

CeBarr      IQNNSNKT V K K L K I Y I I Q V A D I C L F T T A S Y S C E V A R I E S N E G F P V G P G G T L S K V F A V C P L
Contig_01853 IANNSNRT V K K V K V S R Q F A D I C L F S T A Q Y K C T V A E I D S E E G C P V S P G F T L S K V Y Y L R P L
DmBarr      VANNSNRT V K K I K V C V R Q F A D I C L F S T A Q Y K S V V A E I E S E D G C Q V A P G F T L S K V F E L C P L
           : ****:***:*: : *.*****:*.*. **.*:*:*: * .** *****: : **

CeBarr      LSNNKDKRGLALD G Q L K H E D T N L A S S T I L D S K T S K E S L G I V V Q Y R V K V R A V L G --PLNGE
Contig_01853 LANNKDKRGLALD G Q L K H E D T N L A S S T I I T D P A Q K E N L G I I V Q Y K V K V K L C L G --PLGGD
DmBarr      LANNKDKWGLALD G Q L K H E D T N L A S S T L I T N P A Q R E S L G I M V H Y K V K V K L L I S S P L L N G D
           *:***** *****:*****: . .:*.***:*:*:***: . * *

CeBarr      LFAELPFTLTHSKPPEESP E R T-----DRGLPSIE-----ATNGSEPV D I D
Contig_01853 LVAELPFILMHPKPEESSPI R V V-SEP-----KAPGPVPLDTN
DmBarr      LVAELPFTL M H P K P E E E H P L L G E R S P R A S L A G G L P L V S M S D G E T E S A T G G Q D V P T T T N
           *.***** * * * * * . * :

```

Figure 2.S14. Multiple sequence alignment (Clustal Ω) of the deduced amino acid sequence for the putative β -arrestin (BArr; contig 82720) identified exclusively in the Haller's organ spf transcriptome of unfed virgin adult male *D. variabilis* versus the *Caenorhabditis elegans* and *Drosophila melanogaster* β -arrestins (accession no. CCD67242.1 and AAF32365.1, respectively). Asterisks (*) denote conserved residues, colons (:) indicate conservation between groups of strongly similar properties scoring >0.5 in the Gonnet PAM 250 matrix, and periods (.) indicate conservation between groups of weakly similar properties scoring ≤ 0.5 on the Gonnet PAM 250 matrix. The solid black bar shows the arrestin amino terminal domain, and the dashed black bar shows the arrestin carboxyl terminal domain. The acronym consists of the first letter of genus and species (*Caenorhabditis elegans*, Ce; *Drosophila melanogaster*, Dm) followed by the protein name (BArr).

```

contig_69591      -----SAQTLTWTLFALAINPGVQRRVHDELDRVFGKRAACNITKSHVSKLTYLDRVLKET
IsEEC03681.1     GHDTVTSQSLTWTLFVLGIYPDVQSKVHEELDLIFAHDMTRGITRADIADLSYLDRVIKVS
                  *:*****.*.* ** **:*** :*.: : **::::.*:*****:* :
contig_69591      MRIFTIVPWVGRSLTEPLKIGNCTIPEGCTCYVFYGIHRDPHTHYTDPEVDFDPDRFLPEK
IsEEC03681.1     RAFFYHITVSNAS--RVRIFRNYQIPKGTTCFVFYGLHRDPDHYRDPETFDPDRLPEN
                  :* : * . : * **:* **:*****:**** ** ***.*****:
contig_69591      CSRNHPFAFVPPFSAGPRNCIGQKFAMLELKVLLAKVLTNFSVSSCNHRDILLFDADILLR
IsEEC03681.1     CSGRHPFAFVPPFSAGPRNCVGQKFALMELKVTLAKLLRRYQVKSCHQRDLLLLMADMLLR
                  ** .*****:*****:***** **:* .:*.**.:*****: **:***
contig_69591      TKRPIRIRLQPRHDTX
IsEEC03681.1     TRNPIKFQLTERLAPQ
                  *:.**:::* *

```

Figure 2.S15. Multiple sequence alignment (Clustal Ω) of the deduced amino acid sequence for the putative cytochrome p450 (contig 69591) identified exclusively in the Haller’s organ spf transcriptome of unfed virgin adult male *D. variabilis* versus the top BLAST tick hit (lowest expected value; Table 2). Asterisks (*) denote conserved residues, colons (:) indicate conservation between groups of strongly similar properties scoring >0.5 in the Gonnet PAM 250 matrix, and periods (.) indicate conservation between groups of weakly similar properties scoring \leq 0.5 on the Gonnet PAM 250 matrix. The black bar shows the cytochrome p450 domain. The acronym consists of the first letter of genus and species (*Ixodes scapularis*, Is) followed by the GenBank accession number for the protein BLAST hit (EEC03681.1).


```

contig_06898      DFSVSLIVHFLLPGVAKFFRLKFFNPDTLEYFRSLCQRVIKGRIDTKIRQDDDFLQHMIDC
IsEEEC19065.1    -----METRRKTKTKQDDDFLQIMIDA
                  :: * .** :***** **

contig_06898      QQGTYSGDTSKEVADTEERIFDVDSKLADTEDVPSNALSEEEAMAQCFMFLIAGQGTST
IsEEEC19065.1    QERNRTL DVSQGGEE DAVKLF DIDSKLTDEAPLSSKTLSEEEALSQCMMFILAGHTTSS
                  *: . : *.*: : : **:*****: : *:*****:***:***:***:***:

contig_06898      LVAFTLYMLALNPDVQEKLR EEV D LCVKNHGEYPAMEVVAKLEYLHGVI SEMLRMFPPAS
IsEEEC19065.1    VIAFSLYLLALNPEAQNKLRKEVDVCVKENGPKPSMDAIDKLQYLHGVS EALRIFPPAS
                  :*:**:*:*****:.*:***:***:***:.* *:*.:. **:*****:* **.*

contig_06898      RLERETTQDYVLGDTGIKIPKGCVIAVPLYAMHHDPEYFPDPYVFRPERFMGENAANIRP
IsEEEC19065.1    RLERETT E DYVLGNTGIKVPKGCVVAVPVWALHHD PQYFPDPHSFKPERFSKENVDSIPP
                  *****:*****:*****:*****:***:*.**:*****:*****: *:***** ** . * *

contig_06898      YTYLPGAGPRNCVGMRLGLHAAKMAVLHAVRIAQFVRTDKTKVPLEFFKGFVIVSSDI
IsEEEC19065.1    YVYLPGAGPRNCIGVRLGLRAVKMALFHSICNVEFVRTAKTKVPLELFFKGFVIVSSDI
                  *.*****:*.***:*.***:*.***:*.***:*.***:*.***:*.***:*****

contig_06898      TVGVRKRAATSK*NIHIDLKAI*TPTPLLIYLDFFA**FRKVTSDFHSEDNTMTLTESAV
IsEEEC19065.1    TVGVRKRTS-----
                  *****:

```

Figure 2.S17. Multiple sequence alignment (Clustal Ω) of the deduced amino acid sequence for the putative cytochrome p450 (contig 06898) identified exclusively in the Haller’s organ spf transcriptome of unfed virgin adult male *D. variabilis* versus the top BLAST tick hit (lowest expected value; Table 2). Asterisks (*) denote conserved residues, colons (:) indicate conservation between groups of strongly similar properties scoring >0.5 in the Gonnet PAM 250 matrix, and periods (.) indicate conservation between groups of weakly similar properties scoring \leq 0.5 on the Gonnet PAM 250 matrix. The black bar shows the cytochrome p450 domain. The acronym consists of the first letter of genus and species (*Ixodes scapularis*, Is) followed by the GenBank accession number for the protein BLAST hit (EEC19065.1).

```

contig_14383      -----ARTNIQRGDASSLALYKAARKSVGQFGGSKLFFLNLLPPSRLLHKIIFAVQSIF
AtJAC34536.1     LQFFAGALTDVQRNDAAVAALSEAARQSVGQFGGAVLFLNLLPDSPLLHKTLGVRSLF
                  * * ::* * *::* * :***:*****: **:* ** * ** * :.:*:*
                  _____
contig_14383      TQLPSDEVIERMLPIINHRRENPDPTKEDLLQLLLNSEKEDRKNNGKIEGLESSSIMSH
AtJAC34536.1     TQLPSDEMMDRMTPIINHRREHPDPTKEDVLQLLLNSEQEELSSNGKAEGRQLSSTMMSH
                  *****:.* * *****.*****:*****:*. . * ** * : * * **
                  _____
contig_14383      PLELRASNTAICVIAGMDNIASPLAFASYLLSEHQEVQDKVRAEVQALLKKEGELTYDG
AtJAC34536.1     PLTLRTASNTCIFVIASIDAVASPLAFTSYLLSEHPDIQEKVRTEVQAILKKEGKFTYEN
                  ** *****.* * * .:* :*****:***** :.*:***:*****:*****:***:
                  _____
contig_14383      LGELTYLGQVLSETLRLYPALPGWVPRVCEDEYENGVRIKGMNSVSVLPLDVHYDPVLW
AtJAC34536.1     IMELTYLGQVLSESLRLYPSLPGSIRRICDEDEYHNGVRILKGMNVSVP TLDLHYDPELW
                  : *****:*****:*** : *:*****:*****.* ** **:* **
                  _____
contig_14383      PEPKKFDPERFSKANKDRIHFPFSYFPYGIGPRTCMTLLSRVEFLVTL SLLVMRYRLLPS
AtJAC34536.1     PPKFDPERFSKANKDNIRPMSYFPFGFGPRRCIASALSQELTLVLA MLVARYRILPS
                  *:*****:*****.*:.*:***:*** *:*: **:*: .:*:* **:* **
                  _____
contig_14383      GKYKNEPPKYFTAALAGFPKEGVFVKLQKLQNP*KHL*QSEHVMV IITDYFFHVYNNCF
AtJAC34536.1     GRYEKEPPAYASSSLLGFPKHGIWVKLEKL-----
                  *:*:* ** * :.* * **.*:***: **

```

Figure 2.S18. Multiple sequence alignment (Clustal Ω) of the deduced amino acid sequence for the putative cytochrome p450 (contig 14383) identified exclusively in the Haller’s organ spf transcriptome of unfed virgin adult male *D. variabilis* versus the top BLAST tick hit (lowest expected value; Table 2). Asterisks (*) denote conserved residues, colons (:) indicate conservation between groups of strongly similar properties scoring >0.5 in the Gonnet PAM 250 matrix, and periods (.) indicate conservation between groups of weakly similar properties scoring \leq 0.5 on the Gonnet PAM 250 matrix. The black bar shows the cytochrome p450 domain. The acronym consists of the first letter of genus and species (*Amblyomma triste*, At) followed by the GenBank accession number for the protein BLAST hit (JAC34536.1).

```

contig_12057      PAVAARAGGPGLNDAPSSALLATATTRQTRNQQLSRGLSFSVSGSQKGAASSSAITMPV
AtJAC32978.1     -----MPI
                                                         **:

contig_12057      VLYNLVGSPPCGFIRCLAKHIGVELNLNLDFAKGEHRTEQFLKVNPFHKVPAIDDDGFI
AtJAC32978.1     VLYNLNGSPPCGFIRSLAKEIGVELSVKTLDFAKKEHLSDFLKVNPFHKVPTIDDDGFI
*****
*****:***.*****.:.***** ** :*:*****:*****

contig_12057      VYESNAIAYYLLRKYSPELDLYPACIETRTRIDQVLAASSNIHPQLGAFFRPRYFQSTK
AtJAC32978.1     VYESNAIAYYLLRKYAPESDLYPNCLRGRTRIDQVLAASSNIQASLGAFFRPRFFQHTK
*****:***** *: . *****: .*****: ** **

contig_12057      PSAEVKAFFENNVKNLENLIGDSKFAVGDKLTAADFCLIGHVTVCLEFPCVDKAKYPKL
AtJAC32978.1     PTDEEVSAFEQNVCKGLENLIGDKKFAVGDKITLADLCLIGHVTLVIEFGYVDKAKYPKL
*: ***.***:* * *****.*****:* **:*****: :** *****

contig_12057      TAYYELVRNTLPYYQEIFGPFTAQTKQLWDRLK*PLFAPLPQRN*D*ARREMGAVGVLK*
AtJAC32978.1     SGYYELVKSELPHYFDEVYGPAVSALKEALAKLK-----
:*****:. ***:***:*** .: * : **

```

Figure 2.S19. Multiple sequence alignment (Clustal Ω) of the deduced amino acid sequence for the putative glutathione S-transferase (contig 12057) identified exclusively in the Haller's organ spf transcriptome of unfed virgin adult male *D. variabilis* versus the top BLAST tick hit (lowest expected value; Table 2). Asterisks (*) denote conserved residues, colons (:) indicate conservation between groups of strongly similar properties scoring >0.5 in the Gonnet PAM 250 matrix, and periods (.) indicate conservation between groups of weakly similar properties scoring ≤ 0.5 on the Gonnet PAM 250 matrix. The solid black bar shows the glutathione S-transferase amino terminal domain, and the dashed black bar shows the glutathione S-transferase carboxyl terminal domain. The acronym consists of the first letter of genus and species (*Amblyomma triste*, At) followed by the GenBank accession number for the protein BLAST hit (JAC32911.1).

```

contig_04931      AARSGPGMPRRPVVGYWNVRLGQYIRNLLVYKGVAFEDKLYRFGPPPDFDRSHWHGEKF
AtJAC32978.1     -----MPPRPVVGWYWNVRALGQHIRNLLIYKGVAFEDKLYRFGPAPDFDRSHWLGEKF
                  *****.*:*****:***** *****
contig_04931      SLGLQFPNLPYYIDGDVKITQSLAIMRYLARKHDLGARNDEETLQLDFLEQQARDLAWGL
AtJAC32978.1     SLGLQFPNLPYYIDGDVKITQSLAILRYLARKHDLAARNEQEMLQMDLLEQQAKDLAWGL
                  *****:*****.**: * *:*****:*****
contig_04931      AMTAFNPTFDEARKKYEENLVNVLKWPANHMRDCTWALGDRLTYVDFFLLYEALDWNHEFN
AtJAC32978.1     AMTAFNPTFDEARKKYEENLVTVLKPWSDLMRDRVWVLGDRLTYVDFFLLYEALDWNHEFN
                  *****.*: * * .*.*****
contig_04931      ADAFAGYPELQOYLRFEELPNIKEYFASENYSKWPILGPMVKWGHFKE*LRDFAS*YRP
AtJAC32978.1     PDAFSGYPVLLLEYLRRFEELPNIKEYFASENYSKWPILGPMKAWGHFKE-----
                  ***:*** * :** *****.*****

```

Figure 2.S20. Multiple sequence alignment (Clustal Ω) of the deduced amino acid sequence for the putative glutathione S-transferase (contig 04931) identified exclusively in the Haller’s organ spf transcriptome of unfed virgin adult male *D. variabilis* versus the top BLAST tick hit (lowest expected value; Table 2). Asterisks (*) denote conserved residues, colons (:) indicate conservation between groups of strongly similar properties scoring >0.5 in the Gonnet PAM 250 matrix, and periods (.) indicate conservation between groups of weakly similar properties scoring ≤ 0.5 on the Gonnet PAM 250 matrix. The solid black bar shows the glutathione S-transferase amino terminal domain, and the dashed black bar shows the glutathione S-transferase carboxyl terminal domain. The acronym consists of the first letter of genus and species (*Amblyomma triste*, At) followed by the GenBank accession number for the protein BLAST hit (JAC32978.1).

```

contig_83534 -----GCLSTGSHYNPNNKNHGAPNAEDRHVGD LGNIVADC-GIA
RpJAA58838.1 TGLQPGAHGLHVHSYGDLTNGCNSTKGFNPMHKDHGGPEDRERHVGD LGNIKAEADGKA
                ** ** .*:** .*:**.*: .:***** *:. * *

contig_83534 VVNLTDHLLTLNGENSIIGRAVVVHADEDDLGLGSHNDSKTTGHAGSRLTCCVIGIARNS
RpJAA58838.1 RVYITDSMISLVGHHNIIGRAMVVHANPDDLKGGTNEKTTGSAGPRLACCVIGFVSGS
                * :** :::* *...*****:*****: ***** *. *:***** ** **:*****:. *

```

Figure 2.S21. Multiple sequence alignment (Clustal Ω) of the deduced amino acid sequence for the putative superoxide dismutase (contig 83534) identified exclusively in the Haller’s organ spf transcriptome of unfed virgin adult male *D. variabilis* versus the top BLAST tick hit (lowest expected value; Table 2). Asterisks (*) denote conserved residues, colons (:) indicate conservation between groups of strongly similar properties scoring >0.5 in the Gonnet PAM 250 matrix, and periods (.) indicate conservation between groups of weakly similar properties scoring ≤ 0.5 on the Gonnet PAM 250 matrix. The black bar shows the copper/zinc superoxide dismutase domain. The acronym consists of the first letter of genus and species (*Rhipicephalus pulchellus*, Rp) followed by the GenBank accession number for the protein BLAST hit (JAA58838.1).

Evidence of Female Sex Pheromones and Characterization of the Cuticular Lipids from Unfed, Adult Male versus Female Blacklegged Ticks, *Ixodes scapularis*

This chapter was formatted for submission to the *Journal of Experimental and Applied Acarology* with the coauthors Dr. Daniel E. Sonenshine¹, John B. Strider² and Dr. R. Michael Roe².

¹ Department of Biological Sciences, Old Dominion University, Norfolk, Virginia, 23529 USA

² Department of Entomology, North Carolina State University, Raleigh, North Carolina, 27695 USA

Abstract

Copulation in *I. scapularis* involves physical contact between the male and female (on or off the host), male mounting of the female, insertion/maintenance of the male chelicerae in the female genital pore (initiates spermatophore production), and the transfer of the spermatophore by the male into the female genital pore. Bioassays determined that male mounting behavior/chelicerae insertion required direct contact with the female likely requiring non-volatile chemical cues with no evidence of a female volatile sex pheromone to attract males. Unfed virgin adult females and replete mated adult females elicited the highest rates of male chelicerae insertion with part fed virgin adult females exhibiting a much lower response. Whole body surface hexane extracts of unfed virgin adult females and males, separately analyzed by GC-MS, identified a number of novel tick surface associated compounds: fatty alcohols (1-hexadecanol and 1-heptanol), a fatty amide (erucylamid), aromatic hydrocarbons, a short chain alkene (1-heptene), and a carboxylic acid ester (5 β -androstane). These compounds are discussed in terms of their potential role in female-male communication. The two most abundant fatty acid esters found were butyl palmitate and butyl stearate present in ratios that were sex specific. Only 6 n-saturated hydrocarbons were identified in *I. scapularis* ranging from 10-18 carbons.

Introduction

Ticks, like many other arthropods rely on chemical communication for courtship and reproduction. In some cases, pheromones help coordinate mating behaviors that bring adult males in contact with conspecific adult females, and guide male probing of the female genital pore. Transfer of the spermatophore follows soon after the successful completion of these

mating behaviors (Sonenshine 2006). Despite similarities in courtship and reproduction among hard ticks in Ixodidae, there are distinct differences between metastriate and prostriate species. Metastriate ticks, such as *Amblyomma*, *Dermacentor*, and *Rhipicephalus* sp., engage in on-host aggregative mating strategies (Kiszewski et al. 2001). In adult females, consumption of blood triggers the production of a volatile sex pheromone that attracts fed or feeding adult males, and stimulates the males to achieve physical contact with emitting females. Following male-female contact, mounting pheromones induce male mounting behavior, which entails males crawling onto the ventral surface of females and locating the female genital pore. Males subsequently commence probing of the female genital pore with their chelicerae to detect genital pore sex pheromones. Perception of conspecific genital pore sex pheromones by sensilla on the male's chelicerae triggers spermatophore synthesis, during which the male's chelicerae are maintained in the female genital pore. Once the spermatophore is formed, the male's chelicerae are removed from the female genital pore, and used to deposit the spermatophore into the female vulva, completing copulation. It is also important to note that metastriate ticks are not reproductively active until they commence feeding (Mulenga 2014).

The sex pheromones regulating mating in metastriate ticks have been well documented. The attractant sex pheromone is 2,6-dichlorophenol (2,6-DCP), and is produced by seven genera of Ixodidae ticks (Carr and Roe in press). Additionally, electrophysiological studies identified chemosensory sensilla in the Haller's organ of adult male *A. americanum* (Haggart and Davis 1981), *A. cajennense* (Soares and Borges 2012), *A. variegatum*, *D. variabilis*, and *R. appendiculatus* (Mulenga 2014) that are responsible for detecting 2,6-DCP, although only fed or feeding males respond to it. Mixtures of cholesteryl esters present on the

female dorsum have been identified as mounting pheromones in *D. variabilis* (Hamilton et al. 1989). Female genital pore sex pheromones have been identified as a combination of saturated fatty acids (C₁₄-C₂₂) and ecdysteroids in *D. andersoni* and *D. variabilis* (Allen et al. 1988; Allen 2002). In comparison to our knowledge of metastriate reproductive pheromones, very little is known about the pheromones involved in prostriate tick courtship and mating.

Prostriate ticks, comprising the genus *Ixodes*, employ nest-based mating strategies, which do not require blood feeding in order to stimulate mating (Kiszewski et al. 2001). Adult female and male *Ixodes* engage in similar coordinated mounting, genital pore probing, and insemination behaviors as metastriate ticks, except that these behaviors can occur before attachment and feeding on the host, while the ticks are on the ground or in vegetation. Since unfed prostriate adult females can successfully retain endospermatophores without degradation for 4 months, mating can take place independent of blood feeding (Kiszewski and Spielman 2002). *Ixodes* virgin and previously mated adult females can also receive spermatophores from conspecific adult males on the host during blood feeding. The identity of compounds serving as pheromones in adult male-female attraction, mounting, genital pore probing, and sperm transfer of prostriate ticks are currently unknown. Evidence of a volatile attractant sex pheromone has been reported for *I. persulcatus* (Dobrotvorsky and Tkachev 1995) and *I. ricinus* (Dusbábek et al. 2001), however the identities of these volatile attractants have not been determined (Tkachev et al. 2000). Additionally, there has been no documentation of volatile sex pheromones, mounting pheromones, or genital pore sex pheromones in *I. scapularis*, which is of special interest as the vector of the organism that causes Lyme disease. Investigations have identified the presence of aggregation pheromones (previously known as assembly pheromones) in *I. holocyclus* (Treverrow et al. 1977), *I.*

ricinus (Graf 1978), *I. scapularis* (Allan et al. 2002; Sonenshine et al. 2003), and *I. uriae* (Benoit et al. 2008), although it is still unclear if aggregation pheromones play a role in courtship and mating.

Due to the limited research available on prostriate reproductive pheromones, this study was conducted to further examine the mating behaviors of *I. scapularis* and determine, by bioassays, whether there is any evidence for pheromone involvement in male-female attraction, mounting and genital pore probing. In view of the widespread use of cuticular lipids in sexual communication in other arthropods, we also investigated potential sex differences in the cuticular lipids of adult *I. scapularis*. Only a few studies have been conducted on cuticular lipids of prostriate ticks, i.e., *I. persulcatus* and *I. ricinus* (Estrada-Peña et al. 1994; Tkachev et al. 2000; Dusbábek et al. 2001).

Materials and methods

Ticks

Adult *I. scapularis* were obtained from laboratory colonies of Dr. Daniel E. Sonenshine at Old Dominion University (Norfolk, VA). Laboratory colonies were started with field collected *I. scapularis* from Armonk, New York and maintained by feeding larval, nymph and adult stages on New Zealand white rabbits, *Oryctolagus cuniculus*. When not feeding, *I. scapularis* larvae, nymphs, adult females and adult males were maintained in distinct containers at $21 \pm 1^{\circ}\text{C}$, 97% humidity, and with a photoperiod of 16-hour light: 8-hour dark (dusk and dawn periods of 1 h each at the beginning and ending of the scotophase).

Bioassays

Bioassays were utilized to investigate the potential role of sex pheromones in *I. scapularis* mating behaviors including male attraction, mounting, and copulation. Copulation in *I. scapularis* is a two-step process: (i) insertion and maintenance of the chelicerae in the female genital pore (which initiates the production of the spermatophore) followed by (ii) male placement of the spermatophore into the female genital pore. Of these two endpoints, bioassays were designed to evaluate male insertion and maintenance of the male chelicerae in the female genital pore only, and will be referenced in this paper as “male insertion/maintenance of chelicerae”. Two types of bioassays were conducted: a 4-port olfactometer assay (Fig. 3.1) and a Petri dish assay (Fig. 3.2). The 4-port olfactometer (ARS, Gainesville, FL) was used to determine whether *I. scapularis* unfed virgin adult females emit volatile sex pheromones that are attractive to unfed virgin adult males. Tests were conducted in the dark for a 24h period at $23 \pm 1^\circ\text{C}$ with a relative humidity of 40%. Adult ticks used in olfactometer assays were 3-4 months post-molt, with females and males stored separately after molting. All ticks were handled wearing gloves and using sterile soft-tipped (metal) forceps cleaned with absolute ethanol to prevent cross contamination between the sexes. Ticks were allowed 30 min to acclimate to experimental conditions prior to being placed into the olfactometer. A nylon mesh (440 squares/cm²) screen was used to isolate 50 *I. scapularis* unfed virgin adult females into one glass bulb of the 4-port olfactometer, and 20 *I. scapularis* unfed virgin adult males placed into the center of the apparatus (Fig. 3.1). Breathing quality air (AirGas, Radnor, PA) was introduced into each glass bulb from a compressed air tank at a rate of 30mL/min. A vacuum pump was used to remove air from the center of the 4-port olfactometer at a rate of 120mL/min. Gases removed from the olfactometer were exhausted

out of the test area. Airflow from the bulbs towards the central vacuum allowed males to detect putative volatile sex pheromones produced by the females without achieving physical contact. The position of males in the 4-port olfactometer was recorded 24h after introduction into the central test arena. Ticks were identified as positive responders, and attracted to volatiles produced by unfed virgin adult females if they moved 1 cm past the choice point (Fig. 3.1), distal to the central arena. The experiment was replicated three times and the glass bulb containing the female ticks randomly rotated between the four positions to compensate for potential positional response bias. All equipment was washed with hot tap water and absolute ethanol, and allowed to air-dry between trials to eliminate contaminants. Results from the olfactometer assays were analyzed with the Student's *t*-test using PrismTM (GraphPad, La Jolla, CA).

Petri dish assays were conducted to determine whether *I. scapularis* unfed virgin adult female sex pheromones function through direct contact or spatially to induce mounting behavior in unfed virgin adult males. Petri dish assays were performed using black glass Petri dishes (148 mm diam x 20 mm) and lids (150 mm diam x 20 mm). No filter paper was employed during these experiments. Tests were conducted during the day between 1100 h and 1500 h at $23 \pm 1^\circ\text{C}$ and a relative humidity of 40%. The use of black Petri dishes eliminated light contamination from ambient (fluorescent) lighting and created a dark testing environment. Adult ticks used in Petri dish assays were 3-4 months post-molt, with females and males stored separately after molting. All ticks were handled wearing gloves and using sterile soft-tipped (metal) forceps cleaned with absolute ethanol to prevent cross contamination between the sexes. Ticks were allowed 30 min to acclimate to experimental conditions prior to being placed into Petri dishes. To observe normal mounting behavior of *I.*

scapularis in the Petri dish assays, 20 unfed virgin adult males and 20 unfed virgin adult females were placed into a Petri dish, and the percentage of males mounting females documented at 5, 10, 15, 30, and 60 min (Fig. 3.2a). The experiment was replicated three times, and all equipment thoroughly washed with hot tap water and absolute ethanol, and allowed to air-dry between replicates. After documenting normal mounting behavior, Petri dish assays were performed under the same experimental conditions using 20 unfed virgin adult males (free to roam) and 20 unfed virgin adult females secluded in nylon mesh (440 squares/cm²) bags to prevent direct contact between the sexes (Fig. 3.2b). The percentage of males mounting females was documented at 5, 10, 15, 30, and 60 min after all ticks were added to the bioassay arena. The experiment was replicated three times and all equipment washed between replicates as previously described. Results were analyzed with an ANOVA and a Sidak's multiple comparison test using PrismTM (GraphPad, La Jolla, CA).

Petri dish assays were also conducted to determine whether *I. scapularis* unfed virgin adult female sex pheromones affect male chelicerae insertion/maintenance behavior in unfed virgin adult males. Using the same Petri dish experimental procedure just described, male chelicerae insertion/maintenance behavior was observed between *I. scapularis* unfed virgin adult males and unfed virgin adult females after whole body washing of the latter with either distilled water or 1% laboratory grade Triton X-100 detergent (Sigma-Aldrich, St. Louis, MO) in distilled water. Using sterile soft-tipped (metal) forceps, 30 female ticks were placed into a 15mL polypropylene centrifuge tube containing either 5mL of distilled water or detergent (in distilled water) and the tubes repeatedly inverted for 5 min. The females were then removed from the tubes, checked for mortality, and rinsed with distilled water using the same procedure. Rinsed females were air-dried for 30 min, and subsequently placed into a

Petri dish with 30 unfed virgin adult males (Fig. 3.2a). The percentage of males inserting/maintaining their chelicerae in the genital pore of females was documented at 0, 2, and 7 d. This behavior was differentiated from mounting by using a sterile probe to attempt to remove males from the ventral surface of females; males firmly affixed to the female genital pore were scored as having successfully inserted/maintained their chelicerae in the genital pore. Each treatment was replicated three times and the results analyzed with an ANOVA and a Sidak's multiple comparison test using PrismTM (GraphPad, La Jolla, CA).

Additional Petri dish assays were performed to determine whether blood feeding of adult female *I. scapularis* affects male chelicerae insertion/maintenance behavior in unfed virgin adult males. Using the same experimental procedure described just above, 20 *I. scapularis* unfed virgin adult males and 20 unfed virgin adult females were placed into a Petri dish, and the percentage of males inserting/maintaining their chelicerae in the genital pore of females was documented at 5, 10, 15, 30, and 60 min. The experiment was replicated three times. To compare the results from this bioassay with the impact of blood feeding, part-fed virgin, and replete mated adult females were paired with unfed virgin adult males in Petri dish assays. Due to the limited number of available *I. scapularis*, these experiments were conducted with only 4 females of each feeding stage. Part-fed virgin and replete mated adult females were paired with 20 unfed virgin adult males. The experiment was replicated three times for each treatment, and the percentage of males inserting/maintaining their chelicerae in the genital pore of females was documented at 5, 10, 15, 30, and 60 min after all ticks were added to the bioassay arena. Results were analyzed with an ANOVA and a Sidak's multiple comparison test using PrismTM (GraphPad, La Jolla, CA).

Cuticular Extractions

A new bottle of high purity hexane (n-hexane) ($\geq 98.5\%$) was purchased for the purpose of these extractions (Thermo Fischer Scientific, Waltham, MA). Hexane extractions were performed using live unfed virgin adult female and male *I. scapularis*. Ticks were 3-4 months post molt, with females and males stored separately since molting and extracted separately. To avoid cross contamination, extractions of opposite sexes were never conducted simultaneously, and each sex was assigned their own set of extraction tools. All extraction tools were autoclaved, washed 5 times with hexane, and allowed to air-dry prior to use. Extractions were conducted using new glass 2mL Agilent GC-MS vials with polypropylene Teflon lined screw caps (Agilent, Santa Clara, CA) also washed 5 times with hexane and air dried prior to use. Additionally, GC-MS vials and lids were never reused. Soft tipped (metal) forceps were used to transfer either 10 live unfed virgin adult female or male *I. scapularis* ticks into a GC-MS vial. Ticks were randomly selected for extraction. Once placed into a pre-weighed GC-MS vial, tick weight was recorded and a glass Hamilton syringe used to transfer 1mL of hexane into the vial. Ticks were washed with hexane for 10 min at room temperature by inverting the GC-MS vial every few sec. Soft-tipped forceps were used to remove the ticks from the vial. The hexane was then immediately concentrated just to dryness by warming the vial in a water bath ($24 \pm 1^\circ\text{C}$) under a constant, slow stream of nitrogen gas ($\geq 99.98\%$; AirGas, Radnor, PA) using an 18 gauge stainless steel syringe needle inserted just into the top of the vial (Sigma-Aldrich, St. Louis, MO). Then, an additional 10 μl of hexane was added to the vial, using a glass Hamilton syringe, to re-dissolve the extracted material. This procedure was replicated 5 times for females and 6 times for males. The number of replicates performed for each sex was based on the *I.*

scapularis availability at the time. All extractions were analyzed using GC-MS (described in more detail later).

GLC Analyses and Operating Conditions

A HP Mass Selective Detector 5973 (MSD) paired with a HP 6899 Gas Chromatograph (GC) System (Palo Alto, CA) was used for all analyses. Instrumental control and program configuration was conducted using the MSD ChemStation software, Agilent G1701DA (Agilent, Santa Clara, CA). Manual injection of extractions (1 μ l) was performed using the single electronic pressure controlled split-less injection port. Separations were performed on a TRACE TR-5MS coated fused silica capillary column (30m length x 0.25 mm ID, 1 μ M film thickness; Thermo Scientific, Waltham, MA). The column oven temperature was programmed to start at 50°C, with no hold period, and a temperature ramp to 180°C at 5°/min, and from 180° to 300°C at 4°/min at the time of sample injection. Both the injector and detector temperature were set to 250°C. The helium carrier gas (\geq 99.999%; AirGas Radnor PA) was set to a constant flow of 1 ml/min, with an average velocity of 36cm/sec. A flame ionization detector was used to detect GC column eluants. The abundance of components identified in extraction samples was determined using GC peak areas without correcting for molar or weight response. Initial analyses focused on comparing retention times, peak areas and ion mass values (m/z) with the mass spectra database (Wiley 143,100). Secondary analysis consisted of manual comparison of m/z values and relative intensities using the MassBank spectrum search (MassBank Project, Tokyo, Japan) and the National Institute of Standards and Technology Chemistry Webbook (NIST, US Department of Commerce) to confirm compound identifications. Compound abundances were compared

between females and males with the Student's unpaired *t*-test with Welch's correction using Prism™ (GraphPad, La Jolla, CA).

Results

Bioassays

In the 4-port olfactometer assays (Fig. 3.1), the majority of *I. scapularis* unfed virgin adult males remained in the central arena and were unresponsive to any potential volatiles produced by unfed virgin adult females (Fig. 3.3). The percentage of unresponsive ticks was significantly higher than the percentage of ticks identified as attracted, i.e., moving towards the bulb containing the females ($t = 40.93$, $dF = 4$, $P = < 0.0001$).

Petri dish assays (Fig. 3.2b) investigating mounting behavior of unfed virgin adult males with unfed virgin adult females secluded in mesh bags determined that *I. scapularis* does not engage in mounting without physical contact (Fig. 3.4). The percentage mounting observed between free roaming adults was significantly higher than that of the physically separated sexes for all time points; 5 min ($t = 2.865$, $dF = 20$, $P = 0.0096$), 10 min ($t = 3.123$, $dF = 20$, $P = 0.0044$), 15 min ($t = 3.302$, $dF = 20$, $P = 0.0036$), 30 min ($t = 4.109$, $dF = 20$, $P = 0.0005$), and 60 min ($t = 4.471$, $dF = 20$, $P = 0.0002$). Additionally, there was no source of significant variation among time points ($F = 0.4719$, $dF = 20$, $P = 0.7507$).

Petri dish assays (Fig. 3.2a) investigating possible sex pheromones that might elicit male chelicerae insertion/maintenance behavior determined that washing unfed virgin adult females with 1% Triton-X 100 detergent resulted in a significant decrease in percent chelicerae insertion/maintenance of unfed virgin adult males when compared to distilled water washing, though only for day 0 ($t = 4.907$, $dF = 30$, $P = < 0.0001$) (Fig. 3.5). There

were no significant differences in percent chelicerae insertion/maintenance of unfed virgin adult males with unfed virgin adult females washed with distilled water or detergent for day 2 ($t = 0.4147$, $dF = 30$, $P = 0.6813$) and day 7 ($t = 1.175$, $dF = 30$, $P = 0.2492$). There was significant variation among time points, most notably at day 0 ($F = 83.29$, $dF = 30$, $P < 0.0001$).

Petri dish assays (Fig. 3.2a) investigating the impact of blood feeding on chelicerae insertion/maintenance behavior in *I. scapularis* identified significant decreases in percent chelicerae insertion/maintenance of unfed virgin adult males with part-fed virgin adult females at 15 min when compared to unfed virgin adult females ($t = 2.903$, $dF = 30$, $P = 0.0069$) and replete mated adult females ($t = 2.869$, $dF = 30$, $P = 0.0075$), at 30 min when compared to unfed virgin adult females ($t = 3.213$, $dF = 30$, $P = 0.0031$) and replete mated adult females ($t = 2.869$, $dF = 30$, $P = 0.0075$), and at 60 min when compared to unfed virgin adult females ($t = 3.523$, $dF = 30$, $P = 0.0014$) and replete mated adult females ($t = 2.869$, $dF = 30$, $P = 0.0075$) (Fig. 3.6). Additionally there was no significant difference observed in percent chelicerae insertion/maintenance of unfed virgin adults males with either unfed virgin adult females or replete mated adult females at 15 min ($t = 0.03442$, $dF = 30$, $P = 0.9728$), 30 min ($t = 0.3442$, $dF = 30$, $P = 0.7331$), and at 60 min ($t = 0.6541$, $dF = 30$, $P = 0.5180$). No significant difference was observed in percent chelicerae insertion/maintenance of unfed virgin adults males with adult females of all three feeding stages at 5 min and 10 min. There was significant variation among time points ($F = 2.704$, $dF = 30$, $P = 0.0491$) and between feeding stages ($F = 20.06$, $dF = 30$, $P < 0.0001$).

GC-MS

Analysis of replicate data for male and female *I. scapularis* whole body hexane extractions identified over 75 distinct compounds (Figs. 3.7, 3.8). n-Hexane was run individually as a control to ensure that peaks identified for analyses did not originate from the hexane or the process of extraction. Due to the variability in data analysis and repeatability, only compounds found in all replicates, of each sex respectively, and with a match probability $\geq 80\%$ were reported. These criteria identified 17 putative cuticle compounds including alkanes, an alkene, an aromatic hydrocarbon, carboxylic acid esters, fatty acid esters, fatty alcohols, a fatty aldehyde, a fatty amide, and terpenes. Despite having a low match probability (70%) one steroid, repeatedly appearing in all replicates of both sexes, was also included in the analyses. These 18 compounds represent 70-75% of the column eluants, and are listed in Table 3.1 and Fig. 3.9. Several additional compounds were identified in female and male whole body extracts, but in small amounts ($<0.05\%$), which impeded their confirmation of match identity. The majority of these unconfirmed, identified compounds were found in both sexes, though a few compounds were exclusive to females including androstanone, estronone, and valeric acid. But due to the difficulty in confirming peak identity, these compounds were excluded from further analyses. Compound abundances were converted to percentages using the sum of abundances for all 18 compounds as a divisor. Mean percent abundances are based on whole body extracts of 10 unfed virgin adult females or males. The two most abundant components identified in both female and male whole body extracts were the fatty acid esters butyl palmitate and butyl stearate (Fig. 3.9a). Butyl palmitate was the most abundant compound identified in male whole body extracts (35.30 ± 1.14) (Mean % \pm SEM), and was identified in a significantly higher abundance than in

female whole body extracts (18.57 ± 0.94 ; $t = 11.32$, $dF = 8.943$, $P < 0.001$). Butyl stearate was the most abundant compound identified in female whole body extracts (27.53 ± 0.48) in a significantly higher abundance than in male whole body extracts (21.40 ± 0.51 ; $t = 8.753$, $dF = 8.977$, $P < 0.001$) (Fig. 3.9a). There was also a substantial difference observed in the abundances of the aromatic hydrocarbons identified in male and female whole body extracts (Fig. 3.9b). 1,2,3-Trimethylbenzene was the third most abundant component identified in male whole body extracts (6.30 ± 0.18), and occurred in a significantly higher abundance than in female whole body extracts (2.13 ± 0.19 ; $t = 15.93$, $dF = 8.970$, $P < 0.001$). The third most abundant component identified in female whole body extracts was not an aromatic hydrocarbon, but the fatty acid amide erucylamide, and occurred in a significantly higher abundance in female whole body extracts (6.53 ± 0.26) than in male whole body extracts (4.90 ± 0.46 ; $t = 3.085$, $dF = 7.720$, $P = 0.0157$) (Fig 3.9b). Alkanes identified in female and male whole body extracts include compounds with 10, 14, 15, 16, 17, and 18 carbons (Fig 3.9c). The abundances in male whole body extracts of C-10 (1.97 ± 0.15), C-15 (1.44 ± 0.031), C-16 (0.70 ± 0.06), and C-18 (1.87 ± 0.09) were all significantly higher than those identified in female whole body extracts; C-10 (1.23 ± 0.14 ; $t = 3.488$, $dF = 8.889$, $P = 0.007$), C-15 (0.97 ± 0.04 ; $t = 10.18$, $dF = 8.578$, $P < 0.001$), C-16 (0.00 ± 0.00 ; $t = 11.67$, $dF = 5.000$, $P < 0.001$), and C-18 (1.43 ± 0.8 ; $t = 3.654$, $dF = 9.000$, $P = 0.0053$). There was no significant difference between the abundances of C-17 identified in female (0.767 ± 0.88) and male (0.767 ± 0.12) whole body extracts. The final alkane identified, C-14, was present only in female whole body extracts (1.69 ± 0.1 ; $t = 16.90$, $dF = 4.00$, $P < 0.001$). In addition to the alkanes there was one alkene C-7, also identified only in female whole body extracts (0.85 ± 0.03 ; $t = 28.33$, $dF = 4.000$, $P < 0.001$) (Fig. 3.9c). The carboxylic acid esters, butyl

benzoate and ethyl-4-ethoxybenzoate, were identified in the whole body extracts of both sexes (Fig. 3.9a). The abundance of ethyl-4-ethoxybenzoate identified in female whole body extracts (5.30 ± 1.0) was significantly higher than the abundance identified in male whole body extracts (2.56 ± 0.35 ; $t = 2.586$, $dF = 4.980$, $P = 0.0492$). There was no significant difference between the abundances of butyl benzoate identified in female (1.26 ± 0.03) and male (1.10 ± 0.10) whole body extracts. Two fatty alcohols were identified in female and male whole body extracts, 1-heptanol and 1-hexadecanol (Fig. 3.9b). 1-Hexadecanol was identified in both female (1.5 ± 0.11) and male (1.67 ± 0.03) whole body extracts with no significant difference in abundance between the sexes. 1-Heptanol was identified in only female whole body extracts (0.65 ± 0.03 ; $t = 21.67$, $dF = 4.000$, $P < 0.001$). The remaining compounds identified in female and male whole body extracts were the steroid 5β -androstane, and the terpenes phytol and thymol (Fig. 3.9b). Significant differences in abundances between the sexes were found for both 5β -androstane and thymol. 5β -androstane was identified in female whole body extracts (2.87 ± 0.30) in a significantly higher abundance than in male whole body extracts (0.76 ± 0.12 ; $t = 6.530$, $dF = 5.274$, $P = 0.0010$). Thymol was identified only in male whole body extracts (0.70 ± 0.06 ; $t = 11.67$, $dF = 5.000$, $P < 0.001$). There was no significant difference between the abundances of phytol identified in female (1.43 ± 0.1) and male (1.90 ± 0.40) whole body extracts.

Discussion

Laboratory bioassays demonstrated that *I. scapularis* adults rely on direct contact for reproduction. If unfed, mate seeking males can respond to sex attractant volatiles from unfed, virgin females, we would have expected the males to aggregate around and/or on top of the

mesh bags in which the females were confined. As shown in Fig. 4, this did not happen. Our findings do not support the hypothesis that volatile pheromones are required for male mating behavior. In our studies, unfed, virgin adult males did not engage in mating behavior unless direct contact with females was possible. Additionally, washing of unfed virgin adult females decreased chelicerae insertion/maintenance behavior of unfed virgin adult males, removing surface compounds that possibly function as sex pheromones in *I. scapularis*. It is interesting to note that washed females apparently were capable of regenerating these compounds after a 48h period, restoring normal mating behavior. Since *I. scapularis* are natural ambushers when it comes to host seeking, it is plausible that their mating strategies employ a similar behavior of waiting for transient male-female contact. This eliminates the need for volatile attractant sex pheromones to engage adult male *I. scapularis* to actively search for emitting adult females. Additionally, prostrate tick reproduction is not dependent on blood feeding, and would not require effective attractant sex pheromones like those in metastriate ticks to markedly influence male behavior, i.e., cessation of blood feeding and initiation of mating. Instead, it is probable that *I. scapularis* couple aggregation behavior with mating activity. These two behaviors act synergistically to congregate conspecific adults that can subsequently mate. As *I. scapularis* encounter each other through aggregation, adult males come in direct contact with adult females, and with putative sex pheromones located on the cuticle providing the necessary chemical cues for successful mounting and insemination. The large size discrepancies between adult and immature *I. scapularis*, as well as the lack of reproductive orifices, makes adults easily distinguishable from other life stages through physical contact. This coupling of aggregation and mating behavior is also evident in blood feeding *I. scapularis*, congregating on the host in protected locations behind ears and in

axilla. Pairing aggregation and mating behaviors ensures the viability of *I. scapularis* populations by increasing the probability of contact between reproductives and subsequent mating.

I. scapularis unfed virgin adult males demonstrated the highest percent chelicerae genital pore insertion/maintenance when paired with unfed virgin adult females and replete mated adult females in laboratory bioassays. Zemek et al. (2002) observed similar results with *I. ricinus*. Unfed virgin adult females had the highest percentage of male chelicerae insertion/maintenance and spermatophore transfer. However, replete mated adult females were deemed more attractive to unfed virgin adult males having the fastest rate of mounting and female genital pore penetration. Further analysis revealed that despite males remaining in copula with replete females, the majority of males did not transfer spermatophores. Zemek et al. (2002) theorized that this decrease in successful insemination of replete mated adult females was due to a “copulation inhibiting system” that is turned on after the females become fully engorged. This may not be necessarily true. It has been shown that unknown factors, likely associated with spermatophores and male saliva, cause males to abort insemination with females that have been previously mated. This re-mating inhibition slowly decreases after females fully engorge, becoming less apparent 5 days post-repletion, when they are capable of being re-inseminated (Kiszewski and Spielman 2002). This decrease in re-mating inhibition may be explained by the degradation of spermatophores and the recapitulation of sperm that have become sessile again during storage, providing an opportunity for sperm displacement (Kiszewski et al. 2001). It is also possible that re-mating inhibiting factors are sequestered from the female genital pore upon completion of blood feeding and initiation of oocyte maturation.

Zemek et al. (2002) concluded that the increase in attractiveness of replete mated adult females was due to an increase in production of attractive pheromones. This seems counter-intuitive for replete mated adult females to focus on re-mating rather than oviposition. It is known that male *I. rubicundus* and *I. holocylus* regard replete females as sources of nourishment, gaining nutrients through copula or by inserting their mouthparts into the body wall of females (Moorhouse and Heath 1975; Fourie et al. 1988). An alternative hypothesis is that prolonged feeding and host association naturally changes the cuticular chemistry of replete females, becoming attractive to males that primarily seek nourishment, engaging in mating after nutritional needs have been met, and if there are no re-mating inhibition factors. This theory may also explain the distinct decrease in mating activity with part-fed females. Changes in the cuticular chemistries of *I. scapularis* adult females from host interactions and feeding may be gradual, and require a prolonged period of time before becoming apparent to males. Since pheromone recognition in ixodid ticks is dependent on the ratio of signals from generalized chemosensory sensilla, *I. scapularis* males may only identify cuticular chemistries of unfed and replete females (Osterkamp et al. 1999; Waladde and Rice 1982). Subtle changes occurring in part-fed females may be distinct enough to distinguish them from unfed females, preventing mating, but not be substantial enough to induce male attraction like replete females. Since it is highly unlikely that adult males would encounter part-fed, virgin adult females in the wild, there may be other factors that deter male mating. The increase rate of mounting between unfed virgin adult males and replete mated adult females also may be explained by the cessation of locomotor activity in replete females. It would be easier for males to contact females when they are not moving. With both sexes wandering, waiting to achieve contact may be more difficult and take longer,

decreasing the speed of mating. This also further illustrates the importance of coupling aggregation and mating behavior to increase the efficacy of mating in *I. scapularis*. More research is needed in general to understand the different male mating preferences in *I. sp.*

Whole body cuticular extractions of male and female *I. scapularis* have identified a few compounds that may be components of reproductive pheromones regulating courtship and mating. Fatty acids function as aggregation pheromones in *Amblyomma* ticks (Carr and Roe, in press) and are also components of genital pore pheromones in *Dermacentor* ticks (Allan et al. 1988). The two most abundant fatty acids in *I. scapularis* whole body extracts, identified as the derivatized esters butyl palmitate and butyl stearate, are also present in *R. annulatus*, *R. bursa*, and *R. sanguineus* body extracts. Both fatty acid esters were present in ratios that were distinct for each *Rhipicephalus* species (Shimshoni et al. 2013). In *I. scapularis*, there are clear distinctions in the ratios of butyl palmitate and butyl stearate between males and females. The fatty acid palmitic acid, which co-elutes with butyl palmitate, is also present in body extracts of *I. persulcatus*, though in combination with additional fatty acids not identified in *I. scapularis* (Tkachev et al. 2000). It is apparent that fatty acids create unique cuticular chemistries that are species and sex specific, and may be important during male-female interactions and mating. Perhaps fatty acids allow for sex differentiation among reproductives searching for conspecifics for mating, though this is still unclear.

In insects, fatty alcohols act as both pheromones and precursors for fatty aldehydes. 1-Hexadecanol and 1-heptanol are the first fatty alcohols to be identified in ixodid tick whole body extracts. 1-Hexadecanol is an important component of female sex pheromone in the cotton bollworm *Helicoverpa armigera* (Zhang et al. 2012). 1-Heptanol is a primary

pheromone component of the female pine beetle *Dendroctonus jeffreyi*, and attractive to both adult females and males (Paine et al. 1999). Since fatty alcohols function as both reproductive and aggregation pheromones in insects, further investigations of their role in *I. scapularis* reproduction is warranted.

There is currently no evidence that cuticular hydrocarbons function as pheromones in ticks (Estrada-Peña et al. 1994). The cuticular hydrocarbons identified in *I. scapularis* whole body extracts are less diverse and shorter overall than those reported in metastriate ticks. Estrada-Peña et al. (1992, 1993) documented over 100 distinct hydrocarbons in varying lengths of 11-39 carbons, and degrees of saturation and branching in whole body extracts of several *Rhipicephalus* and *Amblyomma* species. Only 6 linear, saturated hydrocarbons were identified in *I. scapularis* whole body extracts ranging from lengths of 10-18 carbons. The short chain alkene 1-heptene, previously undocumented in *Ixodes* species, was also identified (Estrada-Peña et al. 1994; Tkachev et al. 2000). Since metastriate ticks actively hunt for or ambush hosts, they are more susceptible to environmental conditions than prostriate ticks, which quest and usually remain on or near plants that offer shelter and protection. Perhaps metastriate ticks have a thicker epicuticular layer consisting of a greater number of more diverse hydrocarbons to provide additional protection when host seeking, though this requires further investigation.

This is the first documentation of fatty amides, specifically erucylamide in ticks. Fatty amides are the major component of cuticle extracts of psocoptera (Howard and Lorde 2003), and in particular erucylamide a component of whole body extracts of the malaria mosquito, *Anopheles gambiae* (Caputo et al. 2005). Fatty amides are also present on the cuticle and in the Dufour gland of the paper wasps *Polistes dominulus* and *P. sulcifer* (Dani

2006). Unfortunately, fatty amides are not well studied because they were previously hypothesized to be plastic contaminants. The majority of plastic contaminants identified in our *I. scapularis* whole body extracts were phthalates, with no fatty amides identified in our controls. Additionally, GC-MS analyses of ants (Lenoir et al. 2012) and spiders (Xiao et al. 2009) housed in similar plastic containers to ours identified the same phthalate contaminants. Thus, we can assume that the identified fatty amide is not a plastic contaminant, and may play a role in prostriate tick chemical communication or cuticular function.

This study is the first documentation of aromatic hydrocarbons in *I. scapularis* whole body extracts. Aromatic hydrocarbons are functional components of insect assembly pheromones rather than sex pheromones (Torto et al. 1994). Aromatic hydrocarbons have also been identified in mite exocrine glands that secrete complex species-specific oils used as alarm pheromones (Heethoff 2012). In some mite species, components of alarm and aggregation pheromones also functions as components of reproductive pheromones. The secretion of these chemical components in distinct concentrations allows mites to discriminate between the pheromones and respond accordingly (Carr and Roe in press). Since ticks are closely related to mites, aromatic hydrocarbons should be further evaluated as functional components of alarm, aggregation, and reproductive pheromones and the concentrations that distinguish one pheromone from another.

Carboxylic acids and acid derivatives are functional components of many insect pheromones. This is the first documentation of carboxylic acid esters in tick whole body extracts. In lepidopterans, carboxylic acids are commonly biosynthesis intermediates for pheromones (Bjostad et al. 1987). Unfortunately, the role of carboxylic acids in ticks is currently unknown. 5 β -Androstane is a steroid hormone and the precursor for all estrogens

and a variety of axillary steroids that function as pheromones in mammals. Since tick steroids have mammalian counterparts, for example tick ecdysteroid and vertebrate testosterone, it is possible that the component currently identified as 5β -androstane in *I. scapularis* body extracts is a closely related steroid regulating mating, which has not yet been discovered (De Loof 2006). Terpenes are typically associated with plants and disregarded as environmental contaminants. With the repeated identification of terpenes in tick whole body extracts, these compounds also should be further studied to determine their exact role in the Ixodidae.

In summary, our bioassays provided no evidence of a volatile female sex pheromone to attract males. It appears that direct male contact with the female and chemical cues from the female are needed to elicit male mounting of the female and the insertion of his chelicerae into the female genital track. This occurs for both virgin unfed and mated replete females but not virgin part-fed females. A number of unique compounds were identified by GC-MS from hexane surface extracts of unfed males and females, not previously described in other ticks, with potential roles in chemical communication. Sex specific differences were found in some compounds extracted from the cuticle, and a preference for shorter and less diverse cuticular hydrocarbons in *I. scapularis* was found compared to metastriate ticks.

Acknowledgments

This work was funded by grants to RMR and DES from NIH (1R21AI096268) and NSF (IOS-0949194) and from support to RMR from the NCSU Ag. Research Station. ALC was also supported in part by a Graduate Student Teaching Assistantship from the Department of Entomology at North Carolina State University.

Compliance with ethical standards

The authors have no conflicts of interest in the publication of the results reported in this paper. Students conducting research on this project have received training in a Graduate School approved ethics course at NC State University, which complies to the NSF standards. No human subjects were used in the research reported in this paper. All use of animals in this study was carried out in strict accordance with the recommendations in the Guide for the Care and Use of Laboratory Animals of the National Institutes of Health. The protocols were approved by the Old Dominion University Institutional Animal Care and Use Committee (#10-018 and #10-032) and are on file at the Office of Research, Old Dominion University, Norfolk, Virginia. Tranquilizers (Acepromazine) were administered to the animals prior to handling to minimize anxiety and/or discomfort. No animal work was conducted at NC State University.

References

- Allen SA, Phillips JD, Taylor D, Sonenshine DE (1988) Genital sex pheromones of ixodid ticks: evidence for the role of fatty acids from the anterior reproductive tract in mating of *Dermacentor variabilis* and *Dermacentor andersoni*. *J Insect Physiol* 34:315–323
- Allen SA, Sonenshine DE, Burrige MJ (2002) Tick pheromones and uses thereof. United States Patent Office, patent no. 6,331,297.
- Benoit JB, Lopez-Martinez G, Philips SA, Elnitsky MA, Yoder JA, Lee Jr. RE, Denlinger DL (2008) The seabird tick, *Ixodes uriae*, uses uric acid in penguin guano as a kairomone and guanine in tick feces as an assembly pheromone on the Antarctic Peninsula. *Polar Biol* 31:1445–451.
- Bjostad LB, Wold WA, Roelofs WL (1987) Pheromone biosynthesis in lepidoptera: desaturation and chain shortening. In: Prestwich GD, Blomquist GJ (eds) *Pheromone Biochemistry*, Academic Press, Orlando, pp 77–120.

- Caputo B, Dani FR, Horne GL, Petrarca V, Turillazzi S, Coluzzi M, Priestmand A, della Torre A (2005) Identification and composition of cuticular hydrocarbons of the major Afrotropical malaria vector *Anopheles gambiae* s.s. (Diptera: Culicidae): analysis of sexual dimorphism and age related changes. *J Mass Spectrom* 40:1595–1604.
- Dani FR (2006) Cuticular lipids as semiochemicals in paper wasps and other social insects. *Ann Zool Fennici* 43:500–514.
- De Loof A (2006) Ecdysteroids: the overlooked sex steroid of insects? Males: the black box. *Insect Science* 13:325–338.
- Dobrotvorský AK, Tkachev AV (1995) Evidence of a volatile sex pheromone in the unfed adult taiga tick *Ixodes persulcatus* Schulze. 2nd Int Conf on Tick-borne Pathogens at the Host-Vector Interface: an Agenda for Research, Proc and Abstr 1:372–375.
- Dusbábek FP, Simek EAP, Bouman R, Zahradnikova H, Zemek R (2001) Composition and effect of several semiochemicals in *Ixodes ricinus* L. (Acari: Ixodidae). In: Blaszkak C, Bucsek A (eds) *Stawonogi Pasozyty i Nosiciele*, Wydawnictwo KGM, Lublin pp 33–43.
- Estrada-Peña A, Estrada-Peña R, Peiro JM (1992) Differentiation of *Rhipicephalus* ticks (Acari, Ixodidae) by gas-chromatography of cuticular hydrocarbons. *J Parasitol* 78:982–993.
- Estrada-Peña A (1993) Climate and cuticular hydrocarbon variations in *Rhipicephalus sanguineus* ticks (Acari: Ixodidae). *Parasitol Res* 79:512–516.
- Estrada-Peña A, Castellá J, Siuda K (1994) Cuticular hydrocarbon composition and pheromone variability in sympatric populations of *Ixodes ricinus* ticks from Poland. *Exp Appl Acarol* 18:247–263.
- Fourie LJ, de Jager T, Petney TN (1988) Prolonger or repeated copulation and male longevity in the tick *Ixodes rubicundus*. *J Parasitol* 74:609–612
- Graf JF (1978) Ecology and ethology of *Ixodes ricinus* (Ixodidae). *B Swiss Entomol Soc* 50:241–253.
- Haggart DA, Davis EE (1981) Neurons sensitive to 2,6-dichlorophenol on the tarsi of the tick *Amblyomma americanum* (Acari: Ixodidae). *J Med Entomol* 3:187–193.
- Hamilton JGC, Sonenshine DE, Lushby WR (1989) Cholesteryl oleate; mounting sex pheromone of the hard tick, *Dermacentor variabilis*. (Say) (Acari: Ixodidae). *J insect Physiol* 35:873–879.
- Heethoff M (2012) Regeneration of complex oil-gland secretions and its importance for chemical defense in an oribatid mite. *J Chem Ecol* 38:1116–1123.

- Howard RW, Lord JC (2003) Cuticular lipids of the booklouse, *Liposcelis bostrychophila*: Hydrocarbons, aldehydes, fatty acids, and fatty acid amides. *J Chem Ecol* 29:615–627.
- Kiszewski AE, Spielman A (2002) Preprandial inhibition of re-mating in *Ixodes* ticks (Acari: Ixodidae). *J Med Entomol* 39:847–853.
- Kiszewski AE, Matuschka F, Spielman A (2001) Mating strategies and spermiogenesis in ixodid ticks. *Annu Rev Entomol* 46:167–182.
- Lenoir A, Cuvillier-Hot V, Devers A, Christidès J, Montigny F (2012) Ant cuticles: a trap for atmospheric phthalate contaminants. *Sci Total Environ* 441:209–212.
- Moorhouse DE, Heath CG (1975) Parasitism of female ticks by males of the genus *Ixodes*. *J Med Entomol* 12:571–572.
- Mulenga A (2014) Molecular biology and physiology of chemical communication. In: Sonenshine DE, Roe RM (eds) *Biology of Ticks Vol. I*, Oxford University Press, New York, pp 368–397.
- Osterkamp J, Wahl U, Schmalfluss G, Haas, W (1999) Host odor recognition in two tick species coded in a blend of vertebrate volatiles, *J. Comp. Physiol.* 185:59–67.
- Paine TD, Millar JG, Hanlon CC, Hwang JS (1999) Identification of semiochemicals associated with Jeffrey pine beetle, *Dendroctonus jeffreyi*. *J Chem Ecol* 25: 433–453.
- Shimshoni JA, Erster O, Cuneah O, Soback S, Shkap V (2013) Cuticular fatty acid profile analysis of three *Rhipicephalus* tick species (Acari: Ixodidae). *Exp Appl Acarol* 61:481–489.
- Soares SF, Borges MLF (2012) Electrophysiological responses of the olfactory receptors of the tick *Amblyomma cajennense* (Acari: Ixodidae) to host-related and tick pheromone-related synthetic compounds. *Acta Trop* 124:192–198.
- Sonenshine DE, Adams T, Allan SA, McLaughlin J, Webster FX (2003) Chemical composition of some components of the arrestment pheromones of the black-legged tick, *Ixodes scapularis* (Acari: Ixodidae) and their use in tick control. *Med Entomol* 40:849–859.
- Sonenshine DE (2006) Tick pheromones and their use in tick control. *Annu Rev Entomol* 51:557–580.
- Tkachev AV, Dobrotvorsky AK, Vjalkov AI, Morozov SV (2000) Chemical composition of lipophylic compounds from the body surface of unfed adult *Ixodes persulcatus* ticks (Acari: Ixodidae). *Exp Appl Acarol* 24:145–158.
- Torto B, Obeng Ofori D, Njagi PGN, Hassanali A, Amiani A (1994) Aggregation pheromones systems of adult gregarious desert locust *Schistocerca gregaria*. *J Chem Ecol* 20:1749–1762.

Treverrow NL, Stone BF, Cowie M (1977) Aggregation pheromone in two Australian hard ticks, *Ixodes holocyclus* and *Aponomma concolor*. *Experientia* 33:680–682.

Waladde SM, Rice MJ (1982) The sensory basis of tick feeding behavior. In: Obenchain FD, Galun R (eds), *Physiology of Ticks*, Pergamon Press, Oxford, pp 71–118.

Xiao YH, Zhang JX, Li SQ (2009) A two-component female produced pheromone of the spider *Pholcus beijingensis*. *J Chem Ecol* 35:769–778.

Zemek R, Bouman EAP, Socha R, Dusbábek (2002) The effect of feeding status on sexual attractiveness of *Ixodes ricinus* (Acari: Ixodidae) females. *Exp Appl Acarol* 27:137–149.

Zhang J, Salcedo C, Fang Y, Zhang R, Zhang Z (2012) An overlooked component: (z)-9-tetradecenal as a sex pheromone in *Helicoverpa armigera*. *J Insect Physiol* 58:1209–1216.

Tables

Table 3.1 Compounds with a match probability $\geq 80\%$ identified in all replicates of whole body hexane extracts of *I. scapularis* unfed, virgin adult females versus unfed, virgin adult males (Cas no. = Chemical abstract service number). Mass spectral data are listed in SI.

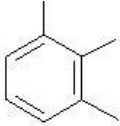
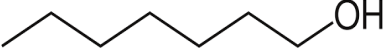
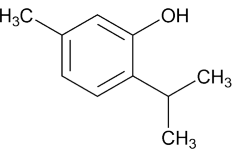
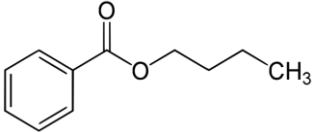
No.	Present in (+/-)		Retention time (min)	Chemical class	Component & match probability % (Cas no.)	Chemical structure
	Females	Males				
1	+	-	4.229	Alkene	1-Heptene, 84.0% (592-76-7)	
2	+	+	6.882	Aromatic hydrocarbon	1,2,3-Trimethylbenzene, 96.4% (526-73-8)	
3	+	-	9.762	Fatty alcohol	1-Heptanol, 81.6% (111-70-6)	
4	+	+	12.345	Alkane	Dodecane, 86.3% (112-40-3)	
5	-	+	13.131	Monoterpene phenol	Thymol, 92.1% (89-83-8)	
6	+	+	17.009	Carboxylic acid ester	Butyl benzoate, 97.7% (136-60-7)	
7	+	-	17.626	Alkane	Tetradecane, 82.4% (629-59-4)	
8	+	+	20.090	Alkane	Pentadecane, 80.0% (629-62-9)	
9	-	+	22.439	Alkane	Hexadecane, 81.4% (544-76-3)	

Table 3.1 Continued

No.	Present in (+/-)		Retention time (min)	Chemical class	Component & match probability % (Cas no.)	Chemical structure
	Females	Males				
10	+	+	23.785	Alkane	Heptadecane, 82.4% (629-78-7)	
11	+	+	25.827	Carboxylic acid ester	Ethyl-4-ethoxybenzoate, 94.9% (23676-09-7)	
12	+	+	27.313	Steroid	5β-Androstane, 70.0% (24887-75-0)	
13	+	+	32.068	Alkane	Octadecane, 84.3% (593-45-3)	
14	+	+	34.685	Diterpene alcohol	Phytol, 80.6% (7541-49-3)	
15	+	+	35.024	Fatty acid ester	Butyl palmitate, 82.1% (111-08-6)	
16	+	+	36.768	Fatty alcohol	1-Hexadecanol, 80.3% (36653-82-4)	
17	+	+	39.063	Fatty acid ester	Butyl stearate, 81.9% (123-95-5)	
18	+	+	46.321	Fatty amide	Erucylamide, 80.4% (93050-58-9)	

Figures

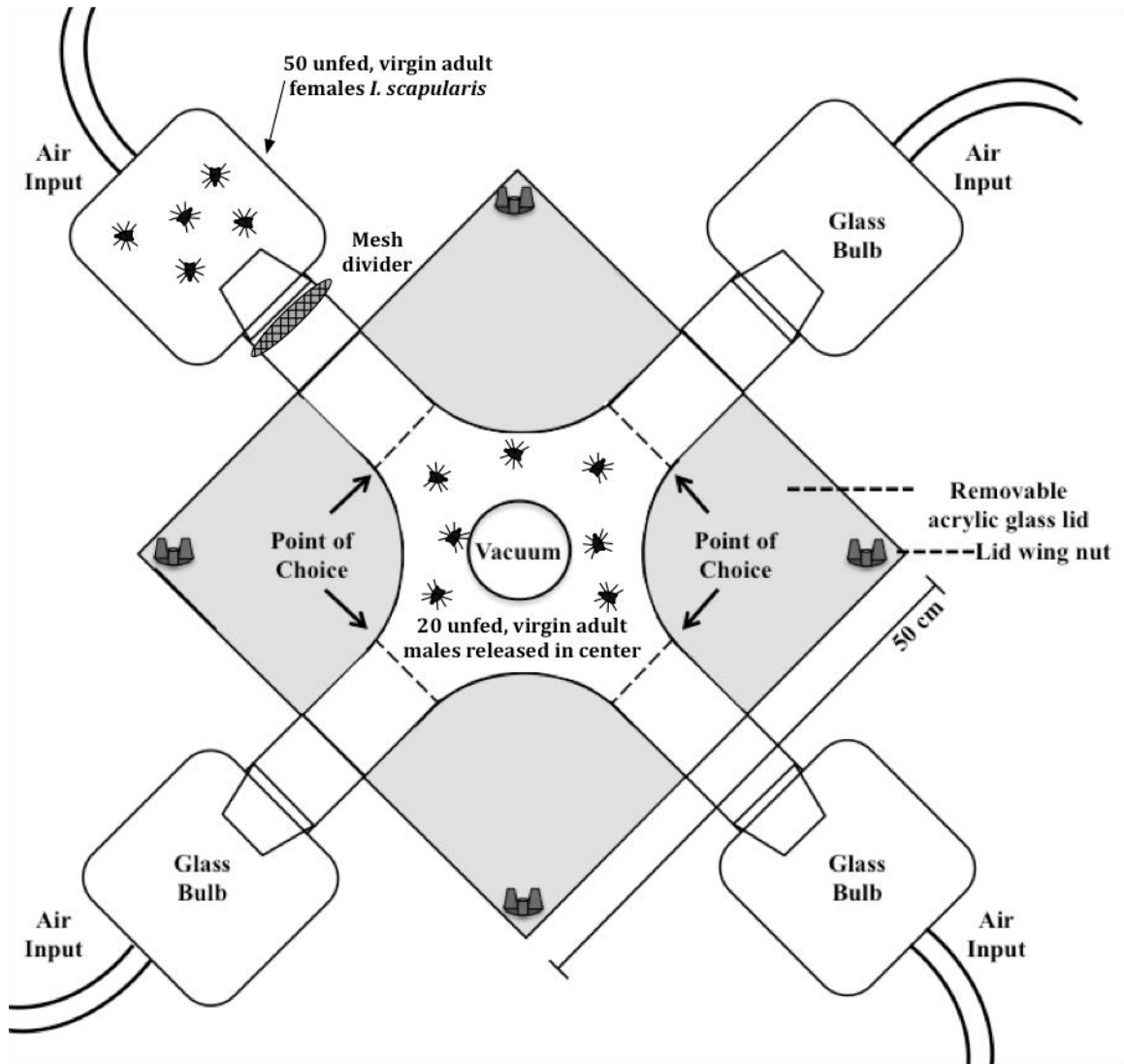


Figure 3.1 The 4-port olfactometer used to examine possible volatile secretions produced by *I. scapularis* unfed virgin adult females that would be attractive to unfed virgin adult males. A vacuum hose attached to the bottom of the central arena of the olfactometer creates a unidirectional airflow from each glass bulb toward the center of the apparatus.

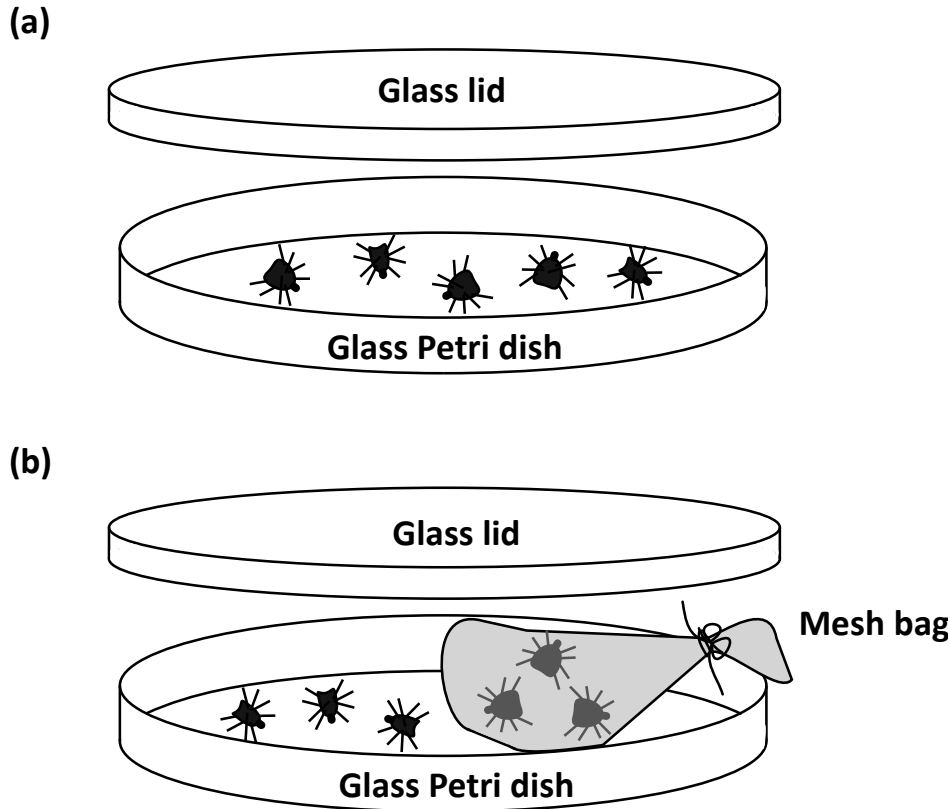


Figure 3.2 (a) Petri dish assays used to examine *I. scapularis* mounting behavior between free roaming unfed virgin adult males and unfed virgin adult females. This experiment was also used to examine the affects of detergent washing and blood feeding on female attraction, and impacts on chelicerae insertion/maintenance behavior in unfed virgin adult males. This Petri dish assay was used to examine chelicerae insertion/maintenance behavior of unfed virgin adult males with 1) detergent washed unfed virgin adult females, 2) unfed virgin adult females, 3) part-fed virgin adult females and 4) replete mated adult females. (b) Petri dish assays used to examine *I. scapularis* mounting behavior between free roaming unfed virgin adult males and unfed virgin adult females secluded inside a mesh to prevent direct contact between the sexes.

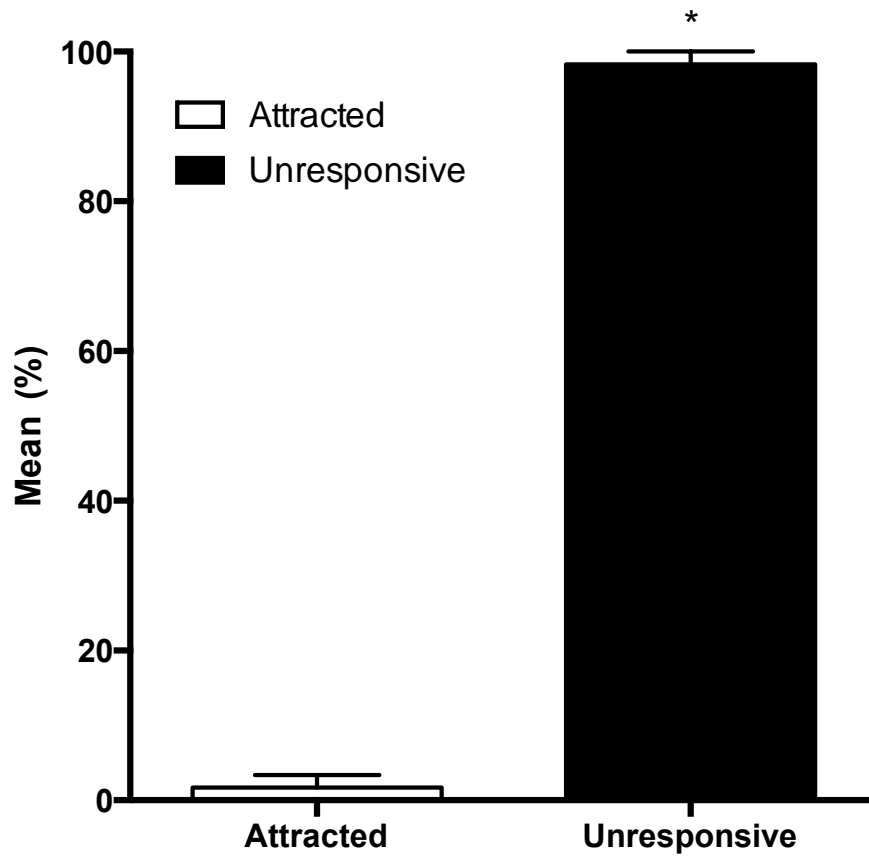


Figure 3.3 Mean percentage (± 1 SEM) of *I. scapularis* unfed virgin adult males attracted to odors produced by unfed virgin adult females in olfactometer assays (Fig. 3.1). Attraction is defined as males found between the females and point of choice (Fig. 3.1) 24h after release in the center of the apparatus. Unresponsive males did not leave the central area of the apparatus. Treatments were compared using a paired Student's *t*-test (* = $P < 0.05$).

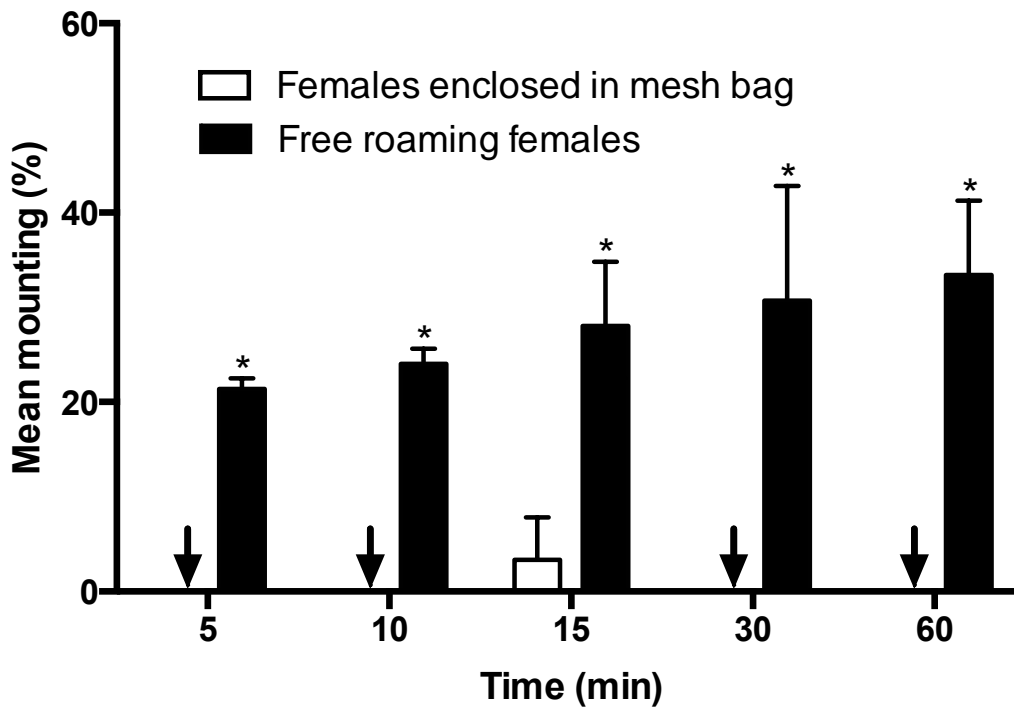


Figure 3. 4 Mean percentage mounting (± 1 SEM) of *I. scapularis* unfed virgin adult males with free roaming unfed virgin adult females, and with unfed virgin adult females enclosed in mesh bags in Petri dish bioassays (Fig. 3.2a and 3.2b). Attraction is defined as males mounting females and orienting towards the female genital pore. Arrows denote zero values. Treatments were compared using a 2-way ANOVA and a Sidak's multiple comparisons test at each time point (* = $P < 0.05$).

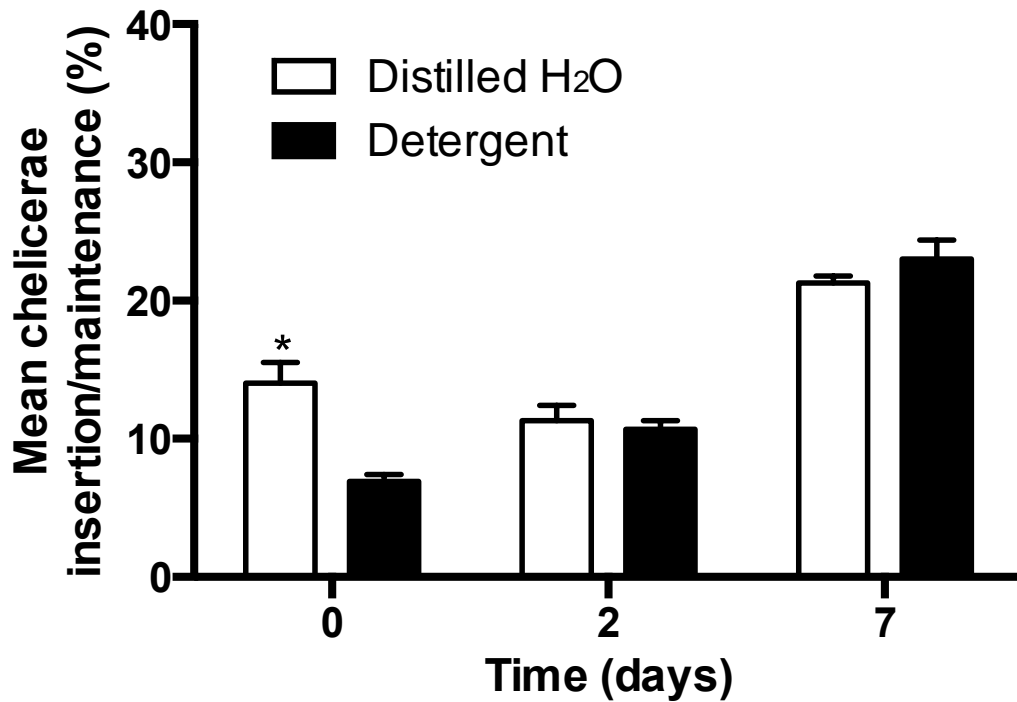


Figure 3.5 Mean percentage chelicerae insertion/maintenance (± 1 SEM) of *I. scapularis* unfed virgin adult males with unfed virgin adult females following female whole body washing with distilled water or with 1% Triton-X 100 detergent in Petri dish bioassays (Fig. 3.2a). Treatments were compared using a 2-way ANOVA and a Sidak's multiple comparison test at each time point (* = $P < 0.05$).

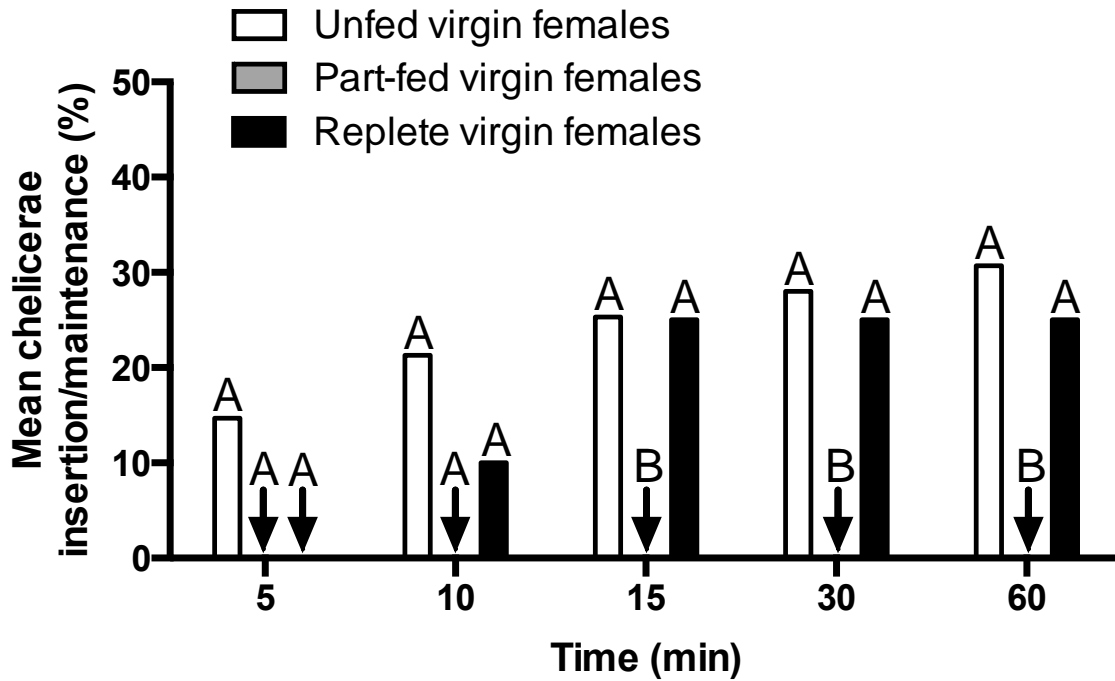


Figure 3.6 Mean percentage chelicerae insertion/maintenance of *I. scapularis* unfed virgin adult males with unfed virgin adult females, part-fed virgin adult females, and replete mated adult females in Petri dish assays (Fig. 3.2a). Arrows denote zero values. Treatments were compared using a 2-way ANOVA and a Tukey's multiple comparison test for each time point. Treatments with the same letter at each time point are not statistically significant ($P < 0.05$).

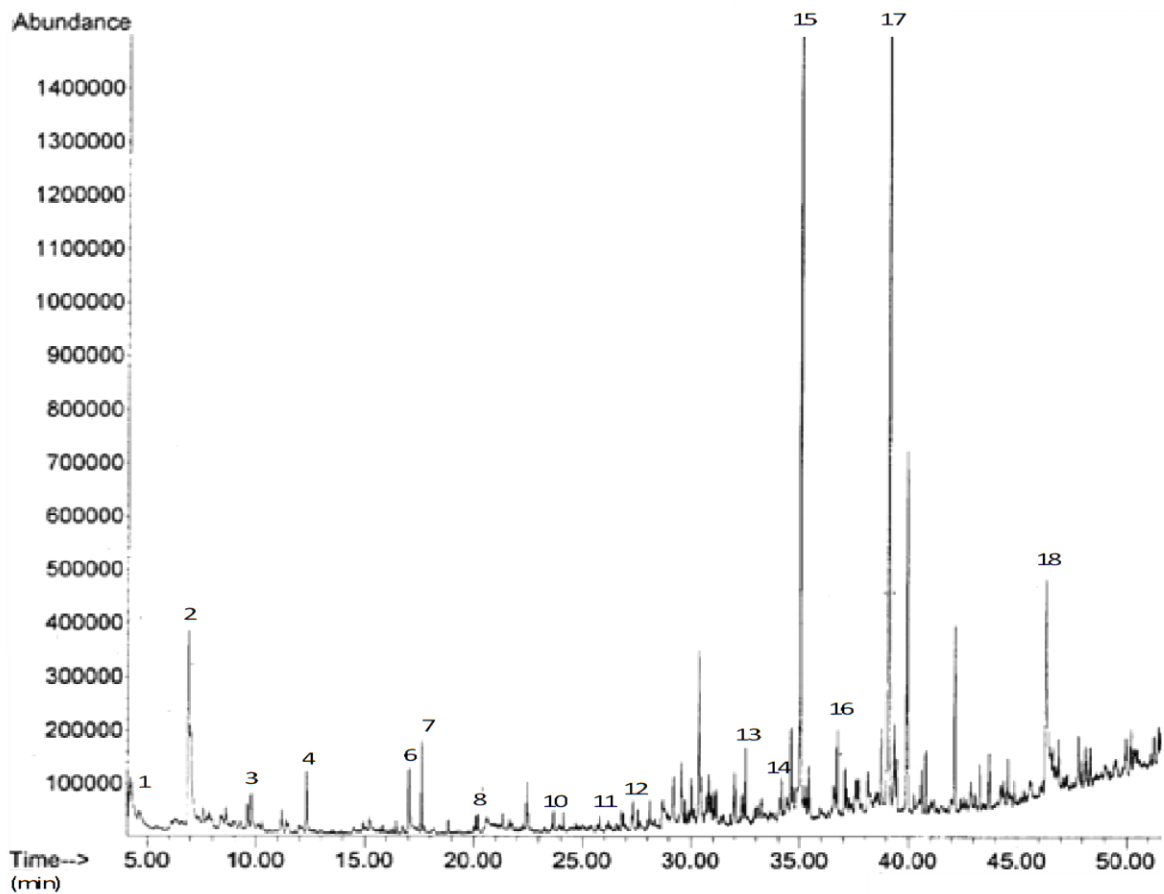


Figure 3.7 Example of a GC-MS chromatogram of a whole body surface hexane extraction of 10 unfed virgin adult female *I. scapularis* ticks. The compounds identified with $\geq 80\%$ match probability are numbered and further described in Table 3.1 and Fig. 3.9. Missing numbers represent compounds not identified in females. Abundances were determined using flame ionization detection. Time = min.

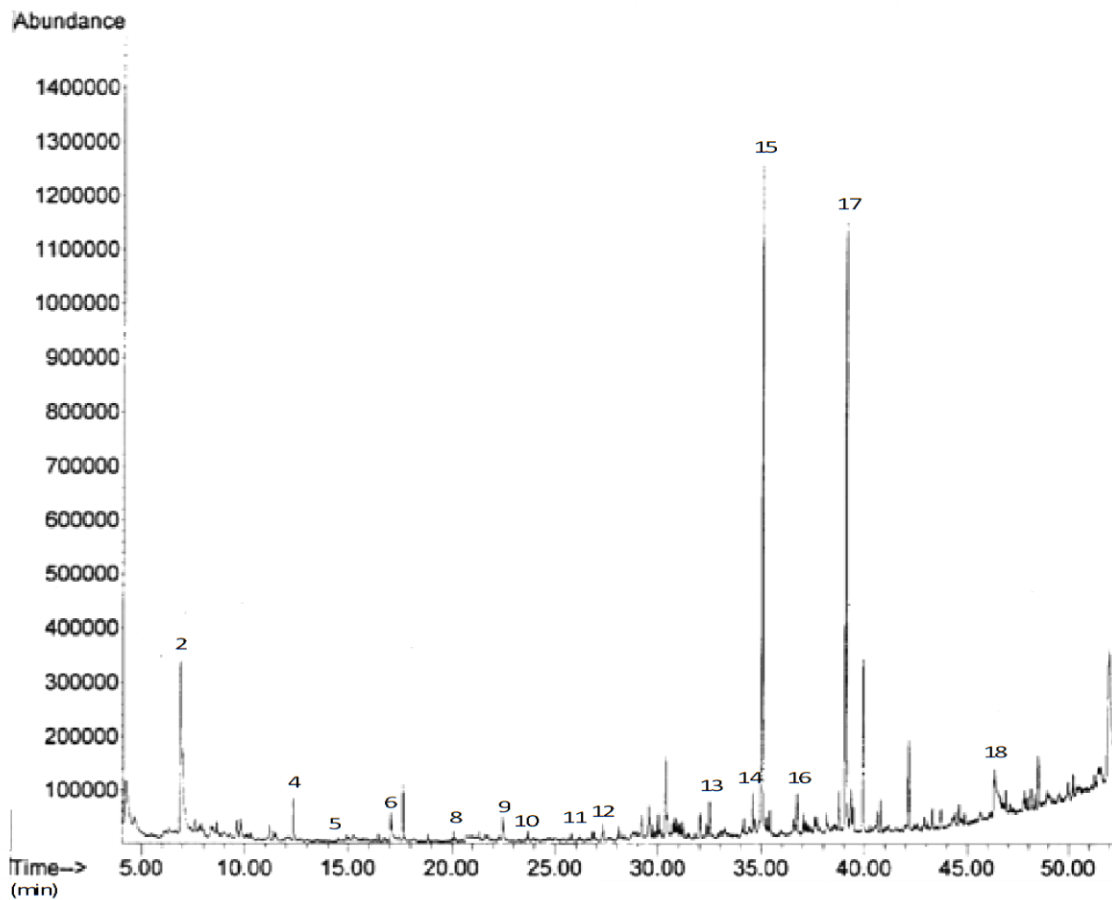


Figure 3.8 Example of a GC-MS chromatogram of a whole body surface hexane extraction of 10 unfed virgin adult male *I. scapularis* ticks. The compounds identified with $\geq 80\%$ match probability are numbered and further described in Table 3.1 and Fig. 3.9. Missing numbers represent compounds not identified in males. Abundances were determined using flame ionization detection. Time = min.

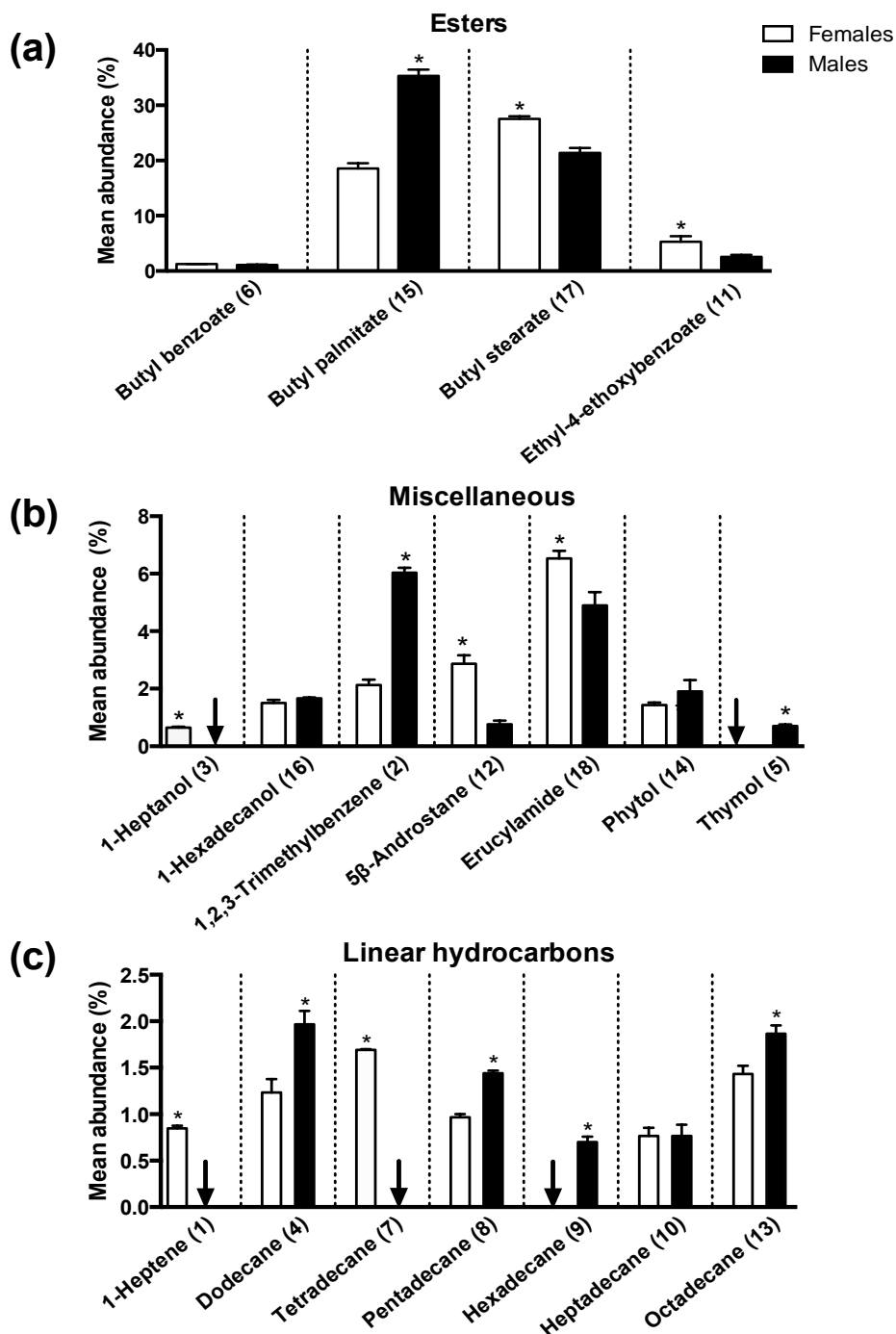


Figure 3.9 Mean percent abundance (± 1 SEM) of compounds identified (Table 3.1) in whole body hexane extractions of *I. scapularis* unfed virgin adult females versus unfed virgin males. Mean abundance for a compound was calculated by averaging the peak areas identified in all 5 female and 6 male replicate GC-MS runs. Percentages were calculated out of the total abundance obtained for all 18 compounds identified. Arrows denote zero values. Treatments were compared using a paired student's *t*-test (* = $P < 0.05$). Numbers in parenthesis correlate to assigned numbers in Table 1 and peak numbers in Fig. 3.7 and Fig. 3.8.

Supplemental Information: Figures

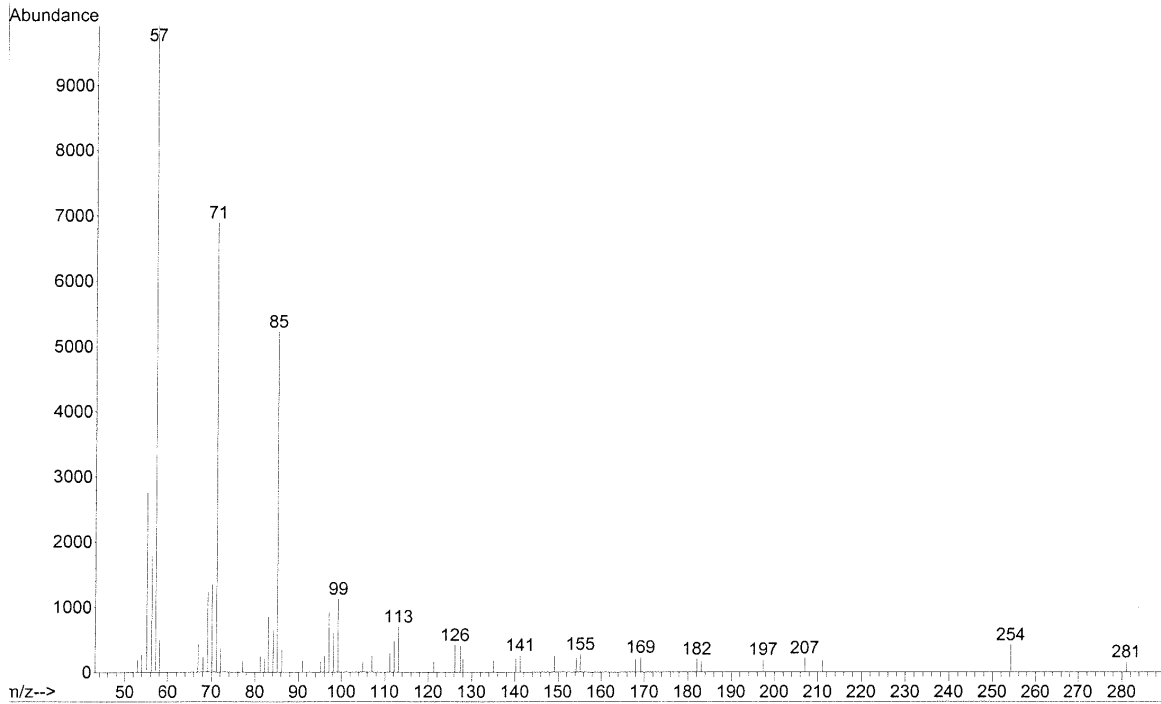


Figure 3.S1 Example of the GC-MS mass spectral data obtained for 1-heptene identified in whole body hexane extractions of *I. scapularis* unfed virgin adult females (Table 3.1 and Fig. 3.9). M/Z = mass to charge ratio for each ion. Abundance = the intensity or abundance of each ion.

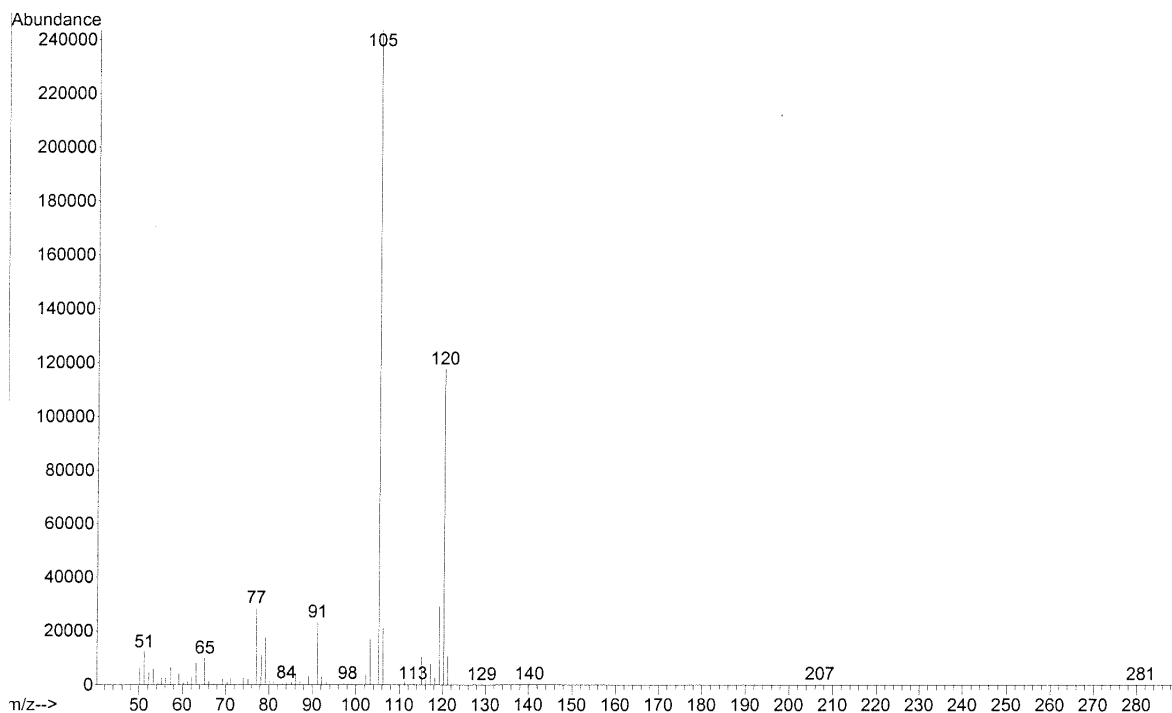


Figure 3.S2 Example of the GC-MS mass spectral data obtained for 1,2,3-trimethylbenzene identified in whole body hexane extractions of *I. scapularis* unfed virgin adult females and males (Table 3.1 and Fig. 3.9). M/Z = mass to charge ratio for each ion. Abundance = the intensity or abundance of each ion.

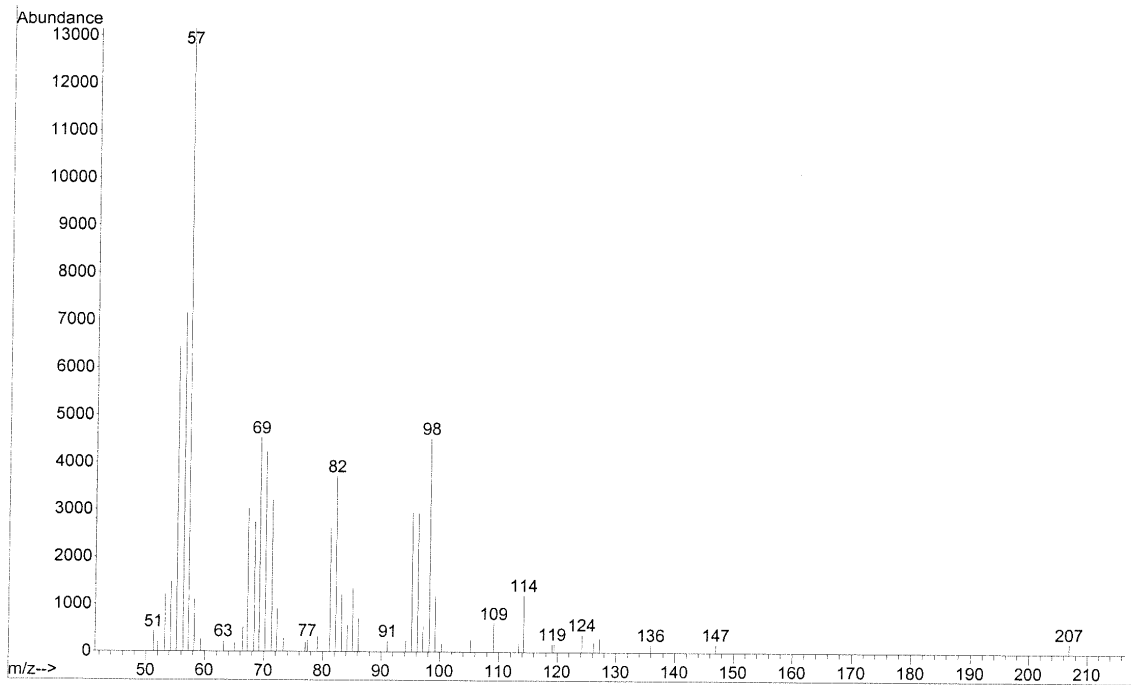


Figure 3.S3 Example of the GC-MS mass spectral data obtained for 1-heptanol identified in whole body hexane extractions of *I. scapularis* unfed virgin adult females (Table 3.1 and Fig. 3.9). M/Z = mass to charge ratio for each ion. Abundance = the intensity or abundance of each ion.

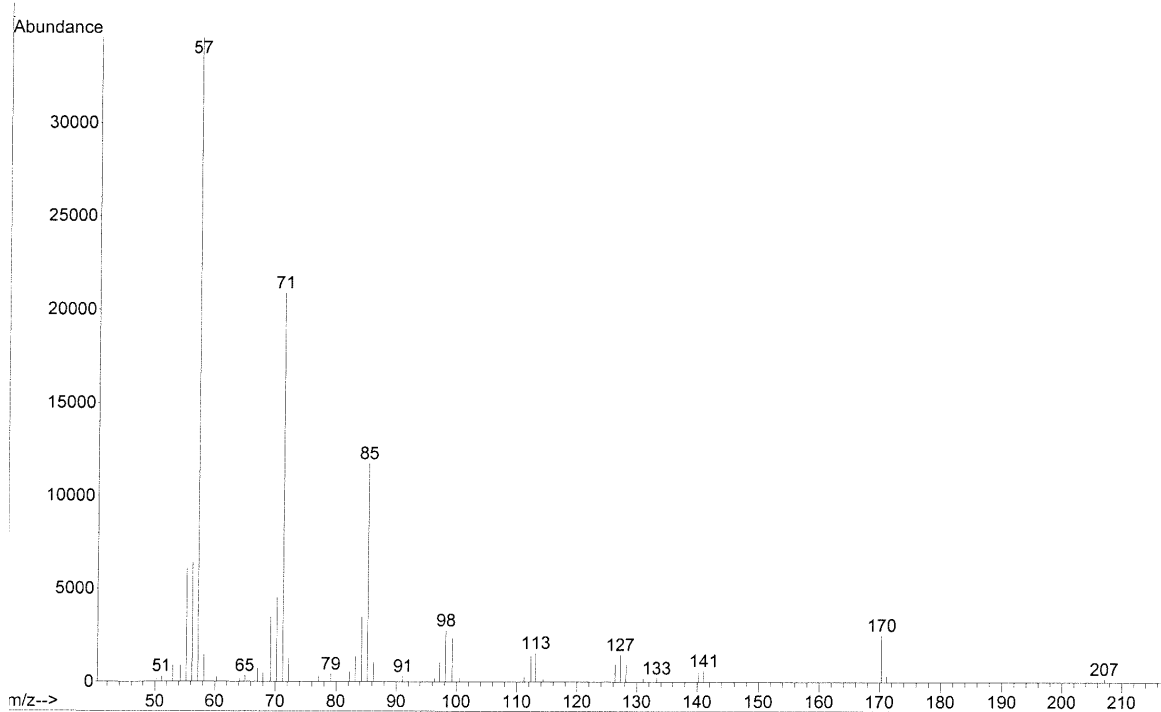


Figure 3.S4 Example of the GC-MS mass spectral data obtained for dodecane identified in whole body hexane extractions of *I. scapularis* unfed virgin adult females and males (Table 3.1 and Fig. 3.9). M/Z = mass to charge ratio for each ion. Abundance = the intensity or abundance of each ion.

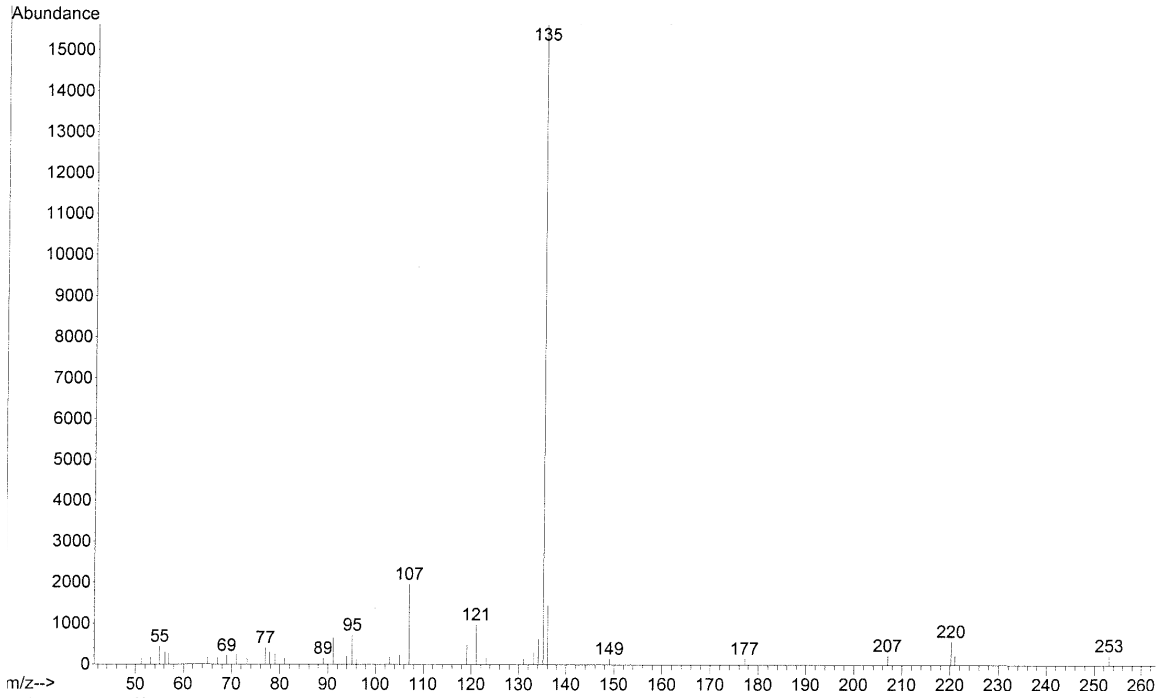


Figure 3.S5 Example of the GC-MS mass spectral data obtained for thymol identified in whole body hexane extractions of *I. scapularis* unfed virgin adult males (Table 3.1 and Fig. 3.9). M/Z = mass to charge ratio for each ion. Abundance = the intensity or abundance of each ion.

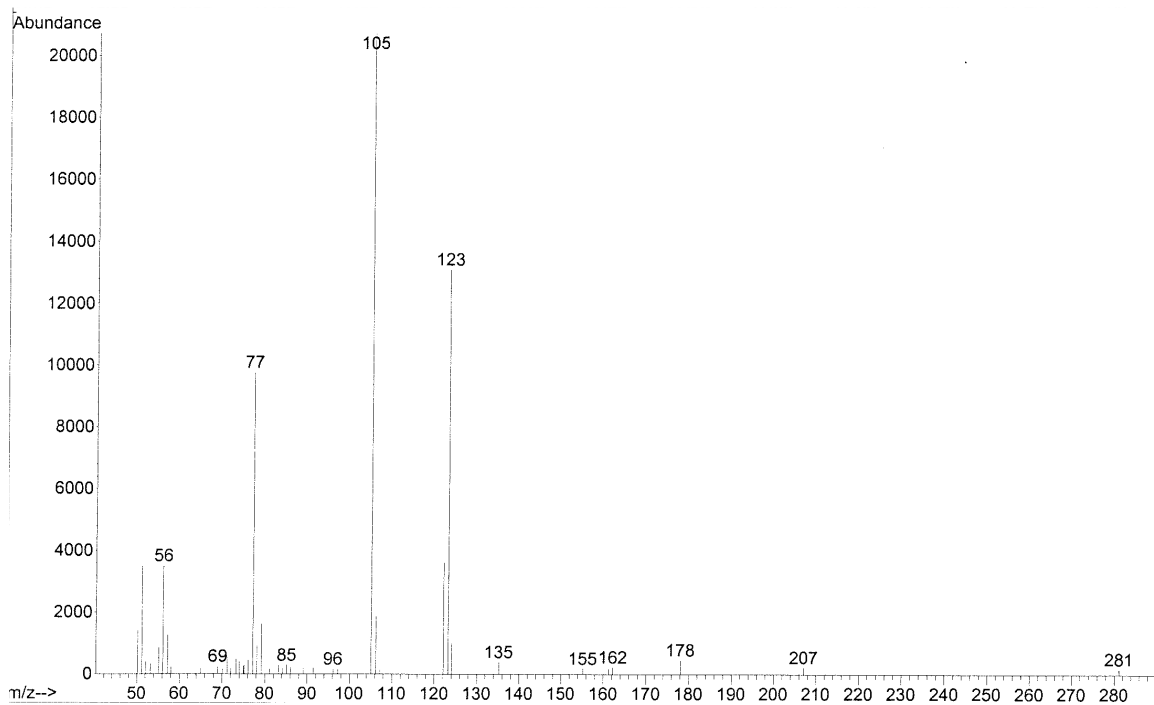


Figure 3.S6 Example of the GC-MS mass spectral data obtained for butyl benzoate identified in whole body hexane extractions of *I. scapularis* unfed virgin adult females and males (Table 3.1 and Fig. 3.9). M/Z = mass to charge ratio for each ion. Abundance = the intensity or abundance of each ion.

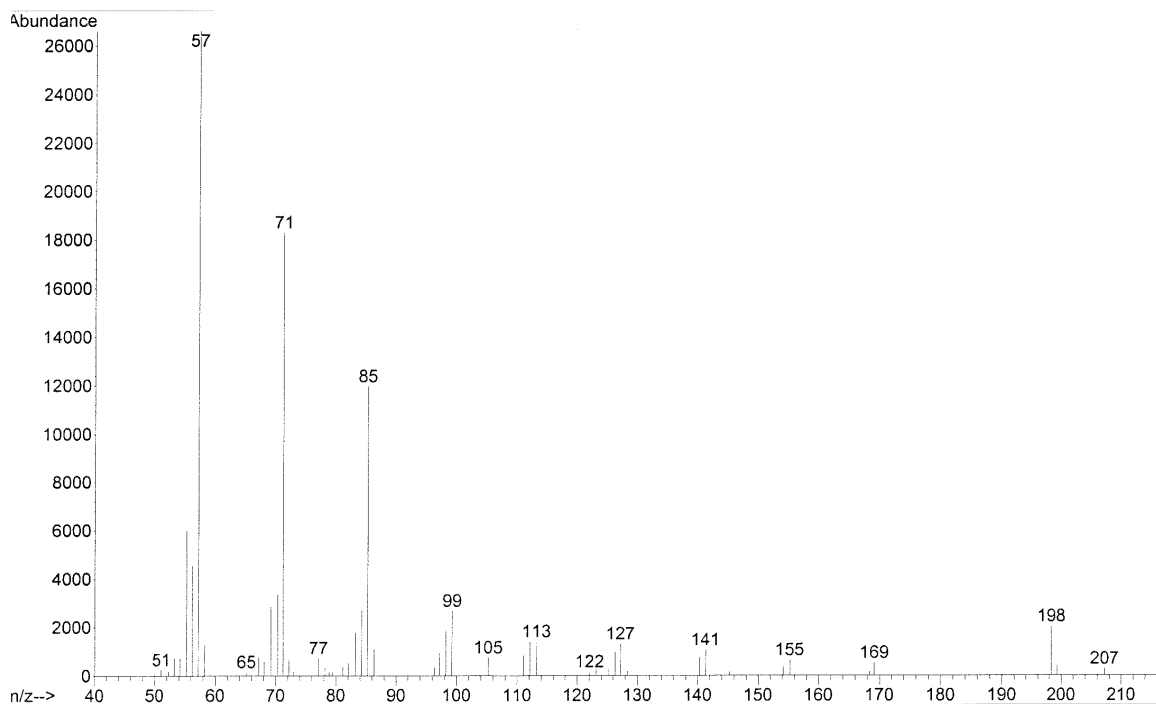


Figure 3.S7 Example of the GC-MS mass spectral data obtained for tetradecane identified in whole body hexane extractions of *I. scapularis* unfed virgin adult females (Table 3.1 and Fig. 3.9). M/Z = mass to charge ratio for each ion. Abundance = the intensity or abundance of each ion.

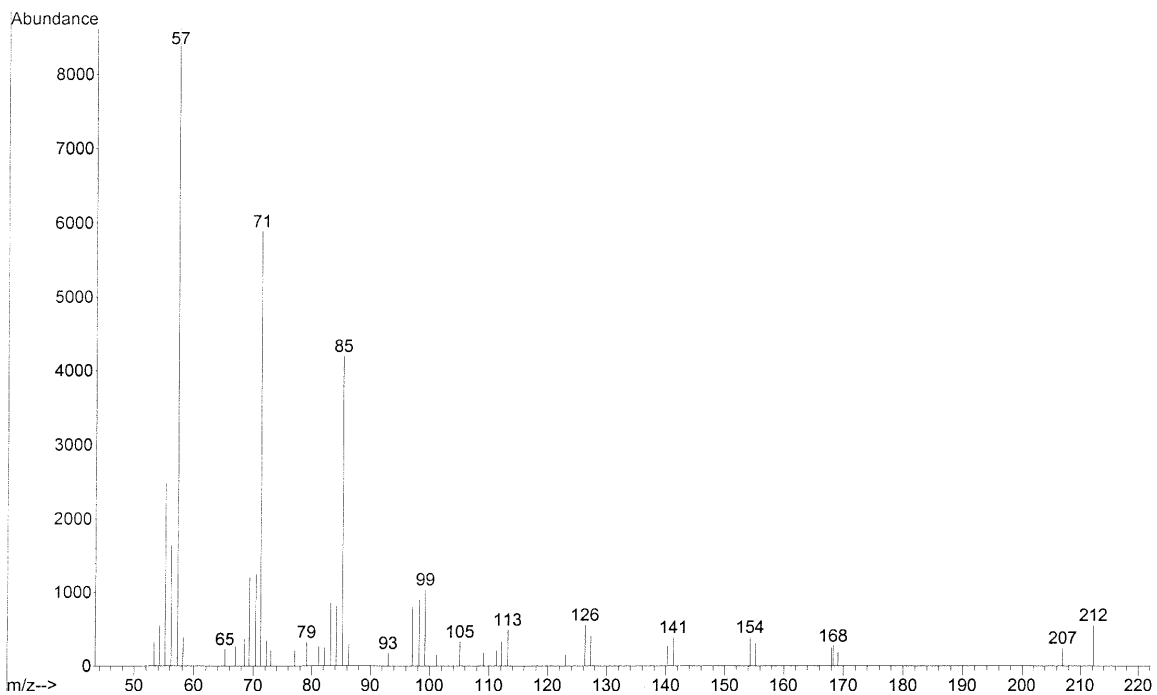


Figure 3.S8 Example of the GC-MS mass spectral data obtained for pentadecane identified in whole body hexane extractions of *I. scapularis* unfed virgin adult females and males (Table 3.1 and Fig. 3.9). M/Z = mass to charge ratio for each ion. Abundance = the intensity or abundance of each ion.

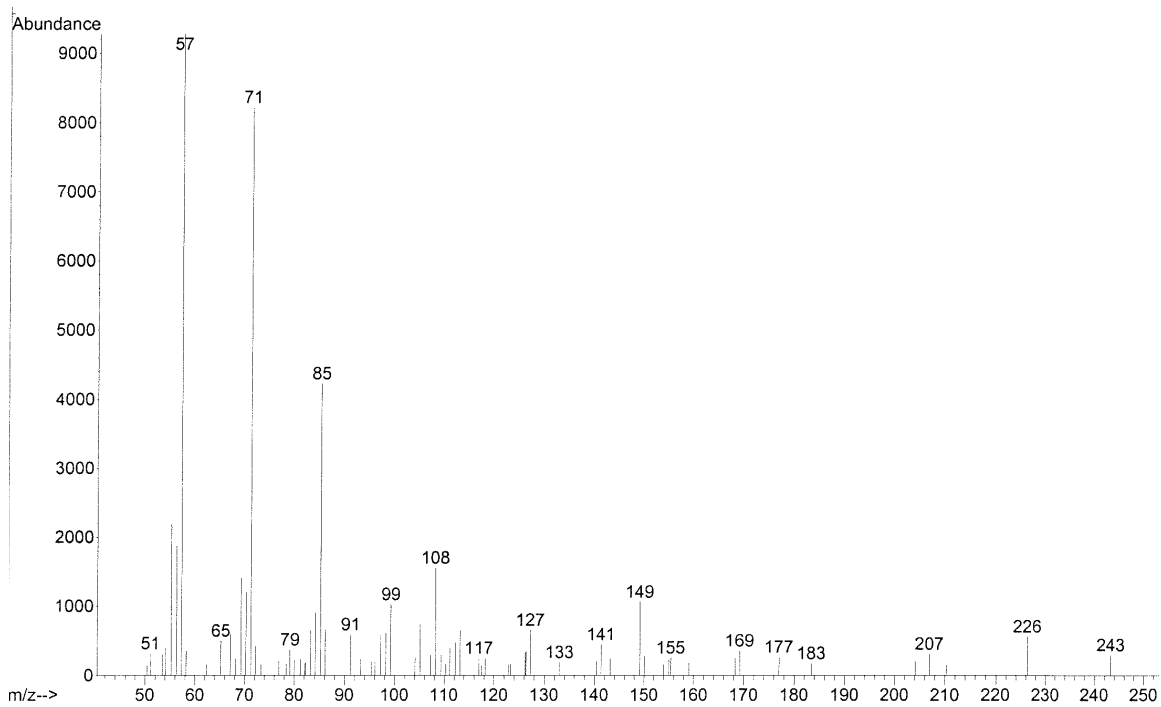


Figure 3.S9 Example of the GC-MS mass spectral data obtained for hexadecane identified in whole body hexane extractions of *I. scapularis* unfed virgin adult males (Table 3.1 and Fig. 3.9). M/Z = mass to charge ratio for each ion. Abundance = the intensity or abundance of each ion.

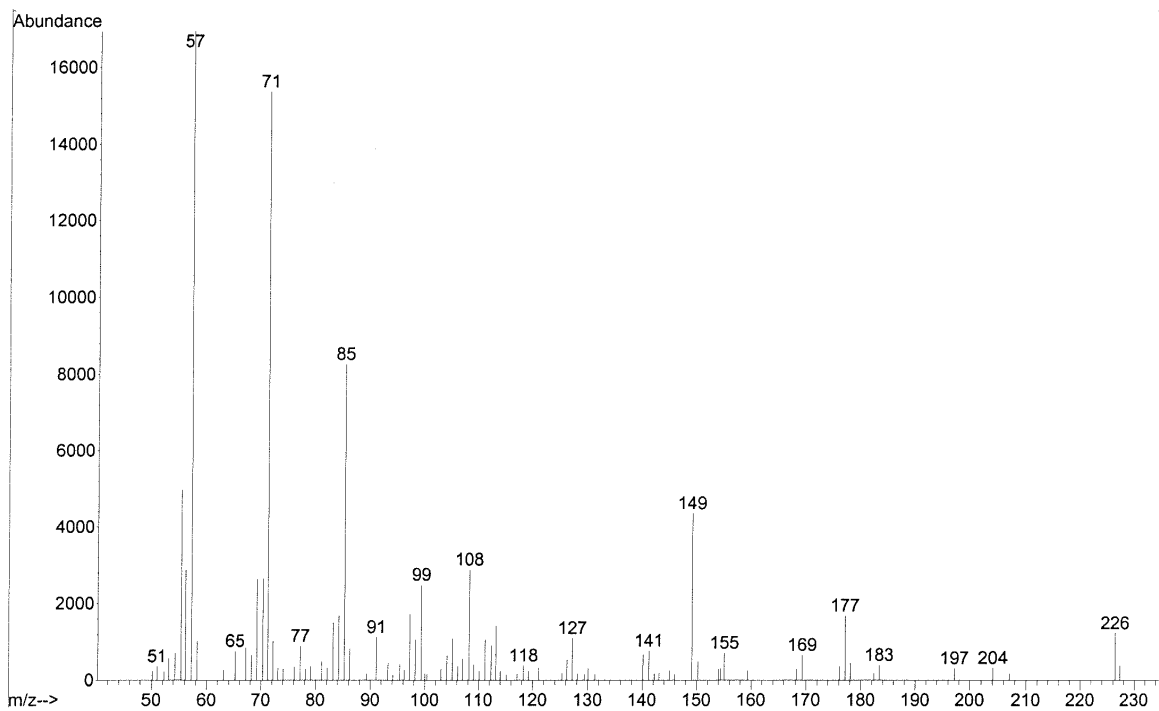


Figure 3.S10 Example of the GC-MS mass spectral data obtained for heptadecane identified in whole body hexane extractions of *I. scapularis* unfed virgin adult females and males (Table 3.1 and Fig. 3.9). M/Z = mass to charge ratio for each ion. Abundance = the intensity or abundance of each ion.

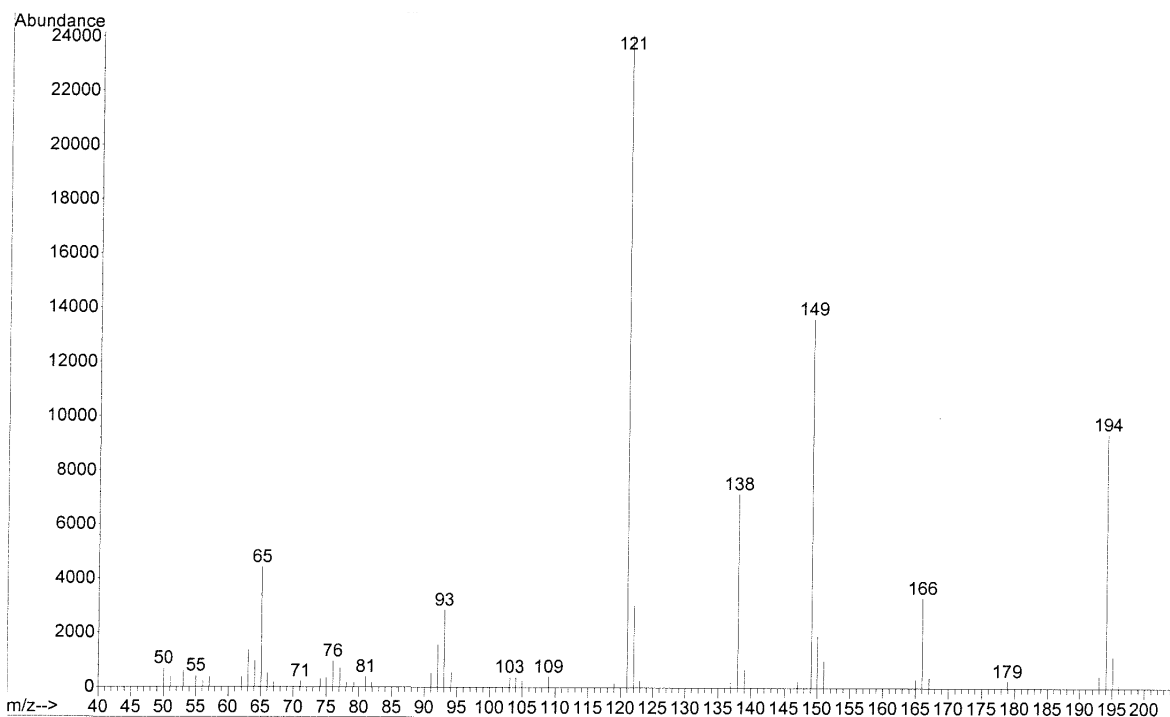


Figure 3.S11 Example of the GC-MS mass spectral data obtained for ethyl-4-ethoxybenzoate identified in whole body hexane extractions of *I. scapularis* unfed virgin adult females and males (Table 3.1 and Fig. 3.9). M/Z = mass to charge ratio for each ion. Abundance = the intensity or abundance of each ion.

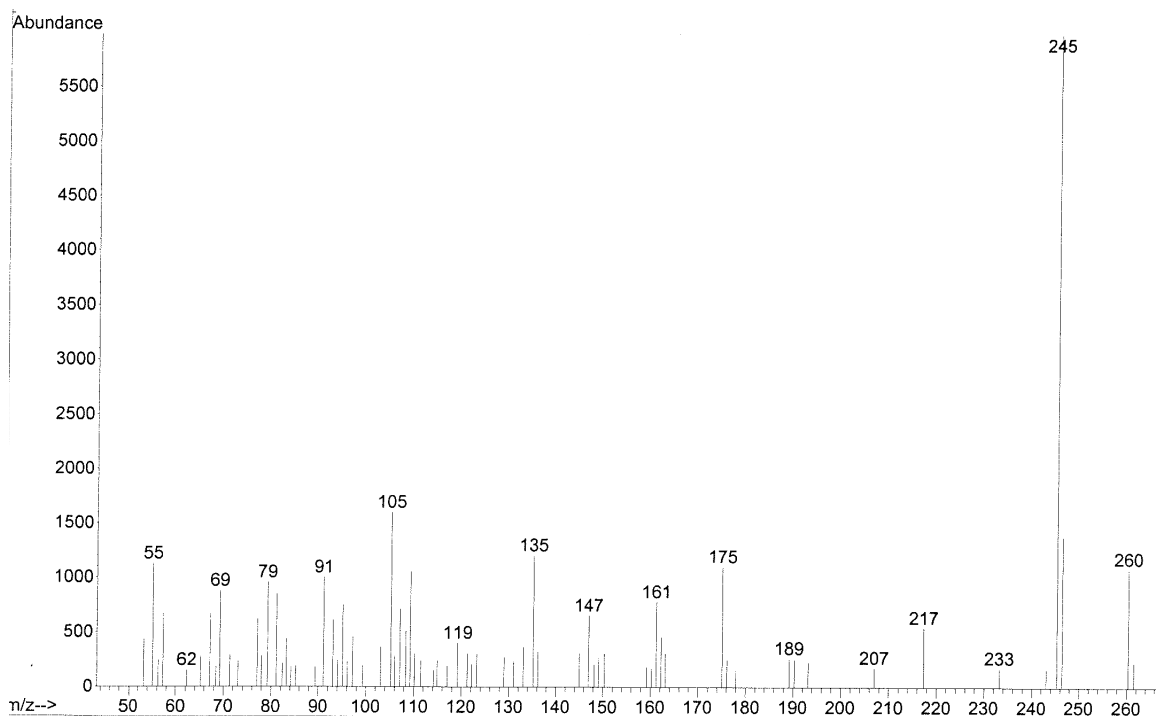


Figure 3.S12 Example of the GC-MS mass spectral data obtained for 5 β -androstane identified in whole body hexane extractions of *I. scapularis* unfed virgin adult females and males (Table 3.1 and Fig. 3.9). M/Z = mass to charge ratio for each ion. Abundance = the intensity or abundance of each ion.

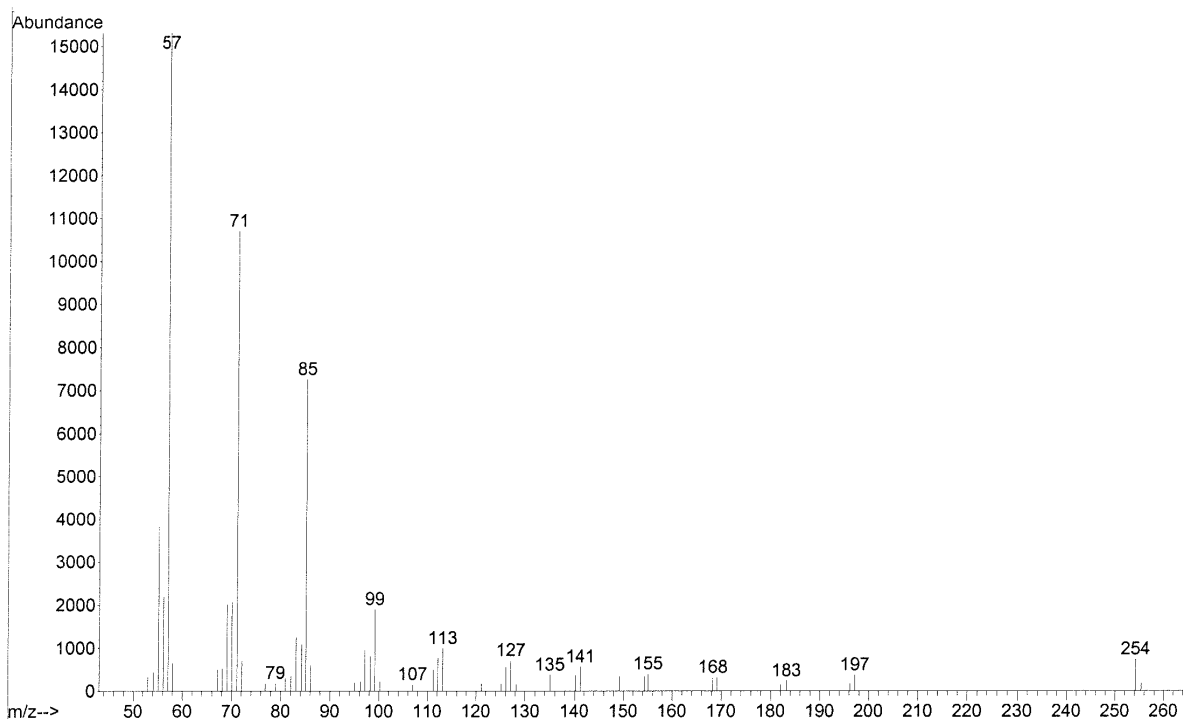


Figure 3.S13 Example of the GC-MS mass spectral data obtained for octadecane identified in whole body hexane extractions of *I. scapularis* unfed virgin adult females and males (Table 3.1 and Fig. 3.9). M/Z = mass to charge ratio for each ion. Abundance = the intensity or abundance of each ion.

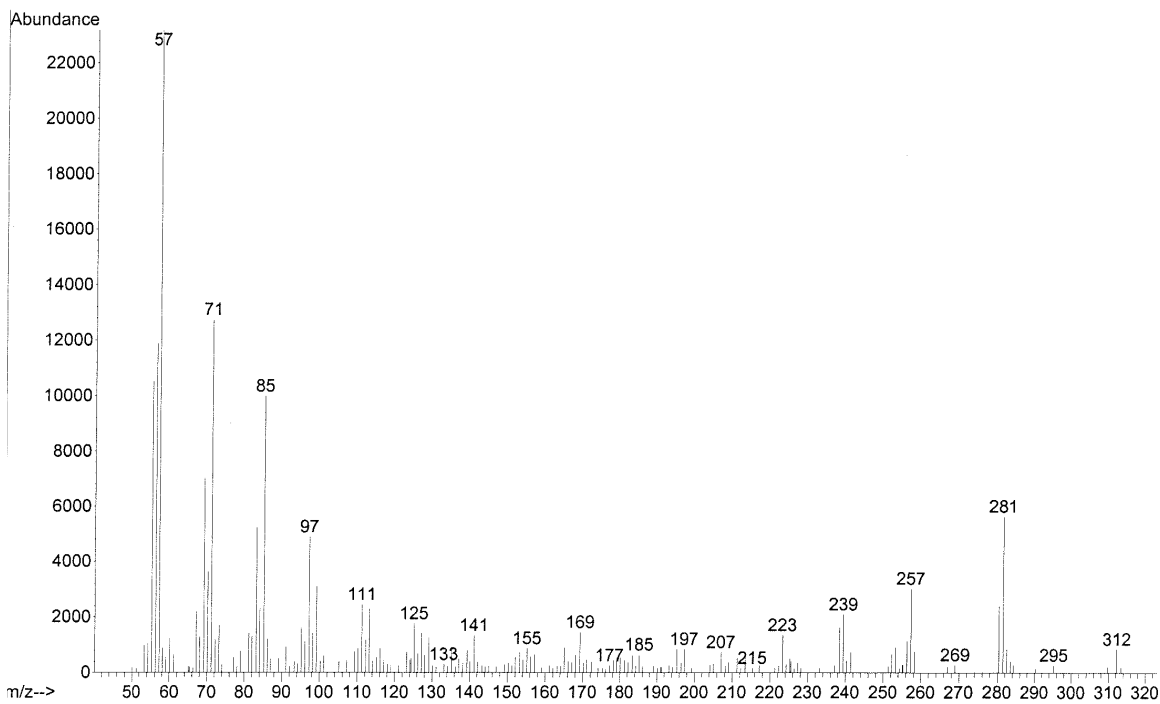


Figure 3.S14 Example of the GC-MS mass spectral data obtained for phytol identified in whole body hexane extractions of *I. scapularis* unfed virgin adult females and males (Table 3.1 and Fig. 3.9). M/Z = mass to charge ratio for each ion. Abundance = the intensity or abundance of each ion.

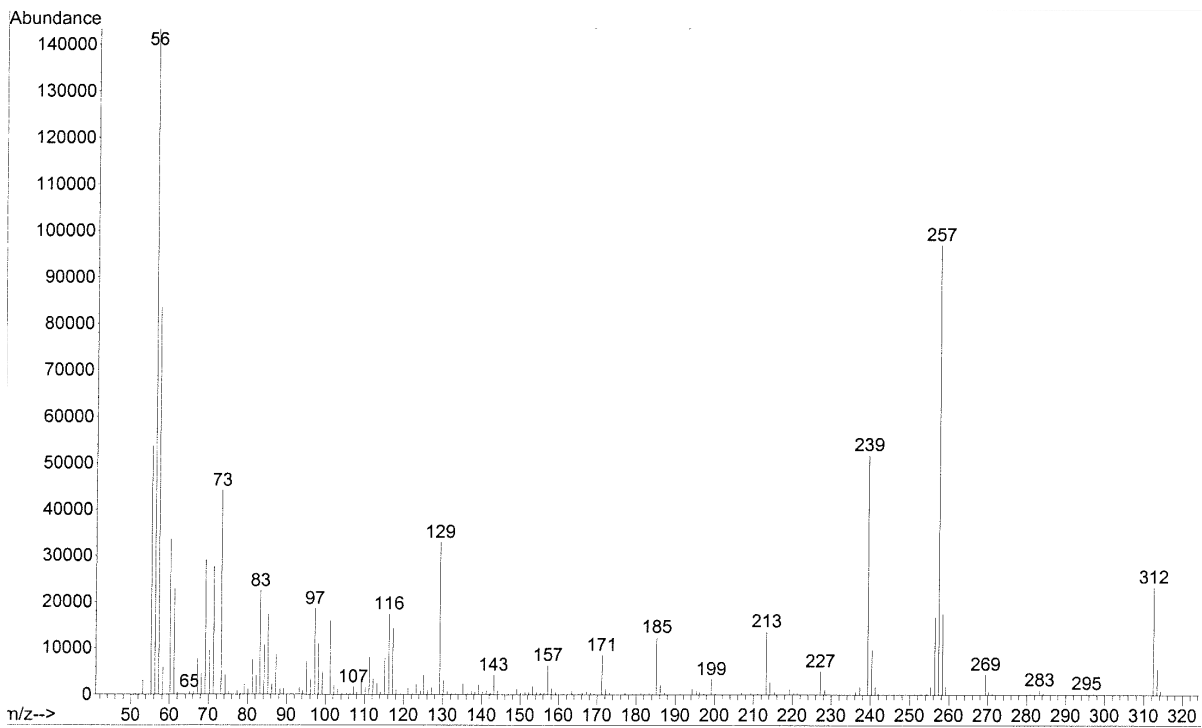


Figure 3.S15 Example of the GC-MS mass spectral data obtained for butyl palmitate identified in whole body hexane extractions of *I. scapularis scapularis* unfed virgin adult females and males (Table 3.1 and Fig. 3.9). M/Z = mass to charge ratio for each ion. Abundance = the intensity or abundance of each ion.

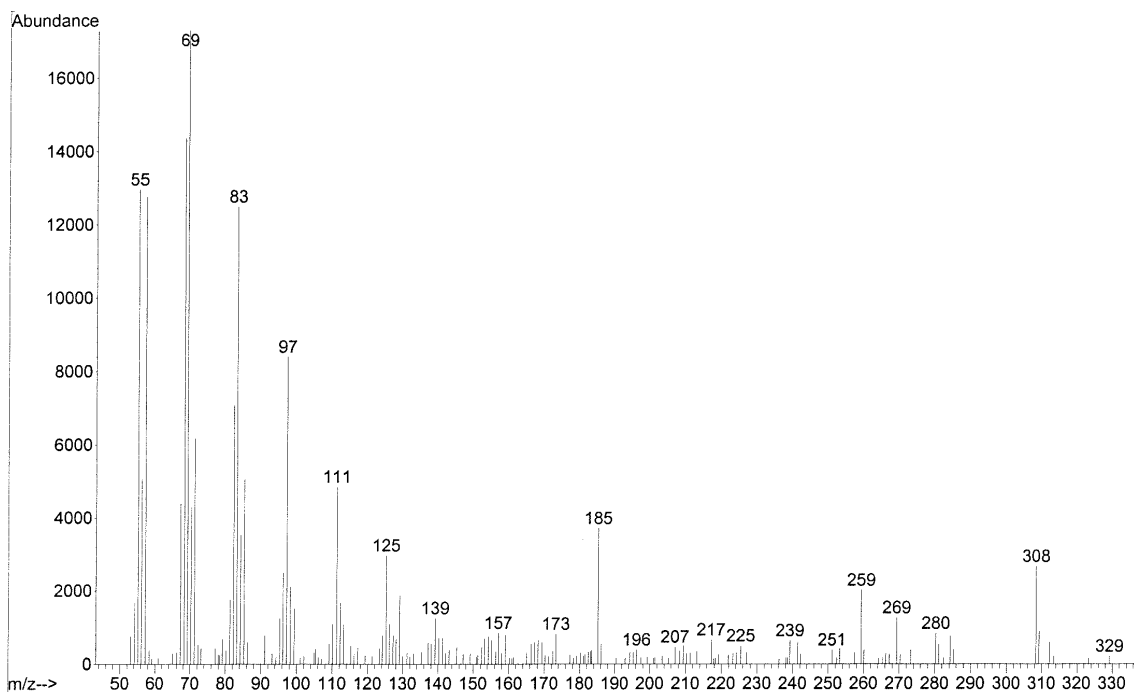


Figure 3.S16 Example of the GC-MS mass spectral data obtained for 1-hexadecanol identified in whole body hexane extractions of *I. scapularis scapularis* unfed virgin adult females and males (Table 3.1 and Fig. 3.9). M/Z = mass to charge ratio for each ion. Abundance = the intensity or abundance of each ion.

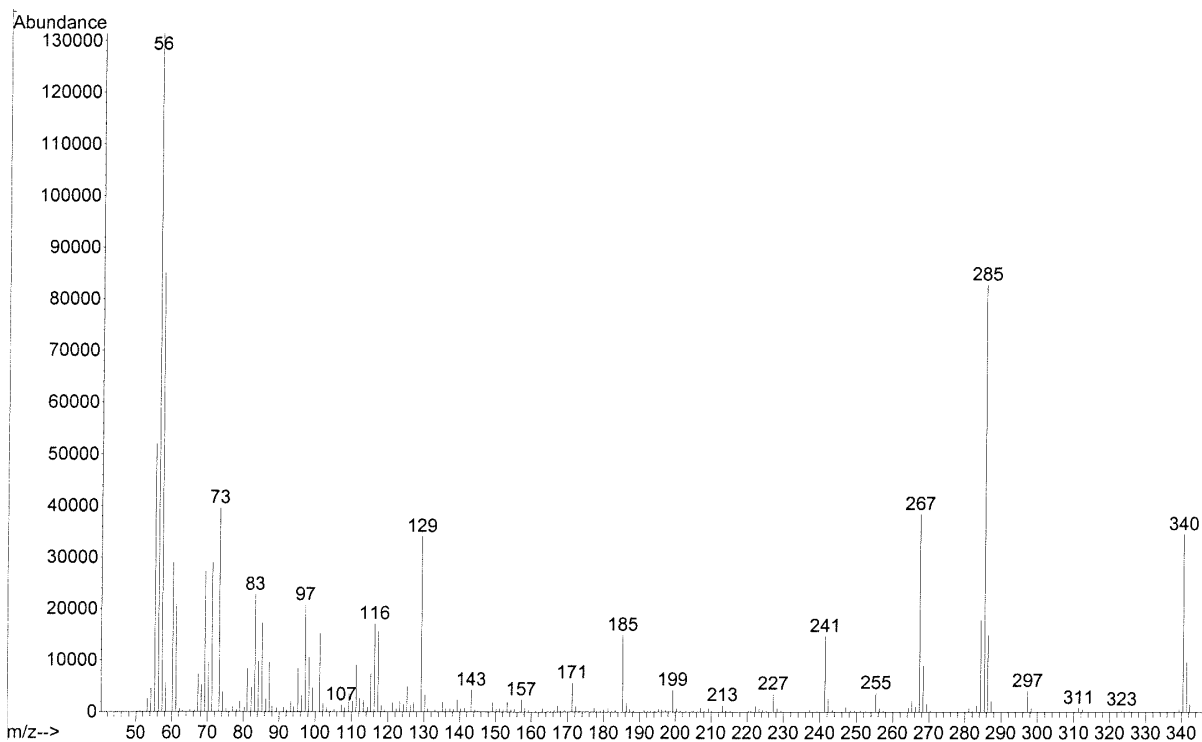


Figure 3.S17 Example of the GC-MS mass spectral data obtained for butyl stearate identified in whole body hexane extractions of *I. scapularis scapularis* unfed virgin adult females and males (Table 3.1 and Fig. 3.9). M/Z = mass to charge ratio for each ion. Abundance = the intensity or abundance of each ion.

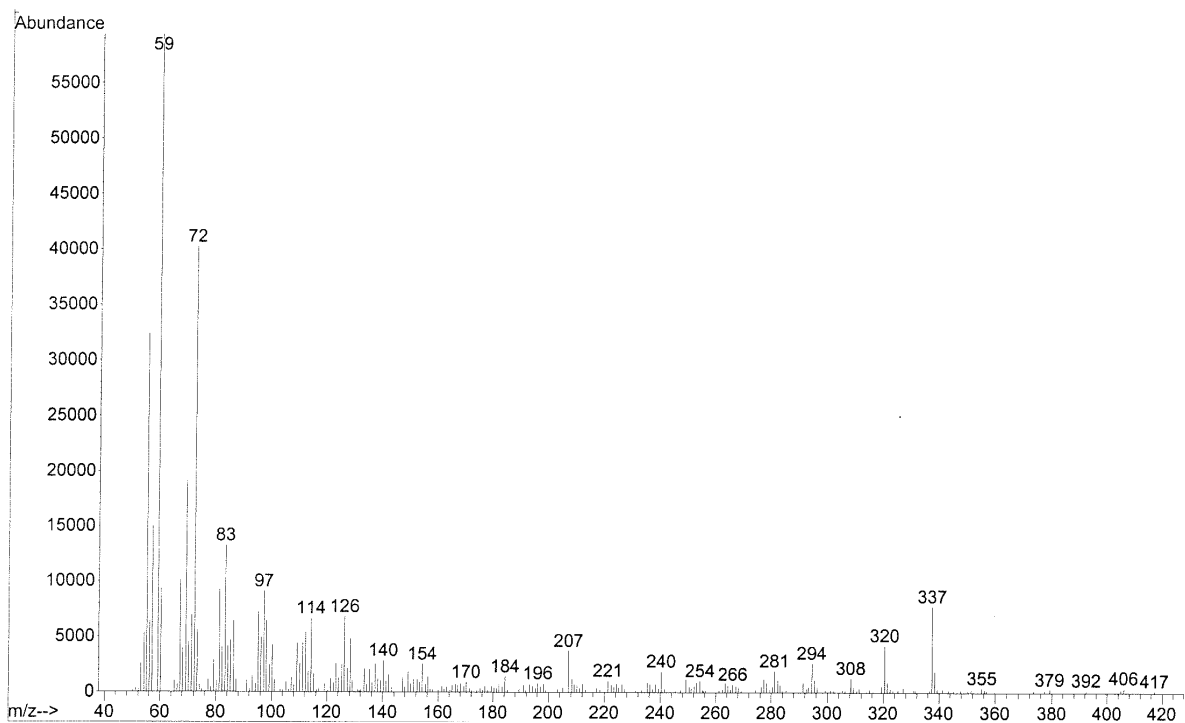


Figure 3.S18 Example of the GC-MS mass spectral data obtained for erucylamide identified in whole body hexane extractions of *I. scapularis scapularis* unfed virgin adult females and males (Table 3.1 and Fig. 3.9). M/Z = mass to charge ratio for each ion. Abundance = the intensity or abundance of each ion.

APPENDICES

Appendix A

Ionotropic Glutamate Receptors with Putative Olfactory Functions Identified in the Haller's Organ of the American Dog Tick, *Dermacentor variabilis* (Acari: Ixodidae)

Introduction

The American dog tick, *Dermacentor variabilis* (Acari: Ixodidae), is the primary vector of *Rickettsia rickettsii*, the causative agent of Rocky Mountain spotted fever, with expanding populations present in the eastern and central portions of the U.S (Sonenshine and Roe, 2014). Pathogen transmission between ticks and hosts occurs during blood feeding. Tick physiology requires blood meals for growth, molting, sexual maturation and reproduction. Ticks depend on chemosensation to detect and locate hosts within the proximate environment. Chemosensory stimuli that induce tick host-seeking and feeding behavior convey information about host species, proximity and directionality. The main external apparatus responsible for chemosensation is the Haller's organ. The Haller's organ is a localization of chemosensilla present on the foretarsus of the first pair of legs (Leonovich, 2006). Through next generation sequencing technology the first transcriptome to the Haller's organ of unfed virgin adult male *D. variabilis* was constructed. Analysis of putative chemosensory transcripts elucidated a possible G-protein coupled receptor (GPCR) mediated chemosensory signal cascade (*unpublished data*). Though in addition to the putative GPCR chemoreceptors, ionotropic glutamate receptors (iGluRs) were also identified exclusively in the Haller's organ transcriptome. iGluRs are membrane bound ligand binding ion channels that are involved in cell mediated responses to extracellular stimuli (Croset et al., 2010). Recently in insects, a novel group of iGluRs was determined to function as olfactory

receptors in the antennae (Croset et al., 2010; Rytz, et al., 2013). Furthermore, similar olfactory iGluRs were identified exclusively in chemosensory organs of crustaceans (Corey et al., 2013). Advances in next generation sequencing have determined that this new group of olfactory iGluRs represents a novel class of iGluRs, which contains iGluRs that function in either olfaction or gustation (Croset et al., 2010). With the pivotal discovery of a novel type of chemoreceptor in insects and crustaceans, it was logical to assess if ticks possess similar types of iGluR chemoreceptors. This research documents the first analyses of putative olfactory iGluRs found exclusively in the Haller's organ of ticks.

Materials and Methods

Bioinformatics

Putative chemosensory iGluR transcripts were identified through BLASTx and BLASTn searches of the unfed virgin adult male *D. variabilis* Haller's organ specific transcriptome (unpublished data). The putative functions of the iGluRs identified were verified against the Uniprot knowledgebase using BLASTx (EBI, Cambridge, UK). The annotations of confirmed iGluRs were determined using Argot² (FEM-IASMA, Trento, Italy) and alignments performed utilizing Clustal Omega (EBI, Cambridge, UK) and MAFFT with L-INS settings (Kato and Standley, 2013). Generated alignments were visualized in Jalview (Waterhouse et al., 2009). Phylogenetic analyses were conducted using the Molecular Evolutionary Genetics Analysis program (MEGA; Biodesign Institute, Tempe, AZ). Membrane topography and domain structures were predicted using Pfam program and database (Finn et al., 2014) and TMHMM (Sonnhammer et al., 1998).

Results and Discussion

Two putative iGluR transcripts (contig 5494 and 9210) were identified exclusively in the unfed virgin adult male *D. variabilis* Haller's organ specific transcriptome (Table A.1).

Alignments of the two putative iGluRs transcripts showed high sequence similarity to two iGluRs identified in the zebra tick, *Rhipicephalus pulchellus* genome (Fig. A1 and A2). In ticks, iGluRs can be divided into three clades, the kainate clade, the α -amino-3-hydroxy-5-methyl-4-isoxazolepropionic acid (AMPA) clade, and the N-methyl-D-aspartate (NMDA) clade (Sonenshine and Roe, 2014). Insects possess iGluRs that can be divided into the same three clades plus a newly discovered fourth clade that contains novel olfactory iGluRs and co-receptors (Croset et al., 2010). Alignment and phylogenetic analyses determined that the two putative iGluR transcripts encoded kainate 2-like receptors (Fig. A3 and A4). Gene ontology annotation and pathway identification for the putative kainate 2-like iGluR transcripts revealed functional roles in the iGluR pathway and glutamate gated ion channel activity (Table A.2). Several kainate 2-like iGluRs have recently been sequenced and linked to olfaction in the sea louse, *Caligus rogercresseyi* (Núñez-Acuña, et al., 2014).

Unfortunately, the exact role of kainate 2-like iGluRs in the olfactory signal transduction still remains unknown. This is the first documentation of kainate 2-like iGluRs exclusively in the Haller's organ of unfed virgin adult male *D. variabilis*. Though with the limited information available documenting kainate 2-like iGluRs in olfactory and gustatory systems it is difficult to draw more in-depth conclusions.

References

- Corey EA, Bobkov Y, Ukhanov K, Ache BW (2013) Ionotropic crustacean olfactory receptors. *PloS One*. 8:e60551.
- Croset V, Rytz R, Cummins SF, Budd A, Brawand D, Kaessmann H, Gibson TJ, Benton R (2010) Glutamate receptors and the evolution of insect taste and olfaction. *PLoS One*, 6:e1001064.
- Katoh K, Standley DM (2013) MAFFT multiple sequence alignment software version 7: improvements in performance and usability. *Mol Biol Evol*, 4:772–778.
- Leonovich SA (2006) *Sensory Systems of Parasitic Ticks and Mites*. Nauka press, St. Petersburg, Russia.
- Macaluso KR, Paddock CD (2014) Tick-borne spotted fever group Rickettsioses and *Rickettsia* species. *In: Sonenshine DE, Roe RM (Eds). Biology of Ticks vol. 2*. Oxford University Press, New York City, New York.
- Núñez-Acuña G, Valenzuela-Muñoz V, Marambio JP, Wadsworth S, Gallardo-Escárate C (2014) Insights into the olfactory system of the ectoparasite *Caligus rogercresseyi*: Molecular characterization and gene transcription analysis of novel ionotropic receptors. *Exp Parasitol*. 145:99–109.
- Rytz R, Croset V, Benton R (2013) Ionotropic receptors (IRs): Chemosensory ionotropic glutamate receptors in *Drosophila* and beyond. *Insect Biochem Molec Biol*.
- Sonenshine DE, Roe RM (2014) *Biology of Ticks vol. 2*. Oxford University Press, New York City, New York.
- Sonnhammer ELL, von Heijne G, Krogh A (1998) A hidden Markov model for predicting transmembrane helices in protein sequences. *Proc Int Conf Syst Mol Biol*, 6:175-182.
- Waterhouse AM, Procter JB, Martin DMA, Clamp M, Barton GJ (2009) Jalview Version 2-a multiple sequence alignment editor and analysis workbench. *Bioinformatics*, 25:1189-1191.

Tables

Table A.1. Putative ionotropic glutamate receptors identified exclusively in the Haller's organ of unfed virgin adult male *Dermacentor variabilis* with their respective tick and non-tick arthropod BLASTx matches with the lowest expected value (e-value).

Contig (length bp)	Best tick match (%identity & e-value)	Best non-tick arthropod match (%identity & e-value)	Conserved domain(s)
5494 (1666)	Putative ionotropic glutamate receptor <i>Rhipicephalus pulchellus</i> JAA54415.1 (88.5%, 7.80E-84)	GK13657 <i>Drosophila willistoni</i> EDW83544.1 (32.0%, 1.10E-10)	None
9210 (218)	Putative ionotropic glutamate receptor <i>Rhipicephalus pulchellus</i> JAA64048.1 (88.9%, 2.20E-36)	Glu-RI_1 protein <i>Fopius arisanus</i> JAG81342.1 (40.8%, 2.90E-8)	None

Table A.2. Biological and molecular level 2 gene ontology annotation of the two putative ionotropic glutamate receptors (contig 5494 and 9210) identified exclusively in the Haller's organ of unfed virgin adult male *Dermacentor variabilis*.

Contig	Level 2	Gene ontology term (GO term no.)
5494	Molecular function	Extracellular glutamate gated ion channel activity (GO:0005234)
		Ionotropic glutamate receptor activity (GO:0004970)
		Transporter activity (GO:0005215)
	Biological process	Ionotropic glutamate receptor signaling pathway (GO:0035235)
		Ion transmembrane transport (GO:0034220)
		Transport (GO:0006810)
9210	Molecular function	Extracellular glutamate gated ion channel activity (GO:0005234)
		Ionotropic glutamate receptor activity (GO:0004970)
	Biological process	Ionotropic glutamate receptor signaling pathway (GO:0035235)
		Ion transmembrane transport (GO:0034220)

Table A.3. Comprehensive list of the acronyms presented in phylogenetic trees and the identifying species and GenBank accession numbers.

Acronym	Species	GeneBank Accession no.
CeAMPA	<i>Caenorhabditis elegans</i>	AAA92006.1
CeIRCo-25a	<i>Caenorhabditis elegans</i>	AAK01099.1
CeKainate	<i>Caenorhabditis elegans</i>	CCD61468.1
CeNMDA	<i>Caenorhabditis elegans</i>	AAK01101.2
CrKainate2-like	<i>Caligus rogercresseyi</i>	AHN49643.1
Dm NDMA	<i>Drosophila melanogaster</i>	CAA50675.1
DmAMPA	<i>Drosophila melanogaster</i>	AAA28575.1
DmIRCo-25a	<i>Drosophila melanogaster</i>	ADU79032.1
DmKainate	<i>Drosophila melanogaster</i>	ABI29183.1
DmKainate-2	<i>Drosophila melanogaster</i>	AAF52268.1
DpAMPA	<i>Daphnia pulex</i>	EFX71861.1
DpIRCo-25a	<i>Daphnia pulex</i>	EFX86214.1
DpKainate	<i>Daphnia pulex</i>	EFX90374.1
DpNMDA	<i>Daphnia pulex</i>	EFX71929.1
IrKainate2-like	<i>Ixodes ricinus</i>	JAC93989.1
IsAMPA1	<i>Ixodes scapularis</i>	EEC03801.1
IsAMPA2	<i>Ixodes scapularis</i>	EEC03802.1
IsKainate	<i>Ixodes scapularis</i>	EEC11135.1
IsNMDA1	<i>Ixodes scapularis</i>	EEC12520.1
IsNMDA2	<i>Ixodes scapularis</i>	EEC15663.1
MoAMPA	<i>Metaseiulus occidentalis</i>	XP_003737303.1
MoIRCo-25a	<i>Metaseiulus occidentalis</i>	XP_003743738.1
MoKainate	<i>Metaseiulus occidentalis</i>	XP_003738808.1
MoNMDA	<i>Metaseiulus occidentalis</i>	XP_003740977.1
RpKainate	<i>Rhipicephalus pulchellus</i>	JAA62812.1

Figures

```

Contig 5494   YALALPKGSAFRSELSAAIIRLKSDGTLQLLRHYWWHEQGAINCPREQPVYRPTPFTVRF
RpJAA54415.1 YAIALPKGSAFRSELSAAIIRLKSEGLQLLRQHWWHERGAVNCPREQPVYRPTPFTVRF
                **:*****:*****:*****:*****:*****:*****
Contig 5494   GRLSLVFVFLLLGLVITMLVMLFIFVVRGHAQKNLSAESMSAVWNTLVEELRAAMLCRKEK
RpJAA54415.1 GRLSLVFVFLLLGLVITMLVMLFIFVVRGHARKNLSAESMSAVWSTLVDELRAAMLCRKEK
                *****:*****.***.******
Contig 5494   RAKEEEDAANKDQEAAAT--TTQPQQPTITTPNDTAPTPVWRWTLGLRHPGRTSQQNRVA
RpJAA54415.1 HPKEEEDETKDQAAAATPAAGQPQQPTITTPNDTAPTKDQAAAA--TPAAGQPQQPTIT
                :*****:*** ***:*****:*****:*****:*****
Contig 5494   GPWHSPVS
RpJAA54415.1 TPND----
                * .

```

Figure A.1. Multiple sequence alignment (Clustal Ω) of the deduced amino acid sequence for the putative ionotropic glutamate receptor (contig 5494) identified exclusively in the Haller's organ transcriptome of unfed virgin adult male *D. variabilis* versus the top BLAST tick hit (lowest e-value). Asterisks (*) denote conserved residues, colons (:) indicate conservation between groups of strongly similar properties scoring >0.5 in the Gonnet PAM 250 matrix, and periods (.) indicate conservation between groups of weakly similar properties scoring ≤ 0.5 on the Gonnet PAM 250 matrix. The acronym consists of the first letter of genus and species (*Rhipicephalus pulchellus*, Rp) followed by the GenBank accession number for the protein BLAST hit (JAA54415.1).

```

Contig 9210  YASVLGEFIIRYRDRPTLDSLDDLLRQKTINYGTLHHGSTHDFRSTFPQYMKLWQGIQ
RpJAA64048.1 YASVLGEFIIRYRDRPTLDSLDDLLRQKEIKYGTLRQGSTHDFRSTFPQYMKLWQGIQ
*****:*****:*****:*****

```

```

Contig 9210  SQGQDAFVNSYA
RpJAA64048.1 SQGDEAFVDSYA
***:***:***

```

Figure A.2. Multiple sequence alignment (Clustal Ω) of the deduced amino acid sequence for the putative ionotropic glutamate receptor (contig 9210) identified exclusively in the Haller's organ transcriptome of unfed virgin adult male *D. variabilis* versus the top BLAST tick hit (lowest e-value). Asterisks (*) denote conserved residues, colons (:) indicate conservation between groups of strongly similar properties scoring >0.5 in the Gonnet PAM 250 matrix, and periods (.) indicate conservation between groups of weakly similar properties scoring ≤ 0.5 on the Gonnet PAM 250 matrix. The acronym consists of the first letter of genus and species (*Rhipicephalus pulchellus*, Rp) followed by the GenBank accession number for the protein BLAST hit (JAA64048.1).

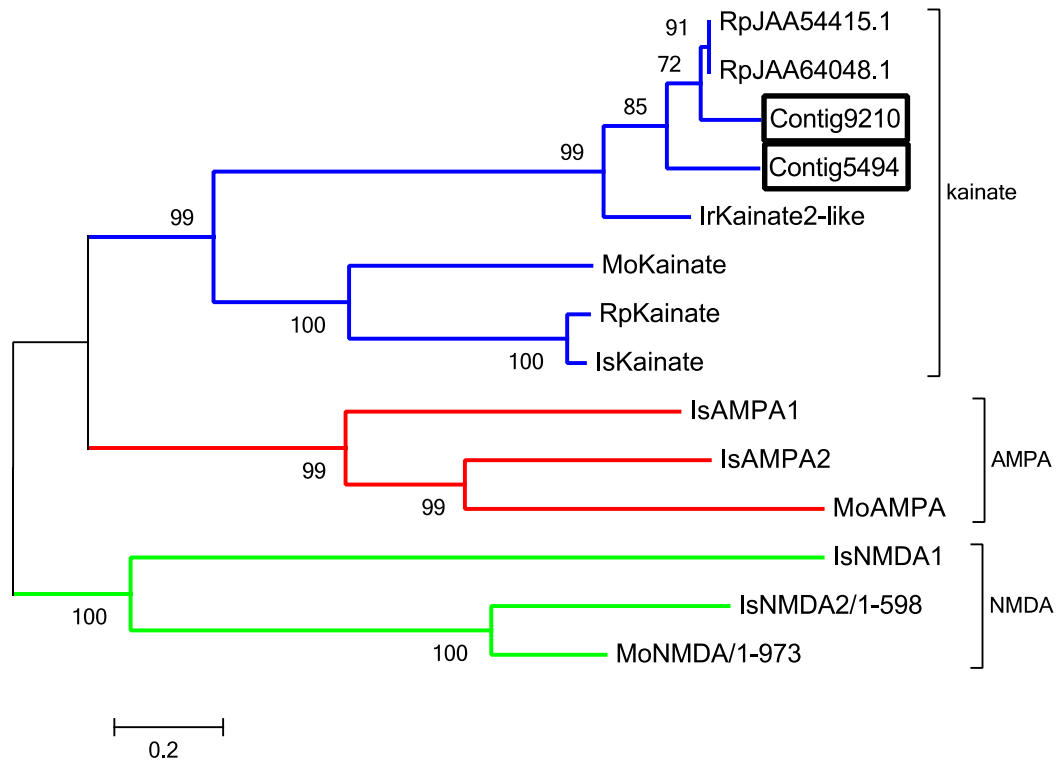


Figure A.3. Phylogenetic relationship of transcripts putatively encoding ionotropic glutamate receptors (iGluRs) identified in the Haller’s organ (contig 5494 and 9210) transcriptome of unfed virgin adult male *D. variabilis* with iGluRs of known clade annotation from *Ixodes scapularis*, *I. ricinus*, *Metaseiulus occidentalis*, and *Rhipicephalus pulchellus*. The phylogenetic tree shows three clades, each represented by a different branch color as follows: blue = kainate clade; red = α -amino-3-hydroxy-5-methyl-4-isoxazolepropionic acid (AMPA) clade; green = N-methyl-D-aspartate (NMDA) clade. Acronyms consist of the first letter of the genus and species (*Ixodes scapularis*, Is; *I. ricinus*, Ir; *Metaseiulus occidentalis*, Mo; *Rhipicephalus pulchellus*, Rp) followed by the associated clade. Putative iGluRs transcripts are boxed. The tree was constructed using Maximum likelihood phylogenetic analysis and bootstrapping set to 500 iterations. Branch values listed are bootstrap percentages (percent confidence), scale set to 20%. The *R. pulchellus* genome orthologs (Table A.1) were included in phylogenetic analyses to ensure the short sequence lengths of the contigs were not resulting in false tree delineation (Acronym Rp followed by GenBank accession no.). A comprehensive list of acronyms and associated Genbank accession numbers are listed in Table A.3.

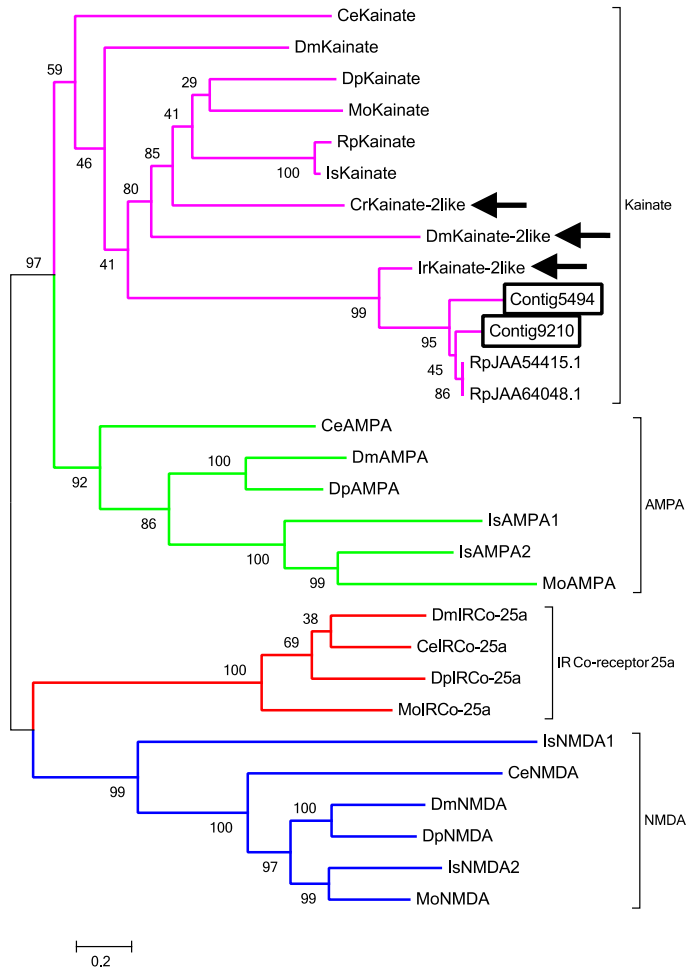


Figure A.4. Phylogenetic relationship of transcripts putatively encoding ionotropic glutamate receptors (iGluRs) identified in the Haller's organ (contig 5494 and 9210) transcriptome of unfed virgin adult male *D. variabilis* with iGluRs of known clade annotation from *Caenorhabditis elegans*, *Caligus rogercresseyi*, *Daphnia pulex*, *Drosophila melanogaster*, *Ixodes scapularis*, *I. ricinus*, *Metaseiulus occidentalis*, and *Rhipicephalus pulchellus*. The phylogenetic tree shows four clades, each represented by a different branch color as follows: purple = kainate clade; green = α -amino-3-hydroxy-5-methyl-4-isoxazolepropionic acid (AMPA); red = novel ionotropic receptor (IR) clade that contains the IR co-receptor 25a; blue = N-methyl-D-aspartate (NMDA) clade. Arrows show clustering of kainate-2 like iGluRs. Acronyms consist of the first letter of the genus and species (*Caenorhabditis elegans*, Ce; *Caligus rogercresseyi*, Cr; *Daphnia pulex*, Dp; *Drosophila melanogaster*, Dm; *Ixodes scapularis*, Is; *I. ricinus*, Ir; *Metaseiulus occidentalis*, Mo; *Rhipicephalus pulchellus*, Rp). The tree was constructed using Maximum likelihood phylogenetic analysis and bootstrapping set to 500 iterations. Branch values listed are bootstrap percentages (percent confidence), scale set to 20%. The *R. pulchellus* genome orthologs (Table A.1) were included in phylogenetic analyses to ensure the short sequence lengths of the contigs were not resulting in false tree delineation (Acronym Rp followed by GenBank accession no.). A comprehensive list of acronyms and associated Genbank accession numbers are listed in Table A.3.

Appendix B

A Novel Method for Micro-dissection of the Cuticle Covering of the Haller's organ

Introduction

Ticks are blood-feeding ectoparasites that rely heavily on chemosensation to locate and identify animal hosts within the proximate environment. In ticks, chemosensation is mainly ascribed to the Haller's organ, a localization of chemosensory sensilla present on the foretarsus of the first pair of legs. The Haller's organ represents a unique chemosensory organ that is exclusive to ticks, and not found in any other animal (Foelix and Axtell, 1972). Chemosensory sensilla in the Haller's organ are organized into two main structures, the anterior pit and the posterior capsule (Fig. B.1). Chemosensory sensilla in the anterior pit are exposed on the exterior surface of the foretarsus, whereas the chemosensory sensilla of the posterior capsule are contained within a pit that is covered with a protective cuticle covering. Due to the physical limitations of the posterior capsule's cuticle covering, the majority of the research documenting chemosensory cell function in the Haller's organ has been restricted to the anterior pit (Waladde, 1982). Attempts to study the chemosensory cells of the posterior capsule have been thwarted by the strength and thickness of the posterior capsule's cuticle covering (Carr and Roe, 2015). Current tick micro-dissection techniques depend on the use of probes, scalpels, and scissors, which are not precise enough to remove the posterior capsule cuticle covering without damaging the sensilla contained within. Recent advancements in micro-dissection techniques have determined that ultrasonic vibrations can be used for cutting mammalian tissue with more precision than laser-based micro-dissection techniques (Sun et al., 2006). Here we describe the first application of ultrasonic vibrations to

cut and remove tick cuticle, specifically the cuticle covering of the Haller's organ posterior capsule.

Materials and Methods

Ticks

Adult *Amblyomma americanum* ticks were purchased from the Oklahoma State University Tick Rearing Facility. Female and male adult *A. americanum* were maintained in different containers at 23 ± 10 C, 97% humidity, and with a photoperiod of 16-hour light: 8-hour dark (dusk and dawn periods of 1 h each at the beginning and ending of the scotophase).

Ultrasonic scaler

A dental piezoelectric ultrasonic scaler (UDS-J; Guilin Woodpecker Medical Instrument Co., Guangxi, China) was modified for use as the cutting instrument for the cuticle covering of the Haller's organ posterior capsule (Fig. B.1). Dental piezoelectric ultrasonic scalers produce ultrasonic linear vibrations that chip away at dental plaque. This same concept was applied to chip away at the cuticle covering of the Haller's organ posterior capsule. The dental piezoelectric ultrasonic scaler consisted of a base unit, handheld scaler instrument and an attached stainless steel scaler tip (Fig. B.2). First, the stainless steel scaler tip was detached from the handheld scaler instrument and sharpened using electropolishing. Electropolishing removes ions individually from the microscopic surface of a metal object by placing set object into an electrolyte solution and applying a direct electrical current (Bauccio, 1993). For electropolishing of the stainless steel scaler tip, a carbon rod was used as the reference electrode, attached to the negative lead, and placed into one opening of a

glass 'U' tube containing 2M NaOH (Fig. B.3). The stainless steel scaler tip was screwed into the base a metal handle, fixed to an upward/downward rotating arm, and the positive lead attached. The stainless steel scaler tip was positioned over the second opening of the glass 'U' tube containing 2M NaOH (Fig. B3). AC current was generated by an Olympus TL3 power supply generator through a variable autotransformer (SGA Scientific Inc., Bloomfield, NJ) to allow for more control and manipulation of the current voltage. During electropolishing the voltage was maintained between 3 and 7 volts. With the current active, the rotating arm was used to lower and raise the stainless steel scaler tip in and out of the charged NaOH solution removing the exterior metal ions along the taper of the tip sharpening it. Turning the active current off, the tip was visualized using a Narishige scope (Model MF 830, Narishige International USA Inc., East Meadow, NY) with 15x eyepieces and a 10x lens. After multiple rounds of electropolishing, the diameter of the stainless steel scaler tip was approximately 0.1 mm.

In addition to sharpening the stainless steel scaler tip, modifications were made to the ultrasonic scaler base unit to reduce the frequency and strength of the ultrasonic vibrations. A wire wound 3Kohm resistor (IRC 8826, 5%; Mouser Electronics, Mansfield, TX) was inserted into the DC circuit of the ultrasonic scaler base unit to reduce the voltage output by 25% (4.18-5.40V). Reducing the voltage output decreased the frequency amplitude of the ultrasonic vibrations allowing for more control and fine-tuning (13.2-16.6kHz).

Micro-dissection technique

Adult *A. americanum* were placed onto a paraffin wax ball and paraffin wax soldered onto the 2nd, 3rd, and 4th pairs of legs to immobilize the tick onto the contour of the wax ball. The

first pair of legs were then strategically stretched and rotated to obtain the best visualization of the Haller's organ. To arrest movement of the first pair of legs after positioning, dental resin was applied to each podomere leg joint, and allowed to cure for 60 sec. The wax ball and affixed tick were then soldered to a glass slide and placed onto the microscope stage. An Olympus SZX116 scope with 1.3x SDF lens and 30x eyepieces were used to visual the cutting field. A LED fiber optics light source (Fiberoptics Technology Inc., Pomfret, CT) was used to illuminate the cutting field. In preparation for cutting the handheld scaler instrument, without the sharpened stainless steel scaler tip, was mounted onto an electronic micromanipulator (American Cyanamid Company, Stamford, CT) and maneuvered into position adjacent to the microscope stage. The sharpened stainless steel scaler tip was then attached to the handheld scaler instrument, and the electronic micromanipulator used to move the scaler tip until it could be visualized in the cutting field, adjacent to the Haller's organ posterior capsule (Fig. B.4). Using the micromanipulator, the modified dental piezoelectric ultrasonic scaler was used to successfully cut and remove the cuticle covering of posterior capsule fully exposing the sensilla contained within.

Summary and future application

Ultrasonic vibrations proved to be an effective cutting tool for micro-dissection in ticks. The modified dental piezoelectric ultrasonic scaler was powerful yet precise in its cutting and removal of the tick cuticle. The ultrasonic vibrations appeared to shave away the cuticle layer by layer, which allowed for the delicate removal of the cuticle covering of the Haller's organ posterior capsule without damaging the sensilla contained within. It should be noted that there were issues associated with removing the cuticle shavings so they would not become

lodged inside the posterior capsule and block visualization of the sensilla. This was quickly resolved by using the piezoelectric ultrasonic scaler to strategically cut the cuticle covering of the posterior capsule starting at the center and working the scaler outwards, and in doing so pushing the cuticle shavings away from the posterior capsule. This is the first documentation of using ultrasonic vibrations to cut the cuticle of live ticks. Ultrasonic vibrations provide a precise cutting instrument that has immense potential as a novel micro-dissection tool for arthropods and warrants further examination.

Acknowledgments

I would like to thank Dr. Vince L. Salgado for all his support and guidance during the development of this novel cutting technique. His mentorship proved to be an invaluable experience.

References

- Bauccio M (1993) ASM Metal Reference Book 3rd Ed., ASM International, Materials Park, OH.
- Carr AL, Roe RM (2015). Acarine attractants: Chemoreception, bioassay, chemistry and control. *Pest. Biochem. Physiol. In press.*
- Foelix RF, Axtell RC (1972) Ultrastructure of the Haller's organ in the tick *Amblyomma americanum*. *Z. Zellforsch. Mikrosk. Anat.* 124:275-292.
- Sun L, Wang H, Chen L, Liu Y (2006) A novel ultrasonic micro-dissection technique for biomedicine. *Ultrasonics.* 44:e255-e260.
- Waladde SM (1982) Tip-recording from Ixodid tick olfactory sensilla: Responses to tick related odors. *J. Comp. Physiol.* 148:411-418.

Figures

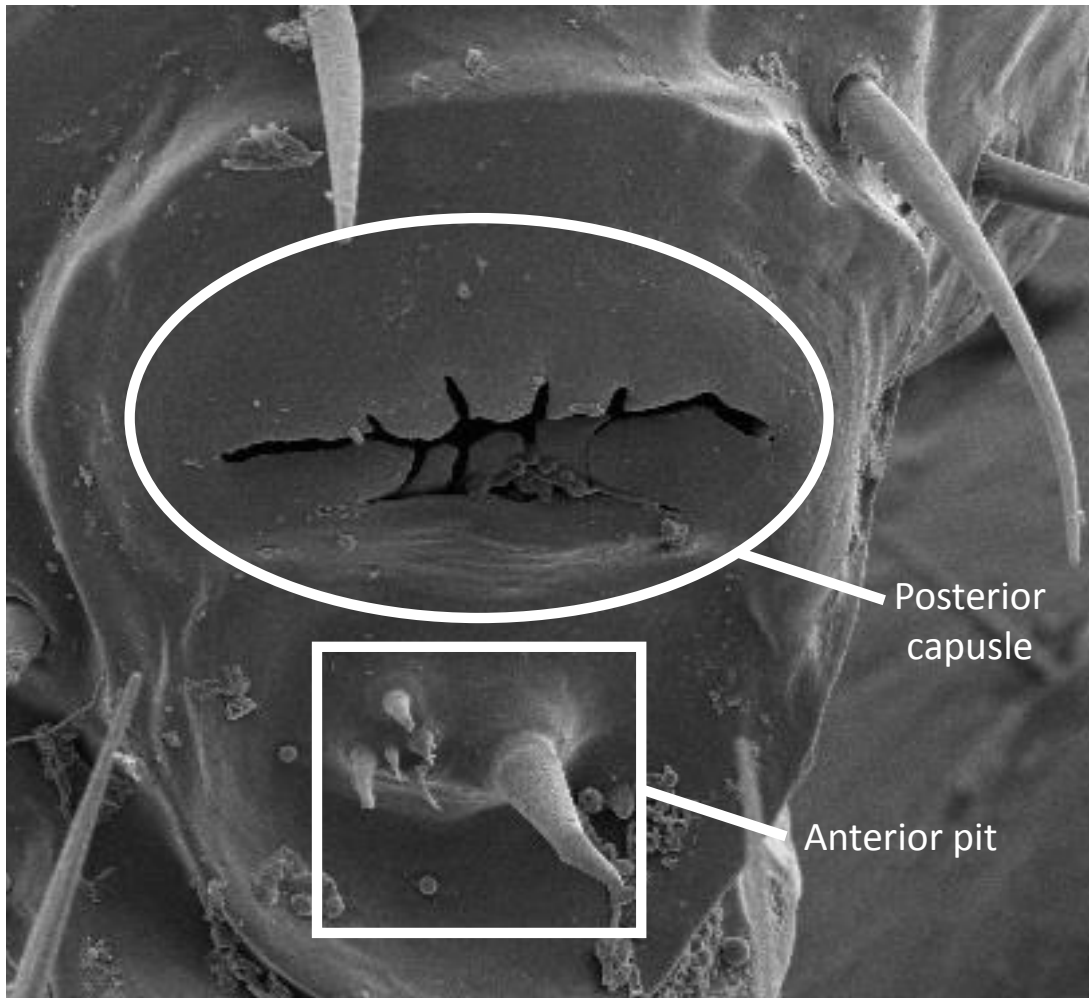


Figure B.1. The Haller's organ located on the foretarsus of the first pair of legs of the American dog tick, *Dermacentor variabilis* and its two structural components the anterior pit (boxed) and the posterior capsule (circled).

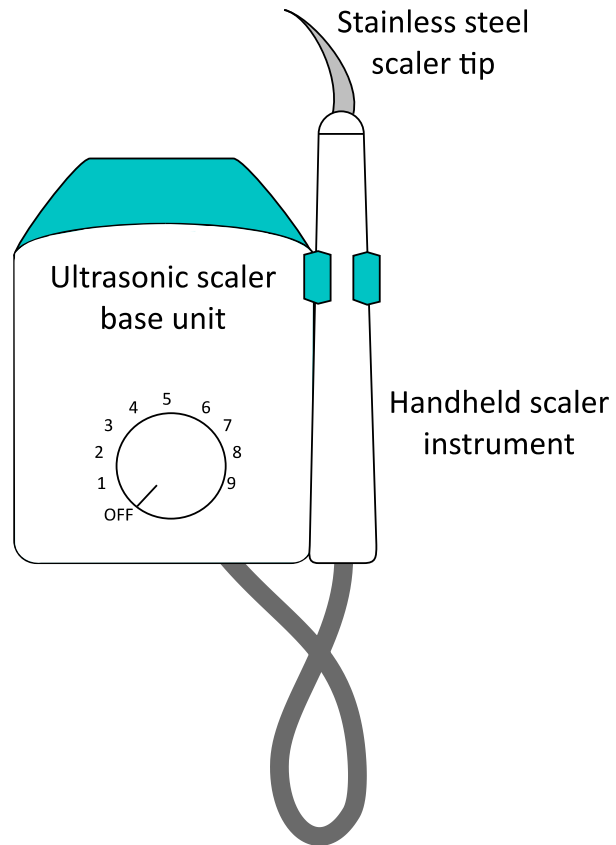


Figure B.2. Schematic of the piezoelectric dental ultrasonic scaler modified for use as the cutting device to remove the cuticle covering of the Haller's organ posterior capsule (UDS-J; Guilin Woodpecker Medical Instrument Co., Guangxi, China).

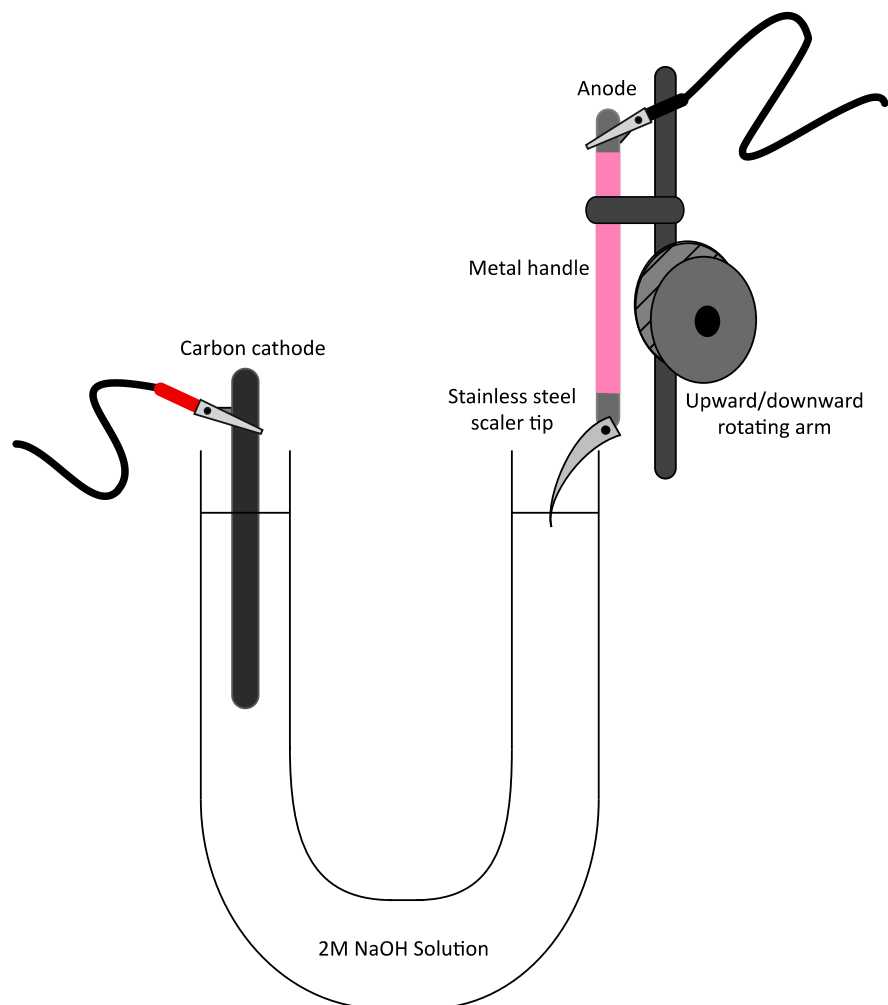


Figure B.3. Schematic representation of the electropolishing set-up used to sharpen the stainless steel scaler tip. The electrolyte solution was 2M NaOH and the voltage through the circuit was maintained between 3 and 7 volts.

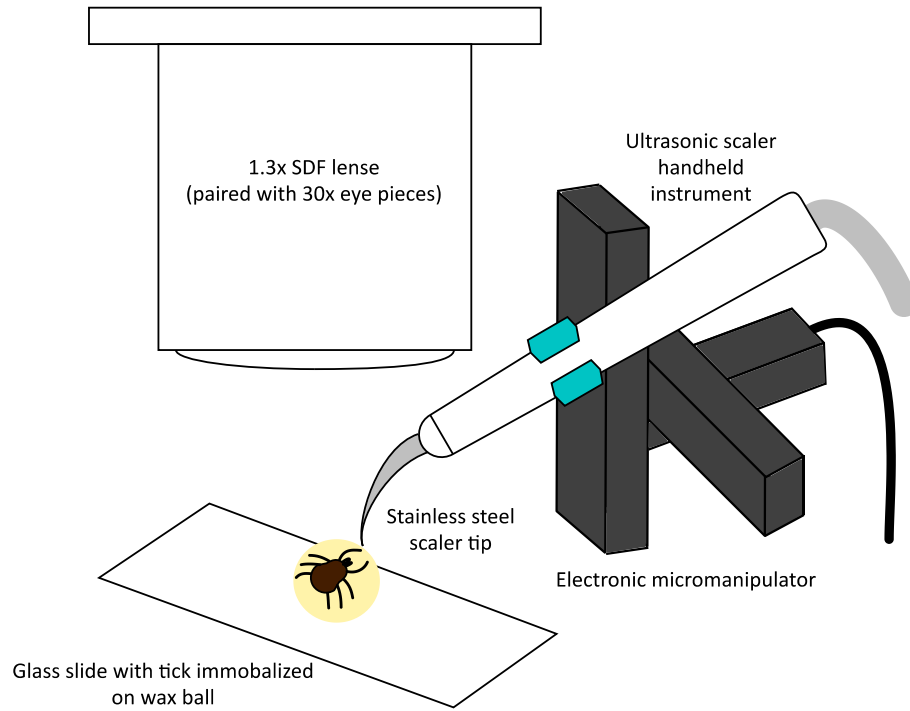


Figure B.4. Schematic representation of the micro-dissection system used to remove the cuticle covering of the posterior capsule of the Haller's organ. The vibration frequency of the dental piezoelectric ultrasonic scaler was set to 13.2-16.6kHz and the voltage 4.18-5.40V.